AFCRL-71-0406

INVESTIGATION OF STABILITY CHARACTERISTICS OF TETHERED BALLOON SYSTEMS

George R. Doyle Jr.
Jerome J. Vorachek

Goodyear Aerospace Corporation
Akron, Ohio 44315

Contract No. F 19628-71-C-0091

Project No. 7659
Task No. 765906
Work Unit No. 76590601

Scientific Report No. 2

30 July 1971

Contract Monitors: Don E. Jackson, Capt., USAF

Approved for public release; distribution unlimited.

Prepared for

AIR FORCE CAMBRIDGE RESEARCH LABORATORIES
AIR FORCE SYSTEMS COMMAND
UNITED STATES AIR FORCE
BEDFORD, MASSACHUSETTS 01730

Unclassified
Security Classification

DOCUMENT CONTROL DATA - R & D

(Security classification of title, body of abstract and indexing annotation must be entered when the overall report is classified)

1. ORIGINATING ACTIVITY (Corporate author) Goodyear Aerospace Corporation Akron, Ohio, 44315	2a. REPORT SECURITY CLASSIFICATION Unclassified 2b. GROUP

3. REPORT TITLE

INVESTIGATION OF STABILITY CHARACTERISTICS OF TETHERED BALLOON SYSTEMS

4. DESCRIPTIVE NOTES (Type of report and inclusive dates)
Scientific - Interim

5. AUTHOR(S) (First name, middle initial, last name)
George R. Doyle Jr.
Jerome J. Vorachek

6. REPORT DATE	7a. TOTAL NO OF PAGES	7b. NO OF REFS
30 July 1971	227	7

8a. CONTRACT OR GRANT NO	9a. ORIGINATOR'S REPORT NUMBER(S)
F19628-71-C-0091	GER- 15325
b. PROJECT, TASK, WORK UNIT NOS. 7659-06-01	Scientific Report No. 2
c. DoD Element: 62101F	9b. OTHER REPORT NO(S) (Any other numbers that may be assigned this report) AFCRL-71-0406
d. DoD Subelement: 687659	

10. DISTRIBUTION STATEMENT
Approved for public release; distribution unlimited

11. SUPPLEMENTARY NOTES	12. SPONSORING MILITARY ACTIVITY
TECH, OTHER	Air Force Cambridge Research Laboratories (LC) L. G. Hanscom Field Bedford, Massachusetts 01730

13. ABSTRACT An analytical investigation of the dynamic behavior of tethered balloons is in progress. This report, the second of three scientific reports, covers a study of stability characteristics of tethered balloon systems. Balloon systems which are investigated use the British BJ Barrage Balloon, the Vee Balloon and a Goodyear Aerospace Model No. 1649 Single-Hull Balloon. The major tether construction is Columbian Rope Company's NOLARO utilizing prestretched polyester filaments. Three design altitudes, 5,000, 10,000 and 20,000 feet, are considered.

The model for the tethered balloon system consists of the streamlined balloon and a tether made up of three discrete links. The derivation of equations of motion for this system in three dimensions is presented. The equations are linearized and treated as uncoupled in the longitudinal and lateral degrees-of freedom. Characteristic equations which incorporate the physical, aerodynamic, and mass characteristics of the system are developed. Computer programs for the IBM 360 digital computer are presented to determine the characteristic equations of the systems, and obtain the roots which represent the frequency and damping qualities.

An exploratory investigation to establish the trends of stability characteristics for various design parameters is reported. Design parameters considered include balloon shape and altitude, trim angle of attack, vertical location of the bridle confluence point, net static lift, tail size, reduced wind profiles, varying altitude as encountered in launch and retrieval, payload location, and winch location above mean sea level.

DD FORM 1 NOV 68 1473

Unclassified
Security Classification

14 KEY WORDS	LINK A		LINK B		LINK C	
	ROLE	WT	ROLE	WT	ROLE	WT
Aerostats						
Balloons						
Balloon Aerodynamics						
Balloon Dynamics						
Balloon Behavior						
Balloon Flying Qualities						
Balloon Mass Characteristics						
Balloon Stability						
Balloon Systems						
Cables						
Cable Dynamics						
Captive Balloons						
Dynamic Simulation Analysis						
Kite Balloons						
Stability Analysis						
Tethered Balloons						
Tethered LTA Vehicles						
Tethers						

AFCRL-71-0406

INVESTIGATION OF STABILITY CHARACTERISTICS OF TETHERED BALLOON SYSTEMS

George R. Doyle Jr.
Jerome J. Vorachek

Goodyear Aerospace Corporation
Akron, Ohio 44315

Contract No. F 19628-71-C-0091

Project No. 7659
Task No. 765906
Work Unit No. 76590601

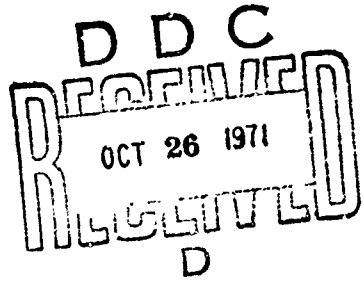

Scientific Report No. 2

30 July 1971

Contract Monitors: Don E. Jackson, Capt., USAF

Prepared for

AIR FORCE CAMBRIDGE RESEARCH LABORATORIES
AIR FORCE SYSTEMS COMMAND
UNITED STATES AIR FORCE
BEDFORD, MASSACHUSETTS 01730

ABSTRACT

An analytical investigation of the dynamic behavior of tethered balloons is in progress. This report, the second of three scientific reports, covers a study of stability characteristics of tethered balloon systems. Balloon systems which are investigated use the British BJ Barrage Balloon, the Vee Balloon and a Goodyear Aerospace Model No. 1649 Single-Hull Balloon. The major tether construction is Columbian Rope Company's NOLARO utilizing prestretched polyester filaments. Three design altitudes, 5,000, 10,000 and 20,000 feet, are considered.

The model for the tethered balloon system consists of the streamlined balloon and a tether made up of three discrete links. The derivation of equations of motion for this system in three dimensions is presented. The equations are linearized and treated as uncoupled in the longitudinal and lateral degrees-of freedom. Characteristic equations which incorporate the physical, aerodynamic, and mass characteristics of the system are developed. Computer programs for the IBM 360 digital computer are presented to determine the characteristic equations of the systems, and obtain the roots which represent the frequency and damping qualities.

An exploratory investigation to establish the trends of stability characteristics for various design parameters is reported. Design parameters considered include balloon shape and altitude, trim angle of attack, vertical location of the bridle confluence point, net static lift, tail size, reduced wind profiles, varying altitude as encountered in launch and retrieval, payload location, and winch location above mean sea level.

FOREWORD

This research was supported by the Air Force Systems Command, USAF, DOD, and was under the technical cognizance of the Air Force Cambridge Research Laboratories under Contract No. F 19628-71-C-0091.

The project is being carried out under the direction of Captain Don Jackson as Contract Monitor for the Air Force Cambridge Research Laboratories. Mr. Jerome Vorachek is the Goodyear Aerospace Corporation Project Engineer. Technical effort has been provided by Mr. George Doyle for derivation of the equations of motion and characteristic equations of the tethered balloon systems, programming of equations for solution with the IBM 360 computer and generation of stability results. Mr. William Ebert developed the aerodynamic characteristics for the balloon system, and mass characteristics were generated by Mr. Walt Stricker. Technical assistance was also provided by Mr. Philip Myers and Mr. Louis Handler.

The contractor's number for this report is GER-15325.

TABLE OF CONTENTS

LIST OF TABLES

LIST OF ILLUSTRATIONS

LIST OF ILLUSTRATIONS (cont'd)

LIST OF ILLUSTRATIONS (cont'd)

SECTION I

INTRODUCTION

The objective of this program is to investigate the dynamic behavior of tethered balloons and in so doing to establish design criteria for tethered balloons, tethers and payloads. The program is organized into three steps:

(1) Definition of balloon systems for dynamic analysis

(2) A study of stability characteristics of tethered balloon systems

(3) A study of dynamic response of tethered balloon systems to wind gusts

Reference 1 presents a definition of tethered balloon systems to be used for dynamic studies. This second scientific report presents a development of the equations of motions describing the behavior of tethered balloons and a parametric study of stability characteristics of the tethered balloon systems presented in Reference 1. Additional aerodynamic and mass characteristics data developed for the dynamic analysis is included in Appendix C to this report.

The system is defined as a balloon tethered at the end of a cable which is fixed to a stationary winch. The tether is represented by "N" straight links, each of the same length. The links are considered rigid and connected to each other by frictionless hinges. Goodyear Aerospace Corporation has employed this method of representation of the tethered system for other studies such as that described in Reference 2.

SECTION II

BALLOON DESCRIPTION

The balloon systems evaluated in this stability investigation have been described in Reference 1. The three balloon types in these systems are the British BJ Balloon, the Vee-Balloon* and the GAC No. 1649 Single Hull Balloon as depicted in Figures 1, 2, and 3. The nominal tethered systems characteristics defined in Reference 1 are summarized in Tables I and II.

Static and dynamic aerodynamic characteristics for the balloons have been determined from experimental data where available and by analytical techniques otherwise. The aerodynamic characteristics are presented and discussed in Appendix C along with additional mass and suspension system geometries which were not included in Reference 1.

Design parameters varied in the stability investigation include the trim angle of attack, vertical location of the suspension system confluence point below the balloons, the free-static lift, and the tail size.

The trim angle of attack can be controlled by locating the confluence point of the suspension system. The location of this point is established by the two coordinates as shown in Figure 1. The fuselage station from the nose and the waterline below the centerline of the balloon defines this point. The trim angle of attack change as a function of bridle apex point location has been calculated and is given in Appendix C.

The free-static lift as used in this report is the excess buoyant lift provided by the balloon after the balloon physical weight and the weight of the tether in no wind is supported.

Nominal tail sizes for each balloon are depicted in Figures 1, 2, and 3. For the British BJ Balloon, tail size is increased and decreased about the nominal by changing the linear dimensions of each of the three tails and maintaining similar proportions. The intersection of the trailing edge of the tails and the hull is maintained at the same point for all tail sizes. For the Vee-Balloon the horizontal tail geometry is maintained. The vertical tails are increased in size in two steps for tails below the hulls. Also investigated are the conditions where vertical tails are located symmetrically above and below the hulls. In addition to establishing aerodynamic characteristics for these tail configurations as noted in Appendix C, the increase in physical mass and additional mass was computed and used in the determination of stability characteristics.

Ascent and descent studies for a specific balloon also incorporate the change in mass characteristics due to air density changes with altitude.

*T.M. Goodyear Aerospace Corporation, Akron, Ohio

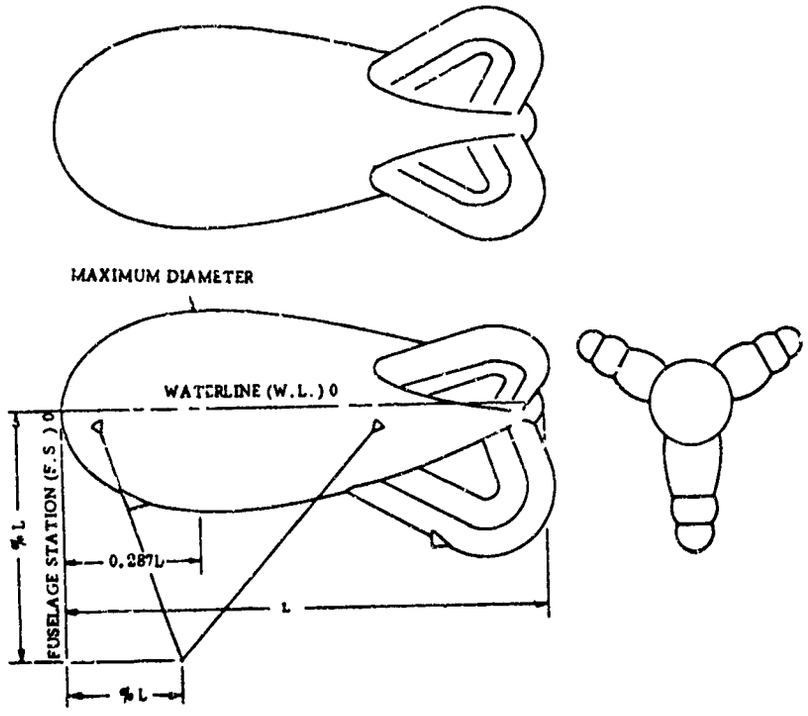

Figure 1. BJ Configuration

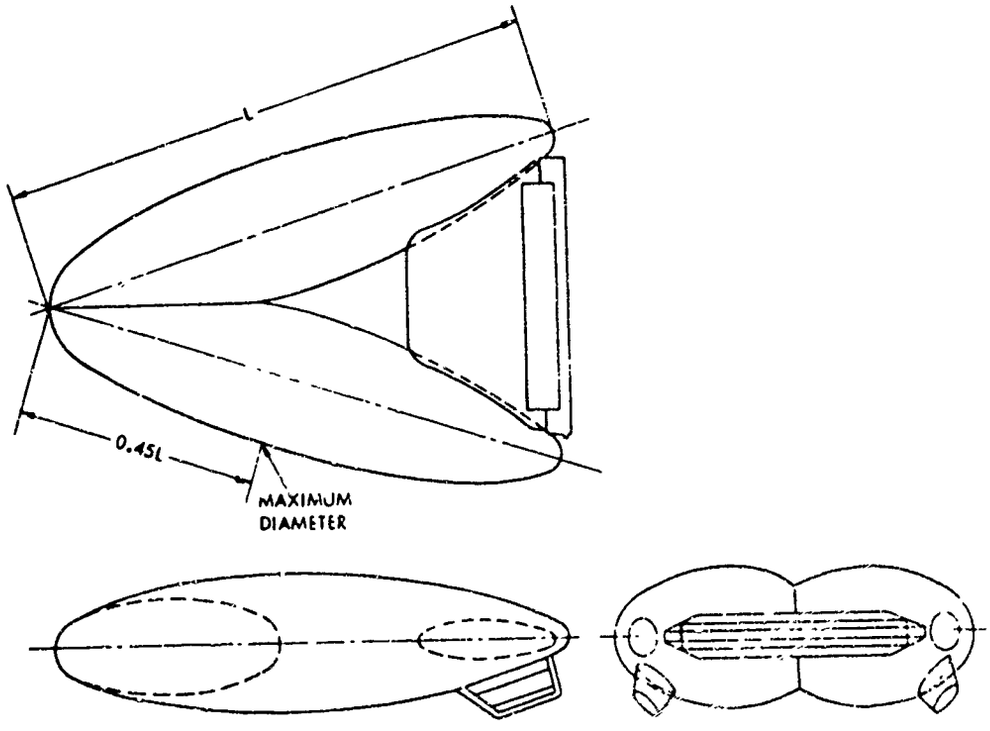

Figure 2. Vee-Balloon Configuration

Table I. Summary of Balloon/Cable Systems

Balloon Type	h	Hull Volume (ft^3)	Gross Static Lift (lb)	L_B (lb)	P (lb)	L_s (lb)	Survival				Operational				Tether		
							L_a (lb)	D (lb)	L_M (lb)	T (lb)	L_a (lb)	D (lb)	L_M (lb)	T (lb)	Type	O.D. (in)	B.S. (lb)
BJ	5,000	46,000	2,534	635	1,500	399	1,391	656	1,790	1,906	659	351	1,058	1,115	NOLARO	0.321	3,813
Vee-Balloon	10,000	80,000 (85,363)[1]	4,029	1,543	1,000	1,488	6,427	2,422	7,916	8,278	4,437	1,514	5,925	6,116	NOLARO	0.585	16,600
		144,000 (153,654)[1]	7,253	2,712	1,000	3,541	9,509	3,583	13,050	13,533	6,564	2,239	10,105	10,350	AMGAL	7/16	20,000
BJ		60,000	2,832	1,031	1,000	801	2,706	1,219	3,507	3,713	1,391	651	2,192	2,287	NOLARO	0.410	7,540
		75,000	3,540	1,276	1,000	1,264	3,140	1,414	4,405	4,626	1,614	755	2,878	2,975	AMGAL	1/4	6,750
ϕ1649 w/ Thin Fins		80,000	3,776	1,548	1,000	1,228	4,963	1,346	6,191	6,336	2,508	757	3,736	3,812	NOLARO	0.520	12,700
		133,000	6,278	2,511	1,000	2,767	6,965	1,887	9,732	9,913	3,529	1,061	6,286	6,376	AMGAL	3/8	14,800
BJ	20,000	500,000	17,037	8,933	600	7,504	15,420	6,785	22,924	23,907	7,571	3,577	15,075	15,494	NOLARO	0.993	47,814

( )[1] Total Helium Volume

Table II. Summary of Cable Solutions

Balloon Type	Altitude (ft)	Hull Volume (ft^3)	Tether Type	B.S. (lb)	O.D. (ft)	Wt/Ft (lb/ft)	X (ft)	ϑ (deg)	T (lb)	Length (ft)	Total Tether Weight (lb)
BJ	5,000	46,000	NOLARO	3,813	0.02679	0.03211	0	161.6	1,115	0	--
h = 5,000 ft P = 1,500 lb	S.L.						2,672	144.2	956	5,692	183
Vee-Balloon	10,000	30,000	NOLARO	16,600	0.04875	0.11400	0	165.7	6,115	0	--
	5,000						1,775	154.7	5,552	5,314	606
h = 10,000 ft P = 1,000 lb	S.L.						4,594	146.6	4,991	11,060	1,260
	10,000	144,000	AMGAL	20,000	0.03642	0.30400	0	167.5	10,350	0	--
	5,000						1,389	160.8	8,836	5,193	1,580
	S.L.						3,452	153.9	7,300	10,605	3,230
BJ	10,000	60,000	NOLARO	7,340	0.03420	0.05600	0	163.4	2,287	0	--
	5,000						2,456	143.6	2,036	5,600	314
h = 10,000 ft P = 1,000 lb	S.L.						7,377	127.7	1,761	12,639	708
	10,000	75,000	AMGAL	6,750	0.02083	0.09970	0	165.3	2,975	0	--
	5,000						1,843	153.2	2,482	5,340	532
	S.L.						5,072	140.3	1,989	11,305	1,128
#1649 w/Thin Fins	10,000	80,000	NOLARO	12,700	0.04330	0.0900	0	168.5	3,612	0	--
	5,000						1,702	153.0	3,374	5,298	476
h = 10,000 ft P = 1,000 lb	S.L.						4,950	141.1	2,930	11,274	1,015
	10,000	133,000	AMGAL	14,800	0.03125	0.22000	0	170.4	6,375	0	--
	5,000						1,193	161.6	5,281	5,245	1,132
	S.L.						3,253	152.7	4,187	10,559	2,325
BJ	20,000	500,000	NOLARO	47,814	0.08281	0.32427	0	166.7	15,494	0	--
	15,000						1,646	155.9	13,897	5,272	1,710
h = 20,000 ft P = 600 lb	10,000						4,495	143.7	12,171	11,039	3,580
	5,000						9,106	130.2	10,702	17,856	5,790
	S.L.						17,231	112.0	9,107	27,436	8,900

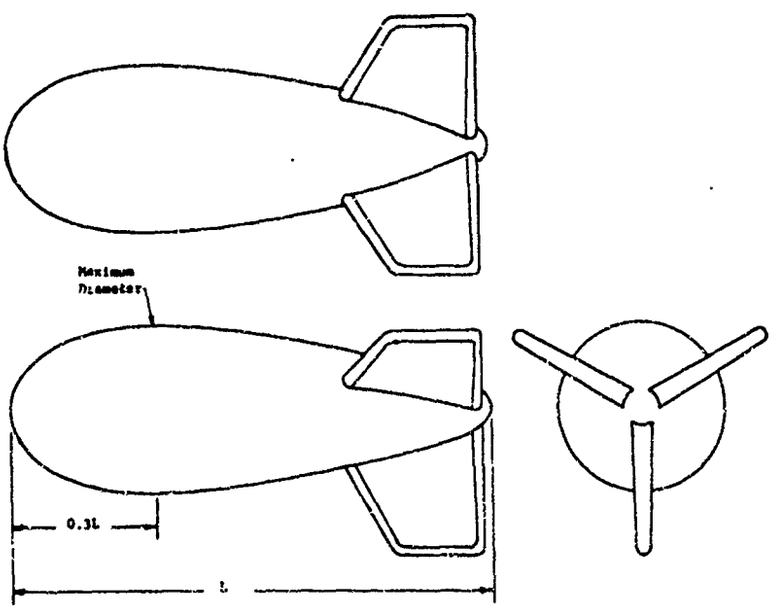

Figure 3. GAC No. 1649 Balloon Configuration

SECTION III

PARAMETRIC DESIGN CONDITIONS

In this study, a number of parameters were chosen that would demonstrate how different design conditions would affect the stability of a tethered balloon system. The major parameter was a balloon type. The BJ Balloon, Vee-Balloon, and the GAC 1649 Balloon are compared with variations in trim angle, waterline location of the bridle apex, and free-static lift. In addition to these parameters, the BJ balloon was studied extensively.

One BJ Balloon was designed for operation at 5000 feet and another at 20,000 feet. An Amgal tether was used with a balloon trim angle-of-attack variation. The tail size on the BJ Balloon was both decreased and increased in area. The steady-state wind profile was reduced in discrete increments. To show the effect of stability during ascent and retrieval, the BJ Balloon designed for 10,000 feet was flown at lower altitudes by shortening the tether length. Three separate payload locations were investigated. Lastly, it was assumed that the winch was positioned at 5000 feet altitude.

A further investigation on the Vee-Balloon was vertical tail sizes on the top and bottom of the hulls.

All of the above variations were studied in both the longitudinal and lateral degrees-of-freedom. Tables III and IV tabulate all of the conditions investigated by run number.

Tables III and IV also contain the remaining input data used for each run as numbered in the first column. Note that it is necessary to use one row in Table III, Sheet 1 or Table IV, Sheet 1 and the corresponding row in Table III, Sheet 2 or Table IV, Sheet 2 to make one longitudinal run and one lateral run for a given system condition. The variable headings at the top of each column are defined in the nomenclature of Appendix B.

Table V is the standard operational wind profile (100%) used in all of the runs. Runs 15 to 19 used smaller percentages of these values as indicated in Table III. Table VI is a list of the moment, lift, and drag coefficients versus angle-of-attack used for each balloon. The only variation in these curves occurred in runs 13 and 14 when a small (81% of nominal area) and large (144% area) tail were studied on the BJ Balloon. These coefficients were changed from the test values by subtracting the calculated effect of the standard tail and adding the calculated effect of the new tail size. The drag change is mainly due to induced drag. The following equations were used:

Table III. Design Parameters and Computer Input Data for BJ Balloon (Sheet 1)

Run No.	Balloon Type	Balloon Altitude (ft)	Tether Type	Tail Area Conf	Free Static Lift (%)	α_T (°)	Water-Line	Volume $(ft)^3$	Wind Profile (%)	LONGITUDINAL RJM (ft)	LONGITUDINAL RKM (ft)	LATERAL RJM (ft)	LATERAL RKM (ft)
1	BJ	10,000	NOLARO	Nominal	9.3	8.5	0.5L	60 K	100	19.6	-44.6	20.5	-42.6
2						6.4	0.5L			21.4	-44.6	22.3	-42.6
3						10.5	0.5L			17.9	-44.6	18.8	-42 6
4						8.5	0.4L			19.1	-35.4	20.0	-33.4
5					9.3	8.4	0.6L			20.2	-53.8	21.1	-51.8
6					4.7	9.7	0.5L			19.6	-44.6	20.5	-42.6
7		10,000			0.0	11.0		60 K		19.6	-44.6	20.5	-42.6
8		5,000			10.4	5.3		46 K		16.9	-41.1	17.8	-39.1
9		20,000	NOLARO		6.4	8.4		500 K		45.6	-89.7	47.2	-85.8
10		10,000	ANSAL		8.2	8.3		75 K		20.7	-48.4	21.7	-45.9
11			ANSAL		8.2	6.3		75 K		22.6	-48.4	23.6	-45.9
12			ANSAL	Nominal	8.2	10.3		75 K		18.9	-48.4	19.9	-45.9
13			NOLARO	81%		11.0		60 K		19.5	-44.6	18.3	-43.2
14				144%		7.4			100	21.5	-44.4	24.7	-41 3
15				Nominal	9.3	6.7			80	19.6	-44.6	20.5	-42 6
16						4.6			60	19.6	-44.6	20.5	-42.6
17						3.0			40	19.6	-44.6	20.5	-42.6
18						1.5			20	19.6	-44.6	20.5	-42 6
19		10,000				0.9			0.1	19.6	-44.6	20.5	-42.6
20		7,000				9.8			100	21.8	-44.3	22.7	-42.3
21		4,000				8.8				21.4	-44.2	22.3	-42.2
22		1,000				7.3				20.9	-44.1	21.8	-42.2
23		10,000				13.0				18.0	-42.1	18.8	-40.4
24						8.5				24.0	-42.1	24 6	-40.4
25						10.7				17.7	-38.0	18.5	-36.3
26						8.5				20.7	-38.0	21.5	-36.3
27	BJ	10,000	NOLARO	Nominal	9.3	8.5	0.5L	60 K	100	19.6	-44.6	20.5	-42.6

Run No.	RJA (ft)	RKA (ft)	RJG (ft)	RKG (ft)	RJB (ft)	RKB (ft)	WB (lb)	LS (lb)	MPL Slugs	WTC (lb)	IXB $Slug-Ft^2$	MAL Slug	MAV Slug
1	6.7	-46.0	23.7	-42.3	12.6	-45.4	2,157	3,942	31.06	708	116,000	15.7	110
2	8.5	-46.0	25.5	-42.3	14.4	-45.4	2,157						
3	5.0	-46.0	22.0	-42.3	10.9	-45.4	2,157						
4	6.2	-36.8	23.2	-33.1	12.1	-36.2	2,157						
5	7.3	-55.2	24.3	-51.5	13.2	-54.6	2,157						
6	6.7	-46.0	23.7	-42.3	12.6	-45.4	2,278						
7	6.7	-46.0	23.7	-42.3	12.6	-45.4	2,399	3,942	31.06	708	116,000	15.7	110
8	4.9	-42.1	21.7	-39.2	10.3	-4' 5	1,627	3,526	46.58	183	75,000	12.0	86
9	19.9	-93.3	51.4	-84.7	31.9	-92.0	15,624	23,715	18.63	8,900	3,204,000	95.0	666
10	6.8	-49.6	25.1	-45.6	13.2	-48.9	2,665	4,928	31.06	1,128	167,000	20.0	138
11	8.7	-49.6	27.0	-45.6	15.1	-48.9	2,665	4,928		1,128	167,000	20.0	138
12	5.0	-49.6	23.3	-45.6	11.4	-48.9	2,665	4,928		1,128	167,000	20.0	138
13	8.9	-46.0	23.8	-42.5	13.4	-45.6	1,970	3,811		708	104,100	14.7	103
14	4.5		25.4	-42.0	13.3	-44.9	2,680	4,340		708	142,000	18.8	131
15	6.7		23.7	-42.3	12.6	-45.4	2,157	3,942		710	116,000	15.7	110
16			23.7	-42.3			2,157	3,942		582			
17			23.7	-42.3			2,157	3,942		602			
18			23.7	-42.3			2,157	3,942		561			
19			23.7	-42.3			2,157	3,942		558	116,000	15.7	110
20			25.2	-41.7			2,476	4,320		439	127,400	28.3	198
21			23.8	-41.4			2,877	4,740		234	142,400	31.7	222
22			22.5	-41.5			3,358	5,190	31.06	54	159,400	35 5	249
23			19.1	-37.8	12.6		3,157	3,942	0.0	708	124,300	15.7	110
24	12.7		25.1	-37.8	18.6		3,157	3,942	0.0	708	124,300	15.7	110
25	6.7		18.3	-28.9	12.6		3,157	3,942	0.0	708	171,300	15.7	110
26	9.7		21.3	-28.0	15.6		3,157	3,942	0.0	708	171,300	15.7	110
27	6.7	-46.0	23.7	-42.3	12.6	-45.4	2,157	3,942	31.06	314	116,000	15.7	110

Table III. Design Parameters and Computer Input Data for BJ Balloon (Sheet 2)

Run No.	SB $(ft)^3$	DB (ft)	CDC	DC (ft)	TBTH (ft)	CMTDB RAD^{-1}	CLTDB RAD^{-1}	ISB $slug\text{-}ft^2$	IYB $slug\text{-}ft^2$	IYSB $slug\text{-}ft^2$	MAS slug	CYPSDB RAD^{-1}	CYPHDR RAD^{-1}
1	1,533	39.15	1.1	0.0342	12,639	-2.01	1.58	119,000	26,000	12,300	115	1.79	0.142
2													
3													
4													
5													
6													
7	1,533	39.15		0.0342	12,639			119,000	26,000	12,500	115		
8	1,264	35.83		0.0268	5,692			75,300	17,000	8,200	86		
9	6,300	79.37		0.0828	27,436			3,374,000	771,000	295,000	690		
10	1,778	42.17		0.0208	11,305			172,000	40,000	18,000	143		
11	1,778	42.17		0.0208	11,305			177,000	40,000	18,000	143		
12	1,778	42.17		0.0208	11,305	-2.01	1.68	172,000	40,000	18,300	143	1.79	0.142
13	1,533	39.15		0.0342	12,639	-1.58	1.25	106,400	17,600	10,200	107	1.55	0.104
14					12,639	-2.61	2.14	145,000	53,900	18,600	146	2.27	0.224
15					12,680	-2.01	1.68	119,000	26,000	12,500	115	1.79	0.142
16					12,170								
17					10,740								
18					10,020								
19					9,960			119,000	26,000	12,500	115		
20					7,840			131,000	32,800	12,800	203		
21					4,170			146,800	35,800	13,400	227		
22					970			164,700	39,300	14,500	255		
23					12,639			116,200	27,700	7,800	115		
24								116,200	27,700	7,800	115		
25								122,700	68,300	4,000	115		
26					12,639			122,700	68,300	4,000	115		
27	1,533	39.15	1.1	0.0342	5,600	-2.01	1.68	119,000	26,000	12,500	115	1.79	0.142

Run No.	CHPSDB RAD^{-1}	CHPHDB RAD^{-1}	CLPSDB RAD^{-1}	CLPHDB RAD^{-1}	CYPSB (-CYVB) RAD^{-1}	CHPSB (-CHVB) RAD^{-1}	CLPSB (-CLVB) RAD^{-1}	CMC	CDC1	CDC2	CLC
1	-2.31	-0.122	-0.347	-0.327	2.08	-0.105	-0.351	0.0	0.0	0.0	0.0
2											
3											
4											
5											
6											
7											
8											
9											
10											
11											
12	-2.31	-0.122	-0.347	-0.327	2.08	-0.105	-0.351	0.0	0.0	0.0	0.0
13	-2.08	-0.096	-0.280	-0.210	1.85	0.08	-0.260	0.270	-0.125	0.123	-0.30
14	-2.67	-0.170	-0.484	-0.609	2.65	-0.498	-0.553	-0.405	-0.125	0.127	0.49
15	-2.31	-0.122	-0.347	-0.327	2.08	-0.105	-0.351	0.0	0.0	0.0	0.0
16											
17											
18											
19											
20											
21											
22											
23											
24											
25											
26											
27	-2.31	-0.122	-0.347	-0.327	2.08	-0.105	-0.351	0.0	0.0	0.0	0.0

Table IV. Design Parameters and Computer Input Data for VEE and GAC 1649 Balloons (Sheet 1)

Run No.	Balloon Type	Balloon Altitude (ft)	Tether Type	Tail Area Conf	Free Static Lift (%)	σ_T (°)	Water-Line	Volume $(ft)^3$	Wind Profile (%)	LONGITUDINAL RJM (ft)	LONGITUDINAL RKM (ft)	LATERAL RJM (ft)	LATERAL RKM (ft)
28	VEE	10,000	NOLARO	100%	9.4	7.0	0.35L	80,000	100	21.3	-37.5	13.7	-36.7
29						5.0	0.35L			24.2	-37.5	16.6	-36.7
30						9.1	0.35L			18.6	-37.5	11.0	-36.7
31						6.9	0.20L			20.8	-32.0	13.2	-31.2
32					9.4	7.0	0.40L			21.8	-43.0	14.2	-42.2
33					4.7	7.3	0.35L			21.3	-37.5	13.7	-36.7
34				100%	0.0	7.7				21.3	-37.5	13.7	-36.7
35				200%	-	7.2				21.4	-37.4	13.8	-36.0
36				300%	-	7.5				21.6	-37.3	14.0	-35.4
37				100+100%	-	7.3				21.5	-37.6	13.9	-37.3
38	VEE			200+200%	-	7.9				21.7	-37.6	14.1	-37.5
39	VEE	10,000	NOLARO	200+300%	-	8.4	0.35L	80,000	100	22.0	-37.6	14.4	-37.6
40	1649 A/T.F.	10,000	NOLARO	100%	9.5	7.9	0.5L	80,000	100	18.3	-56.6	16.2	-55.0
41						6.0	0.5L			22.5	-56.6	20.4	-55.0
42						10.0	0.5L			14.6	-56.6	12.5	-55.0
43						7.9	0.6L			18.1	-45.1	16.0	-43.5
44					9.5	8.0	0.5L			18.6	-68.1	16.5	-66.5
45					4.8	8.4	0.5L			18.3	-56.6	16.2	-55.0
46	1649 W/T.F.	10,000	NOLARO	100%	0.0	8.4	0.5L	80,000	100	18.3	-56.6	16.2	-55.0

Run No.	RJA (ft)	RKA (ft)	RJG (ft)	RKG (ft)	RJB (ft)	RKB (ft)	WB (lb)	LS (lb)	MPL Slugs	WTC (lb)	IXB Slug-Ft^2	MAL Slug	MAV Slug
28	9.4	-38.6	17.0	-34.5	11.7	-38.5	2,334	4,822	31.06	1,260	166,300	47.0	189.0
29	12.3	-38.6	19.9	-34.5	14.6	-38.5							
30	6.7	-38.6	14.3	-34.5	9.0	-38.5							
31	8.9	-33.1	16.5	-29.0	11.2	-33.0							
32	9.9	-44.1	17.5	-40.0	12.2	-44.0	2,334						
33	9.4	-38.6	17.0	-34.5	11.7	-38.5	2,508						
34			17.0	-34.5			2,682	4,822			166,300		
35			17.5	-34.3			2,408	4,832			167,900		
36			18.1	-33.9			2,476	4,842			170,000		
37			17.8	-35.1			2,408	4,832			168,000		
38			18.8	-35.3			2,550	4,852			172,300		
39	9.4	-38.6	19.9	-35.4	11.7	-38.5	2,680	4,872	31.06	1,260	176,000	47.0	189.0
40	-0.5	-57.5	18.4	-54.7	4.7	-57.5	2,788	5,016	31.06	1,015	249,400	14.7	169.4
41	3.7	-57.5	23.6	-54.7	8.7	-57.5							
42	-4.2	-57.5	14.7	-54.7	0.8	-57.5							
43	-0.7	-46.0	18.2	-43.2	4.5	-46.0							
44	-0.2	-69.0	18.7	-66.2	4.8	-69.0	2,788						
45	-0.5	-57.5	18.4	-54.7	4.7	-57.5	2,952						
46	-0.5	-57.5	18.4	-54.7	4.7	-57.5	3,116	5,016	31.06	1,015	249,400	14.7	169.4

Table IV. Design Parameters and Computer Input Data for VEE and GAC 1649 Balloons (Sheet 2)

Run No.	SB $(ft)^3$	DB (ft)	CDC	DC (ft)	TBTM (ft)	CMTDB RAD^{-1}	CLTDB RAD^{-1}	IEB $Slug\text{-}ft^2$	IYB $Slug\text{-}ft^2$	IYEB $Slug\text{-}ft^2$	MAS Slug	CYPSDB RAD^{-1}	CYPHDB RAD^{-1}
28	1836.7	43.09	1.1	0.0488	11,060	-2.483	2.495	173,300	84,000	3,900	127	0.439	0.054
29													
30													
31													
32													
33													
34								173,300	84,000	3,900	127	0.439	0.054
35								187,000	86,200	7,500	135	0.718	0.108
36								198,700	88,300	10,700	143	0.997	0.162
37								191,600	86,300	400	135	0.718	0.0
38								217,900	90,500	1,000	151	1.276	0.0
39	1856.7	43.09	1.1	0.0488	11,060	-2.483	2.495	238,400	94,600	1,400	166	1.834	0.0
40	1836.7	43.09	1.1	0.0433	11,274	-2.07	1.49	226,800	106,500	10,500	154.4	1.94	0.0
41													
42													
43													
44													
45													
46	1856.7	43.09	1.1	0.0433	11,274	-2.07	1.49	228,800	106,500	10,500	154.4	1.94	0.0

Run No.	CNPSDB RAD^{-1}	CNPHDB RAD^{-1}	CLPSDC RAD^{-1}	CLPHDB RAD^{-1}	CYPSB (-CYVB) RAD^{-1}	CNPSB (-CNVB) RAD^{-1}	CLPSB (-CLVB) RAD^{-1}	CNC	CDC1	CDC2	CLC
28	-0.482	-0.0505	-0.0212	-0.3758	0.857	-0.004	-0.0578	0.0	0.0	0.0	0.0
29											
30											
31											
32											
33											
34	-0.487	-0.0505	-0.0212	-0.3758	0.857	-0.004	-0.0578				
35	-0.784	-0.101	-0.0494	-0.393	1.439	-0.441	-0.135				
36	-1.066	-0.1515	-0.0810	-0.412	2.021	-0.878	-0.220				
37	-0.784	0.0	-0.0	-0.389	1.439	-0.441	0.0				
38	-1.388	0.0	0.0	-0.427	2.603	-1.315	0.0				
39	-1.992	0.0	0.0	-0.461	3.767	-2.189	0.0	0.0	0.0	0.0	0.0
40	-2.07	0.0	-0.298	-0.508	1.9	-0.22	-0.374	0.0	0.0	0.0	0.0
41											
42											
43											
44											
45											
46	-2.07	0.0	-0.298	-0.508	1.9	-0.22	-0.374	0.0	0.0	0.0	0.0

$$C_{mB}(I) = C_{mBO}(I) + C_{mC}\ \alpha(I) \quad (1)$$

$$C_{LB}(I) = C_{LBO}(I) + C_{LC}\ \alpha(I) \quad (2)$$

$$C_{DB}(I) = C_{DBO}(I) + C_{DC1}\ C_{LBO}(I)^2 + C_{DC2}\ C_{LB}(I)^2 \quad (3)$$

where the "0" subscript indicates the nominal value and C_{mC}, C_{LC}, C_{DC1}, and C_{DC2} are given in Table III. (I) indicates a specific angle of attack.

Table V. Standard Operational Wind Profile

Altitude (feet)	0.0	5000	10,000	20,000	25,000
Wind Velocity (ft/sec)	16.9	52.3	67.5	91.1	99.9

Table VI. Moment, Lift, and Drag Coefficients vs Angle-of-Attack

Angle-of-Attack (Deg.)		-5	0	5	10	12	15	20	25
BJ	C_m	0.0137	0.0103	-0.0005	0.0044	0.0050	-0.0075	-0.0410	-0.0780
	C_L	-0.1100	0.0063	0.1368	0.2514	0.2991	0.3710	0.5100	0.6200
	C_D	0.1100	0.0764	0.0865	0.1133	0.1279	0.1527	0.2200	0.3000
Vee	C_m	-0.010	0.030	0.103	0.110	0.113	0.102	0.090	0.022
	C_L	-0.400	0.0	0.400	0.800	0.970	1.210	1.610	2.030
	C_D	0.150	0.160	0.170	0.230	0.265	0.340	0.510	0.740
GAC	C_m	0.074	-0.010	-0.074	-0.120	-0.170	-0.190	-0.310	-0.460
	C_L	-0.240	0.0	0.210	0.380	0.450	0.560	0.830	1.080
	C_D	0.105	0.085	0.090	0.100	0.110	0.140	0.230	0.390

SECTION IV

GENERAL STABILITY THEORY

The purpose of this study is to analyze the stability of a tethered balloon around its equilibrium configuration (References 3, 4, and 5). The equilibrium configuration can be defined as that position which demands that the summation of all applied moments equals zero. The equilibrium is said to be stable if, for any small disturbance, the system ultimately returns to its equilibrium conditions. Two types of stability are of interest. In the first (statically stable), a small displacement of the system will create forces which tend to return the system to its equilibrium position. The second (dynamically stable) produces a motion which eventually restores equilibrium. If the motion is periodic, it is characterized by a damped frequency and a damping ratio. Similar definitions apply for statically and dynamically unstable motions. A third possibility is for the system to be neutrally stable during which the motion neither diverges nor converges.

It was necessary during this study to develop techniques to investigate and understand the stability of the system. To this end, characteristic equations are derived. Appendix A is a complete derivation of the equations needed for the establishment of the characteristic equations. The general approach is as follows:

(1) Derive the nonlinear equations of motion in three dimensions for each degree-of-freedom

(2) Assume the motion is near equilibrium so that the equations can be linearized and separated into a longitudinal motion and a lateral motion.

(3) Laplace transform the linear equations from the time domain to the "S" doman assuming that the initial conditions are zero. This establishes a matrix equation of the following form:

$$\left[A\right] \quad \left\{X\ (S)\right\} \quad = \quad \left\{0\right\} \tag{1}$$

where $\left\{X\ (S)\right\}$ is the eigenvector and $\left[A\right]$ is a square matrix whose elements are quadratics in S containing the physical properties of the system.

(4) Expand the determinant of $\left[A\right]$ such that the characteristics polynominal is obtained.

Each root of the characteristic equation represents a term in the general solution of the form, $A_i e^{S_i t}$, where S_i is the "i"th root and A_i is an amplitude, dependent on the initial conditions of the system. Both real and complex roots may appear where the complex roots occur in conjugate pairs. In general for "n" degrees of freedom, the characteristic equation will yield "2n" roots. Each pair of complex conjugate roots represents one oscillatory motion, while each real root represents one aperiodic motion.

First consider an oscillatory system. This motion is characterized by two roots of the form $S_i = X \pm i\,Y$, where X and Y are real numbers and $i = \sqrt{-1}$. Several important quantities can be found from the root. The natural frequency associated with this motion is $\omega_n = \sqrt{X^2 + Y^2}$. The damping ratio is $\zeta = \frac{-X}{\omega_n}$. The damped frequency is $\omega_d = \omega_n \sqrt{1 - \zeta^2} = Y$. It is also of interest to know the time to half amplitude for a stable root or the time to double amplitude for an unstable root. This quantity can easily be found by considering one oscillatory motion. The general solution for free vibration is

$$Z = Ce^{-\zeta \omega_n t} \sin (\omega_d t + \phi) \tag{2}$$

where

ϕ is the phase angle dependent upon initial conditions

C is a constant dependent upon initial conditions

It is the factor $e^{-\zeta \omega_n t}$ that establishes the nature of divergent or convergent part of the solution. If the system is convergent ζ will be positive and the half amplitude time can be found by comparing the ratio of the magnitudes of the factor $e^{-\zeta \omega_n t}$ at t_2 and t_1.

$$\frac{Z_2}{Z_1} = e^{-\zeta \omega_n (t_2 - t_1)} = \frac{1}{2} \tag{3}$$

$$\ell n \frac{1}{2} = -\zeta \omega_n (t_2 - t_1) \tag{4}$$

Finally, $$t_2 - t_1 = \frac{0.693}{\zeta \omega_n} \tag{5}$$

A similar procedure will lead to the same expression for time to double amplitude for a diverging motion (ζ is negative). The time to double amplitude is an important quantity for a diverging motion because it essentially gives a speed to the divergence. A short time to double amplitude is of more concern than a slowly diverging oscillation.

The second possibility is an aperiodic motion given by the expression

$$Z = Ce^{Xt} \tag{6}$$

where X is the real part of one root and the imaginary part (Y) is zero

If X is negative, Z approaches zero as time increases indefinitely and the motion is said to be overdamped. Like the oscillatory motion, roots which give overdamped motions will also occur in pairs. However, unlike the complex conjugate roots which result in one oscillatory motion, each real root is a distinct motion. Therefore, it is possible for a "n" degree-of-freedom system to have "2n" distinct motions if the system is so heavily damped that all the roots to the characteristic equation are real. Equation (5) also applies to aperiodic motion.

There is a third possible motion which is a borderline case. If two roots are real and equal, the system is said to be critically damped. The motion will be aperiodic and both roots will give the same motion.

The general solution to the motion of the system is a linear combination of all the motions defined by the roots to the characteristic equation. Associated with each root is a mode shape which gives the relative amplitudes of each degree-of-freedom when the system is responding to one particular root. It is of interest to establish these mode shapes so that each stability curve can be associated with a definite motion of the whole system. For example, one mode shape may show that the pitching motion of the balloon is very large compared to the motion of the tether. To find the mode shapes, the following procedure is used (Reference 6). The characteristic equation is found by expanding the determinant of $[A]$, equation (1) and setting it equal to zero. If one of the roots is substituted into equation (1), the equation becomes

$$\left[A_{ij}\right]_{n,\,n} \left\{X_i\right\}_n = 0 \tag{7}$$

Because $|A_{ij}| = 0$, the X_i's are linearly dependent and the rank of $\left[A_{ij}\right]_{n,n}$ is $n - 1$.

In order to make the X_i's linearly independent, eliminate the first row and the equation becomes:

$$\left[A_{ij}\right]_{n-1,\,n} \left\{X_i\right\}_n = 0 \tag{8}$$

Equation (8) can be expanded as follows:

$$\left[A_{ij}\right]_{n-1,n} \left\{X_i\right\}_n = \left[A_{ij}\right]_{n-1,n-1} \left\{X_i\right\}_{n-1} + \left\{A_{i1}\right\}_{n-1,\,1} (X_1) = 0 \tag{9}$$

or

$$\left[A_{ij}\right]_{n-1,\,n-1} \left\{\frac{X_i}{X_1}\right\}_{n-1} = - \left\{A_{i1}\right\}_{n-1,\,1} \tag{10}$$

The elements of the $[A_{ij}]$ matrix are complex and the eigenvector will also be complex. With this in mind, rewrite equation (10) assuming $X_1 = 1 + 0i$. Thus, the mode shapes will be normalized.

$$[G_{ij} + i\,\bar{G}_{ij}]_{n-1,\,n-1} \{r_i + i\,S_i\}_{n-1} = -\{H_{i1} + i\,\bar{H}_{i1}\}_{n-1,\,1} \tag{11}$$

or

$$[G_{ij}]\{r_i\} - [\bar{G}_{ij}]\{S_i\} + i\,[G_{ij}]\{S_i\} + i[\bar{G}_{ij}]\{r_i\} = -\{H_{i1}\} - i\{\bar{H}_{i1}\} \tag{12}$$

where G_{ij}, H_{ij} and r_i are the real parts of the complex elements of the matrices and $\bar{G}_{ij}$, $\bar{H}_{ij}$ and S_i are the imaginary parts of complex elements. Equation (12) is rewritten in partitioned form as follows:

$$\begin{bmatrix} [G_{ij}] & [-\bar{G}_{ij}] \\ [\bar{G}_{ij}] & [G_{ij}] \end{bmatrix} \begin{Bmatrix} \{r_i\} \\ \{S_i\} \end{Bmatrix} = \begin{Bmatrix} -\{H_{i1}\} \\ -\{\bar{H}_{i1}\} \end{Bmatrix} \tag{13}$$

All elements in equation (13) are real and the solution of the eigenvectors r_i and S_i will give the mode shape in component form. The matrix equation (13) is a set of linear real algebraic equations which can be solved by Crout reduction. The eigenvectors which are solutions to (7) are finally:

$$\{X_i\} = \begin{Bmatrix} 1 \\ r_1 + i\,S_1 \\ r_2 + i\,S_2 \\ \cdots \\ r_{n-1} + i\,S_{n-1} \end{Bmatrix} \tag{14}$$

In an undamped system only the relative amplitudes are arbitrary; but in a damped system both the amplitude and the phase angle are arbitrary. It has already been stated that the eigenvectors have been normalized by assuming that $X_1 = 1$. The magnitude and phase angle of the other elements are:

$$|X_i| = [r_i^2 + S_i^2]^{1/2} \tag{15}$$

$$\phi_i = \tan^{-1}\left(\frac{S_i}{r_i}\right) \tag{16}$$

Since each complex element may possess a different phase angle, the corresponding degree-of-freedom may reach its maximum at a different time than the remaining coordinates. However, the motion is synchronous and the cyclic pattern will repeat itself with the maximum excursions decaying exponentially if the system is stable. The main interest in this report is the relative amplitudes associated with each mode and more will be said about this when discussing the results.

SECTION V

RESULTS AND CONCLUSIONS

1. SUMMARY

Mathematical tools have been developed to investigate dynamic stability of tethered balloons. The model for the tethered balloon system consists of the streamlined balloon and a tether made up of three discrete links. This system then has four longitudinal degrees of freedom (balloon pitch and three tether link pitchs), and five lateral degrees of freedom (balloon yaw and roll), and three tether link yaws i.e. lateral rotation).

In general, the tethered systems have five longitudinal modes of motion, three oscillatory, and two aperiodic. Some conditions investigated have four oscillatory modes. Generally, the modes of motion are similar for the three balloon types. The first mode is a low frequency motion with strongly coupled balloon and tether link pitching. Under many conditions examined this long period mode is near neutrally stable for small oscillations about equilibrium which are assumed in the analysis. The second and third modes are balloon pitching modes and are moderately damped. For the tethered systems at design altitude, the fourth mode is an overdamped coupled balloon and tether pitching mode and the fifth mode represents an overdamped motion in balloon pitch.

Considering the BJ balloon at 10,000 feet, the longitudinal dynamic characteristics of the tethered system are not changed in a major manner as a result of angle-of-attack trim changes, location of the confluence point below the hull centerline, free static lift, payload location (when the balloon is retrimmed to nominal angle of attack) or tail size. The first mode becomes slightly stable with the largest tails, with the payload located on the belly, and for a system with AMGAL tether. As the system designed for 10,000 feet is brought to lower altitudes, the second and third modes become less damped, and the fourth and fifth modes become an oscillatory mode with less stability. Generally the stability of the system designed for 10,000 feet reduces as the operational wind is reduced. An exception is the first mode where stability improves at intermediate wind speeds.

Tethered systems with BJ balloons designed for the three altitudes of 5000, 10,000 and 20,000 feet show significant increase in frequency for the second and third modes for the lower altitude systems.

The longitudinal stability characteristics of tethered systems with the other two balloon types have some notable differences as compared to the BJ balloon system. For the Vee-balloon, at low angle of attack, the first mode has an aperiodic divergence at a trim angle of 5 degrees. At higher trim angles of attack, the unstable characteristic of this mode is reduced. The GAC No. 1649 single hull balloon exhibits a more stable first mode as compared to the other two balloon types.

Turning to the lateral degrees of freedom, the lateral modes of motion have a different character for each of the three balloon types. The BJ balloon system has two oscillatory and six overdamped aperiodic modes, the Vee-balloon system has four oscillatory and two overdamped aperiodic modes, and the GAC No. 1649 single hull balloon system has three oscillatory and four overdamped aperiodic modes. The first mode is a low frequency neutrally damped motion with strongly coupled balloon yaw and lateral tether link rotation. The higher modes are various combinations of the lateral degrees of freedom including coupled balloon yaw and roll modes, balloon roll modes and coupled balloon yaw and roll and lateral link rotations.

Design parameter changes on the BJ tethered balloon system designed for 10,000 feet altitude resulted in no major effects to lateral dynamic stability characteristics. As would be expected, larger tail sizes provided greater damping of the balloon modes. During retrieval of the 10,000 foot altitude BJ balloon design, balloon damping was reduced at the lower altitude and frequency of the balloon tether modes was increased. The first mode became unstable at 1000 feet altitude. For BJ balloons designed for various altitudes, the oscillatory modes show greater damped frequency and less damping at the lower altitudes.

The lateral dynamic characteristics of the Vee-balloon are notably different in that four oscillatory modes exist. The second, third and fourth balloon coupled yaw roll modes are oscillatory and well damped. Tail size affects the frequency and damping of these modes although all tail sizes do provide a stable behavior. The lateral dynamic characteristics of the GAC No. 1649 single hull balloon are similar to the BJ balloon although an additional oscillatory mode exists.

2. LONGITUDINAL MODES OF MOTION

Before discussing the stability characteristics as given in complex plot form, it is advantageous to study the mode shapes of the different roots to the characteristic equations. The mathematical approach has been summarized in Section IV. Figures 4 thru 8 are typical mode shape plots for the longitudinal motions of the tethered balloon (normalized on θ); Figures 9 thru 14 are mode shapes for the lateral motions (normalized on ψ). Each mode shape has a circled number associated with it for identification purposes. The mode numbering sequence starts with the oscillatory mode with lowest natural frequency and numbers the oscillatory modes in the order of ascending natural frequency followed by aperiodic modes in ascending natural frequency. The mode shapes are presented only as a means of identifying the type of motion associated with a stability root. In the longitudinal plots, each vector from the origin is labeled as θ ξ_1, ξ_2, or ξ_3 which identify the longitudinal degrees-of-freedom where ξ_1 is the link rotation closest to the ground. θ is the pitch angle of the balloon and ξ_i is the pitch angle of the "i"th link. For the lateral plots the vectors are labeled ψ, ϕ, σ_1, σ_2, σ_3 and identify balloon yaw and roll and tethered link yaw angles (lateral rotations) where σ_1 is the link rotation closest to the ground.

Figure 4 is the mode shapes for the nominal tethered balloon in the longitudinal plane. The first mode is seen to respond strongly to moderately in all four degrees-of-freedom with each degree-of-freedom reaching a maximum at different times. This motion seems to be a whipping phenomenon. The second and third modes are primarily balloon pitching modes with secondary response in the tether. The fourth mode shows significant response in all four degrees-of-freedom but is strongest in the balloon's pitching. Mode(5)is entirely a balloon pitching mode.

Figure 5 is presented to show how the mode shapes change at a lower wind velocity profile. The first mode shows a weaker response in ξ_2 and ξ_3 and stronger response in ξ_1. The second to fifth modes show quite a different response than that shown in Figure 4. The second mode has become strongly to moderately responsive to all degrees-of-freedom while the third mode is now responsive to only the balloon's pitching motion. The fourth mode is strongly responsive to ξ_1 and decreasingly responsive to ξ_2, ξ_3, and θ. In mode(5)all degrees-of-freedom except $\xi_2$are equally responsive.

Figure 6 shows the mode shapes for the system when the BJ Balloon has been retrieved to an altitude of 1000 feet. First, notice that there are only four mode shapes associated with the balloon's motion because the two overdamped modes (4 and 5 in Figure 4) have become one oscillatory mode. Mode(1)is primarily a tether mode with secondary response in the balloon. Note that all three link angles have the same phase angle. Mode(2)is a balloon pitching mode only, while

mode (4) is completely a tether motion mode. The third mode is primarily a response to ξ_1 and ξ_3 with a very light response from θ and no response from ξ_2 .

Figure 7 is the mode shapes for the nominal VEE tethered balloon. All mode shapes are very similar to the modes shown in Figure 4 and are not discussed further.

Figure 8 is the mode shapes for the nominal GAC single hull balloon. The first mode is seen to have a strong response in the tether degrees-of-freedom and a moderate response in the balloon's pitching degree-of-freedom. The second mode is primarily a balloon pitching motion with weak response from the tether. Mode (3) is entirely a balloon pitching mode. Modes (4) and (5) are primarily balloon pitching modes with weak to moderate response from the tether degrees-of-freedom.

3. LATERAL MODES OF MOTION

The first lateral mode shapes shown in Figure 9 are for the nominal BJ tethered balloon. The first mode is oscillatory with the greatest response being in balloon yaw (ψ) and moderate response in balloon roll (ϕ) and link yaw (σ_i). The second oscillatory mode is primarily a balloon roll mode with secondary motion in balloon yaw. Modes (3), (4), and (5) are strong overdamped tetner yaw modes with small to moderate response in balloon yaw and roll degrees-of-freedom. Modes (6) and (7) are balloon roll modes with weak response in balloon yaw and tether yaw. The last mode, (8), is a coupled balloon yaw-roll mode.

Figure 10 presents the lateral mode shapes for the nominal BJ tethered balloon under a 20% wind profile. It can be seen that the character of the motions has changed significantly from the standard operational wind conditions (Figure 9). The first mode is primarily a balloon yaw mode with a weak response in σ_1. The second mode is a coupled balloon-tether mode with the strongest response in balloon yaw. Mode (3) is also a coupled balloon-tether mode with stronger tether responses than in mode (2). Mode (4) is a balloon roll mode with secondary response in balloon yaw. Modes (5) and (6) are overdamped balloon yaw modes with weak response in balloon roll.

Figure 11 shows the lateral mode shapes for the nominal BJ tethered balloon when it has been retrieved to 1000 ft. Again the character of the motions has changed substantially from the design altitude (10,000 ft). There are 6 mode shapes compared to 8 for the design altitude. Mode (1) is primarily a balloon yaw mode with moderate response in balloon roll and in the tether degrees-of-freedom. Mode (2) is a balloon roll mode with light response in balloon yaw. In modes (3) and (4), the tether yaw motion are predominant. Note: Modes (3) and (4) are oscillatory but the imaginary components of the eigenvector (mode shapes) are very small compared to the real parts. Mode (5) is an overdamped balloon mode with moderate coupling in tether yaw. Mode (6) is an overdamped balloon yaw mode with lesser response in balloon roll.

Figure 12 is the mode shapes for the nominal VEE tethered balloon in the lateral degrees-of-freedom. The first mode is a balloon yaw mode with light to moderate response in tether yaw and balloon roll. Modes (2) and (3) are primarily balloon roll modes with moderate response in balloon yaw and weak response in the tether. Mode (5) is an overdamped mode with strong to weak response from the tether, moderate response in balloon yaw and no response in balloon roll. In mode (6), balloon roll is the predominant response with lesser response in the tether yaw motion and balloon yaw.

Figure 13 presents the mode shapes for the VEE tethered balloon in the lateral degrees-of-freedom with a 300% increase in area of the lower tail fins. Mode (1) is, as usual, a coupled balloon tether motion with greatest response in balloon yaw. Mode (2) is also a coupled mode with good response in all degrees-of-freedom. Modes (3) and (4) are balloon roll modes with lesser responses in balloon yaw. Mode (5) is an overdamped tether yaw mode coupled with balloon yaw. Mode (6) is an overdamped balloon roll mode with moderate response in balloon yaw and tether yaw.

The last mode shape plot (Figure 14) is for the nominal GAC single hull tethered balloon in the lateral degrees of freedom. Modes (1) and (2) are coupled balloon tether modes with balloon yaw being predominant in mode (1) and least responsive in mode (2). Mode (3) is a balloon roll mode with a smaller response in balloon yaw. Mode (4) is a coupled balloon yaw and tether yaw mode with the greatest response in σ_1. In mode (3), the balloon roll is very predominant with small responses in the other degrees-of-freedom. Mode (6) is an overdamped balloon-tether mode with balloon roll having the strongest response. Mode (7) is a coupled balloon yaw-roll mode.

The mode shapes were found for each stability configuration but only the above plots are presented because the other mode shapes are similar to the nominal configurations or to the off-nominal mode shapes presented. When discussing the stability plots, it will be useful to refer back to the mode shapes so that each stability root can be identified as a particular motion. But it must be remembered that the actual motion of the tethered balloon system is a linear combination of all possible mode shapes, and is dependent upon initial conditions and forcing functions.

4. GENERAL STABILITY CHARACTERISTICS

As in the mode shape plots, a circled number is associated with each set of stability roots for easy identification. The stability plots are actually plots of the roots to the characteristics equation in the complex plane. Only the second quadrant of the complex plane is shown because the oscillatory roots are symmetric about the negative real axis. The aperiodic roots are real and therefore lie on the real axis. Stable roots have negative real parts and unstable roots have positive real parts. Since most of the roots are stable, only the second quadrant is shown in detail, although a few roots are also shown in the first quadrant.

5. LONGITUDINAL STABILITY CHARACTERISTICS

The first stability plot (Figure 15) shows the effect of changing the trim angle-of-attack on the BJ tethered balloons on longitudinal stability. The roots corresponding to the first mode are seen to be very slightly unstable and unaffected by trim angle. However, because of the low frequency associated with these roots, the time to double the amplitude of the diverging oscillation is in the order of several 100 seconds. This mode (shown in Figure 4) has already been identified as a whipping-type motion of the whole system. The second and third modes which have been identified as being primarily balloon pitching modes (Figure 4) are significantly affected by the trim angle because the aerodynamics of the balloon is a function of the trim angle. The stability trend in these two modes shows that a higher angle-of-attack increases the damped frequency moderately and changes the damping ratio slightly. Modes (4 and 5)are overdamped modes. Mode (4)shows a response in all degrees-of-freedom (Figure 4) and is unaffected by balloon angle-of-attack change because of the change in aerodynamics.

Figure 16 presents the effect of waterline location of the bridle apex below the balloon. In the figure, "L" is the length of the balloon and waterline is the

distance below the balloon centerline to the confluence of the suspension lines. The first mode (whipping) is unaffected. The second mode shows a moderate increase in damped frequency and a slight increase in damping with an increase in waterline. This is because mode(2)is primarily a balloon pitch mode, and an increase in waterline increases the moment arm which increases the restoring torques on the balloon. The third mode shows only a slight change in damping with increase waterline. The fourth mode is unaffected. The fifth mode, although it remains overdamped, shows a strong tendency to become less damped as the waterline increases.

In Figure 17, the effect of decreasing the free-static lift over a small range is shown to be minor in all modes. The free-static lift can be decreased by pumping air into the ballonets and valving helium.

Figure 18 gives the stability roots for three different size BJ balloons. Each balloon was designed to fly at a specific altitude (5000, 10,000, and 20,000 feet). In the first mode, both the balloons at the highest and lowest altitudes were very slightly stable. The second and third modes show moderate and strong increases respectively in damped frequency, and a slight change and decrease respectively in damping ratio. The higher frequency at lower altitudes is somewhat attributed to a smaller inertia associated with the smaller balloon. The fourth and fifth modes show moderate changes but remain overdamped.

Figure 19 is a parameter study of trim angle-of-attack using an Amgal tether. The results in this figure should be compared to Figure 15. However, because the Amgal tether is heavier, a larger balloon is needed to support it (75,000 ft^3 compared to 60,000 ft^3). The first mode is unaffected by trim angle but becomes slightly stable when the Amgal tether is used compared to the Nolaro tether in Figure 15. The damping ratio ξ is of the order of 0.1 for Amgal tether as compared to -.04 (slightly unstable) for the nominal BJ balloon with Nolaro tether. The second mode increases in frequency and damping with an increase in trim angle-of-attack, while the third mode increases in frequency and decreases in damping at higher trim angles-of-attack. The fourth mode shows only a slight effect to trim angle, while the fifth mode is moderately affected because it is a balloon pitching mode.

The effect of tail area on the BJ tethered balloon is shown in Figure 20. Mode(1)shows that the system becomes slightly stable as the balloon tail is increased. This is to be expected because a larger tail gives more balloon aerodynamic damping. The damping ratio ξ for the large, nominal, and small tails are .21, -.04 and -.30 respectively. The balloon pitching modes (2 and 3) both display a similar trend to become slightly less stable with a smaller tail. However, the larger tail sizes show increase damping in modes(2 and 3.) Again both modes(4 and 5)remain overdamped with only mode(5)showing a moderate change in stability roots. Overall a larger tail size does increase the damping in the balloon system but not a great deal with the tail sizes considered. A further attempt was made to investigate the stability of a balloon with 64 percent nominal tail area. This attempt was futile because the balloon would not trim at a positive angle-of-attack.

The single most complicated parametric study was the effect of wind velocity (Figure 21). The wind velocity profile was decreased from its nominal to 0.1 percent of nominal. In order to maintain a 10,000-foot altitude, the tether line was adjusted. This does effectively change the balloon system. A more important consideration is that the trim angle-of-attack steadily decreased as the wind velocity decreased, causing the balloon aerodynamics to change. These two changes were also seen to effect the mode shapes as already discussed for Figure 5. The first mode is seen to change from a slightly unstable condition,

to slightly stable, to very stable, and back to slightly stable as the wind velocity profile decreases. The second mode, which is a moderate to strong response to all degrees-of-freedom, shows a tendency to become less stable at the lower wind velocities. Mode(3) which is a strong balloon pitching mode, also is seen to be less stable at the lower wind velocities. This is to be expected because a lower free stream velocity means lower damping forces. Modes(4)and(5)show trends to decrease in damping as the wind velocity decreases. In fact, modes(4)and(5)combine to give one oscillatory mode at a 60 percent wind, but then return to two aperiodic modes for the lower wind velocities finally ending up as one oscillatory mode for 0.1 percent wind. In general, Figure 21 shows that it is desirable to have a strong steady wind to maintain longitudinal stability, a result not unexpected.

Figure 22 presents the effect of balloon launch and retrieval on stability. As with the wind velocity study, the wind velocity is decreased because of the lower altitudes and this results in an angle-of-attack change. Also, the tether is decreased in length giving the system a greater effective buoyancy. The effect on mode 1 is to increase its damping at the lower altitudes. The damping ratio for the first mode increased to $\zeta = 0.55$ at 4000-foot altitude and then decreases to $\zeta = 0.27$ at 1000-foot altitude. The second mode which becomes a very strong balloon pitching mode (Figure 6) at the lower altitudes demonstrates an increase in damped frequency and a moderately strong decrease in damping ratio. The third mode shows an even stronger change. Both the damped frequency increases and the damping ratio decreases very strongly. Modes(4)and(5)react similar to a one degree-of-freedom system. Two aperiodic modes join to become one oscillatory mode at lower altitudes and then becomes less stable at the lowest altitude. The same trend would be seen in a one-degree-of-freedom system if the damping was steadily decreased.

The next parameter investigated was payload location. In Figure 23 the payload location was changed and the balloon was allowed to retrim itself. In Figure 24 the payload location was changed, and then the bridle apex was moved forward in order to achieve a nominal 8.5° trim attitude. By comparing the two figures it can be seen that the large changes in stability roots in modes 2 and 3 are due almost entirely to angle-of-attack change. In fact, moving the payload aft of the apex (5.9 feet) causes the balloon to trim at 10.7°. The payload location on the belly of the hull is 5.9 feet aft of the apex but it is also closer to the dynamic mass center of the balloon. Comparing Figures 23 and 24, the effect of modes(2)and(3)is again primarily an angle-of-attack change. The true effect of payload location can be seen to be minor in Figure 24 except for mode(5)which is an overdamped mode. Note that the first mode does become slightly stable when the payload is on the belly. The damping ratio ζ is .35 for the payload on the belly and -.04 for the payload at the bridle apex point.

The last parametric study on the BJ balloon system was the effect of winch location (Figure 25). In this case the balloon is still flown at 10,000 feet M.S.L., but the winch is at 5,000 feet M.S.L. Mode one has gone from very slightly unstable to very slightly stable. Modes(2)and(3)show a large increase in frequency due to a shortening of the tether somewhat similar to Figure 22. Frequency is substantially increased because net static lift has substantially increased with less tether supported by the balloon.

Figure 26 investigates the effect of trim angle on the Vee balloon. Comparing this figure to Figure 15, the effect is seen to be much greater. In fact a low angle-of-attack is seen to be undesirable in the first mode. Not only does the motion become more unstable, but the time to double amplitude decreases. The positive real root, with value 0.18, has a time to double amplitude of only 3.9 seconds. The second mode, which is a balloon pitching mode, becomes moderately more stable at the higher trim angles and

also shows a strong increase in damped frequency. Mode(3)demonstrates moderate changes in frequency and a slight change in damping having its best damping at the intermediate trim angle.

The effect of waterline of bridle apex on the longitudinal stability of the Vee Balloon (Figure 27) is seen to be small in all modes as it was with the BJ Balloon (Figure 16).

The effect of free static lift (Figure 28) is minor for the Vee Balloon as it is for the BJ (Figure 17) over the range of variations investigated.

Figure 29 cannot be compared to any of the BJ stability plots. This figure shows the effect of increasing the area of two fins located on the lower aft end of each hull. Physically, this change does not affect the aerodynamics in the longitudinal plane but only increases the weight of the tail. This is seen to have little effect on longitudinal stability.

Figure 30 is similar to Figure 29 except that the tail size is not only increased on the bottom of each hull, but an identical fin is placed on the top of each hull so that the tail assembly is symmetric. Again the effect on the stability plots is due only to an increase in weight.

The third balloon investigated was a GAC single hull balloon. Figure 31 presents the effects of trim angle-of-attack. The most favorable change for the single hull balloon is that the first mode has become stable and is moderately damped. The second and third modes which are balloon modes (Figure 8) show trends similar to the BJ Balloon (Figure 15) but do have significantly higher frequencies. The four and fifth modes show little effect.

The effect of waterline of the bridle apex on the GAC balloon is shown in Figure 32. Again mode(1)is stable and shows a tendency to become more stable at lesser waterline locations. Mode(2)shows no significant trend, while mode(3)shows a slight decrease in damping and an increase in damped frequency with greater waterline locations. Modes(4)and(5)are slightly effected.

As with the BJ and Vee Balloons, free static lift has no effect on the stability of the balloon system (Figure 33).

6. LATERAL STABILITY CHARACTERISTICS

Now consider the lateral stability roots. In general there is a lateral stability plot for each parameter studied in the longitudinal plane. It is of interest to compare the corresponding lateral and longitudinal plots to see which parameters affect the lateral modes, which affect the longitudinal modes, and which affect neither mode or both modes. Note that there is one more degree-of-freedom associated with the lateral motions, than associated with the longitudinal motions.

Before proceeding to the parametric study, it is of interest to observe the effect of cable drag coefficient on the stability roots. This is seen in Figure 34. All three modes shown are neutrally stable if the cable drag coefficient is zero (cable drag = 0). As the drag coefficient increases, all three modes become more stable and modes (2) and (3) are overdamped at the nominal cable drag coefficient of 1.1. However, mode (1), which is overdamped when the drag coefficient is about .3, becomes less damped at higher drag coefficients but remains moderately stable.

The first lateral stability plot is for the effect of balloon trim angle on a BJ tethered balloon (Figure 35), Figure 9 shows the mode shapes corresponding to this tethered balloon. All modes demonstrate little or no effect due to trim angle change. Figure 36 is the stability effect due to changes in the waterline of the bridle apex. Mode (2) shows a slight increase in damping at lesser waterline locations, a trend which is opposite in the longitudinal plane (Figure 16). Note that mode (2) is predominantly a balloon roll mode (Figure 9). Mode (8) is also slightly affected by waterline location.

The effect of free static lift on the lateral modes is shown in Figure 37, as in the longitudinal plane (Figure 17) the effect is small.

The next plot (Figure 38) presents the lateral stabilities of a BJ balloon designed for different altitudes. In general the oscillatory modes show greater damped frequency and less damping at the lower altitudes. The increase in frequency can be explained by the fact that smaller balloon systems are designed for lower altitudes meaning smaller inertia characteristics and therefore higher frequencies. A decrease in damping ratio also results with smaller balloon systems because effective moment arms are smaller giving less resistance to motions. Note that modes (3) and (4) combine to give one oscillatory mode at 5000 feet.

Figure 39 is the effect of balloon trim angle when using an Amgal tether. The effect is negligible as in Figure 35 where a Nolaro tether was used. The first mode has greater damping with Amgal tethered than with Nolaro tether as observed by comparing Figures 39 and 35.

The effect of tail size of the BJ balloon on lateral stability is demonstrated in Figure 40. Significant changes in frequency and damping are noted in mode (2) which is a roll mode. It would be expected that a smaller tail would give less damping. Mode (1) also shows a moderate increase in damping with the larger tail size. Stability roots (3) to (8) are all affected by tail size but they do keep their overdamped characteristic.

Wind velocity effects are shown in Figure 41 for the lateral motions of the BJ balloon. As with the longitudinal stability roots (Figure 21), some of the trends are difficult to follow. In general all the roots tend to become less stable as the operational wind velocity is decreased until each mode is only very slightly damped at the .1% wind condition. Therefore, it is desirable to have a strong operational wind to maintain stability.

Figure 42 presents the effects of retrieving a BJ balloon. The first mode, which is responsive in all degrees-of-freedom, shows a very important result. At 1000 ft altitude, this mode becomes unstable and has a time to double amplitude of 66 seconds. Also of interest is that two pairs of aperiodic modes become oscillatory at lower altitudes and decrease in damping as the altitude decreases. These two oscillatory modes are similar to modes (3) and (4) in the longitudinal plane (Figure 22).

Figures 43 and 44 show the effect of payload location on lateral stability. The effect on longitudinal stability is shown in Figures 23 and 24. The only difference in Figures 43 and 44 is the trim angle-of-attack as noted on the plots. Modes (2) and (6) are strongly affected when the payload is removed from the bridle apex and assumed to be rigidly attached to the balloon, changing the balloons inertia characteristics. Note that modes (2) and (6) are both strong balloon roll modes (Figure 9). In Figure 44, the aperiodic modes

(6) and (8) combine to give one heavily damped oscillatory mode when the payload is on the belly.

Finally, the effect of winch altitude was considered in the lateral degrees-of-freedom for the BJ balloon. Modes (3) and (5) which are overdamped tether modes for the nominal design condition become an oscillatory mode when the winch altitude is increased to 5000 ft. Mode (1) also shows a moderate decrease in frequency.

The lateral stability plots for the tethered Vee Balloon are presented next. Perhaps the most significant comparison between the VEE balloon Figure 46) and the BJ balloon (Figure 35) is that there are four oscillatory roots associated with the Vee Balloon and only two associated with the BJ balloon. However, these extra oscillatory roots are well damped. Figure 46 shows that trim angle-of-attack has little effect on lateral stability.

Figure 47 gives the effect of waterline of the bridle apex on the VEE balloon in the lateral degrees-of-freedom. The effect is small.

Figure 48 presents the effect of free static lift on the lateral stability of the tethered balloon. The most significant change is in the second mode which becomes more stable at lower free static lift values. From Figure 12, it is seen that mode(2)is a strong roll mode. The increase in damping can be attributed to the fact that the damping ratio is inversely proportional to the square root of the stiffness in the system and decreasing free static lift decreases stiffness thereby increasing damping. This effect is also noticeable to a lesser extent in mode (4) which is a strong roll mode (Figure 12).

A very significant change is seen in Figure 49 when the lower fins are increased in area. Mode(1) which is a coupled balloon-tether mode decreases in frequency when the tail area is increased. Mode(2)increases in frequency and decreases in damping with an increase in tail area. Mode(4),which is a strong roll mode, increases in frequency and damping as the tail area increases. Mode(3) which is also a strong roll mode, shows a slight decrease in damping with larger tail areas. The overdamped modes(5)and(6)are unaffected.

Figure 50 shows the effect of increasing lower and upper tail area. All trends are the same as in Figure 49.

Figure 51 presents the effect of trim angle-of-attack on the lateral stability of a GAC single hull balloon. In comparison to the BJ balloon (Figure 35), there is seen to be one more oscillatory mode with the GAC balloon. The effect of trim angle is negligible with the GAC balloon as it was with the BJ and Vee Balloons.

Figure 52 demonstrates that bridle apex waterline has little effect on the lateral stability of the GAC balloon except in mode (3) which is a strong roll mode (Figure 14).

In Figure 53, the free static lift is decreased in the GAC single hull balloon. The resulting stability trend is similar to the Vee-Balloon (Figure 48). The second mode shows a strong increase in damping as free static lift decreases, as mode (2) in Figure 48 did.

Longitudinal BJ-Nominal, Run No. 1

Mode Shapes

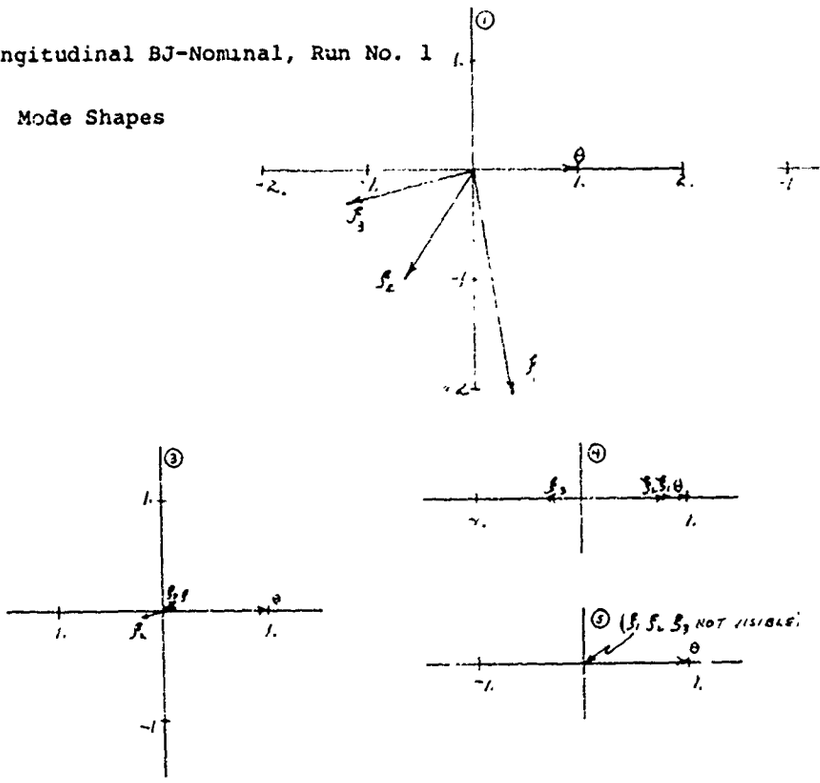

FIGURE 4

Longitudinal BJ-20% Wind, Run No. 18

Mode Shapes

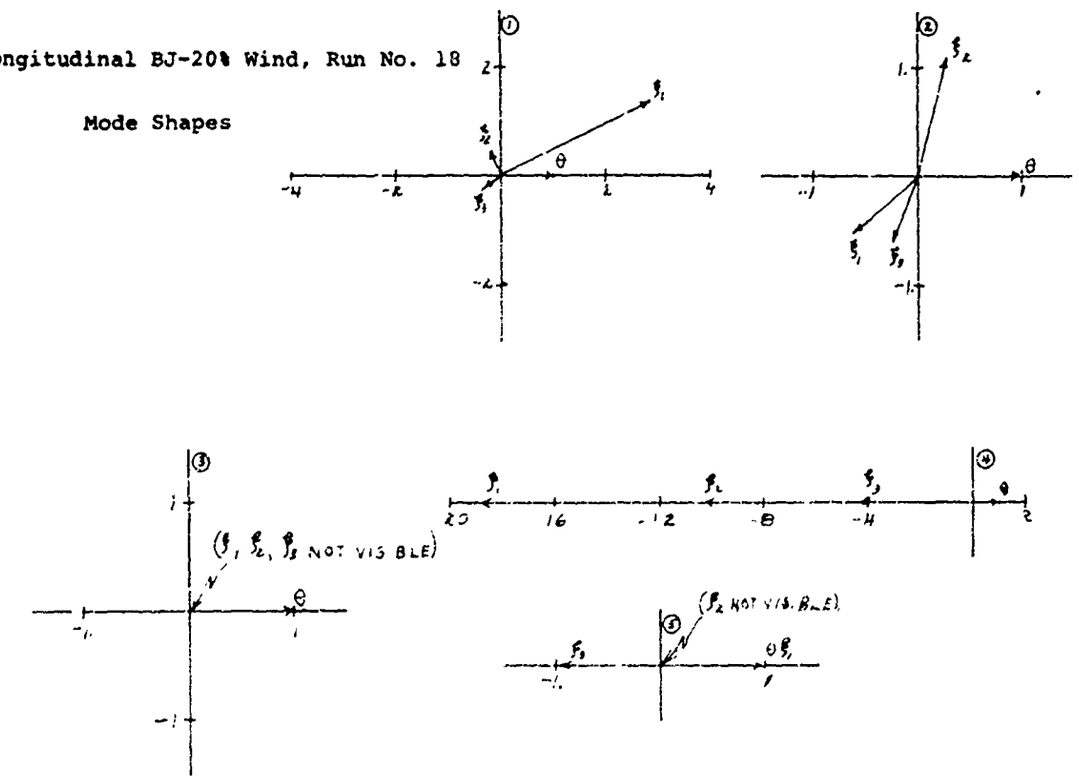

FIGURE 5

Longitudinal BJ-1000 Ft Alt., Run No. 22

Mode Shapes

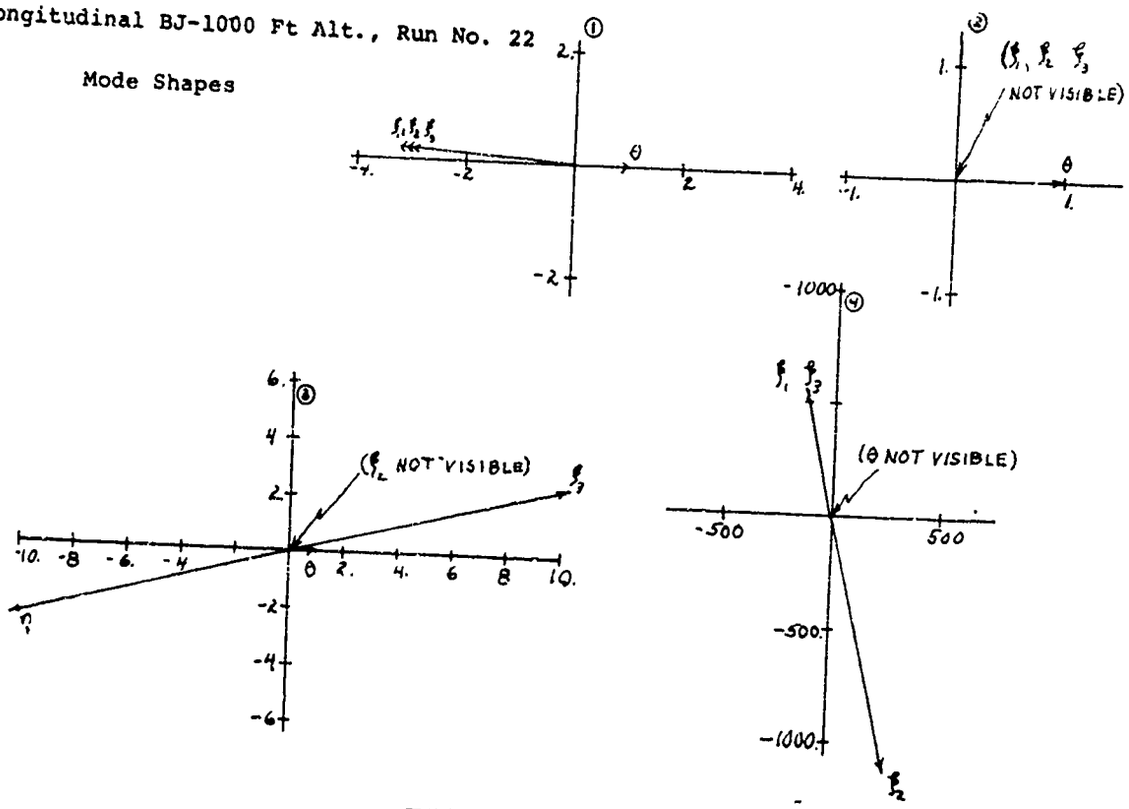

FIGURE 6

Longitudinal Vee-Nominal, Run No. 28

Mode Shapes

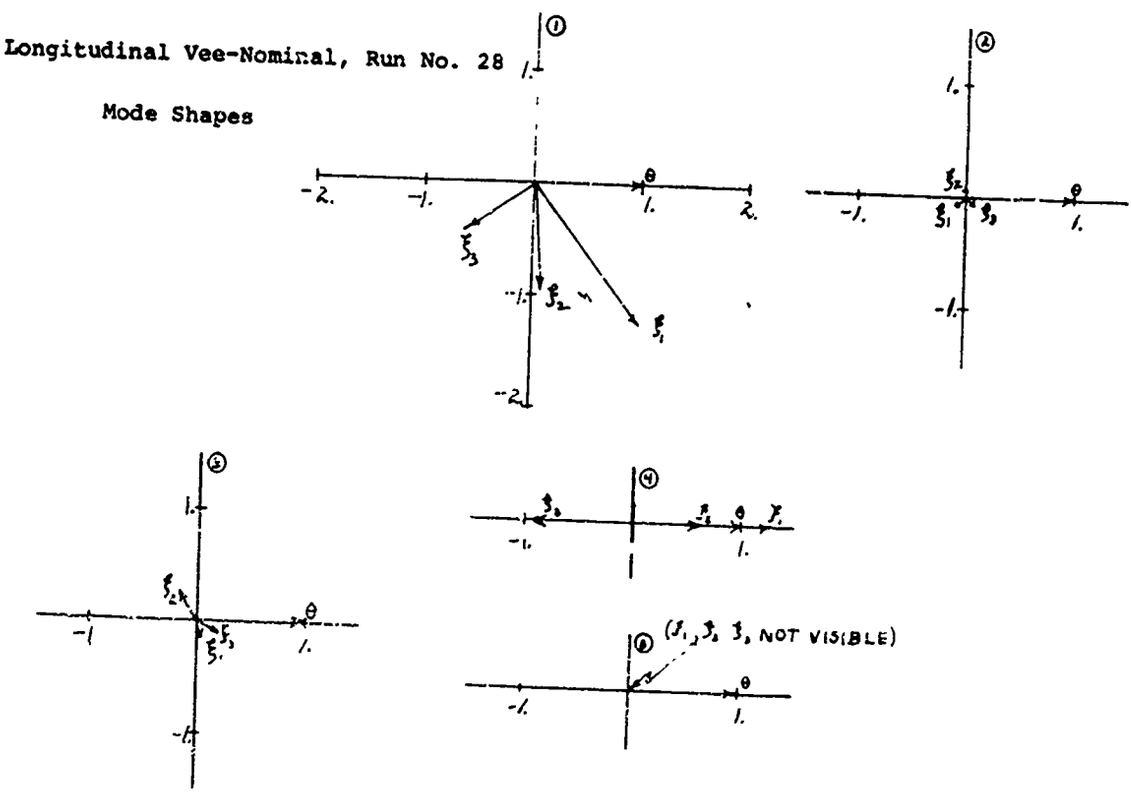

FIGURE 7

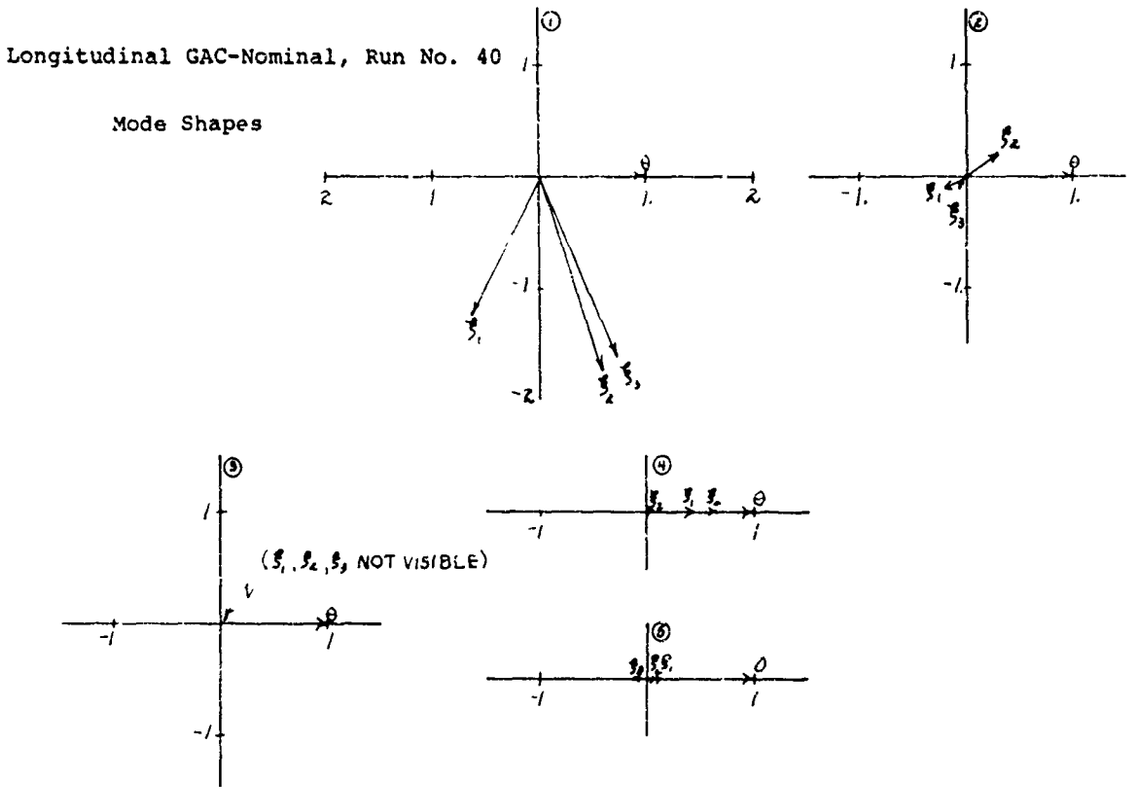

FIGURE 8

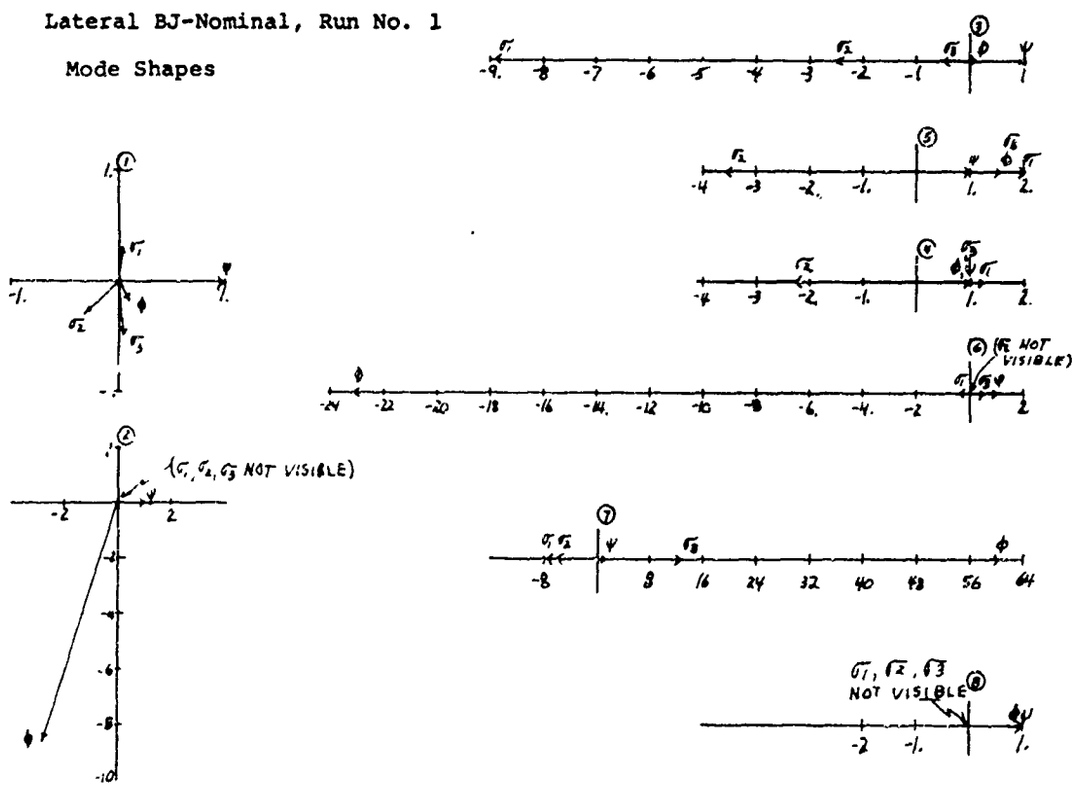

FIGURE 9

Lateral BJ-20% Wind, Run No. 18

Mode Shapes

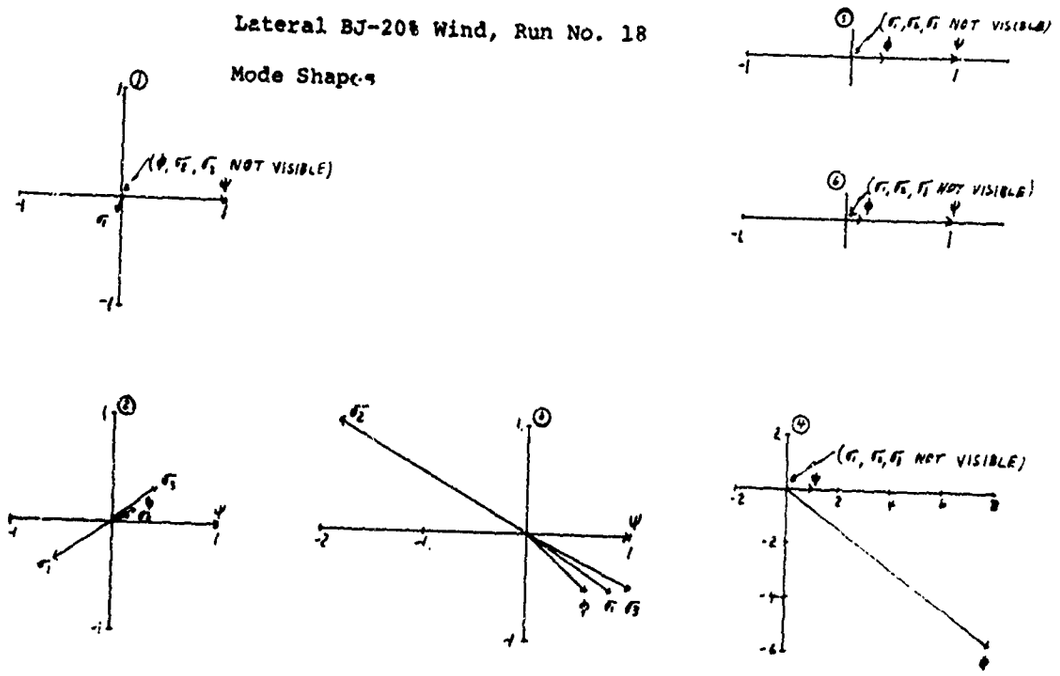

FIGURE 10

Lateral BJ-1000 Ft Alt., Run No. 22

Mode Shapes

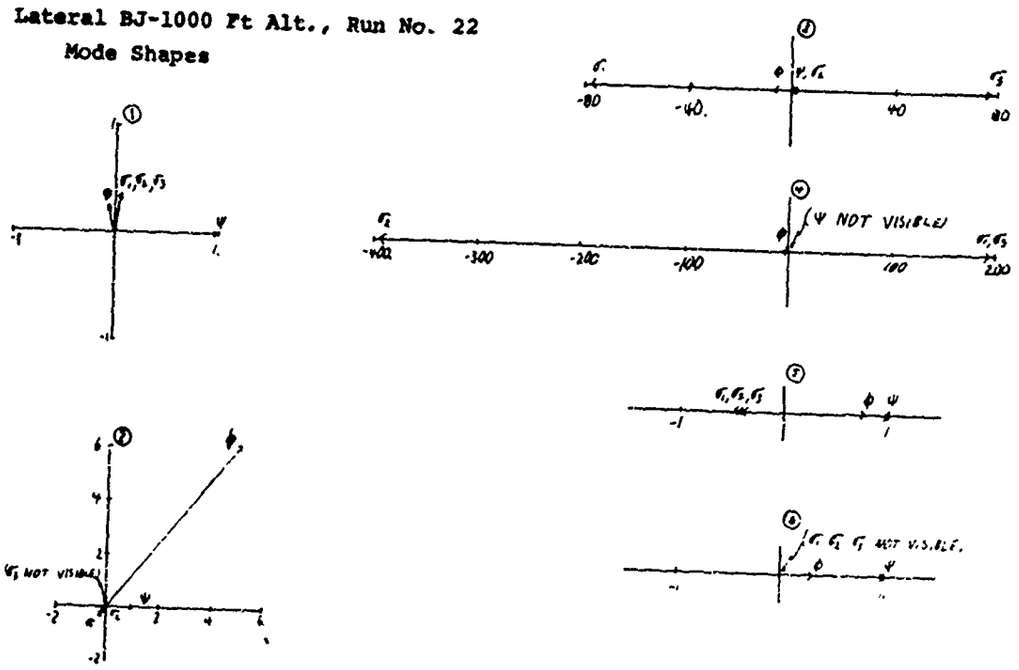

FIGURE 11

Lateral Vee-Nominal, Run No. 28

Mode Shapes

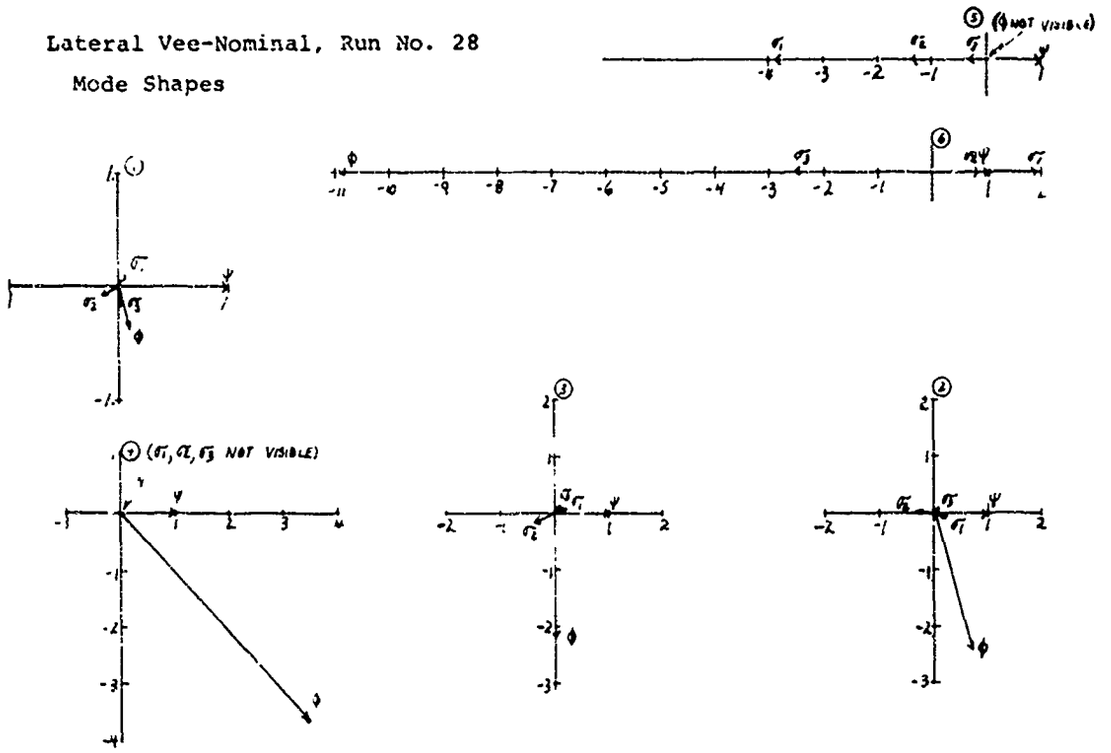

FIGURE 12

Lateral Vee-300% Tail Area, Run No. 36

Mode Shapes

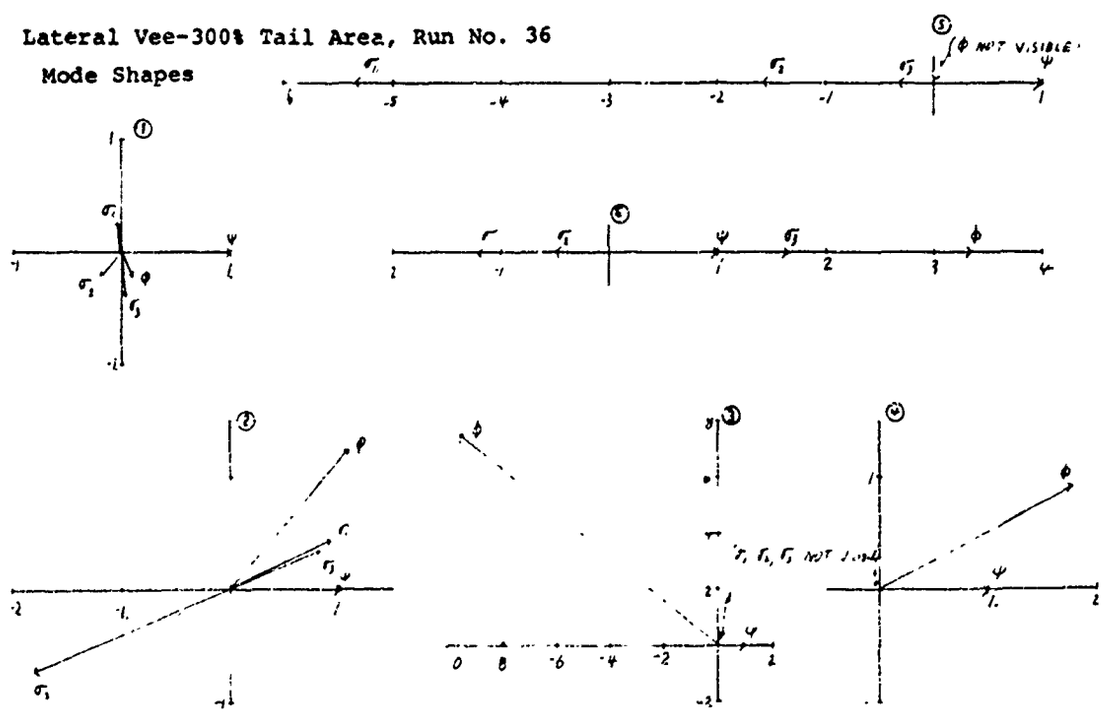

FIGURE 13

Lateral GAC-Nominal, Run No. 40

Mode Shapes

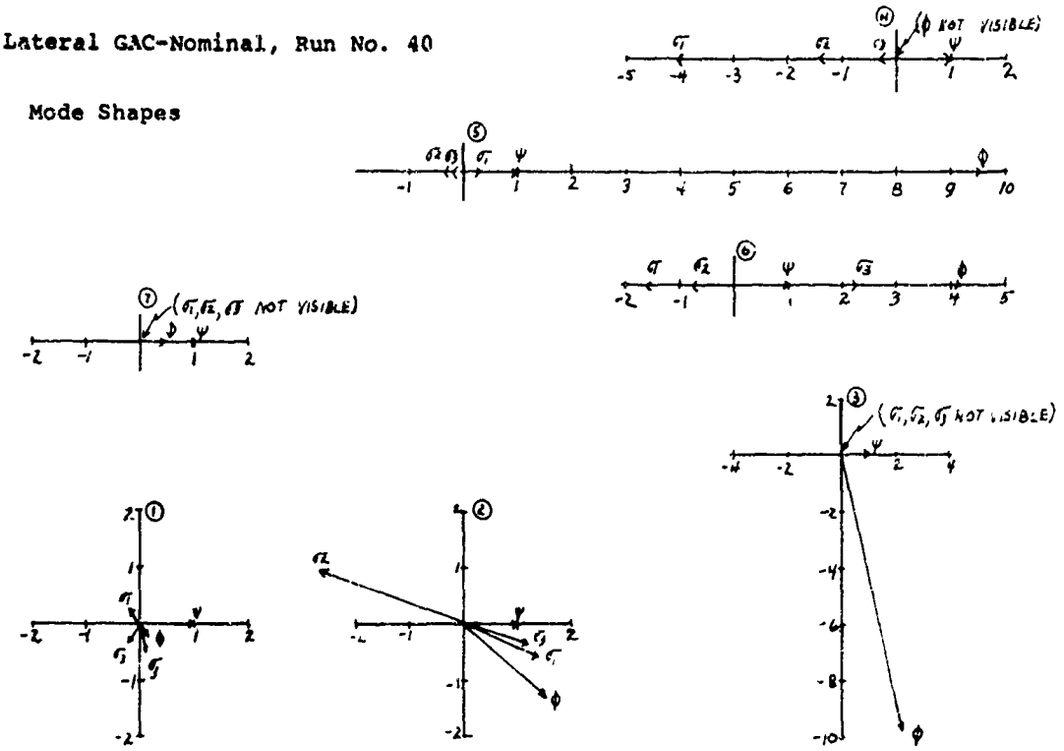

FIGURE 14

Longitudinal BJ-Effect of Trim Angle,
Run Nos. 1,2,3

○ α_T = 8.5° (NOMINAL)

□ α_T = 6.5°

◇ α_T = 10.5°

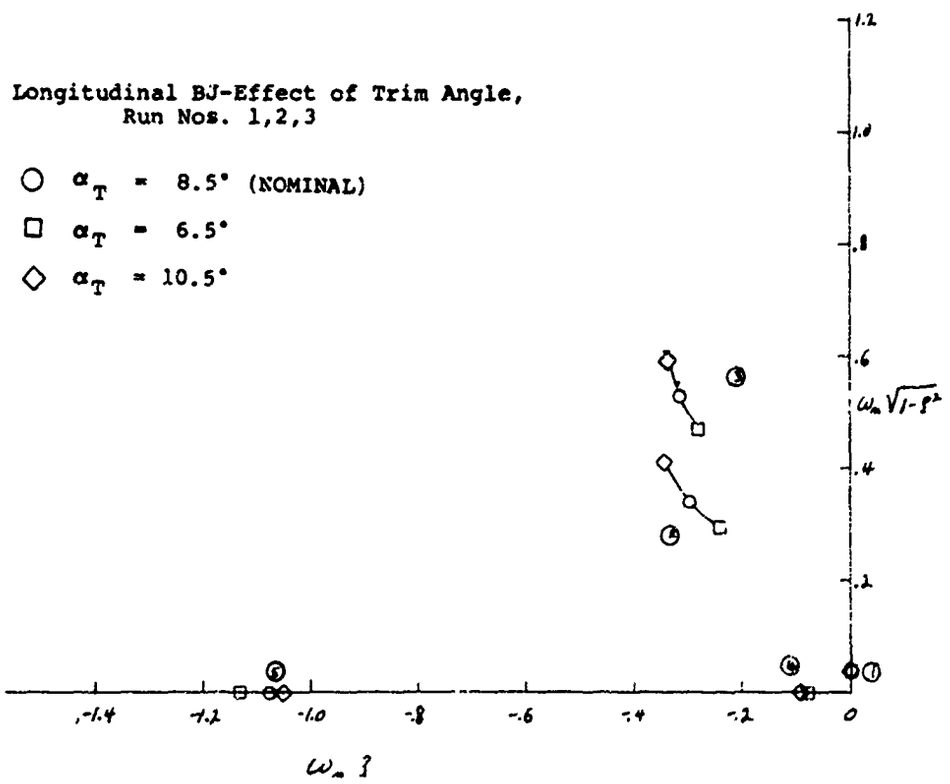

FIGURE 15

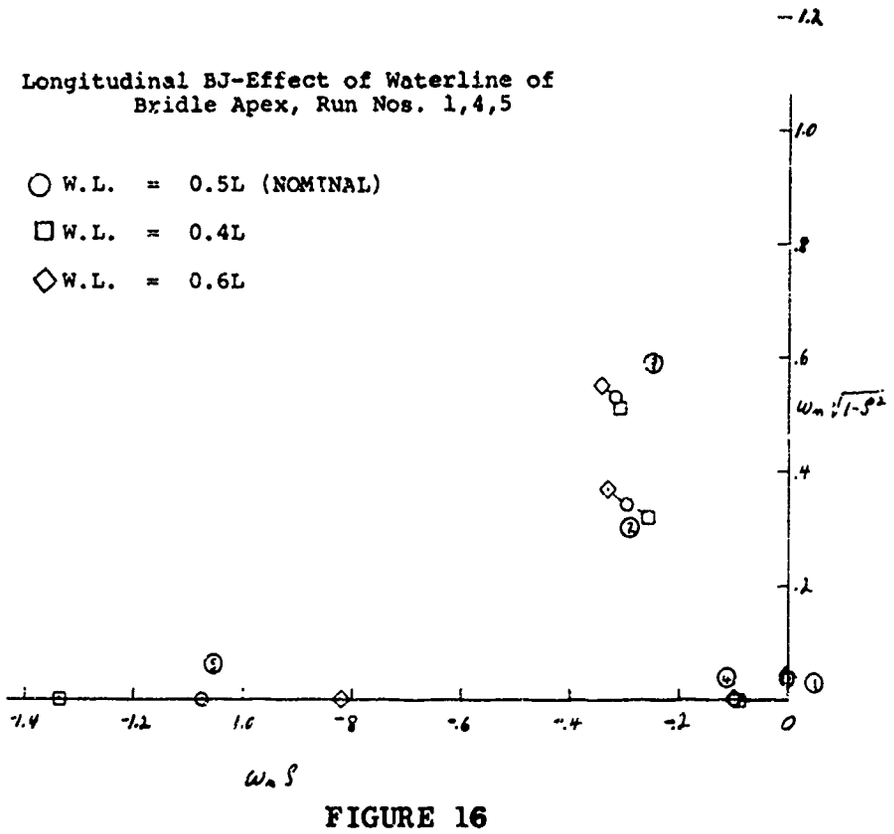

FIGURE 16

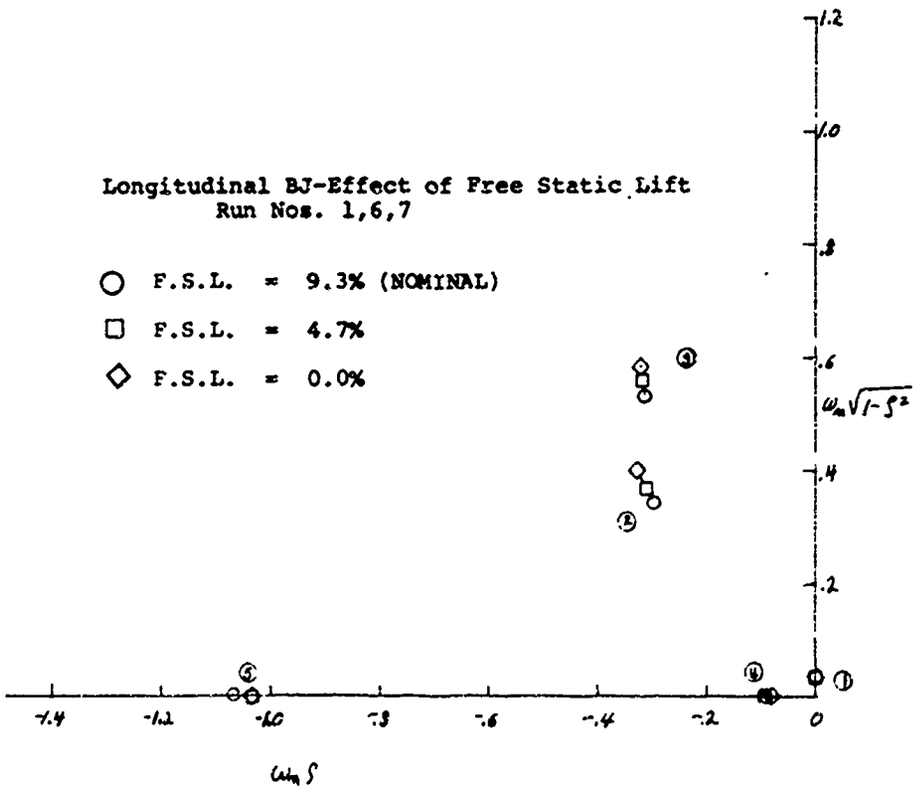

FIGURE 17

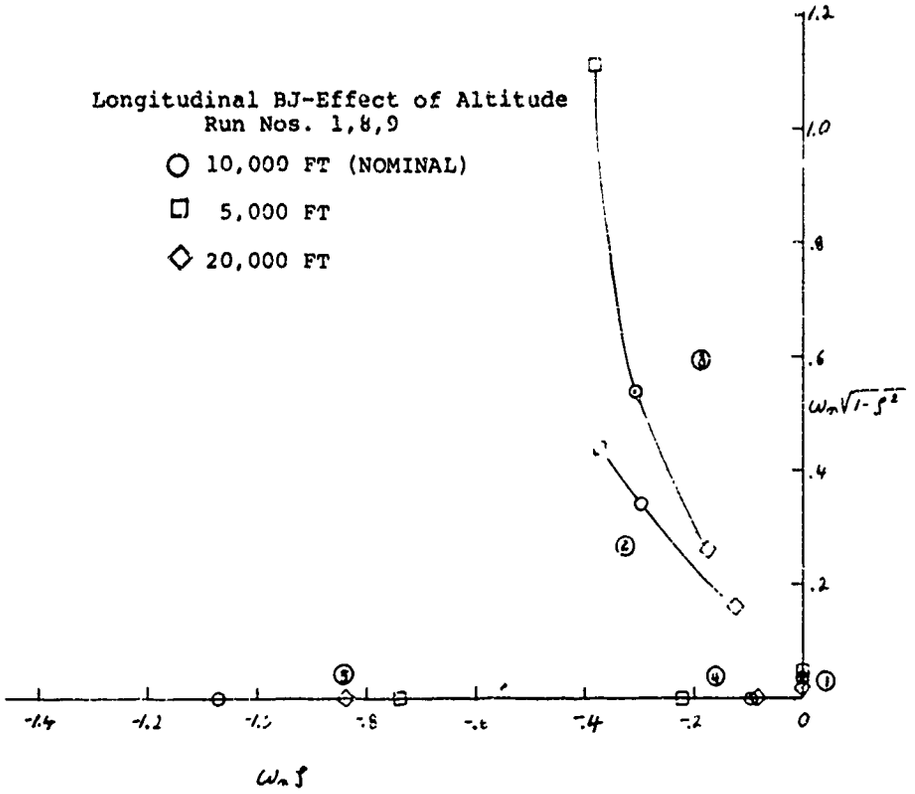

FIGURE 18

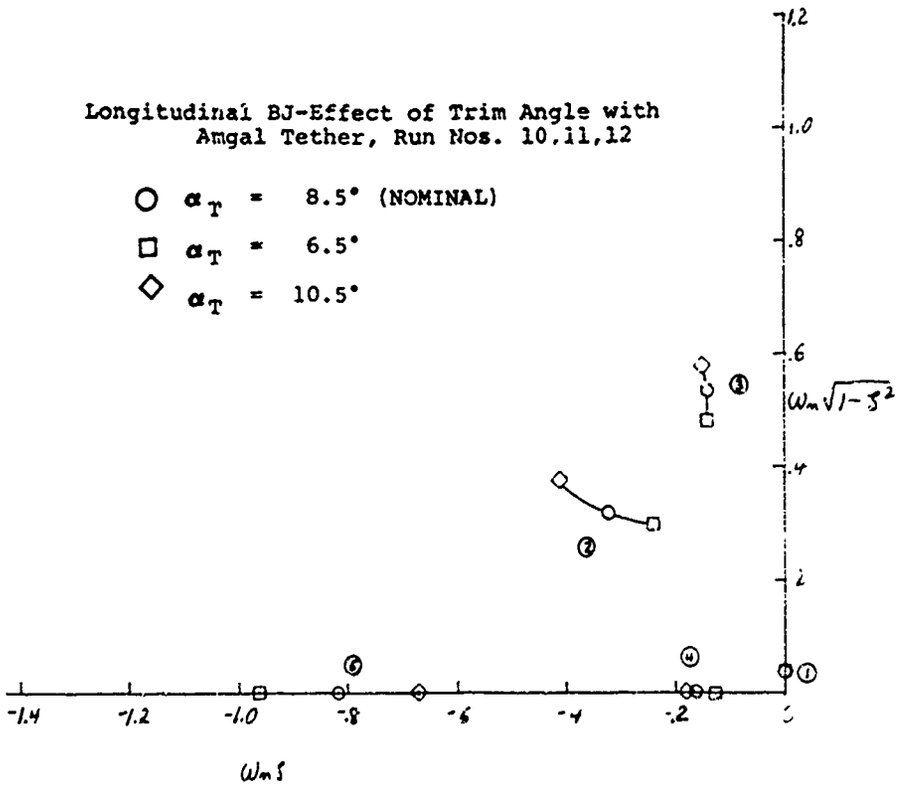

FIGURE 19

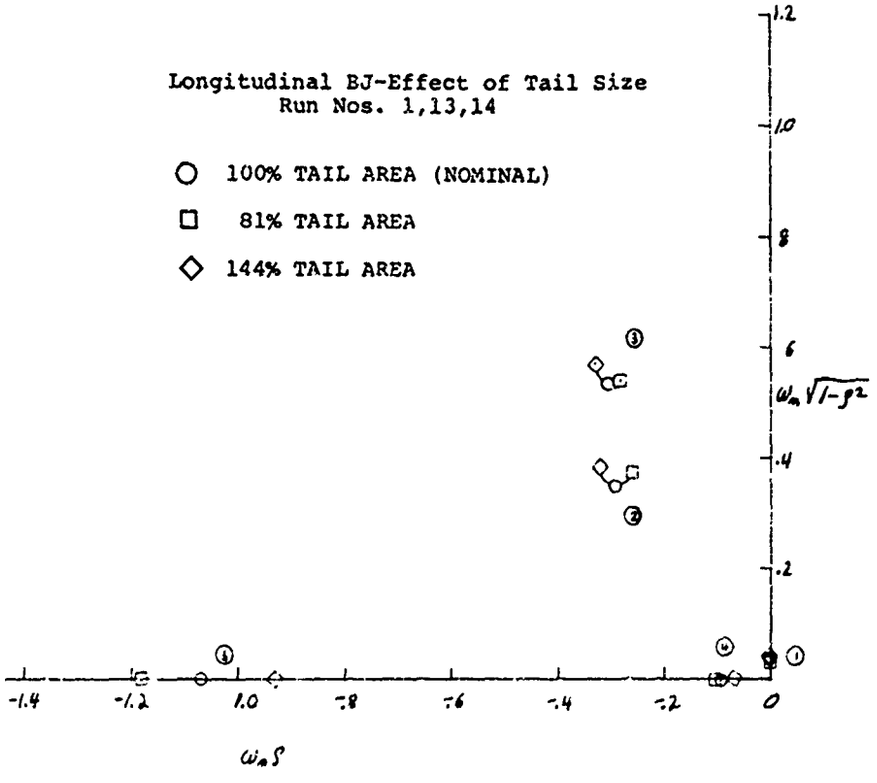
Longitudinal BJ-Effect of Tail Size
Run Nos. 1,13,14
100% TAIL AREA (NOMINAL)
81% TAIL AREA
144% TAIL AREA
1.2
1.0
.8
.6
.4
.2
0
-1.4
-1.2
1.0
-.8
-.6
-.4
-.2
$\omega_n\sqrt{1-\zeta^2}$
$\omega_n\zeta$

FIGURE 20

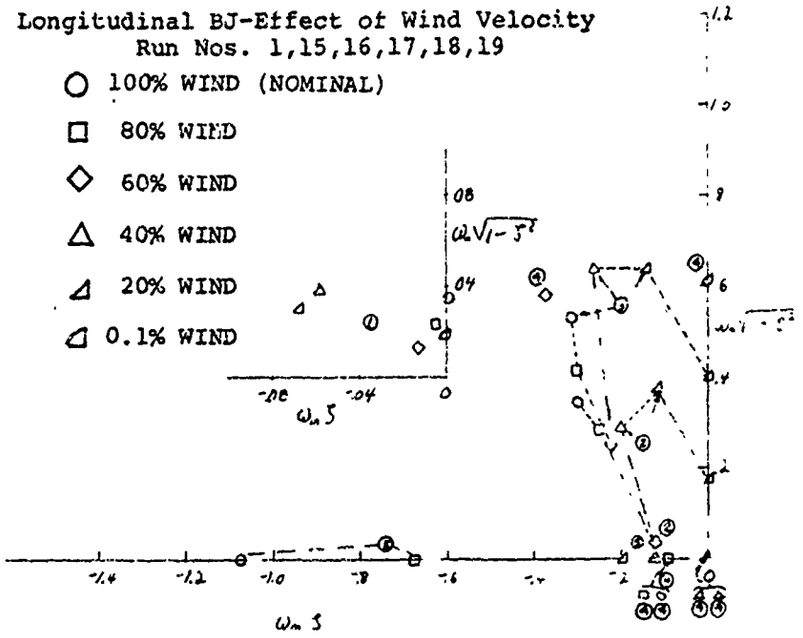

FIGURE 21

LONGITUDINAL BJ
EFFECT OF WIND VELOCITY

MODE NUMBER	WIND 100% ○	80% □	60% ◇	40% △	20% ◿	0.1% ◿
1	0	0	0	0	0	0
2	0	0	0	0	0	0
3	0	0	0	0	0	0
4	A	A	0	A	A	0
5	A	A	-	A	A	-

0 - OSCILLATORY
A - APERIODIC

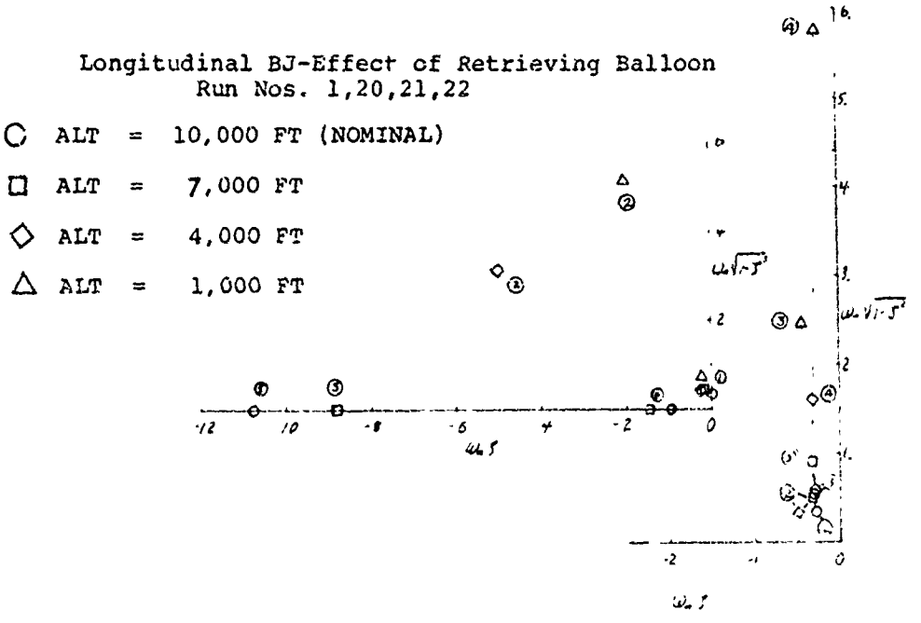

FIGURE 22

LONGITUDINAL BJ
EFFECT OF RETRIEVING BALLOON

MODE NUMBER	10,000' ○	7,000' □	4,000' ◇	1,000' △
1	0	0	0	0
2	0	0	0	0
3	0	0	0	0
4	A	A	0	0
5	A	A	-	-

0 - OSCILLATORY
A - APERIODIC

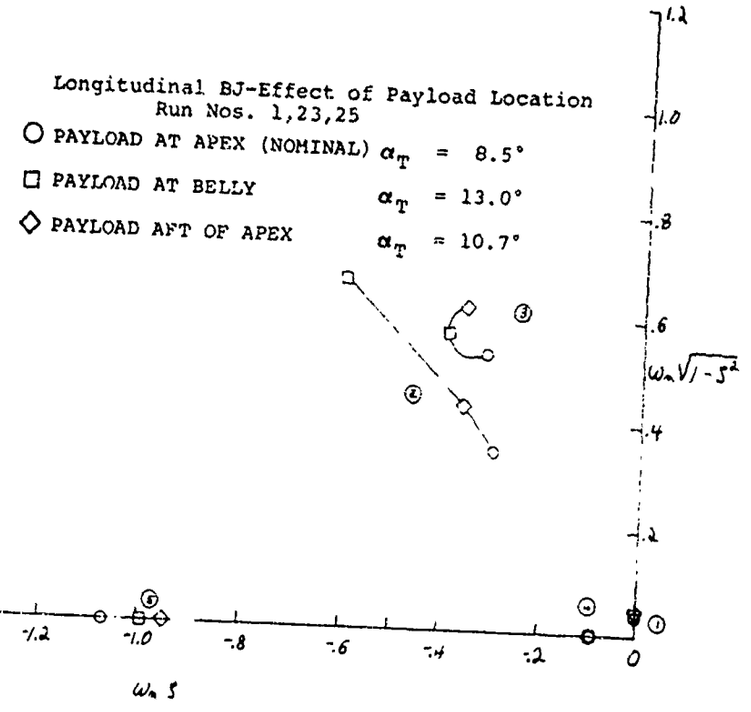

FIGURE 23

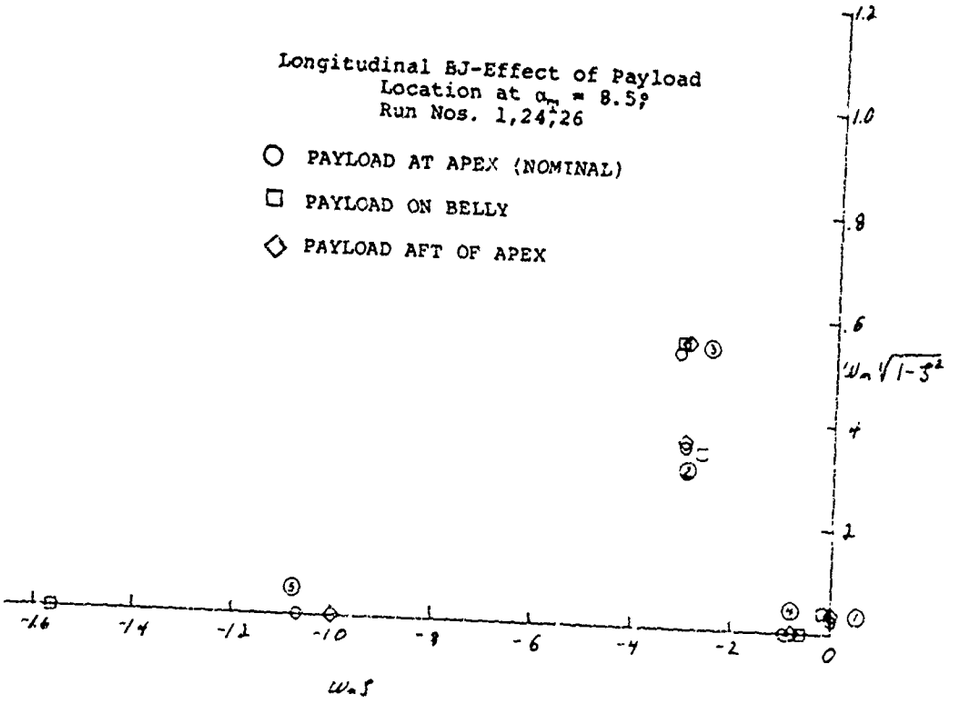

FIGURE 24

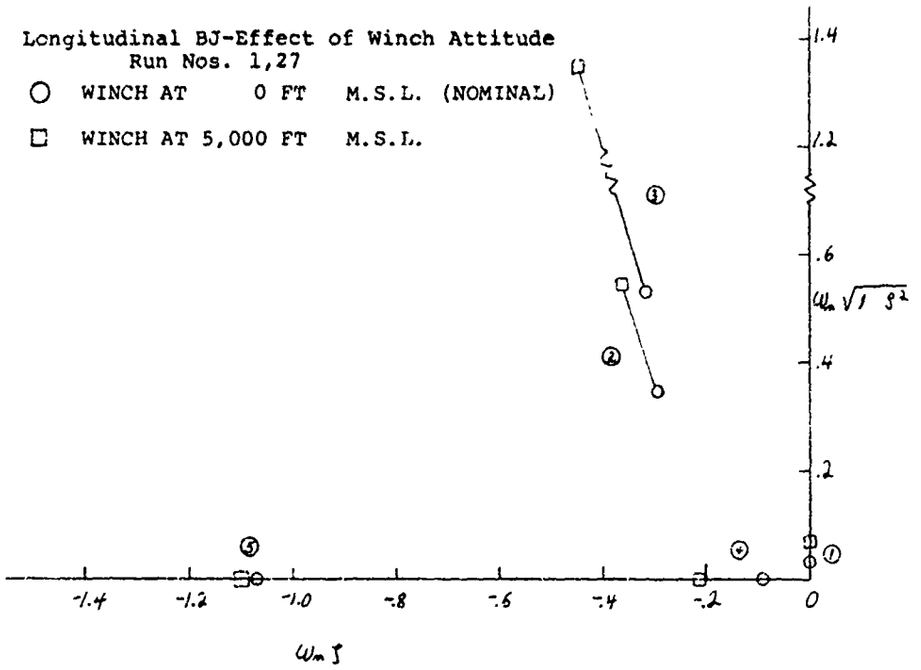

FIGURE 25

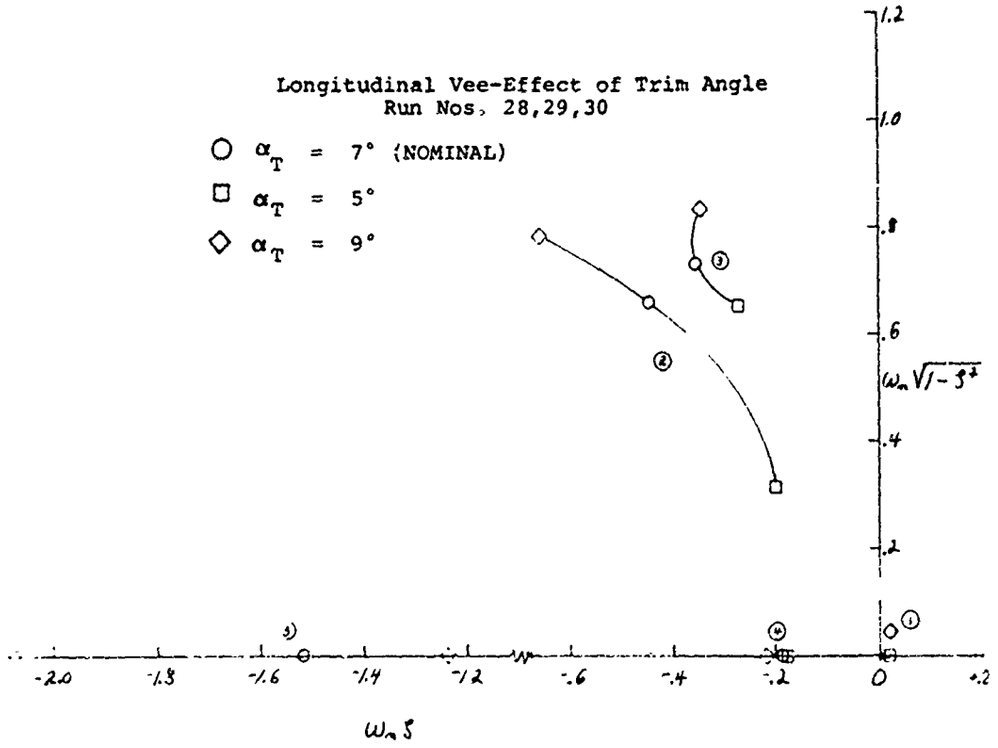

FIGURE 26

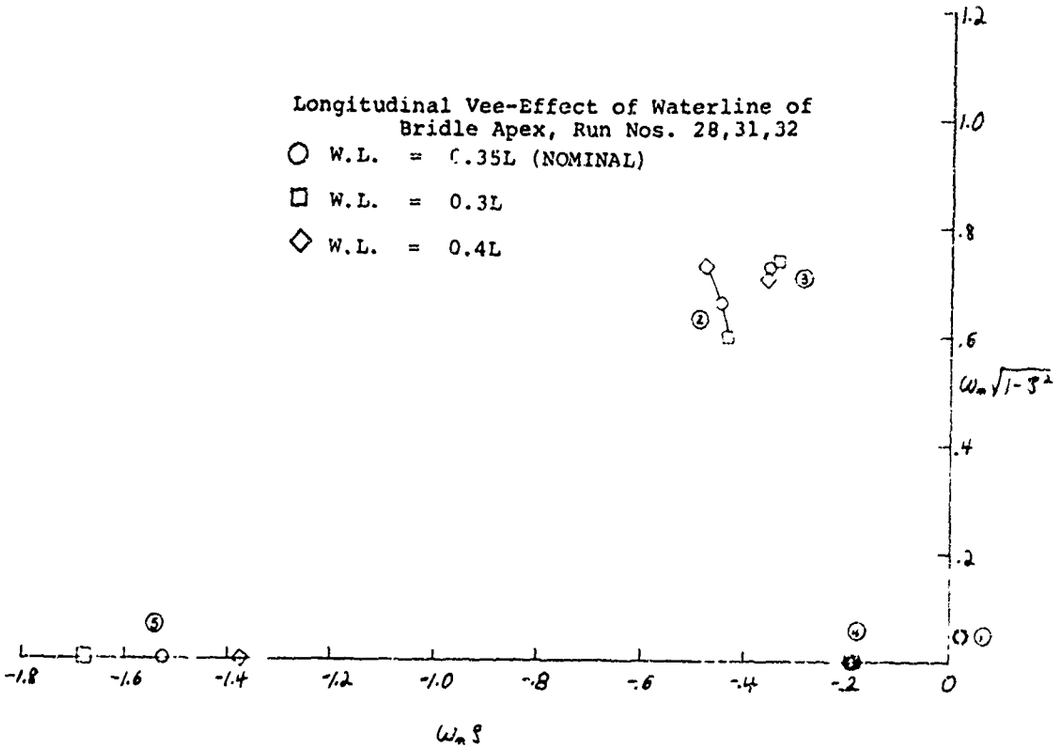

FIGURE 27

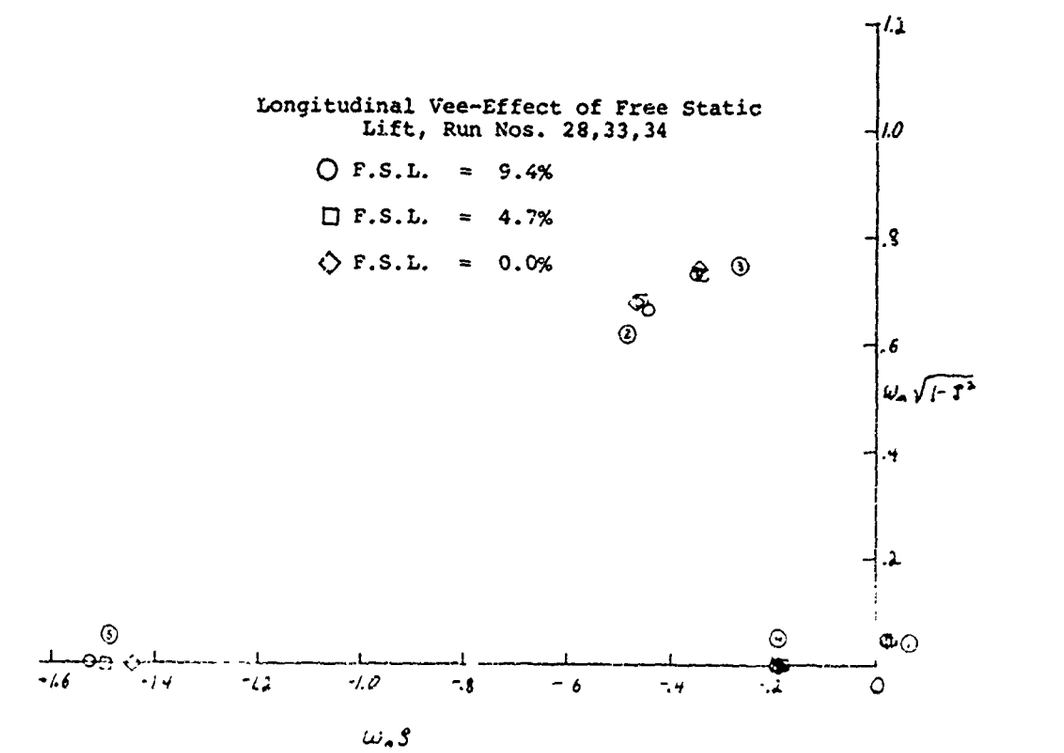

FIGURE 28

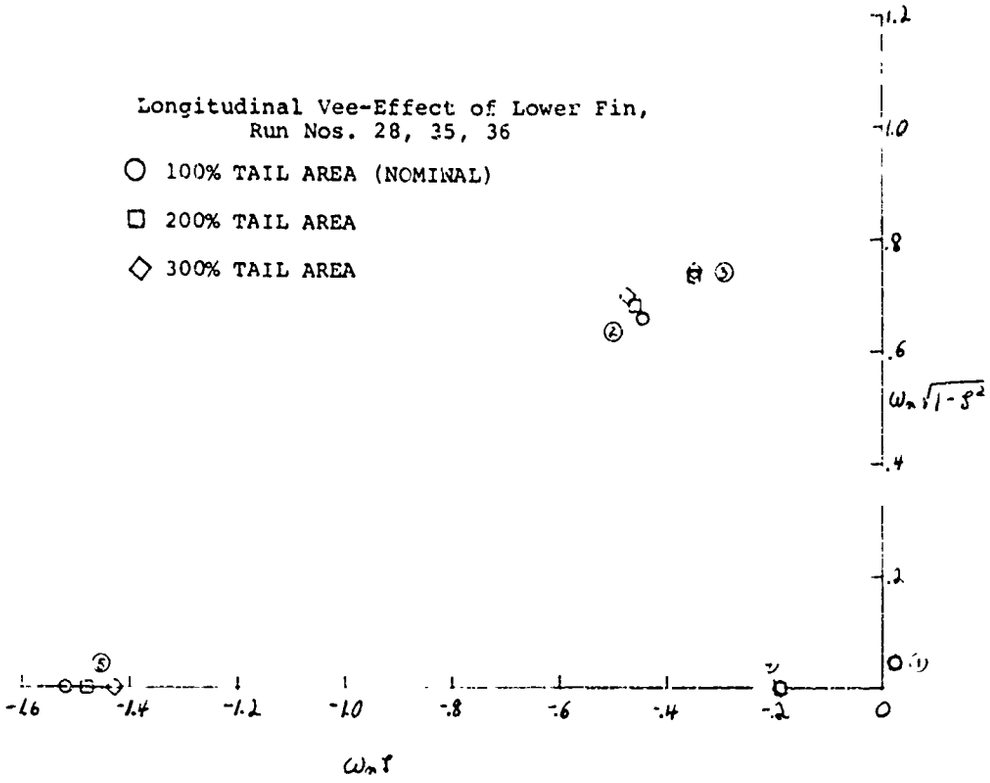

FIGURE 29

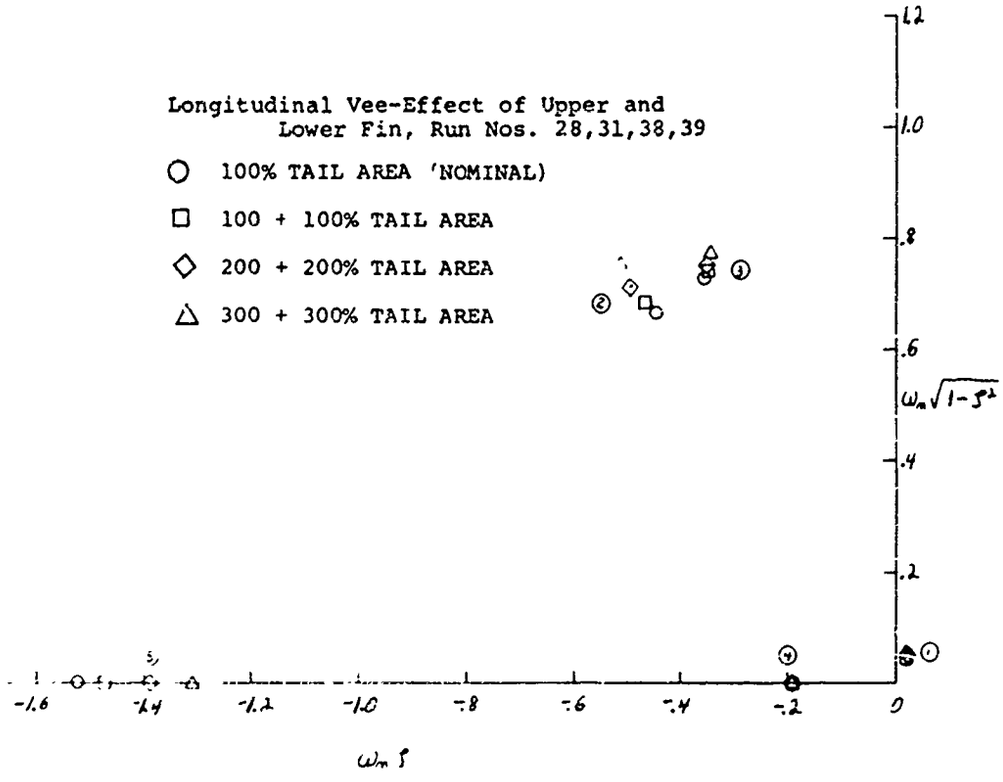

FIGURE 30

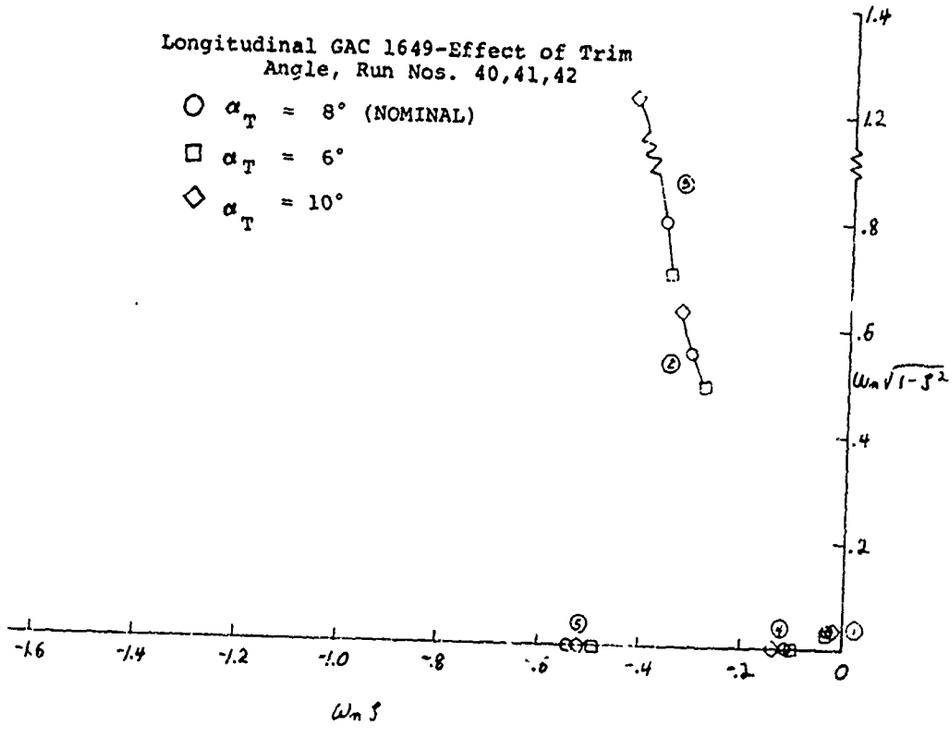

FIGURE 31

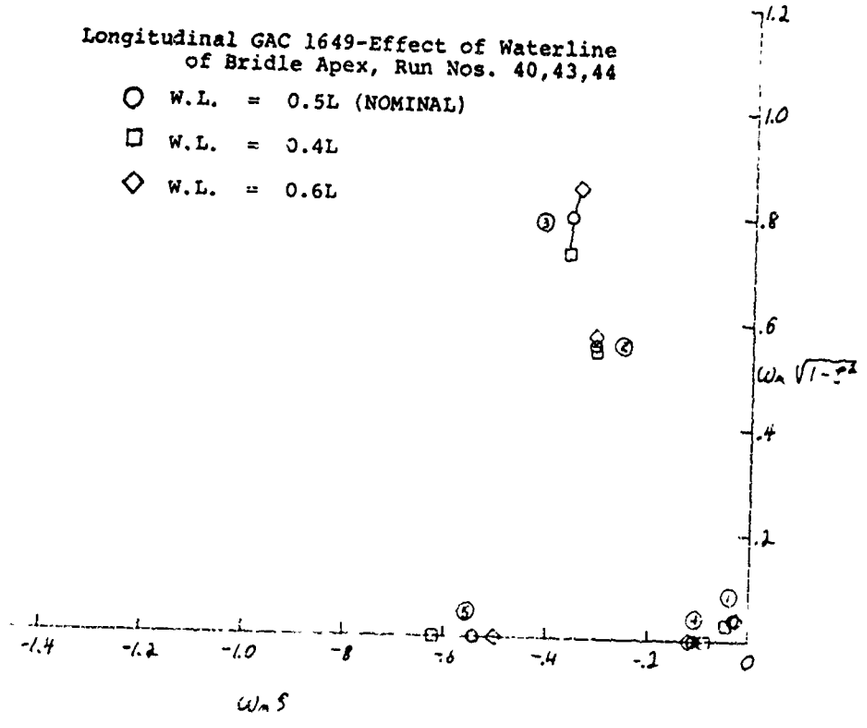

FIGURE 32

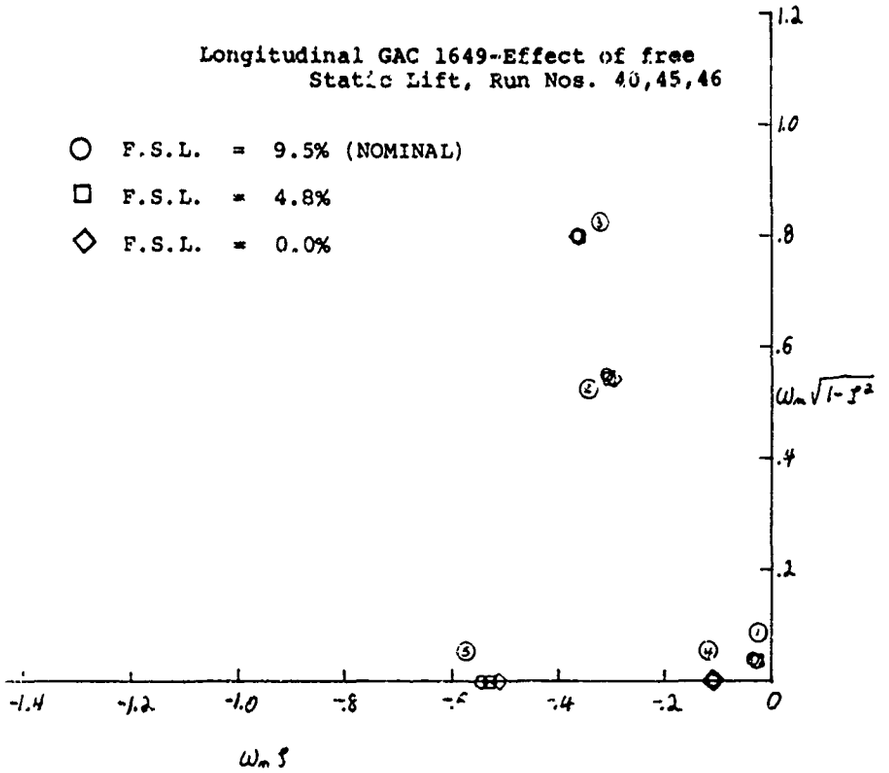

FIGURE 33

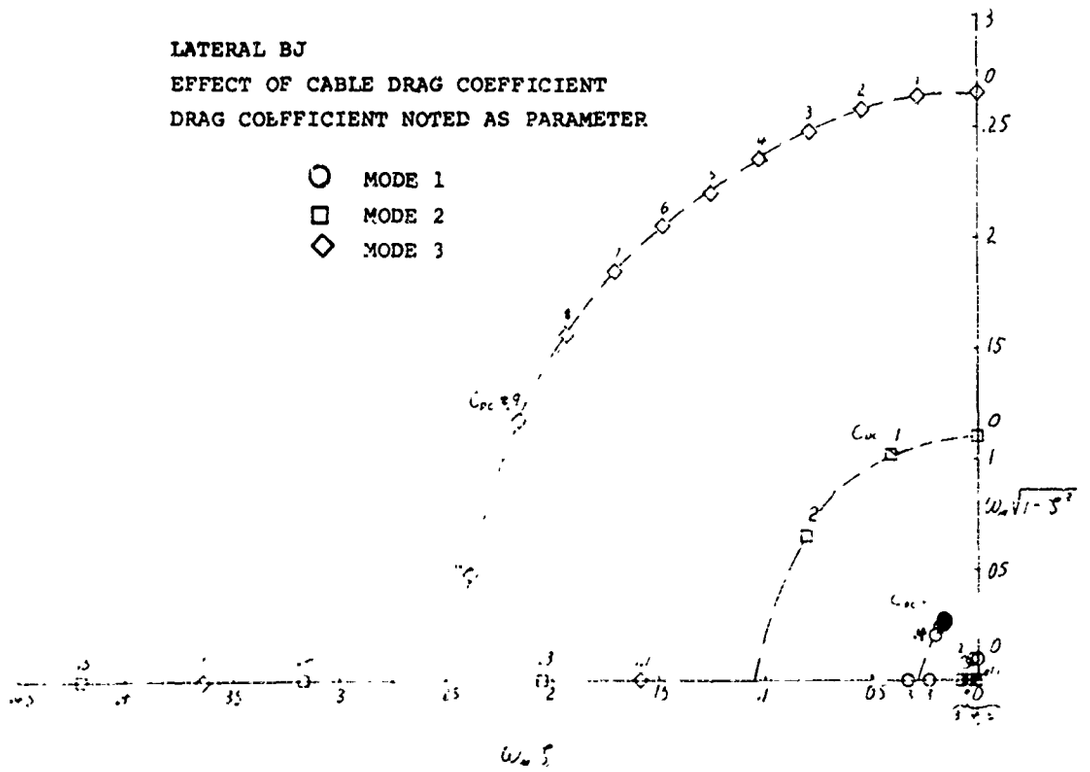

FIGURE 34

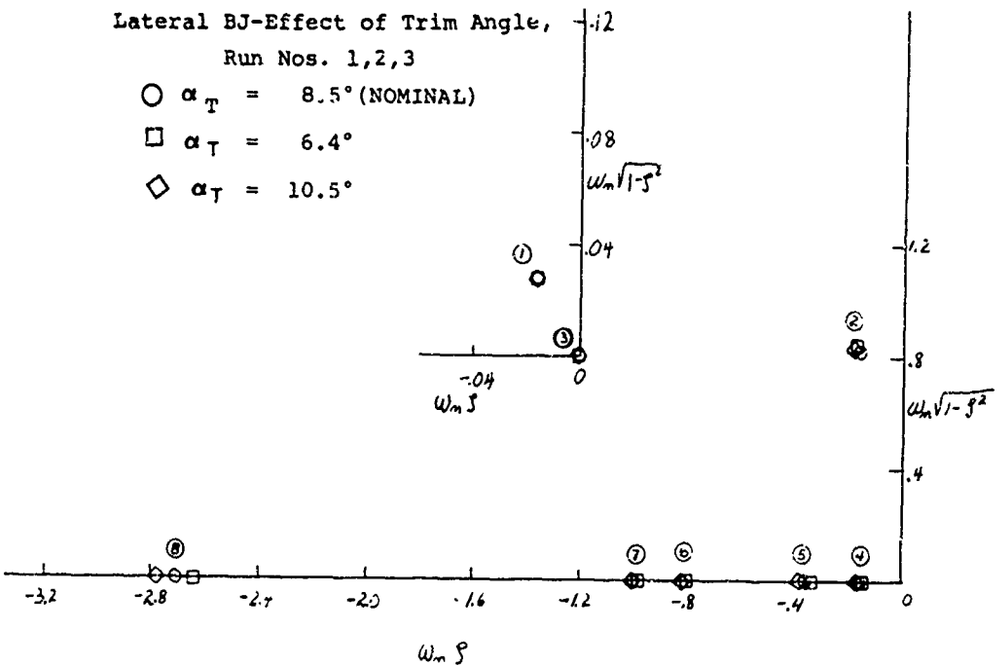

FIGURE 35

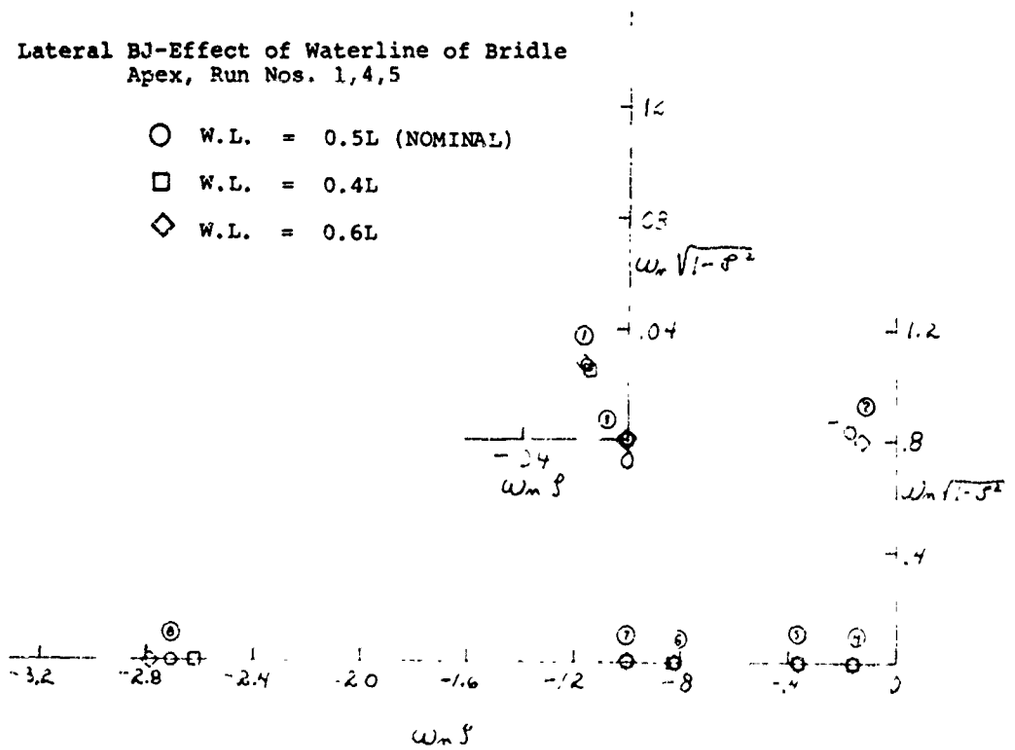

FIGURE 36

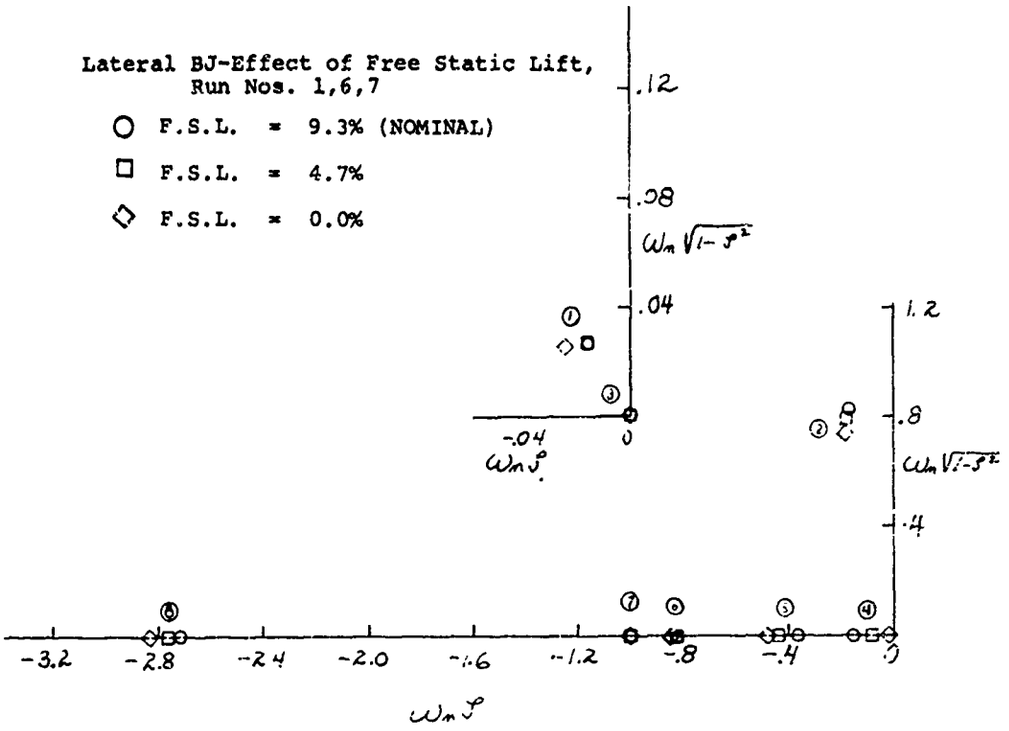
Lateral BJ-Effect of Free Static Lift,
Run Nos. 1,6,7
F.S.L. = 9.3% (NOMINAL)
F.S.L. = 4.7%
F.S.L. = 0.0%
.12
.08
$\omega_n\sqrt{1-\zeta^2}$
.04
1.2
.8
.4
-.04
$\omega_n\zeta$
0
-3.2
-2.8
-2.4
-2.0
-1.6
-1.2
-.8
-.4
0
$\omega_n\zeta$

FIGURE 37

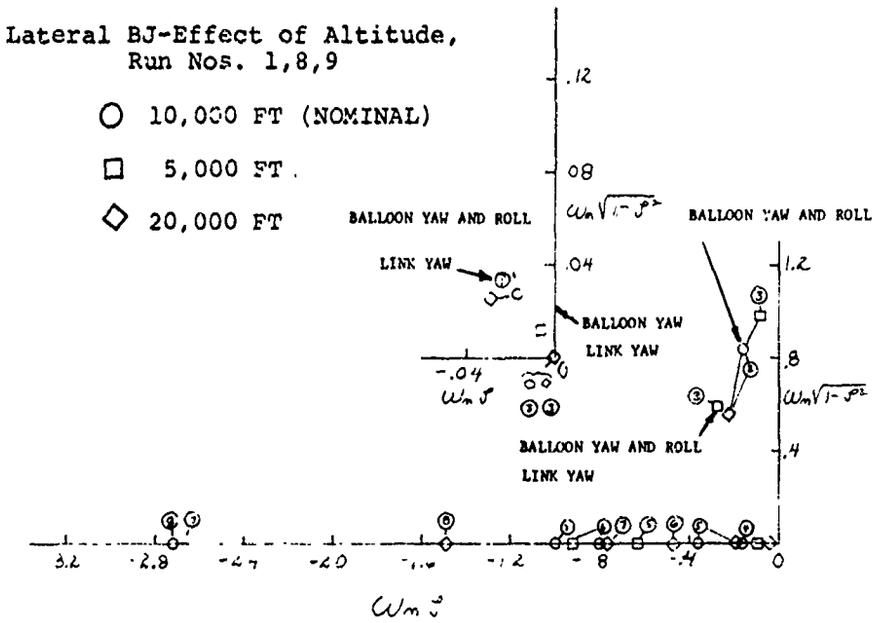

FIGURE 38

LATERAL BJ
EFFECT OF ALTITUDE

MODE NUMBER	DESIGN ALTITUDE		
	5,000 □	10,000 ○	20,000 ◇
1	0	0	0
2	0	0	0
3	0	A	A
4	A	A	A
5	A	A	A
6	A	A	A
7	A	A	A
8	-	A	A

0 - OSCILLATORY
A - APERIODIC

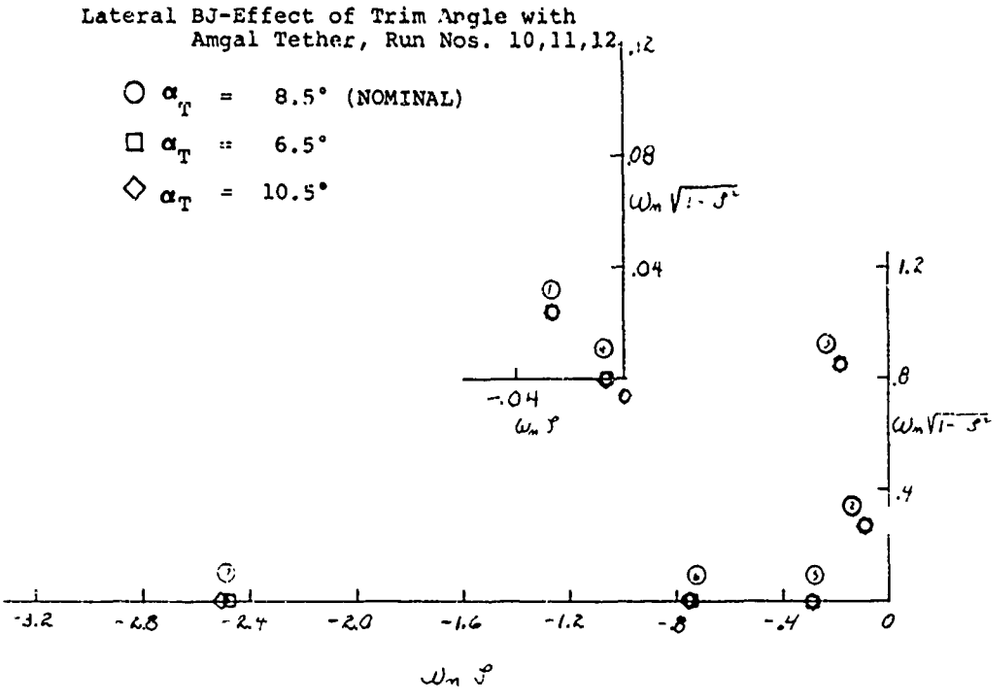

FIGURE 39

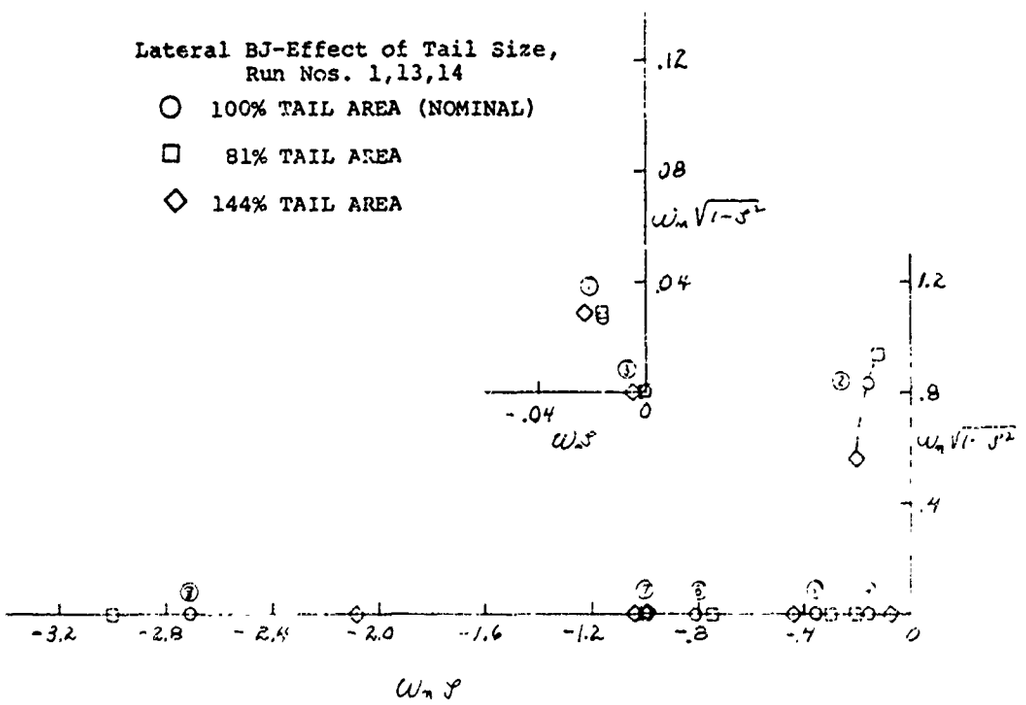

FIGURE 40

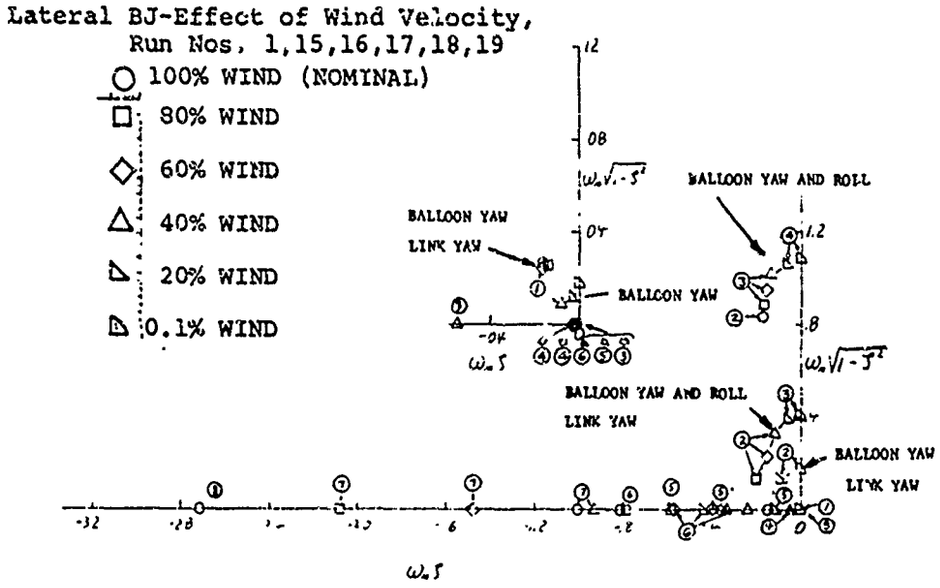

FIGURE 41

LATERAL BJ

EFFECT OF WIND VELOCITY

MODE NUMBER	WIND 100% ○	80% □	60% ◇	40% △	20% ▷	0.1% ▷
1	0	0	0	0	0	0
2	0	0	0	0	0	0
3	A	0	0	0	0	0
4	A	A	A	A	0	0
5	A	A	A	A	A	A
6	A	A	A	A	A	A
7	A	A	A	A	-	-
8	A	-	-	-	-	-

0 - OSCILLATORY
A - APERIODIC

Lateral BJ-Effect of Payload Location,
Run Nos. 1,23,25

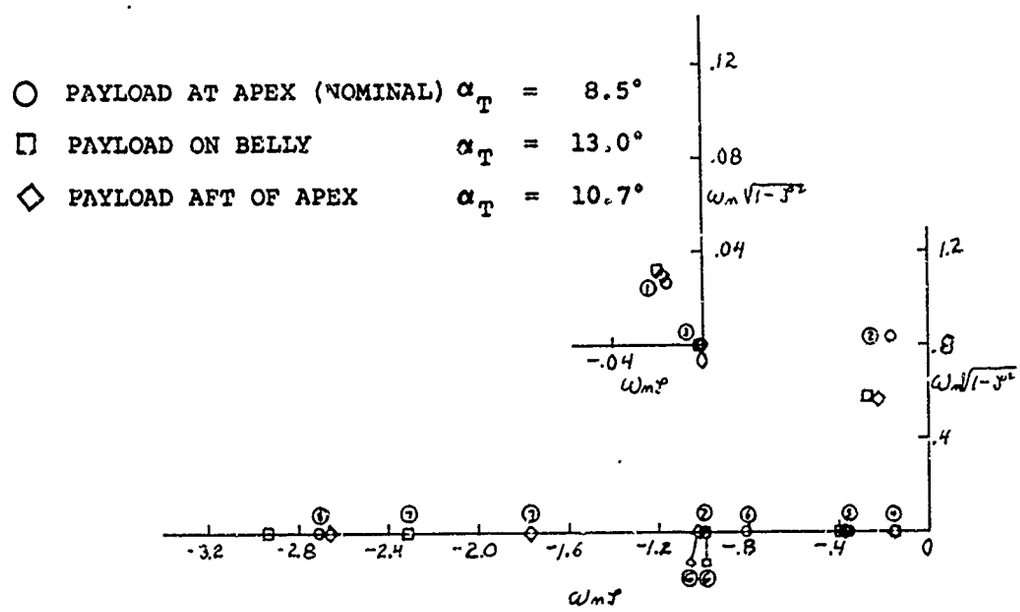

FIGURE 43

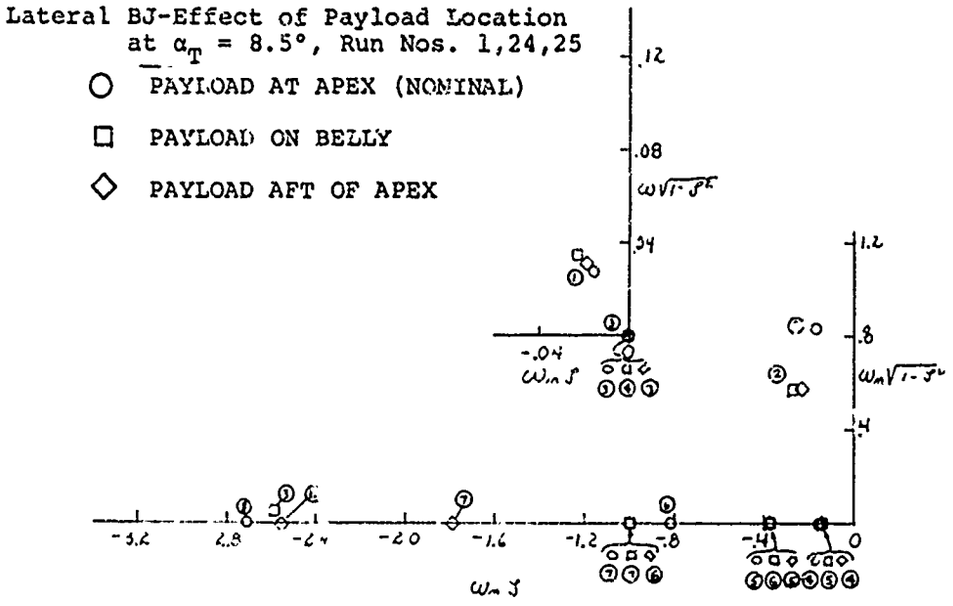

FIGURE 44

LATERAL BJ
EFFECT OF PAYLOAD LOCATION

MODE NUMBER	APEX ○	BELLY □	AFT OF APEX ◇
1	0	C	0
2	0	0	0
3	A	0	A
4	A	A	A
5	A	A	A
6	A	A	A
7	A	A	A
8	A	-	A

0 - OSCILLATORY
A - APERIODIC

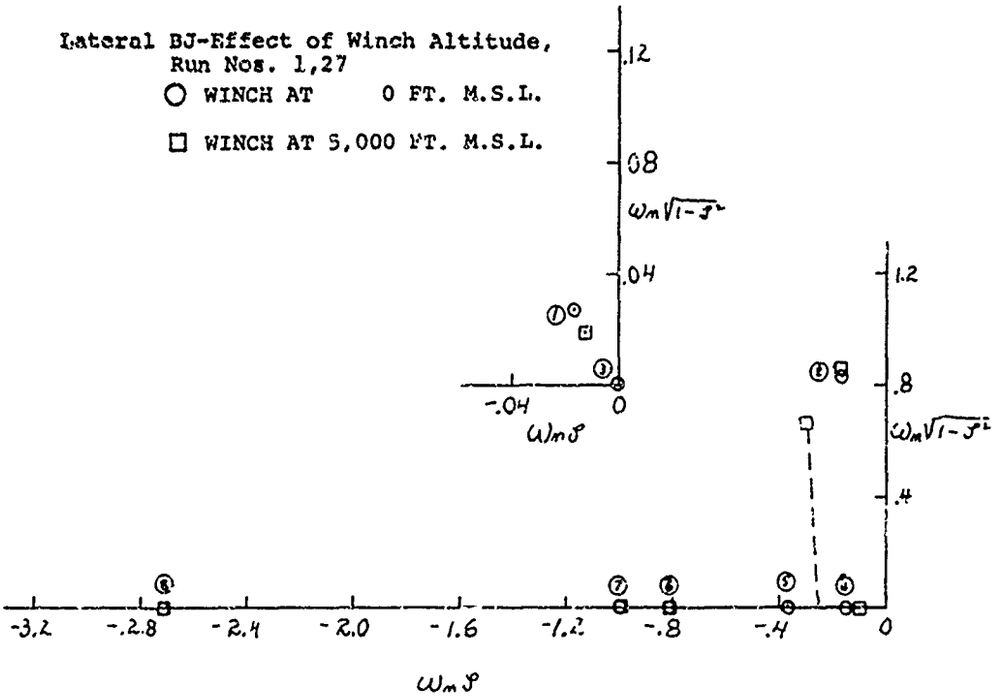

FIGURE 45

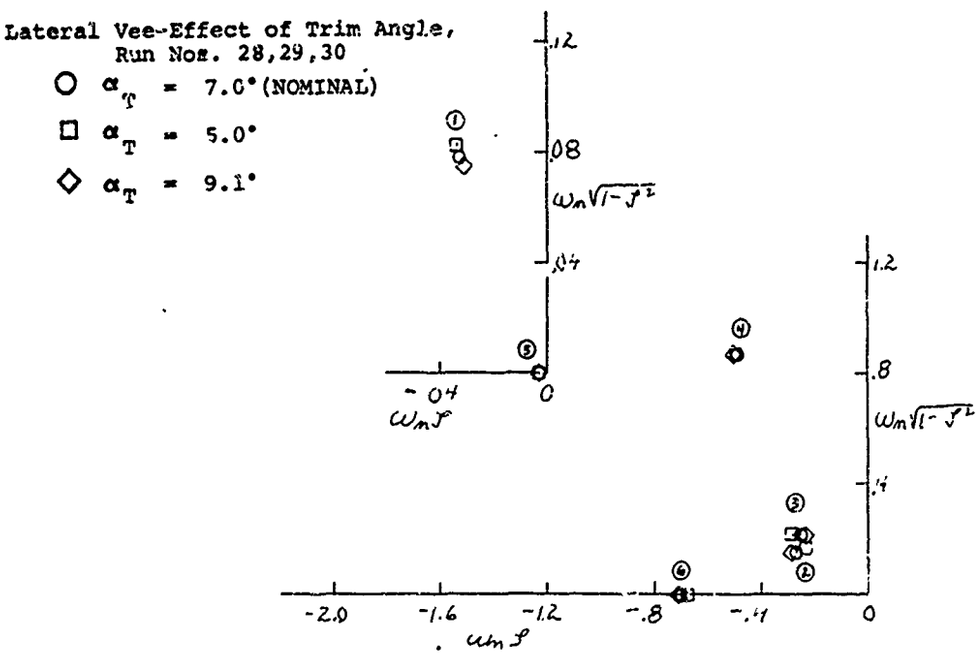

FIGURE 46

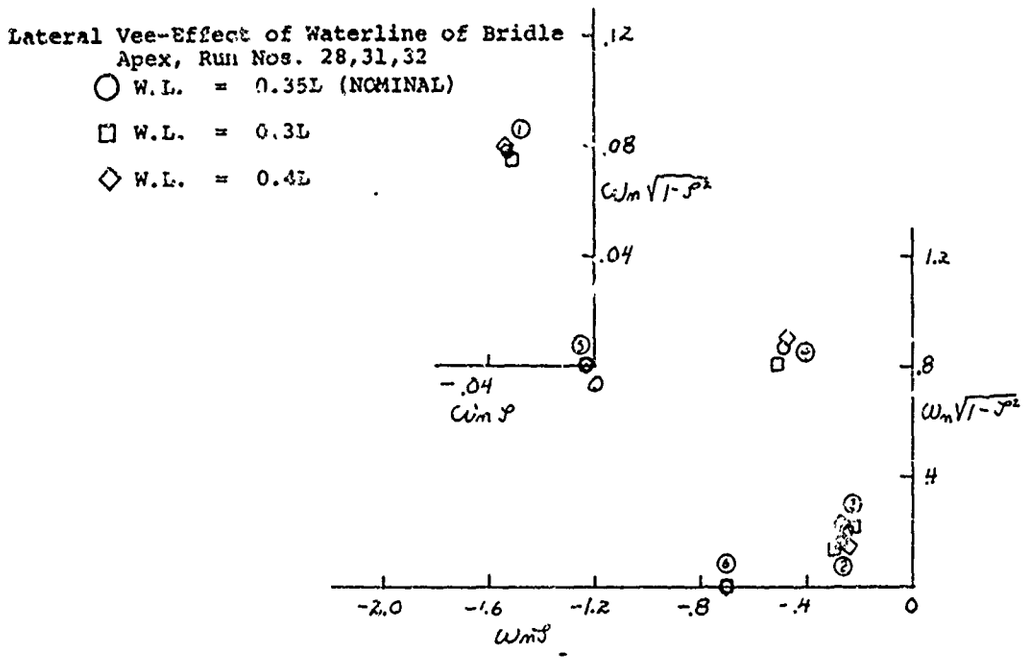

FIGURE 47

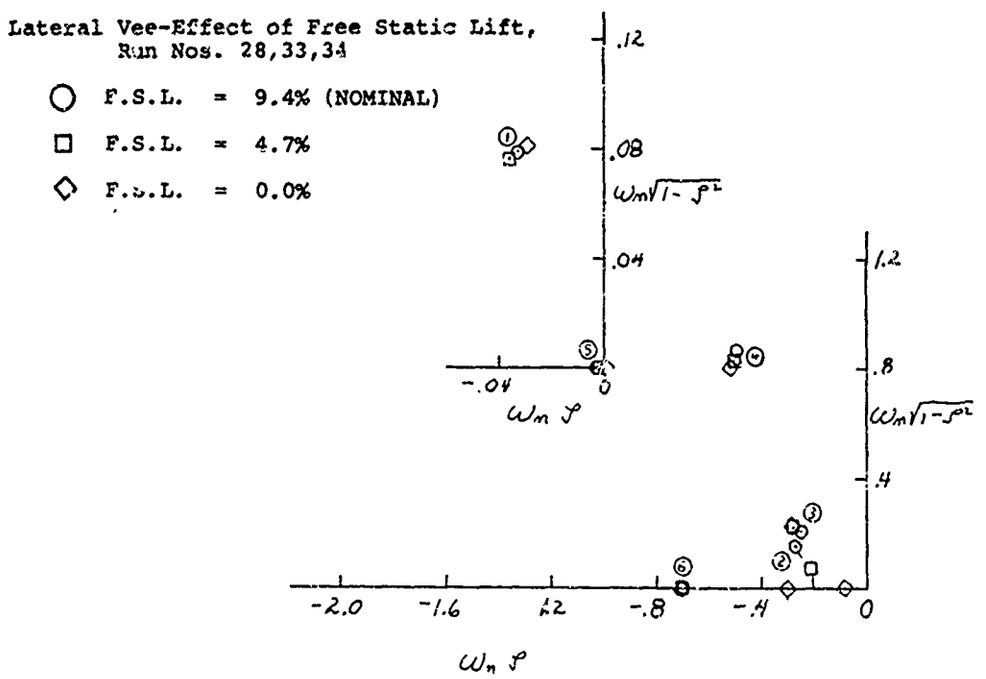

FIGURE 48

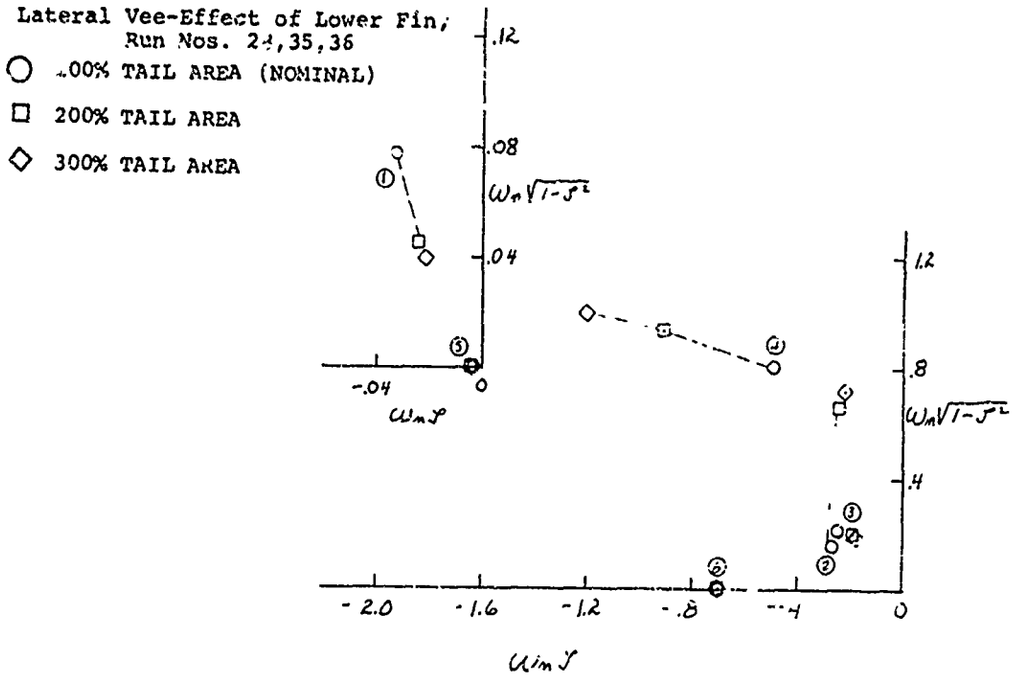

FIGURE 49

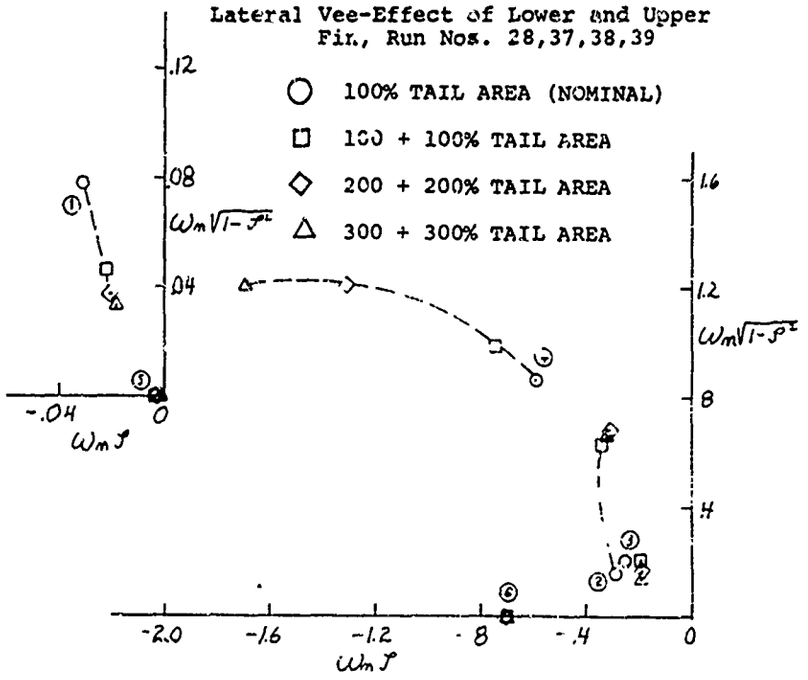

FIGURE 50

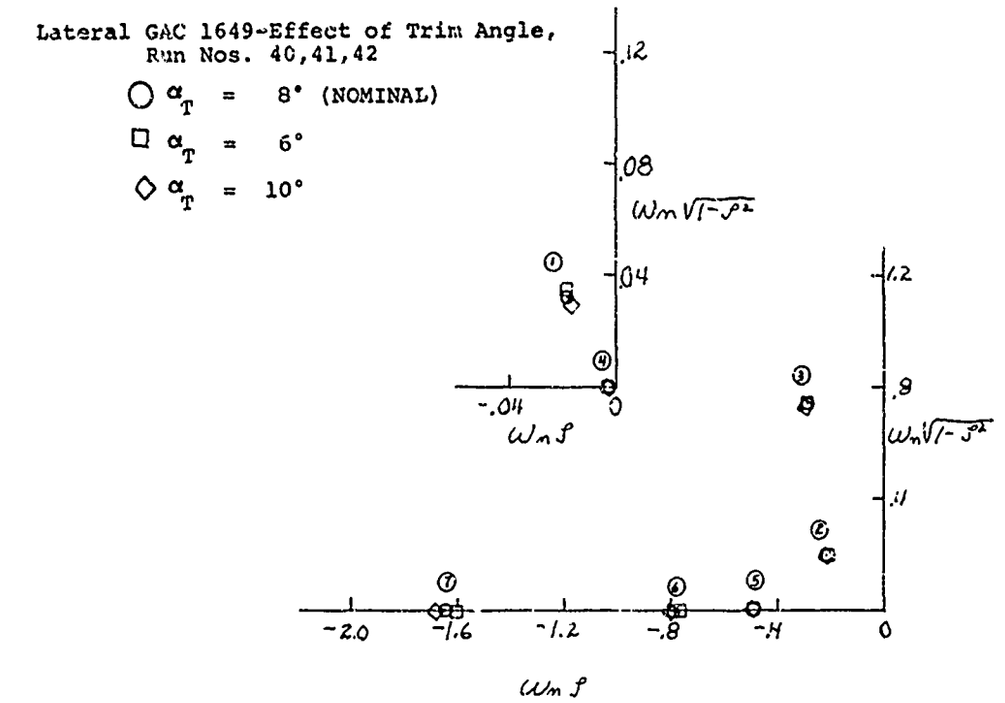

FIGURE 51

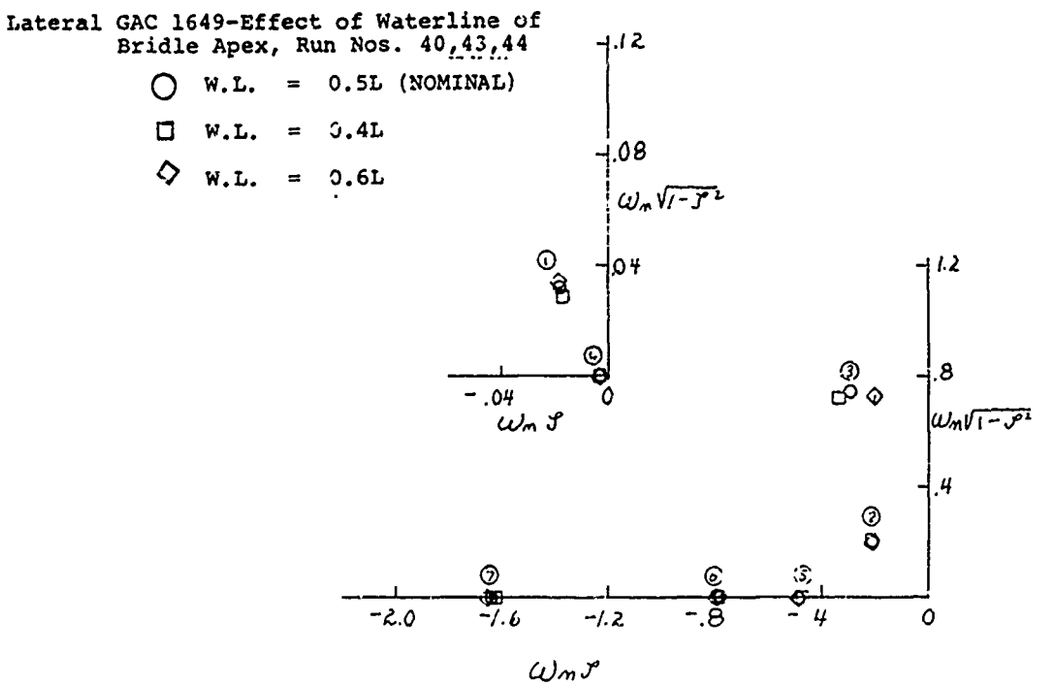

FIGURE 52

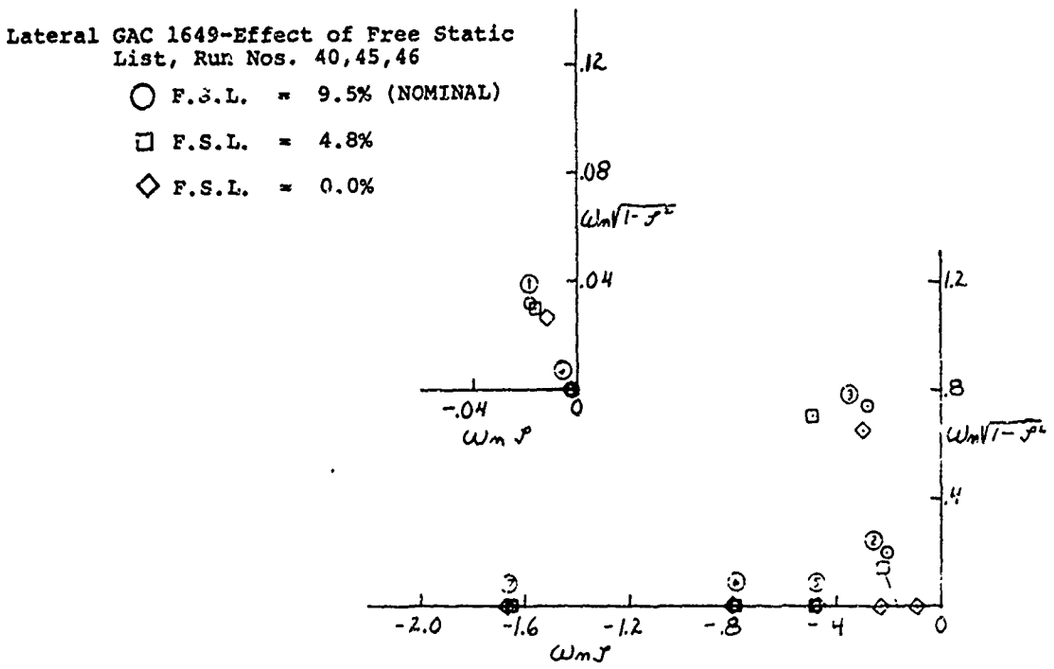
Lateral GAC 1649-Effect of Free Static List, Run Nos. 40,45,46
F.S.L. = 9.5% (NOMINAL)
F.S.L. = 4.8%
F.S.L. = 0.0%
.12
.08
.04
-.04
0
1.2
.8
.4
-2.0
-1.6
-1.2
-.8
-.4
0

FIGURE 53

APPENDIX A

DERIVATION OF THREE DIMENSIONAL EQUATIONS OF MOTION OF A TETHERED BALLOON, AND LONGITUDINAL AND LATERAL CHARACTERISTIC EQUATIONS

TABLE OF CONTENTS

LIST OF ILLUSTRATIONS

SECTION I

INTRODUCTION

This Appendix presents the details of the derivation of the differential equations of motion of a tethered balloon. The derivation is done in three dimensional space with the assumption that all angular velocities are small. It is then assumed for stability analysis that the system is near equilibrium, so that the motion can be described as two independent sets of equations (longitudinal and lateral). From this assumption, two sets of linear equations can be generated and two characteristic equations are formed. By solving for the roots of these characteristic equations, stability information can be generated.

SECTION II

EQUATIONS OF MOTION

1. General

The system is defined as a balloon tethered (by means of a bridle) at the end of a cable which is fixed to a stationary winch at the other end. The position of the winch on a flat non-rotating earth is considered to be the origin of an inertial three-dimensional coordinate system (Figure 54). Also included in the system is a payload situated at the bridle tether connection. The balloon and bridle are assumed to be one rigid body.

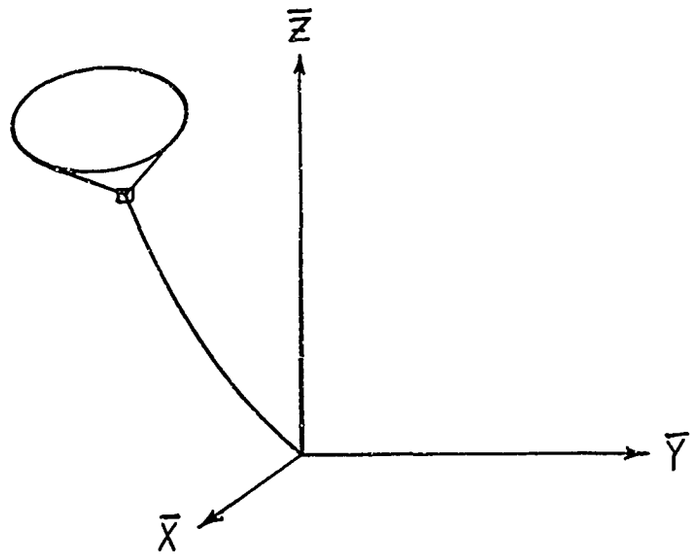

Figure 54. Balloon Tether System

Using Lagrangian techniques, the system can be simulated by five differential equations of motion. The first three equations are the yawing, pitching and rolling motion of the balloon; the last two equations are the pitching and yawing motion of the tether. The rotational motion of the tether about its own centerline is neglected.

Lagrange's differential equation for the system are:

$$\frac{d}{dt}\left(\frac{\partial \bar{T}}{\partial \dot{\psi}}\right) - \frac{\partial \bar{T}}{\partial \psi} = F_{\psi} \tag{1}$$

$$\frac{d}{dt}\left(\frac{\partial \bar{T}}{\partial \dot{\theta}}\right) - \frac{\partial \bar{T}}{\partial \theta} = F_{\theta} \tag{2}$$

$$\frac{d}{dt}\left(\frac{\partial \bar{T}}{\partial \dot{\phi}}\right) - \frac{\partial \bar{T}}{\partial \phi} = F_{\phi} \tag{3}$$

$$\frac{d}{dt}\left(\frac{\partial \bar{T}}{\partial \dot{\rho}_n}\right) - \frac{\partial \bar{T}}{\partial \rho_n} = F_{\rho_n} \tag{4}$$

$$\frac{d}{dt}\left(\frac{\partial \bar{T}}{\partial \dot{\sigma}_n}\right) - \frac{\partial \bar{T}}{\partial \sigma_n} = F_{\sigma_n} \tag{5}$$

where $\bar{T}$ is the total kinetic energy of the system

$\psi, \theta, \phi, \rho_n, \sigma_n$ (r = 1, 2, 3, $\cdots$ N) are generalized coordinates.

$F_{\psi}, F_{\theta}, F_{\phi}, F_{\rho_n}, F_{\sigma_n}$ (r = 1, 2, 3, $\cdots$ N)

are generalized forces

2. Cable Representation

The tether is represented by "N" straight links, each of the same length. The links are considered rigid and connected to each other by frictionless hinges. Therefore,

all forces but no moments may be transferred through the hinges. The angle that each link makes with the horizontal in the longitudinal plane (measured positive for clockwise rotations) is ξ_i (i = 1, 2,•••N). A second rotation σ_i (i = 1, 2,•••N) is given to each link, so that the system may move in the lateral direction. These angles are measured relative to planes parallel to the longitudinal plane. If an observer (located at the winch) looks down range in the direction of the balloon, he will observe a positive angle (σ_i) if the link rotates to his left. Figure 55 shows a schematic of the tether. σ_1 is positive if the first link rotates up out of the plane of the paper (longitudinal plane); σ_2 is positive if the second link rotates up out of a plane parallel to the longitudinal plane. This second plane is defined by a plane parallel to the longitudinal plane and through the end point (P_1) of the first link.

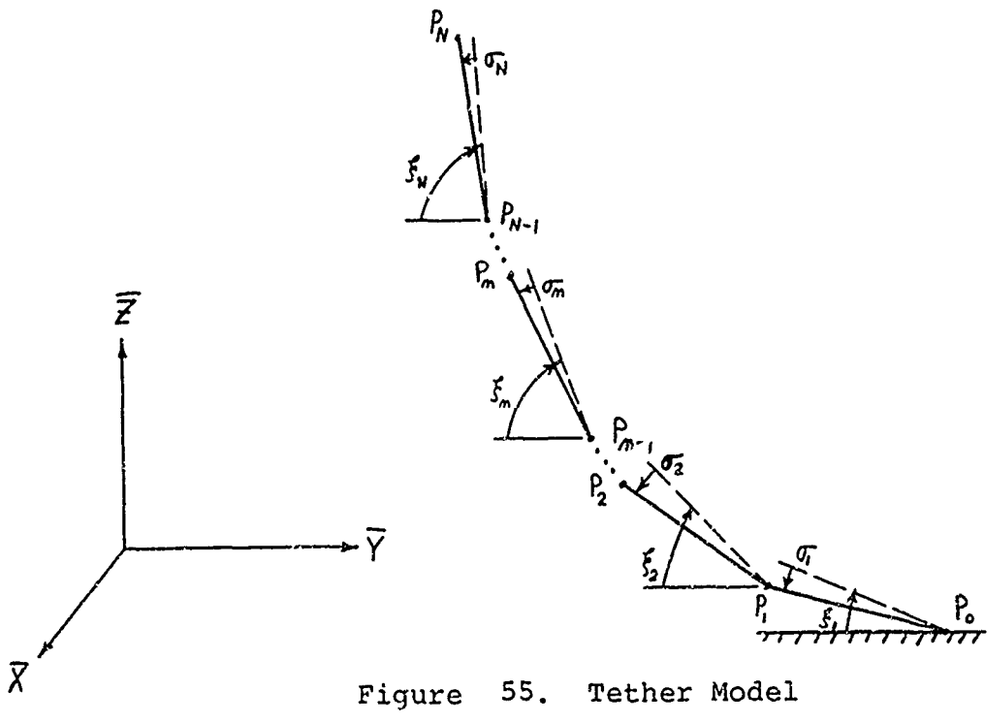

Figure 55. Tether Model

It is assumed that the links of the tether are of constant diameter, and the c.g. of each link is located at the geometric center. To find the position of the link relative to the inertia coordinate system, two rotations are made as shown in Figure 56. The first rotation is a pitch about the $O\bar{X}$ inertia axis such that the negative $O\bar{Y}$ axis rotates into the positive Oe_i axis and the positive $O\bar{Z}$ axis rotates into the positive Oe_i' axis. The second rotation is a yaw about the Oe_i' axis such that Oe_i rotates into Of_i and $O\bar{X}$ rotates into Of_i'.

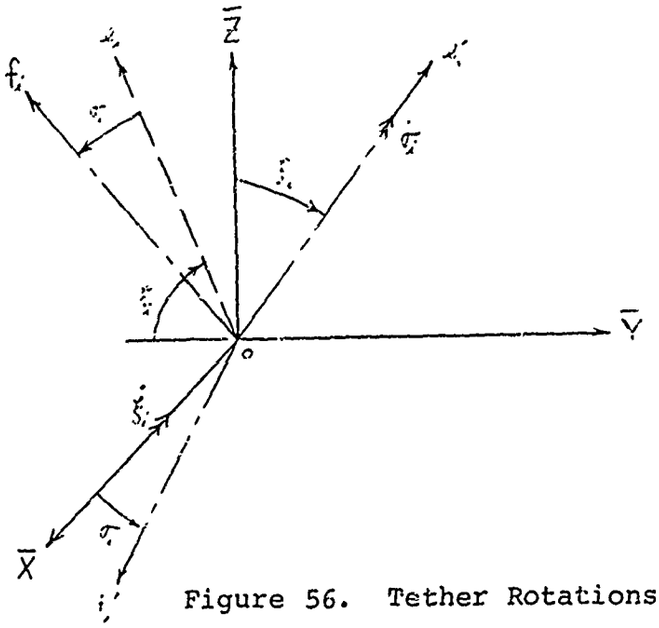

Figure 56. Tether Rotations

The body axis rates are given in terms of the angular rates $\dot{\xi}_i$ and $\dot{\sigma}_i$. The components of $\dot{\xi}_i$ in the body axes coordinates (f_i, f_i', e_i') are:

$$\omega_{\xi_i}\Big)_{f_i} = -\dot{\xi}_i \, s\sigma_i \quad ; \quad \omega_{\xi_i}\Big)_{f_i'} = -\dot{\xi}_i \, c\sigma_i \quad ; \quad \omega_{\xi_i}\Big)_{e_i'} = 0 \tag{6}$$

The components of $\dot{\sigma}_i$ are:

$$\omega_{\sigma_i})_{f_i} = 0 \quad ; \quad \omega_{\sigma_i})_{f_i'} = 0 \quad ; \quad \omega_{\sigma_i})_{e_i'} = \dot{\sigma}_i \tag{7}$$

Note: Throughout this derivation, the letters "s" and "c" will be used for sine and cosine, e.g. $s\sigma_i = \sin\sigma_i$, $c\sigma_i = \cos\sigma_i$.

Adding the components of the angular velocities gives:

$$\omega_{f_i} = -\dot{\xi}_i \, s\sigma_i \tag{8}$$

$$\omega_{f_i'} = -\dot{\xi}_i \, c\sigma_i \tag{9}$$

$$\omega_{e_i'} = \dot{\sigma}_i \tag{10}$$

The angular velocity of the "i" th link is:

$$\vec{\omega}_i = \omega_{f_i} \vec{f}_i + \omega_{f_i'} \vec{f}_i' + \omega_{e_i'} \vec{e}_i' \tag{11}$$

$$\vec{\omega}_i = (-\dot{\xi}_i \, s\sigma_i)\vec{f}_i + (-\dot{\xi}_i \, c\sigma_i)\vec{f}_i' + (\dot{\sigma}_i)\vec{e}_i' \tag{12}$$

Let P_i^* denote the mass center of the "i" th link as shown in Figure 57. It is assumed to be a distance $\ell/2$ from the hinge point P_{i-1}. Since P_1 is fixed to the ground, the velocity of P_1^* is

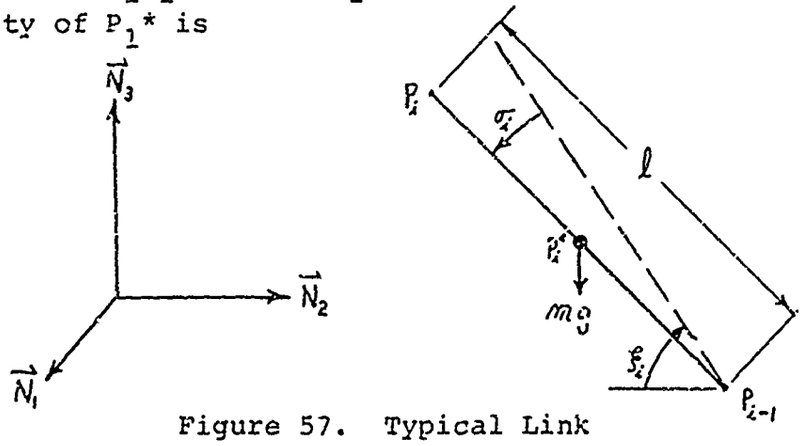

Figure 57. Typical Link

$$\vec{V}^{P_1^*} = \vec{\omega}_1 \times \frac{\ell}{2} \vec{f}_1 \tag{13}$$

$$\vec{V}^{P_1^*} = \left[(-\dot{\beta}_1 s\sigma_1) \vec{f}_1 + (-\dot{\beta}_1 c\sigma_1) \vec{f}_1' + (\dot{\sigma}_1) \vec{e}_1' \right] \times \left[\frac{\ell}{2} \vec{f}_1 \right] \tag{14}$$

$$\vec{V}^{P_1^*} = \frac{\ell}{2} \left[(\dot{\beta}_1 c\sigma_1) \vec{e}_1' + (\dot{\sigma}_1) \vec{f}_1' \right] \tag{15}$$

Also

$$\vec{V}^{P_1} = \ell \left[(\dot{\beta}_1 c\sigma_1) \vec{e}_1' + (\dot{\sigma}_1) \vec{f}_1' \right] \tag{16}$$

In like manner the velocity of P_2^* is:

$$\vec{V}^{P_2^*} = \ell \left[(\dot{\beta}_1 c\sigma_1) \vec{e}_1' + (\dot{\sigma}_1) \vec{f}_1' \right] + \frac{\ell}{2} \left[(\dot{\beta}_2 c\sigma_2) \vec{e}_2' + (\dot{\sigma}_2) \vec{f}_2' \right] \tag{17}$$

In general, the velocity of the "n" th link (geometric center of the "n" link) is given by

$$\vec{V}^{P_m^*} = \ell \left[\sum_{i=1}^{m-1} \left(\dot{\beta}_i c\sigma_i \vec{e}_i' + \dot{\sigma}_i \vec{f}_i' \right) + \frac{1}{2} \left(\dot{\beta}_m c\sigma_m \vec{e}_m' + \dot{\sigma}_m \vec{f}_m' \right) \right] \tag{18}$$

Also

$$\vec{V}^{P_m} = \ell \sum_{i=1}^{m} \left(\dot{\beta}_i c\sigma_i \vec{e}_i' + \dot{\sigma}_i \vec{f}_i' \right) \tag{19}$$

The kinetic energy of a body is given by:

$$T = \frac{1}{2} m v_o^2 + \frac{1}{2} \left[I_x \omega_x^2 + I_y \omega_y^2 + I_z \omega_z^2 \right.$$

$$\left. - 2 I_{xy} \omega_x \omega_y - 2 I_{xz} \omega_x \omega_z - 2 I_{yz} \omega_y \omega_z \right] \tag{20}$$

For the tether $I_{xy} = I_{xz} = I_{yz} = 0$. v_o is the linear inertial space velocity of the c.g. of the link. I_x is the moment of inertia of a link about its center line. Since I_x is small compared to I_y and I_z (moments of inertia of link about an axis normal to its length at the c.g.), it is ignored.

$$I_y = I_z = \frac{m\ell^2}{12} \tag{21}$$

where m is the mass of one link.

The kinetic energy of the tether is then given by;

$$\bar{T}_t = \sum_{n=1}^{N} \left[\frac{1}{2} m \left(\vec{V}^{P_n} \right)^2 + \frac{1}{2} \left(\frac{m\ell^2}{12} \right) \left(\omega_{t_n}^2 + \omega_{\ell_n}^2 \right) \right] \tag{22}$$

Expanding (22)

$$\bar{T}_t = \sum_{n=1}^{N} \left\{ \frac{1}{2} m\ell^2 \left[\sum_{i=1}^{n-1} \left(\dot{\xi}_i C\sigma_i \vec{\ell}_i + \dot{\sigma}_i \vec{f}_i \right) \right. \right.$$

$$\left. \left. + \frac{1}{2} \left(\dot{\xi}_n C\sigma_n \vec{\ell}_n + \dot{\sigma}_n \vec{f}_n \right) \right] + \frac{m\ell^2}{24} \left[\dot{\xi}_n^2 C^2\sigma_n + \dot{\sigma}_n^2 \right] \right\} \tag{23}$$

3. Payload Representation

The velocity of the payload, which is attached to the top of the tether, is:

$$\vec{V}^{P_L} = \ell \sum_{i=1}^{N} \left(\dot{\xi}_i C\sigma_i \vec{\ell}_i + \dot{\sigma}_i \vec{f}_i \right) = \vec{V}^{P_N} \tag{24}$$

Its kinetic energy is:

$$\bar{T}_{PL} = \frac{1}{2} m_{PL} \left(\vec{V}^{P_N} \right)^2 \tag{25}$$

The moment of inertia of the payload is assumed to be negligible.

4. Balloon - Bridle Representation

The shape of the balloon and bridle assembly is completely arbitrary, except that they are considered as one rigid body. Furthermore, it is assumed that all of the bridle lines are in tension. This restricts the angular displacements of the balloon to less than large angles, where the maximum angle depends on the balloon-bridle configuration. The balloon is assumed to have "directional masses" M_L, M_V, M_S in the direction of the longitudinal, vertical and lateral axes respectively. The "directional masses" are assumed to be concentrated at the apparent mass center of the balloon (Q). In general, the apparent mass center (c.m.) is different from the center of gravity (c.g.). Included in the "directional masses" are the weight of the balloon-bridle, the lifting gas, and the added air mass being accelerated by the balloon's motion.

In order to determine the balloon's attitude with respect to a fixed set of coordinates ($\bar{X}$, $\bar{Y}$, $\bar{Z}$), three angular displacements are made as shown in Figure 58. The three successive angular rotations are yaw ($\dot{\psi}$ about the inertia $Q\bar{Z}$ axis), pitch ($\dot{\theta}$ about the line of nodes QN) and roll ($\dot{\phi}$ about the longitudinal body axis $Q\bar{X}_B$). In Figure 58 the angles ψ, θ, ϕ determine the orientation of the right-handed body triad $\bar{X}_B$, $\bar{Y}_B$, $\bar{Z}_B$ with respect to the right-handed inertial triad $\bar{X}$, $\bar{Y}$, $\bar{Z}$.

First yaw (ψ) about axis $Q\bar{Z}$ such that $Q\bar{X}$ and $Q\bar{Y}$ rotate into QN and Qa respectively. The second rotation is a pitch (θ) about the line of nodes, QN, such that Qa rotates into $Q\bar{Y}_B$ and $Q\bar{Z}$ rotates into Qb. The final rotation is a roll (ϕ) such that Qb rotates into $Q\bar{Z}_B$ and QN rotates into $Q\bar{X}_B$.

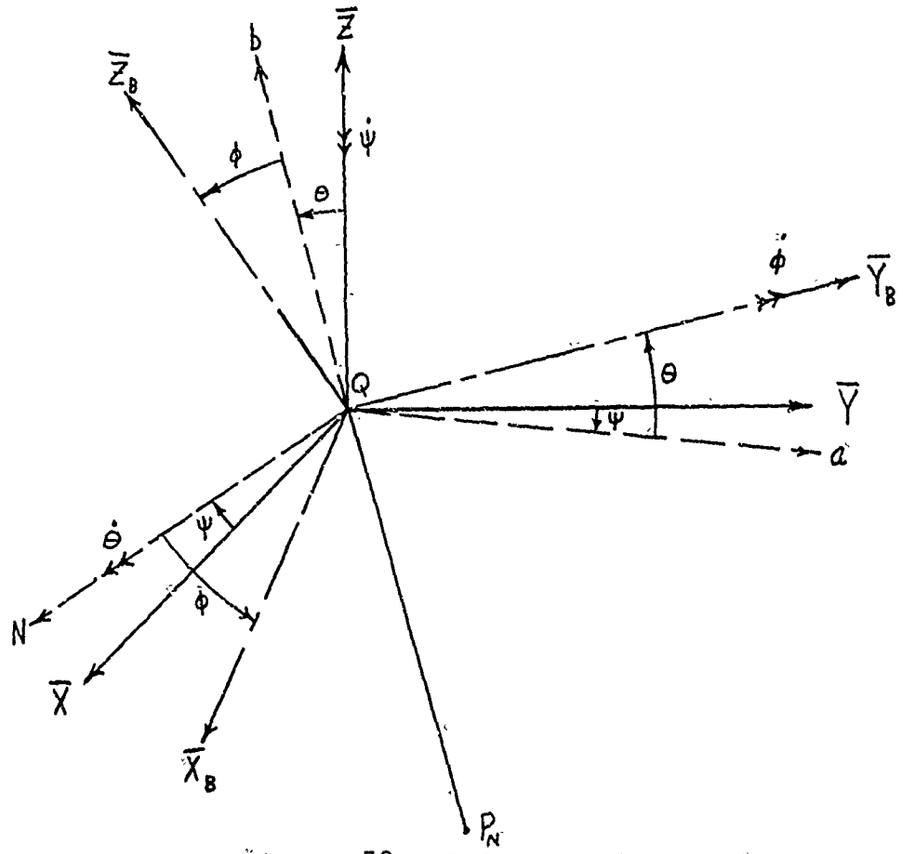

Figure 58. Balloon Euler Angles

The body axes rates (ω_{XB}, ω_{YB}, ω_{ZB}, are given in terms of the Euler angle rates ($\dot{\psi}$, $\dot{\theta}$, $\dot{\phi}$). The components of $\dot{\psi}$ in the $\bar{X}_B$ $\bar{Y}_B$ $\bar{Z}_B$ coordinate system are:

$$\omega_{\psi})_{xB} = \dot{\psi}\, s\phi\, c\theta \quad , \quad \omega_{\psi})_{yB} = -\dot{\psi}\, s\theta \quad , \quad \omega_{\psi})_{zB} = -\dot{\psi}\, c\theta\, c\phi \tag{26}$$

The components of $\dot{\theta}$ are:

$$\omega_{\theta})_{xB} = \dot{\theta}\, c\phi \quad , \quad \omega_{\theta})_{yB} = 0 \quad , \quad \omega_{\theta})_{zB} = \dot{\theta}\, s\phi \tag{27}$$

The components of $\dot{\phi}$ are:

$$\omega_{\phi})_{xB} = 0 \quad , \quad \omega_{\phi})_{yB} = \dot{\phi} \quad , \quad \omega_{\phi})_{zB} = 0 \tag{28}$$

Adding the components of the angular velocities gives:

$$\omega_{xB} = \dot{\psi}\, s\phi\, c\theta + \dot{\theta}\, c\phi \tag{29}$$

$$\omega_{yB} = -\dot{\psi}\, s\theta + \dot{\phi} \tag{30}$$

$$\omega_{zB} = -\dot{\psi}\, c\theta\, c\phi + \dot{\theta}\, s\phi \tag{31}$$

The angular velocity of the balloon about its dynamic mass center is:

$$\vec{\omega} = \omega_{xB}\,\vec{i}_B + \omega_{yB}\,\vec{j}_B + \omega_{zB}\,\vec{k}_B \tag{32}$$

$$\vec{\omega} = (\dot{\psi}\, s\phi\, c\theta + \dot{\theta} c\phi)\,\vec{i}_B + (-\dot{\psi}\, s\theta + \dot{\phi})\,\vec{j}_B + (-\dot{\psi}\, c\theta\, c\phi + \dot{\theta}\, s\phi)\,\vec{k}_B \tag{33}$$

where $\vec{i}_B$, $\vec{j}_B$, and $\vec{k}_B$ are unit vectors along the lateral ($\bar{X}_B$), longitudinal, ($\bar{Y}_B$), and vertical ($\bar{z}_B$) body axes of the balloon.

The location of the bridle apex point is defined with respect to the dynamic mass center as:

$$\vec{\rho} = R_{jm}\,\vec{j}_B + R_{km}\,\vec{k}_B \tag{34}$$

Equation (34) assumes that the bridle apex point is in the $\bar{Y}_B$ $\bar{z}_B$ plane. The velocity of the apex of the bridle with respect to the balloon's dynamic mass center is:

$$\vec{V}_a = \vec{\omega} \times \vec{\rho} \tag{35}$$

The velocity of the balloon's dynamic mass center with respect to the apex of the bridle is:

$$\vec{V}_B = -\vec{\omega} \times \vec{\rho} = \vec{\rho} \times \vec{\omega} \tag{36}$$

The total translational velocity of the dynamic mass center of the balloon with respect to the winch is given by the sum of Equations (24) and (36) with contributions from Equations (33) and (34).

$$\vec{V}^a = \ell \sum_{i=1}^{N} \left(\dot{\xi}_i c\sigma_i \vec{e}_i + \dot{\sigma}_i \vec{f}_i \right) + \left[R_{jm} \vec{j}_B + R_{km} \vec{k}_B \right] \times \left[(\dot{\psi} s\phi c\theta + \dot{\theta} c\phi) \vec{i}_B + (-\dot{\psi} s\theta + \dot{\phi}) \vec{j}_B + (-\dot{\psi} c\theta c\phi + \dot{\theta} s\phi) \vec{k}_B \right] \tag{37}$$

$$\vec{V}^a = \ell \sum_{i=1}^{N} \left(\dot{\xi}_i c\sigma_i \vec{e}_i + \dot{\sigma}_i \vec{f}_i \right) + \left[R_{jm} (-\dot{\psi} c\theta c\phi + \dot{\theta} s\phi) - R_{km} (-\dot{\psi} s\theta + \dot{\phi}) \right] \vec{i}_B + \left[R_{km} (\dot{\psi} s\phi c\theta + \dot{\theta} c\phi) \right] \vec{j}_B + \left[-R_{jm} (\dot{\psi} s\phi c\theta + \dot{\theta} c\phi) \right] \vec{k}_B \tag{38}$$

The general expression for the kinetic energy of a body is given by Equation (20). For the balloon it is assumed that $I_{xy} = I_{xz} = 0$. The kinetic energy of the balloon-bridle is:

$$T_B = \frac{1}{2} M_s (\vec{V}^a \cdot \vec{i}_B)^2 + \frac{1}{2} M_L (\vec{V}^a \cdot \vec{j}_B)^2 + \frac{1}{2} M_v (\vec{V}^a \cdot \vec{k}_B)^2 + \frac{1}{2} \left[I_{XB} \omega_{XB}^2 + I_{YB} \omega_{YB}^2 + I_{ZB} \omega_{ZB}^2 - 2 I_{YZB} \omega_{YB} \omega_{ZB} \right] \tag{39}$$

In Equation (39) $\vec{V}^a$ is given by Equation (38) and ω_{XB}, ω_{YB}, and ω_{ZB} are given in Equation (33). I_{XB}, I_{YB}, I_{ZB}, and I_{YZB} are apparent moments and product of inertia of the balloon referenced to its body axes $\bar{X}_B$ $\bar{Y}_B$ $\bar{Z}_B$. Substituting into Equation (39) the Euler angle rates equivalent to ω_{XB}, ω_{YB}, ω_{ZB} gives:

$$T_B = \frac{1}{2} M_s (\vec{V}^a \cdot \vec{i}_B)^2 + \frac{1}{2} M_L (\vec{V}^a \cdot \vec{j}_B)^2 + \frac{1}{2} M_v (\vec{V}^a \cdot \vec{k}_B)^2$$

$$+\frac{1}{2}\Big\{\dot{\psi}^2\big[C^2\theta(I_{xB}S^2\phi + I_{zB}C^2\phi) + S^2\theta I_{yB} - S2\theta C\phi I_{yzB}\big] + \dot{\phi}^2\big[I_{yB}\big]$$

$$+\dot{\theta}^2\big[I_{xB}C^2\phi + I_{zB}S^2\phi\big] + \dot{\psi}\dot{\theta}\big[S2\phi\, C\theta(I_{xB}-I_{zB}) + 2S\phi S\theta I_{yzB}\big]$$

$$+\dot{\psi}\dot{\phi}\big[-2I_{yB}S\theta + 2I_{yzB}C\theta C\phi\big] + \dot{\theta}\dot{\phi}\big[-2I_{yzB}S\phi\big]\Big\} \qquad (40)$$

5. Inertia Terms

The total kinetic energy of the system is given by the sum of the Equations (23), (25) and (40).

$$T = \sum_{m=1}^{N}\Big[\frac{1}{2}m(\vec{V}^{P_m^a})^2 + \frac{ml^2}{24}(\dot{\xi}_m^2 C^2\sigma_m + \dot{\sigma}_m^2)\Big] + \frac{1}{2}m_{PL}(\vec{V}^{P_L})^2$$

$$+\frac{1}{2}M_S(\vec{V}^a\cdot\vec{i}_a)^2 + \frac{1}{2}M_L(\vec{V}^a\cdot\vec{j}_a)^2 + \frac{1}{2}M_V(\vec{V}^a\cdot\vec{k}_a)^2$$

$$+\frac{1}{2}\Big\{\dot{\psi}^2\big[C^2\theta(I_{xB}S^2\phi + I_{zB}C^2\phi) + S^2\theta I_{yB} - S2\theta C\phi I_{yzB}\big] + \dot{\phi}^2\big[I_{yB}\big]$$

$$+\dot{\theta}^2\big[I_{xB}C^2\phi + I_{zB}S^2\phi\big] + \dot{\psi}\dot{\theta}\big[S2\phi\, C\theta(I_{xB}-I_{zB}) + 2S\phi S\theta I_{yzB}\big]$$

$$+\dot{\psi}\dot{\phi}\big[-2I_{yB}S\theta + 2I_{yzB}C\theta C\phi\big] + \dot{\theta}\dot{\phi}\big[-2I_{yzB}S\phi\big]\Big\} \qquad (41)$$

The differential equations of motion are found by operating on Equation (41) with Equations (1) to (5). But before continuing the derivation, an important observation can be made at this point. Due to the size of the system, its response to a disturbance will be slow. Consequently, it will be assumed that all angular velocities are small and products of angular velocities will be negligible. The immediate effect of this assumption is that the second term in Lagrange's equation is zero. It should also be

noted that many terms will be ignored when operating on the kinetic energy with the first term of Lagrange's equation.

It will be necessary to establish relations between the unit vectors $\vec{e}_i$, $\vec{e}_i'$, $\vec{f}_i$, and $\vec{f}_i'$, and the unit vectors $\vec{i}_B$, $\vec{j}_B$, and $\vec{k}_B$. This can be done by referencing both sets of unit vectors to the inertia reference $\bar{X}$, $\bar{Y}$, $\bar{Z}$ which has unit vectors $\vec{N}_1$, $\vec{N}_2$, $\vec{N}_3$ respectively. Referring to Figure 56, the link vectors can be expressed. The first rotation is a pitch about the negative $O\bar{X}$ axis.

$$\begin{Bmatrix} \vec{N}_1 \\ \vec{e}_i' \\ \vec{e}_i \end{Bmatrix} = \begin{bmatrix} 1 & 0 & 0 \\ 0 & S\varphi_i & C\varphi_i \\ 0 & -C\varphi_i & S\varphi_i \end{bmatrix} \begin{Bmatrix} \vec{N}_1 \\ \vec{N}_2 \\ \vec{N}_3 \end{Bmatrix} \tag{42}$$

The second rotation is about the positive Oe_i' axis.

$$\begin{Bmatrix} \vec{e}_i' \\ \vec{f}_i \\ \vec{f}_i' \end{Bmatrix} = \begin{bmatrix} 0 & 1 & 0 \\ S\sigma_i & 0 & C\sigma_i \\ C\sigma_i & 0 & -S\sigma_i \end{bmatrix} \begin{Bmatrix} \vec{N}_1 \\ \vec{e}_i' \\ \vec{e}_i \end{Bmatrix} \tag{43}$$

Substituting Equation (42) into (43) gives

$$\begin{Bmatrix} \vec{e}_i' \\ \vec{f}_i \\ \vec{f}_i' \end{Bmatrix} = \begin{bmatrix} 0 & 1 & 0 \\ S\sigma_i & 0 & C\sigma_i \\ C\sigma_i & 0 & -S\sigma_i \end{bmatrix} \begin{bmatrix} 1 & 0 & 0 \\ 0 & S\varphi_i & C\varphi_i \\ 0 & -C\varphi_i & S\varphi_i \end{bmatrix} \begin{Bmatrix} \vec{N}_1 \\ \vec{N}_2 \\ \vec{N}_3 \end{Bmatrix} \tag{44}$$

$$\begin{Bmatrix} \vec{e}_i' \\ \vec{f}_i \\ \vec{f}_i' \end{Bmatrix} = \begin{bmatrix} 0 & S\varphi_i & C\varphi_i \\ S\sigma_i & -C\sigma_i C\varphi_i & C\sigma_i S\varphi_i \\ C\sigma_i & S\sigma_i C\varphi_i & -S\sigma_i S\varphi_i \end{bmatrix} \begin{Bmatrix} \vec{N}_1 \\ \vec{N}_2 \\ \vec{N}_3 \end{Bmatrix} \tag{45}$$

Referring to Figure 58, the balloon's unit vectors can be expressed. The first rotation is about the negative $Q\bar{Z}$ axis or the negative $\vec{N}_3$ unit vector.

$$\begin{Bmatrix} \vec{N}_3 \\ \vec{QN} \\ \vec{Qa} \end{Bmatrix} = \begin{bmatrix} 0 & 0 & 1 \\ C\psi & -S\psi & 0 \\ S\psi & C\psi & 0 \end{bmatrix} \begin{Bmatrix} \vec{N}_1 \\ \vec{N}_2 \\ \vec{N}_3 \end{Bmatrix} \tag{46}$$

The second rotation is about the positive $\vec{QN}$ axis.

$$\begin{Bmatrix} \vec{Qb} \\ \vec{j}_B \\ \vec{QN} \end{Bmatrix} = \begin{bmatrix} C\theta & 0 & -S\theta \\ S\theta & 0 & C\theta \\ 0 & 1 & 0 \end{bmatrix} \begin{Bmatrix} \vec{N}_3 \\ \vec{QN} \\ \vec{Qa} \end{Bmatrix} \tag{47}$$

The third rotation is about the positive $\vec{j}_B$ axis,

$$\begin{Bmatrix} \vec{i}_B \\ \vec{j}_B \\ \vec{k}_B \end{Bmatrix} = \begin{bmatrix} -S\phi & 0 & C\phi \\ 0 & 1 & 0 \\ C\phi & 0 & S\phi \end{bmatrix} \begin{Bmatrix} \vec{Qb} \\ \vec{j}_B \\ \vec{QN} \end{Bmatrix} \tag{48}$$

Substituting Equation (46) into (47) and (47) into (48) gives:

$$\begin{Bmatrix} \vec{i}_B \\ \vec{j}_B \\ \vec{k}_B \end{Bmatrix} = \begin{bmatrix} -S\phi & 0 & C\phi \\ 0 & 1 & 0 \\ C\phi & 0 & S\phi \end{bmatrix} \begin{bmatrix} C\theta & 0 & -S\theta \\ S\theta & 0 & C\theta \\ 0 & 1 & 0 \end{bmatrix} \begin{bmatrix} 0 & 0 & 1 \\ C\psi & -S\psi & 0 \\ S\psi & C\psi & 0 \end{bmatrix} \begin{Bmatrix} \vec{N}_1 \\ \vec{N}_2 \\ \vec{N}_3 \end{Bmatrix} \tag{49}$$

$$\begin{Bmatrix} \vec{i}_B \\ \vec{j}_B \\ \vec{k}_B \end{Bmatrix} = \begin{bmatrix} -S\phi & 0 & C\phi \\ 0 & 1 & 0 \\ C\phi & 0 & S\phi \end{bmatrix} \begin{bmatrix} -S\theta S\psi & -S\theta C\psi & C\theta \\ C\theta S\psi & C\theta C\psi & S\theta \\ C\psi & -S\psi & 0 \end{bmatrix} \begin{Bmatrix} \vec{N}_1 \\ \vec{N}_2 \\ \vec{N}_3 \end{Bmatrix} \tag{50}$$

$$\begin{Bmatrix} \vec{i}_B \\ \vec{j}_B \\ \vec{k}_B \end{Bmatrix} = \begin{bmatrix} S\phi S\theta S\psi + C\phi C\psi & S\phi S\theta C\psi - C\phi S\psi & -S\phi C\theta \\ C\theta S\psi & C\theta C\psi & S\theta \\ -C\phi S\theta S\psi + S\phi C\psi & -C\phi S\theta C\psi - S\phi S\psi & C\phi C\theta \end{bmatrix} \begin{Bmatrix} \vec{N}_1 \\ \vec{N}_2 \\ \vec{N}_3 \end{Bmatrix} \tag{51}$$

Matrix Equations (45) and (51) give the relation between the link unit vectors and the inertia frame, and the balloon unit vectors and the inertia frame. The following dot products will be needed.

$$\vec{f}_i \cdot \vec{i}_B = S\sigma_i (S\phi S\theta S\psi + C\phi C\psi) - C\sigma_i C\xi_i (S\phi S\theta C\psi - C\phi S\psi) + C\sigma_i S\xi_i (-S\phi C\theta) \quad (52)$$

$$\vec{f}_i \cdot \vec{j}_B = S\sigma_i (C\theta S\psi) - C\sigma_i C\xi_i (C\theta C\psi) + C\sigma_i S\xi_i (S\theta) \quad (53)$$

$$\vec{f}_i \cdot \vec{k}_B = S\sigma_i (-C\phi S\theta S\psi + S\phi C\psi) - C\sigma_i C\xi_i (-C\phi S\theta C\psi - S\phi S\psi) + C\sigma_i S\xi_i (C\phi C\theta) \quad (54)$$

$$\vec{f}_i' \cdot \vec{i}_B = C\sigma_i (S\phi S\theta S\psi + C\phi C\psi) + S\sigma_i C\xi_i (S\phi S\theta C\psi - C\phi S\psi) - S\sigma_i S\xi_i (-S\phi C\theta) \quad (55)$$

$$\vec{f}_i' \cdot \vec{j}_B = C\sigma_i (C\theta S\psi) + S\sigma_i C\xi_i (C\theta C\psi) - S\sigma_i S\xi_i (S\theta) \quad (56)$$

$$\vec{f}_i' \cdot \vec{k}_B = C\sigma_i (-C\phi S\theta S\psi + S\phi C\psi) + S\sigma_i C\xi_i (-C\phi S\theta C\psi - S\phi S\psi) - S\sigma_i S\xi_i (C\phi C\theta) \quad (57)$$

$$\vec{e}_i \cdot \vec{i}_B = S\xi_i (S\phi S\theta C\psi - C\phi S\psi) + C\xi_i (-S\phi C\theta) \quad (58)$$

$$\vec{e}_i \cdot \vec{j}_B = S\xi_i (C\theta C\psi) + C\xi_i (S\theta) \quad (59)$$

$$\vec{e}_i \cdot \vec{k}_B = S\xi_i (-C\phi S\theta C\psi - S\phi S\psi) + C\xi_i (C\phi C\theta) \quad (60)$$

Also from Equations (42) and (51):

$$\vec{e}_i \cdot \vec{i}_B = -C\xi_i (S\phi S\theta C\psi - C\phi S\psi) + S\xi_i (-S\phi C\theta) \quad (61)$$

$$\vec{e}_i \cdot \vec{j}_B = -C\xi_i (C\theta C\psi) + S\xi_i (S\theta) \quad (62)$$

$$\vec{e}_i \cdot \vec{k}_B = -C\xi_i (-C\phi S\theta C\psi - S\phi S\psi) + S\xi_i (C\phi C\theta) \quad (63)$$

Now operate on Equation (41) with Equation (1).

$$\frac{\partial \bar{T}}{\partial \dot{\psi}} = M_S(\vec{V}^a \cdot \vec{i}_B)\left(\frac{\partial \vec{V}^a}{\partial \dot{\psi}} \cdot \vec{i}_B\right) + M_L(\vec{V}^a \cdot \vec{j}_B)\left(\frac{\partial \vec{V}^a}{\partial \dot{\psi}} \cdot \vec{j}_B\right)$$

$$+ M_V(\vec{V}^a \cdot \vec{k}_B)\left(\frac{\partial \vec{V}^a}{\partial \dot{\psi}} \cdot \vec{k}_B\right) + \dot{\psi}\left[c^2\theta\left(I_{xB}s^2\phi + I_{zB}c^2\phi\right) + s^2\theta\, I_{yB}\right.$$

$$\left. - s2\theta\, c\phi\, I_{yzB}\right] + \dot{\theta}\left[\tfrac{1}{2}s2\phi\, c\theta\left(I_{xB} - I_{zB}\right) + s\phi\, s\theta\, I_{yzB}\right]$$

$$+ \dot{\phi}\left[-I_{yB}s\theta + I_{yzB}c\theta\, c\phi\right] \qquad (64)$$

From Equation (38):

$$\frac{\partial \vec{V}^a}{\partial \dot{\psi}} = \left(-R_{jm}c\theta c\phi + R_{km}s\theta\right)\vec{i}_B + \left(R_{km}s\phi c\theta\right)\vec{j}_B + \left(-R_{jm}s\phi c\theta\right)\vec{k}_B \qquad (65)$$

The dot products in Equation (64) are:

$$\vec{V}^a \cdot \vec{i}_B = \ell\sum_{i=1}^{N}\left\{\dot{\xi}_i c\sigma_i\left[s\xi_i\left(s\phi s\theta c\psi - c\phi s\psi\right) + c\xi_i\left(-s\phi c\theta\right)\right]\right.$$

$$+ \dot{\sigma}_i\left[c\sigma_i\left(s\phi s\theta s\psi + c\phi c\psi\right) + s\sigma_i c\xi_i\left(s\phi s\theta c\psi - c\phi s\psi\right)\right.$$

$$\left.\left. + s\sigma_i s\xi_i\left(s\phi c\theta\right)\right]\right\} + \left[R_{jm}\left(-\dot{\psi}c\theta c\phi + \dot{\theta}s\phi\right) - R_{km}\left(-\dot{\psi}s\theta + \dot{\phi}\right)\right] \qquad (66)$$

$$\vec{V}^a \cdot \vec{j}_B = \ell\sum_{i=1}^{N}\left\{\dot{\xi}_i c\sigma_i\left[s\xi_i\left(c\theta c\psi\right) + c\xi_i\left(s\theta\right)\right] + \dot{\sigma}_i\left[c\sigma_i\left(c\theta s\psi\right)\right.\right.$$

$$\left.\left. + s\sigma_i c\xi_i\left(c\theta c\psi\right) - s\sigma_i s\xi_i\left(s\theta\right)\right]\right\} + \left[R_{km}\left(\dot{\psi}s\phi c\theta + \dot{\theta}c\phi\right)\right] \qquad (67)$$

$$\vec{V}^a \cdot \vec{k}_B = \ell\sum_{i=1}^{N}\left\{\dot{\xi}_i c\sigma_i\left[s\xi_i\left(-c\phi s\theta c\psi - s\phi s\psi\right) + c\xi_i\left(c\phi c\theta\right)\right]\right.$$

$$+ \dot{\sigma}_i\left[c\sigma_i\left(-c\phi s\theta s\psi + s\phi c\psi\right) + s\sigma_i c\xi_i\left(-c\phi s\theta c\psi - s\phi s\psi\right)\right.$$

$$\left.\left. - s\sigma_i s\xi_i\left(c\phi c\theta\right)\right]\right\} + \left[-R_{jm}\left(\dot{\psi}s\phi c\theta + \dot{\theta}c\phi\right)\right] \qquad (68)$$

$$\frac{\partial \vec{V}^a}{\partial \dot{\psi}} \cdot \vec{i}_B = -R_{jm}\, C\theta\, C\phi + R_{km}\, S\theta \tag{69}$$

$$\frac{\partial \vec{V}^a}{\partial \dot{\psi}} \cdot \vec{j}_B = R_{km}\, S\phi\, C\theta \tag{70}$$

$$\frac{\partial \vec{V}^a}{\partial \dot{\psi}} \cdot \vec{k}_B = -R_{jm}\, S\phi\, C\theta \tag{71}$$

Substituting Equations (66) to (71) into Equation (64) gives:

$$\begin{aligned}
\frac{\partial \bar{\bar{T}}}{\partial \dot{\psi}} = {} & M_S \Big\langle \ell \sum_{i=1}^{N} \Big\{ \dot{\xi}_i C\sigma_i \left[S\xi_i (S\phi S\theta C\psi - C\phi S\psi) + C\xi_i (-S\phi C\theta) \right] \\
& + \dot{\sigma}_i \left[C\sigma_i (S\phi S\theta S\psi + C\phi C\psi) + S\sigma_i C\xi_i (S\phi S\theta C\psi - C\phi S\psi) + S\sigma_i S\xi_i (S\phi C\theta) \right] \Big\} \\
& + \left[R_{jm} (-\dot{\psi} C\theta C\phi + \dot{\theta} S\phi) - R_{km} (-\dot{\psi} S\theta + \dot{\phi}) \right] \Big\rangle \Big\langle -R_{jm}\, C\theta\, C\phi + R_{km}\, S\theta \Big\rangle \\
& + M_L \Big\langle \ell \sum_{i=1}^{N} \Big\{ \dot{\xi}_i C\sigma_i \left[S\xi_i (C\theta C\psi) + C\xi_i (S\theta) \right] + \dot{\sigma}_i \left[C\sigma_i (C\theta S\psi) \right. \\
& \left. + S\sigma_i C\xi_i (C\theta C\psi) - S\sigma_i S\xi_i (S\theta) \right] \Big\} + \left[R_{km} (\dot{\psi} S\phi C\theta + \dot{\theta} C\phi) \right] \Big\rangle \Big\langle R_{km}\, S\phi\, C\theta \Big\rangle \\
& + M_V \Big\langle \ell \sum_{i=1}^{N} \Big\{ \dot{\xi}_i C\sigma_i \left[S\xi_i (-C\phi S\theta C\psi - S\phi S\psi) + C\xi_i (C\phi C\theta) \right] \\
& + \dot{\sigma}_i \left[C\sigma_i (-C\phi S\theta S\psi + S\phi C\psi) + S\sigma_i C\xi_i (-C\phi S\theta C\psi - S\phi S\psi) \right. \\
& \left. - S\sigma_i S\xi_i (C\phi C\theta) \right] \Big\} + \left[-R_{jm} (\dot{\psi} S\phi C\theta + \dot{\theta} C\phi) \right] \Big\rangle \Big\langle -R_{jm}\, S\phi\, C\theta \Big\rangle \\
& + \dot{\psi} \left[C^2\theta (I_{xB} S^2\phi + I_{zB} C^2\phi) + S^2\theta I_{yB} - S2\theta C\phi I_{yzB} \right] \\
& + \dot{\theta} \left[\tfrac{1}{2} S2\phi C\theta (I_{xB} - I_{zB}) + S\phi S\theta I_{yzB} \right] + \dot{\phi} \left[-I_{yB} S\theta + I_{yzB} C\theta C\phi \right]
\end{aligned} \tag{72}$$

Neglecting products of angular velocities the balloon yaw equation is written.

$$\frac{d}{dt}\left(\frac{\partial \overline{T}}{\partial \dot{\psi}}\right) = M_s\left\langle \ell \sum_{i=1}^{N} \left\{ \ddot{\xi}_i\, c\sigma_i \left[s\xi_i (s\phi\, s\theta\, c\psi - c\phi\, s\psi) + c\xi_i (-s\phi\, c\theta) \right] \right.\right.$$

$$+ \ddot{\sigma}_i \left[c\sigma_i (s\phi\, s\theta\, s\psi + c\phi\, c\psi) + s\sigma_i\, c\xi_i (s\phi\, s\theta\, c\psi - c\phi\, s\psi) \right.$$

$$\left.\left. + s\sigma_i\, s\xi_i (s\phi\, c\theta) \right] \right\} + \left[R_{jm} (-\ddot{\psi}\, c\theta\, c\phi + \ddot{\theta}\, s\phi) \right.$$

$$\left.\left. - R_{km} (-\ddot{\psi}\, s\theta + \ddot{\phi}) \right] \right\rangle \left\langle -R_{jm}\, c\theta\, c\phi + R_{km}\, s\theta \right\rangle$$

$$+ M_L \left\langle \ell \sum_{i=1}^{N} \left\{ \ddot{\xi}_i\, c\sigma_i \left[s\xi_i (c\theta\, c\psi) + c\xi_i (s\theta) \right] + \ddot{\sigma}_i \left[c\sigma_i (c\theta\, s\psi) \right.\right.\right.$$

$$\left.\left.\left. + s\sigma_i\, c\xi_i (c\theta\, c\psi) - s\sigma_i\, s\xi_i (s\theta) \right] \right\} \right.$$

$$\left. + \left[R_{km} (\ddot{\psi}\, s\phi\, c\theta + \ddot{\theta}\, c\phi) \right] \right\rangle \left\langle R_{km}\, s\phi\, c\theta \right\rangle$$

$$+ M_V \left\langle \ell \sum_{i=1}^{N} \left\{ \ddot{\xi}_i\, c\sigma_i \left[s\xi_i (-c\phi\, s\theta\, c\psi - s\phi\, s\psi) + c\xi_i (c\phi\, c\theta) \right] \right.\right.$$

$$+ \ddot{\sigma}_i \left[c\sigma_i (-c\phi\, s\theta\, s\psi + s\phi\, c\psi) + s\sigma_i\, c\xi_i (-c\phi\, s\theta\, c\psi - s\phi\, s\psi) \right.$$

$$\left.\left. - s\sigma_i\, s\xi_i (c\phi\, c\theta) \right] \right\} + \left[-R_{jm} (\ddot{\psi}\, s\phi\, c\theta + \ddot{\theta}\, c\phi) \right] \right\rangle \left\langle -R_{jm}\, s\phi\, c\theta \right\rangle$$

$$+ \ddot{\theta} \left[\tfrac{1}{2} s2\phi\, c\theta\, (I_{xB} - I_{zB}) + s\phi\, s\theta\, I_{yzB} \right] + \ddot{\phi} \left[-I_{yB}\, s\theta + I_{yzB}\, c\theta\, c\phi \right]$$

$$+ \ddot{\psi} \left[c^2\theta (I_{xB}\, s^2\phi + I_{zB}\, c^2\phi) + s^2\theta\, I_{yB} - s2\theta\, c\phi\, I_{yzB} \right] = F_\psi \qquad (73)$$

Operating on Equation (41) with Equation (2) gives:

$$\frac{\partial \dot{T}}{\partial \dot{\theta}} = M_S(\vec{V}^a \cdot \vec{i}_B)\left(\frac{\partial \vec{V}^a}{\partial \dot{\theta}} \cdot \vec{i}_B\right) + M_L(\vec{V}^a \cdot \vec{j}_B)\left(\frac{\partial \vec{V}^a}{\partial \dot{\theta}} \cdot \vec{j}_B\right)$$

$$+M_V(\vec{V}^a \cdot \vec{k}_B)\left(\frac{\partial \vec{V}^a}{\partial \dot{\theta}} \cdot \vec{k}_B\right) + \dot{\theta}\left[I_{xB}\, c^2\phi + I_{zB}\, s^2\phi\right]$$

$$+\dot{\psi}\left[\tfrac{1}{2}\, s2\phi\, c\theta\,(I_{xB} - I_{zB}) + s\phi\, s\theta I_{yzB}\right] + \dot{\phi}\left[-I_{yz_B}\, s\phi\right] \qquad (74)$$

From Equation (38):

$$\frac{\partial \vec{V}^a}{\partial \dot{\theta}} = (R_{jm}\, s\phi)\vec{i}_B + (R_{km}\, c\phi)\vec{j}_B + (-R_{jm}\, c\phi)\vec{k}_B \qquad (75)$$

$$\frac{\partial \vec{V}^a}{\partial \dot{\theta}} \cdot \vec{i}_B = R_{jm}\, s\phi \qquad (76)$$

$$\frac{\partial \vec{V}^a}{\partial \dot{\theta}} \cdot \vec{j}_B = R_{km}\, c\phi \qquad (77)$$

$$\frac{\partial \vec{V}^a}{\partial \dot{\theta}} \cdot \vec{k}_B = -R_{jm}\, c\phi \qquad (78)$$

Substituting Equations (66), (67), (68), (76), (77), and (78) into Equation (74) gives:

$$\frac{\partial \dot{T}}{\partial \dot{\theta}} = M_S\left\langle \ell \sum_{i=1}^{N} \left\{ \dot{\xi}_i\, c\sigma_i \left[s\xi_i (s\phi\, s\theta\, c\psi - c\phi\, s\psi) + c\xi_i (-s\phi\, c\theta) \right] \right.\right.$$

$$\left. + \dot{\sigma}_i \left[c\sigma_i (s\phi\, s\theta\, s\psi + c\phi\, c\psi) + s\sigma_i\, c\xi_i (s\phi\, s\theta\, c\psi - c\phi\, s\psi) + s\sigma_i\, s\xi_i (s\phi\, c\theta) \right] \right\}$$

$$\left. + \left[R_{jm}(-\dot{\psi}\, c\theta\, c\phi + \dot{\theta}\, s\phi) - R_{km}(-\dot{\psi}\, s\theta + \dot{\phi}) \right] \right\rangle \left\langle R_{jm}\, s\phi \right\rangle$$

$$+ M_L\left\langle \ell \sum_{i=1}^{N} \left\{ \dot{\xi}_i\, c\sigma_i \left[s\xi_i (c\theta\, c\psi) + c\xi_i (s\theta) \right] + \dot{\sigma}_i \left[c\sigma_i (c\theta\, s\psi) \right.\right.\right.$$

$$\left.\left. + s\sigma_i\, c\xi_i (c\theta\, c\psi) - s\sigma_i\, s\xi_i (s\theta) \right] \right\} + \left[R_{km}(\dot{\psi}\, s\phi\, c\theta + \dot{\theta}\, c\phi) \right] \left. \right\rangle \left\langle R_{km}\, c\phi \right\rangle$$

$$+M_v\Big\langle \ell\sum_{i=1}^{N}\Big\{\ddot{\xi}_i\, c\sigma_i\big[s\xi_i(-c\phi s\theta c\psi - s\phi s\psi)+c\xi_i(c\phi c\theta)\big]$$

$$+\ddot{\sigma}_i\big[c\sigma_i(-c\phi s\theta s\psi + s\phi c\psi)+s\sigma_i c\xi_i(-c\phi s\theta c\psi - s\phi s\psi)-s\sigma_i s\xi_i(c\phi c\theta)\big]\Big\}$$

$$+\big[-R_{jm}(\dot{\psi}s\phi c\theta+\dot{\theta}c\phi)\big]\Big\rangle\big\langle -R_{jm}c\phi\big\rangle$$

$$+\ddot{\theta}\big[I_{xB}c^2\phi + I_{zB}s^2\phi\big]+\dot{\psi}\big[\tfrac{1}{2}s2\phi c\theta(I_{xB}-I_{zB})+s\phi s\theta I_{yzB}\big]$$

$$+\dot{\phi}\big[-I_{yzB}s\phi\big] \qquad (79)$$

Neglecting products of angular velocities, the balloon pitch equation is written.

$$\frac{d}{dt}\left(\frac{\partial T}{\partial\dot{\theta}}\right)=M_s\Big\langle \ell\sum_{i=1}^{N}\Big\{\ddot{\xi}_i\, c\sigma_i\big[s\xi_i(s\phi s\theta c\psi - c\phi s\psi)+c\xi_i(-s\phi c\theta)\big]$$

$$+\ddot{\sigma}_i\big[c\sigma_i(s\phi s\theta s\psi + c\phi c\psi)+s\sigma_i c\xi_i(s\phi s\theta c\psi - c\phi s\psi)+s\sigma_i s\xi_i(s\phi c\theta)\big]\Big\}$$

$$+\big[R_{jm}(-\ddot{\psi}c\theta c\phi+\ddot{\theta}s\phi)-R_{km}(-\ddot{\psi}s\theta+\ddot{\phi})\big]\Big\rangle\big\langle R_{jm}s\phi\big\rangle$$

$$+M_L\Big\langle \ell\sum_{i=1}^{N}\Big\{\ddot{\xi}_i\, c\sigma_i\big[s\xi_i(c\theta c\psi)+c\xi_i(s\theta)\big]+\ddot{\sigma}_i\big[c\sigma_i(c\theta s\psi)$$

$$+s\sigma_i c\xi_i(c\theta c\psi)-s\sigma_i s\xi_i(s\theta)\big]\Big\}+\big[R_{km}(\ddot{\psi}s\phi c\theta+\ddot{\theta}c\phi)\big]\Big\rangle\big\langle R_{km}c\phi\big\rangle$$

$$+M_v\Big\langle \ell\sum_{i=1}^{N}\Big\{\ddot{\xi}_i\, c\sigma_i\big[s\xi_i(-c\phi s\theta c\psi - s\phi s\psi)+c\xi_i(c\phi c\theta)\big]$$

$$+\ddot{\sigma}_i\left[c\sigma_i(-c\phi s\theta s\psi+s\phi c\psi)+s\sigma_i c\xi_i(-c\phi s\theta c\psi-s\phi s\psi)\right.$$

$$\left.-s\sigma_i s\xi_i(c\phi c\theta)\right]\}+\left[-R_{jm}(\ddot{\psi}s\phi c\theta+\ddot{\theta}c\phi)\right]\rangle\langle -R_{jm}c\phi\rangle$$

$$+\ddot{\theta}\left[I_{xB}c^2\phi+I_{zB}s^2\phi\right]+\ddot{\psi}\left[\tfrac{1}{2}s2\phi c\theta(I_{xB}-I_{zB})+s\phi s\theta I_{yzB}\right]$$

$$+\ddot{\phi}\left[-I_{yzB}s\phi\right]=F_\theta \tag{80}$$

Operating on Equation (41) with Equation(3) gives:

$$\frac{\partial\bar{T}}{\partial\dot{\phi}}=M_S(\vec{V}^a\cdot\vec{i}_B)\left(\frac{\partial\vec{V}^a}{\partial\dot{\phi}}\cdot\vec{i}_B\right)+M_L(\vec{V}^a\cdot\vec{j}_B)\left(\frac{\partial\vec{V}^a}{\partial\dot{\phi}}\cdot\vec{j}_B\right)$$

$$+M_V(\vec{V}^a\cdot\vec{k}_B)\left(\frac{\partial\vec{V}^a}{\partial\dot{\phi}}\cdot\vec{k}_B\right)+\dot{\phi}\left[I_{yB}\right]$$

$$+\dot{\psi}\left[-I_{yB}s\theta+I_{yzB}c\theta c\phi\right]+\dot{\theta}\left[-I_{yzB}s\phi\right] \tag{81}$$

From Equation (38):

$$\frac{\partial\vec{V}^a}{\partial\dot{\phi}}=-R_{km}\vec{i}_B \tag{82}$$

$$\frac{\partial\vec{V}^a}{\partial\dot{\phi}}\cdot\vec{i}_B=-R_{km} \tag{83}$$

$$\frac{\partial\vec{V}^a}{\partial\dot{\phi}}\cdot\vec{j}_B=\frac{\partial\vec{V}^a}{\partial\dot{\phi}}\cdot\vec{k}_B=0 \tag{84}$$

Substituting Equation (66), (83), and (84) into (81) gives:

$$\frac{\partial\bar{T}}{\partial\dot{\phi}}=M_S\langle\ell\sum_{i=1}^{N}\left\{\dot{\xi}_i c\sigma_i\left[s\xi_i(s\phi s\theta c\psi-c\phi s\psi)+c\xi_i(-s\phi c\theta)\right]\right.$$

$$+\dot{\sigma}_i\left[c\sigma_i(s\phi s\theta s\psi+c\phi c\psi)+s\sigma_i c\xi_i(s\phi s\theta c\psi-c\phi s\psi)\right.$$

$$+S\sigma_i S\xi_i (S\phi C\theta)]\}+[R_{jm}(-\dot\psi C\theta C\phi+\dot\theta S\phi)-R_{km}(-\dot\psi S\theta+\dot\phi)]\rangle\langle -R_{km}\rangle$$

$$+\dot\phi[I_{yB}]+\dot\psi[-I_{yB}S\theta+I_{yzB}C\theta C\phi]+\dot\theta[-I_{yzB}S\phi] \qquad (85)$$

Neglecting products of angular velocities the balloon roll equation is written.

$$\frac{d}{dt}\left(\frac{\partial\bar T}{\partial\dot\phi}\right)=M_S\left\langle \ell\sum_{i=1}^{N}\{\ddot\xi_i C\sigma_i[S\xi_i(S\phi S\theta C\psi-C\phi S\psi)+C\xi_i(-S\phi C\theta)]\right.$$

$$+\ddot\sigma_i[C\sigma_i(S\phi S\theta S\psi+C\phi C\psi)+S\sigma_i C\xi_i(S\phi S\theta C\psi-C\phi S\psi)+S\sigma_i S\xi_i(S\phi C\theta)]\}$$

$$+[R_{jm}(-\ddot\psi C\theta C\phi+\ddot\theta S\phi)-R_{km}(-\ddot\psi S\theta+\ddot\phi)]\rangle\langle -R_{km}\rangle+\ddot\phi[I_{yB}]$$

$$+\ddot\psi[-I_{yB}S\theta+I_{yzB}C\theta C\phi]+\ddot\theta[-I_{yzB}S\phi]=F_\phi \qquad (86)$$

Operating on Equation (41) with Equation (4) gives:

$$\frac{\partial\bar T}{\partial\dot\xi_n}=\sum_{m=1}^{N} m\vec V^{P_m}\cdot\frac{\partial\vec V^{P_m}}{\partial\dot\xi_n}+\frac{1}{12}m\ell^2\dot\xi_n C\sigma_n+m_{PL}\vec V^{PL}\cdot\frac{\partial\vec V^{PL}}{\partial\dot\xi_n}$$

$$+M_S(\vec V^{Q}\cdot\vec i_B)\left(\frac{\partial\vec V^{Q}}{\partial\dot\xi_n}\cdot\vec i_B\right)+M_L(\vec V^{Q}\cdot\vec j_B)\left(\frac{\partial\vec V^{Q}}{\partial\dot\xi_n}\cdot\vec j_B\right)$$

$$+M_V(\vec V^{Q}\cdot\vec k_B)\left(\frac{\partial\vec V^{Q}}{\partial\dot\xi_n}\cdot\vec k_B\right) \qquad (87)$$

$$\frac{\partial\vec V^{P_m}}{\partial\dot\xi_n}=\begin{cases}\ell C\sigma_n\vec u_n' & n<m\\ \frac{\ell}{2}C\sigma_n\vec u_n' & n=m\\ 0 & n>m\end{cases} \qquad (88)$$

$$\frac{\partial \vec{V}^{PL}}{\partial \dot{\xi}_n} = l\, c\sigma_n\, \vec{e}_n' \tag{89}$$

$$\frac{\partial \vec{V}^{R}}{\partial \dot{\xi}_n} = l\, c\sigma_n\, \vec{e}_n' \tag{90}$$

$$\frac{\partial \vec{V}^{R}}{\partial \dot{\xi}_n} \cdot \vec{i}_R = l\, c\sigma_n \left[s\xi_n \left(s\phi\, s\theta\, c\psi - c\phi\, s\psi \right) + c\xi_n \left(-s\phi\, c\theta \right) \right] \tag{91}$$

$$\frac{\partial \vec{V}^{R}}{\partial \dot{\xi}_n} \cdot \vec{j}_R = l\, c\sigma_n \left[s\xi_n \left(c\theta\, c\psi \right) + c\xi_n \left(s\theta \right) \right] \tag{92}$$

$$\frac{\partial \vec{V}^{R}}{\partial \dot{\xi}_n} \cdot \vec{k}_R = l\, c\sigma_n \left[s\xi_n \left(-c\phi\, s\theta\, c\psi - s\phi\, s\psi \right) + c\xi_n \left(c\phi\, c\theta \right) \right] \tag{93}$$

The following dot products will be necessary.

$$\vec{e}_i' \cdot \vec{e}_n' = s\xi_i\, s\xi_n + c\xi_i\, c\xi_n = c\left(\xi_n - \xi_i \right) \tag{94}$$

$$\vec{f}_i' \cdot \vec{e}_n' = s\sigma_i\, c\xi_i\, s\xi_n - s\sigma_i\, s\xi_i\, c\xi_n = s\sigma_i\, s\left(\xi_n - \xi_i \right) \tag{95}$$

Substituting Equations (18), (24), (66), (67), (68), (88), (89), (91), (92), and (93) into Equation (87) yields:

$$\frac{\partial T}{\partial \dot{\xi}_n} = \sum_{m=n+1}^{N} m \left\{ l^2 c\sigma_n \sum_{i=1}^{n-1} \left[\dot{\xi}_i\, c\sigma_i\, c\left(\xi_n - \xi_i \right) + \dot{\sigma}_i\, s\sigma_i\, s\left(\xi_n - \xi_i \right) \right] + \frac{l^2}{2} c\sigma_n \left[\dot{\xi}_m\, c\sigma_m\, c\left(\xi_n - \xi_m \right) \right.\right.$$

$$\left.\left. + \dot{\sigma}_m\, s\sigma_m\, s\left(\xi_n - \xi_m \right) \right] \right\} + m \left\{ \frac{l^2}{2} c\sigma_n \sum_{i=1}^{n-1} \left[\dot{\xi}_i\, c\sigma_i\, c\left(\xi_n - \xi_i \right) + \dot{\sigma}_i\, s\sigma_i\, s\left(\xi_n - \xi_i \right) \right] \right.$$

$$\left. + \frac{l^2}{4} c\sigma_n \left[\dot{\xi}_n\, c\sigma_n \right] \right\} + \frac{1}{12} m l^2 c^2\sigma_n\, \dot{\xi}_n + m_{PL} l^2 c\sigma_n \sum_{i=1}^{N} \left[\dot{\xi}_i\, c\sigma_i\, c\left(\xi_n - \xi_i \right) \right.$$

$$\left. + \dot{\sigma}_i\, s\sigma_i\, s\left(\xi_n - \xi_i \right) \right] + M_S \left\langle l \sum_{i=1}^{N} \left\{ \dot{\xi}_i\, c\sigma_i \left[s\xi_i \left(s\phi\, s\theta\, c\psi - c\phi\, s\psi \right) + c\xi_i \left(-s\phi\, c\theta \right) \right] \right.\right.$$

$$\left.\left. + \dot{\sigma}_i \left[c\sigma_i \left(s\phi\, s\theta\, s\psi + c\phi\, c\psi \right) + s\sigma_i\, c\xi_i \left(s\phi\, s\theta\, c\psi - c\phi\, s\psi \right) + s\sigma_i\, s\xi_i \left(s\phi\, c\theta \right) \right] \right\}$$

$$+\left[R_{jm}(-\dot{\psi}\,c\theta\,c\phi+\dot{\theta}\,s\phi)-R_{km}(-\dot{\psi}\,s\theta+\dot{\phi})\right]\Big\rangle\Big\langle l\,c\sigma_n\left[s\beta_n(s\phi\,s\theta\,c\psi-c\phi\,s\psi)\right.$$

$$\left.+c\beta_n(-s\phi\,c\theta)\right]\Big\rangle+M_n\Big\langle l\sum_{i=1}^{N}\Big\{\ddot{\beta}_i\,c\sigma_n\left[s\beta_n(c\theta\,c\psi)+c\beta_n(s\theta)\right]$$

$$+\dot{\sigma}_i^2\left[c\sigma_n(c\theta\,s\psi)+s\sigma_n\,c\beta_n(c\theta\,c\psi)-s\sigma_n\,s\beta_n(s\theta)\right]\Big\}$$

$$+\left[R_{km}(\dot{\psi}\,s\phi\,c\theta+\dot{\theta}\,c\phi)\right]\Big\rangle\Big\langle l\,c\sigma_n\left[s\beta_n(c\theta\,c\psi)+c\beta_n(s\theta)\right]\Big\rangle$$

$$+M_V\Big\langle l\sum_{i=1}^{N}\Big\{\ddot{\beta}_i\,c\sigma_n\left[s\beta_i(-c\phi\,s\theta\,c\psi-s\phi\,s\psi)+c\beta_i(c\phi\,c\theta)\right]$$

$$+\dot{\sigma}_i^2\left[c\sigma_i(-c\phi\,s\theta\,s\psi+s\phi\,c\psi)+s\sigma_i\,c\beta_i(-c\phi\,s\theta\,c\psi-s\phi\,s\psi)-s\sigma_i\,s\beta_i(c\phi\,c\theta)\right]\Big\}$$

$$+\left[-R_{jm}(\dot{\psi}\,s\phi\,c\theta+\dot{\theta}\,c\phi)\right]\Big\rangle\Big\langle l\,c\sigma_n\left[s\beta_n(-c\phi\,s\theta\,c\psi-s\phi\,s\psi)+c\beta_n(c\phi\,c\theta)\right]\Big\rangle \tag{96}$$

Neglecting products of angular velocities the, link pitch equation is written.

$$\frac{d}{dt}\left(\frac{\partial\bar{T}}{\partial\dot{\beta}_n}\right)=\sum_{m=n+1}^{N}m l^2 c\sigma_n\Big\{\sum_{i=1}^{m-1}\left[\ddot{\beta}_i\,c\sigma_i\,c(\beta_n-\beta_i)+\ddot{\sigma}_i\,s\sigma_i\,s(\beta_n-\beta_i)\right]+\frac{1}{2}\left[\ddot{\beta}_m\,c\sigma_m\,c(\beta_n-\beta_m)\right.$$

$$\left.+\ddot{\sigma}_m\,s\sigma_m\,s(\beta_n-\beta_m)\right]\Big\}+\frac{1}{2}ml^2c\sigma_n\sum_{i=1}^{n-1}\left[\ddot{\beta}_i\,c\sigma_i\,c(\beta_n-\beta_i)+\ddot{\sigma}_i\,s\sigma_i\,s(\beta_n-\beta_i)\right]$$

$$+\frac{1}{3}ml^2c^2\sigma_n\,\ddot{\beta}_n+m_{PL}\,l^2c\sigma_n\sum_{i=1}^{N}\left[\ddot{\beta}_i\,c\sigma_i\,c(\beta_n-\beta_i)+\ddot{\sigma}_i\,s\sigma_i\,s(\beta_n-\beta_i)\right]$$

$$+M_S\Big\langle l\sum_{i=1}^{N}\Big\{\ddot{\beta}_i\,c\sigma_n\left[s\beta_n(s\phi\,s\theta\,c\psi-c\phi\,s\psi)+c\beta_n(-s\phi\,c\theta)\right]$$

$$+\ddot{\sigma}_i\left[c\sigma_i\left(s\phi\, s\theta\, s\psi + c\phi\, c\psi\right) + s\sigma_i\, c\beta_i\left(s\phi\, s\theta\, c\psi - c\phi\, s\psi\right) + s\sigma_i\, s\beta_i\left(s\phi\, c\theta\right)\right]\Big\}$$

$$+\left[R_{jm}\left(-\ddot{\psi}\, c\theta\, c\phi + \ddot{\theta}\, s\phi\right) - R_{km}\left(-\ddot{\psi}\, s\theta + \ddot{\phi}\right)\right]\Big\rangle\Big\langle \ell\, c\sigma_n\left[s\beta_n\left(s\phi\, s\theta\, c\psi\right.\right.$$

$$\left.\left. - c\phi\, s\psi\right) + c\beta_n\left(-s\phi\, c\theta\right)\right]\Big\rangle$$

$$+M_L\Big\langle \ell \sum_{i=1}^{N}\Big\{\ddot{\beta}_i\, c\sigma_i\left[s\beta_i\left(c\theta\, c\psi\right) + c\beta_i\left(s\theta\right)\right] + \ddot{\sigma}_i\left[c\sigma_i\left(c\theta\, s\psi\right) + s\sigma_i\, c\beta_i\left(c\theta\, c\psi\right)\right.$$

$$\left. - s\sigma_i\, s\beta_i\left(s\theta\right)\right]\Big\} + \left[R_{km}\left(\ddot{\psi}\, s\phi\, c\theta + \ddot{\theta}\, c\phi\right)\right]\Big\rangle\Big\langle \ell\, c\sigma_n\left[s\beta_n\left(c\theta\, c\psi\right) + c\beta_n\left(s\theta\right)\right]\Big\rangle$$

$$+M_V\Big\langle \ell \sum_{i=1}^{N}\Big\{\ddot{\beta}_i\, c\sigma_i\left[s\beta_i\left(-c\phi\, s\theta\, c\psi - s\phi\, s\psi\right) + c\beta_i\left(c\phi\, c\theta\right)\right]$$

$$+\ddot{\sigma}_i\left[c\sigma_i\left(-c\phi\, s\theta\, s\psi + s\phi\, c\psi\right) + s\sigma_i\, c\beta_i\left(-c\phi\, s\theta\, c\psi - s\phi\, s\psi\right) - s\sigma_i\, s\beta_i\left(c\phi\, c\theta\right)\right]\Big\}$$

$$+\left[-R_{jm}\left(\ddot{\psi}\, s\phi\, c\theta + \ddot{\theta}\, c\phi\right)\right]\Big\rangle\Big\langle \ell\, c\sigma_n\left[s\beta_n\left(-c\phi\, s\theta\, c\psi - s\phi\, s\psi\right) + c\beta_n\left(c\phi\, c\theta\right)\right]\Big\rangle$$

$$= F_{\beta_n} \tag{97}$$

Operating on Equation (41) with Equation (5) gives:

$$\frac{\partial \bar{T}}{\partial \dot{\sigma}_n} = \sum_{m=1}^{N} m\, \vec{V}^{P_m^*} \cdot \frac{\partial \vec{V}^{P_m^*}}{\partial \dot{\sigma}_n} + \frac{1}{12} m \ell^2 \ddot{\sigma}_n + m_{P_L} \vec{V}^{P_L} \cdot \frac{\partial \vec{V}^{P_L}}{\partial \dot{\sigma}_n}$$

$$+M_S\left(\vec{V}^{a} \cdot \vec{i}_a\right)\left(\frac{\partial \vec{V}^{a}}{\partial \dot{\sigma}_n} \cdot \vec{i}_a\right) + M_L\left(\vec{V}^{a} \cdot \vec{j}_a\right)\left(\frac{\partial \vec{V}^{a}}{\partial \dot{\sigma}_n} \cdot \vec{j}_a\right) \tag{98}$$

$$+M_V\left(\vec{V}^{a} \cdot \vec{k}_a\right)\left(\frac{\partial \vec{V}^{a}}{\partial \dot{\sigma}_n} \cdot \vec{k}_a\right)$$

$$\frac{\partial \vec{V}^{P_n^*}}{\partial \dot{\sigma}_n} \begin{cases} \ell \vec{f}_n' & n < m \\ \frac{\ell}{2} \vec{f}_n' & n = m \\ 0 & n > m \end{cases} \tag{99}$$

$$\frac{\partial \vec{V}^{P_n}}{\partial \dot{\sigma}_n} = \ell \vec{f}_n' \tag{100}$$

$$\frac{\partial \vec{V}^{Q}}{\partial \dot{\sigma}_n} = \ell \vec{f}_n' \tag{101}$$

$$\frac{\partial \vec{V}^{Q}}{\partial \dot{\sigma}_n} \cdot \vec{i}_B = \ell \left[C\sigma_n (S\phi S\theta S\psi + C\phi C\psi) + S\sigma_n C\beta_n (S\phi S\theta C\psi - C\phi S\psi) + S\sigma_n S\beta_n (S\phi C\theta) \right] \tag{102}$$

$$\frac{\partial \vec{V}^{Q}}{\partial \dot{\sigma}_n} \cdot \vec{j}_B = \ell \left[C\sigma_n (C\theta S\psi) + S\sigma_n C\beta_n (C\theta C\psi) - S\sigma_n S\beta_n (S\theta) \right] \tag{103}$$

$$\frac{\partial \vec{V}^{Q}}{\partial \dot{\sigma}_n} \cdot \vec{k}_B = \ell \left[C\sigma_n (-C\phi S\theta S\psi + S\phi C\psi) + S\sigma_n C\beta_n (-C\phi S\theta C\psi - S\phi S\psi) - S\sigma_n S\beta_n (C\phi C\theta) \right] \tag{104}$$

The following dot products will be necessary.

$$\vec{i}_i \cdot \vec{f}_n' = S\beta_i S\sigma_n C\beta_n - C\beta_i S\sigma_n S\beta_n = -S\sigma_n S(\beta_i - \beta_n) \tag{105}$$

$$\begin{aligned} \vec{f}_i \cdot \vec{f}_n' &= C\sigma_i C\sigma_n + S\sigma_i C\beta_i S\sigma_n C\beta_n + S\sigma_i S\beta_i S\sigma_n S\beta_n \\ &= C\sigma_i C\sigma_n + S\sigma_i S\sigma_n C(\beta_n - \beta_i) \end{aligned} \tag{106}$$

Substituting Equations (18), (24), (66), (67), (68), (99) (100), (102), (103) and (104) into Equation (98) yields:

$$\frac{\partial \bar{T}}{\partial \dot{\sigma}_n} = \sum_{m=n+1}^{N} m\ell^2 \Big\{ \sum_{i=1}^{n-1} \Big[-\dot{\xi}_i \, c\sigma_i s\sigma_n s(\xi_n - \xi_i) + \dot{\sigma}_i (c\sigma_i c\sigma_n + s\sigma_i s\sigma_n c(\xi_n - \xi_i)) \Big]$$

$$+ \tfrac{1}{2} \Big[-\dot{\xi}_m c\sigma_m s\sigma_n s(\xi_n - \xi_m) + \dot{\sigma}_m (c\sigma_m c\sigma_n + s\sigma_m s\sigma_n c(\xi_n - \xi_m)) \Big] \Big\}$$

$$+ m \Big\{ \tfrac{\ell^2}{2} \sum_{i=1}^{n-1} \Big[-\dot{\xi}_i c\sigma_i s\sigma_n s(\xi_n - \xi_i) + \dot{\sigma}_i (c\sigma_i c\sigma_n + s\sigma_i s\sigma_n c(\xi_n - \xi_i)) \Big] + \tfrac{\ell^2}{4} \dot{\sigma}_n \Big\}$$

$$+ \tfrac{m}{12} \ell^2 \dot{\sigma}_n + m_{PL} \ell^2 \sum_{i=1}^{N} \Big[-\dot{\xi}_i c\sigma_i s\sigma_n s(\xi_n - \xi_i) + \dot{\sigma}_i (c\sigma_i c\sigma_n + s\sigma_i s\sigma_n c(\xi_n - \xi_i)) \Big]$$

$$+ M_S \Big\langle \ell \sum_{i=1}^{N} \Big\{ \dot{\xi}_i c\sigma_i \big[s\xi_n (s\phi s\theta c\psi - c\phi s\psi) + c\xi_n (-s\phi c\theta) \big]$$

$$+ \dot{\sigma}_i \big[c\sigma_n (s\phi s\theta s\psi + c\phi c\psi) + s\sigma_n c\xi_n (s\phi s\theta c\psi - c\phi s\psi) + s\sigma_n s\xi_n (s\phi c\theta) \big] \Big\}$$

$$+ \big[R_{jm} (-\dot{\psi} c\theta c\phi + \dot{\theta} s\phi) - R_{km} (-\dot{\psi} s\theta + \dot{\phi}) \big] \Big\rangle \Big\langle \ell \big[c\sigma_n (s\phi s\theta s\psi + c\phi c\psi)$$

$$+ s\sigma_n c\xi_n (s\phi s\theta c\psi - c\phi s\psi) + s\sigma_n s\xi_n (s\phi c\theta) \big] \Big\rangle$$

$$+ M_L \Big\langle \ell \sum_{i=1}^{N} \Big\{ \dot{\xi}_i c\sigma_i \big[s\xi_n (c\theta c\psi) + c\xi_n (s\theta) \big] + \dot{\sigma}_i \big[c\sigma_n (c\theta s\psi) + s\sigma_n c\xi_n (c\theta c\psi)$$

$$- s\sigma_n s\xi_n (s\theta) \big] \Big\} + \big[R_{km} (\dot{\psi} s\phi c\theta + \dot{\theta} c\phi) \big] \Big\rangle \Big\langle \ell \big[c\sigma_n (c\theta s\psi) + s\sigma_n c\xi_n (c\theta c\psi)$$

$$- s\sigma_n s\xi_n (s\theta) \big] \Big\rangle + M_V \Big\langle \ell \sum_{i=1}^{N} \Big\{ \dot{\xi}_i c\sigma_i \big[s\xi_n (-c\phi s\theta c\psi - s\phi s\psi) + c\xi_n (c\phi c\theta) \big]$$

$$+ \dot{\sigma}_i \big[c\sigma_n (-c\phi s\theta s\psi + s\phi c\psi) + s\sigma_n c\xi_n (-c\phi s\theta c\psi - s\phi s\psi) - s\sigma_n s\xi_n (c\phi c\theta) \big] \Big\}$$

$$+ \big[-R_{jm} (\dot{\psi} s\phi c\theta + \dot{\theta} c\phi) \big] \Big\rangle \Big\langle \ell \big[c\sigma_n (-c\phi s\theta s\psi + s\phi c\psi)$$

$$+ s\sigma_n c\xi_n (-c\phi s\theta c\psi - s\phi s\psi) - s\sigma_n s\xi_n (c\phi c\theta) \big] \Big\rangle \qquad (107)$$

Neglecting products of angular velocities, the link yaw equation is written.

$$\frac{d}{dt}\left(\frac{\partial \bar{T}}{\partial \dot{\sigma}_n}\right) = \sum_{m=n+1}^{N} m\ell^2 \Bigg\{ \sum_{i=1}^{n-1} \Big[-\ddot{\xi}_i \, c\sigma_i s\sigma_n s(\xi_n - \xi_i) + \ddot{\sigma}_i \big(c\sigma_i c\sigma_n + s\sigma_i s\sigma_n c(\xi_n - \xi_i) \big) \Big]$$

$$+ \frac{1}{2} \Big[-\ddot{\xi}_m \, c\sigma_m s\sigma_n s(\xi_n - \xi_m) + \ddot{\sigma}_m \big(c\sigma_m c\sigma_n + s\sigma_m s\sigma_n c(\xi_n - \xi_m) \big) \Big] \Bigg\}$$

$$+ \frac{m}{2} \ell^2 \sum_{i=1}^{n-1} \Big[-\ddot{\xi}_i \, c\sigma_i s\sigma_n s(\xi_n - \xi_i) + \ddot{\sigma}_i \big(c\sigma_i c\sigma_n + s\sigma_i s\sigma_n c(\xi_n - \xi_i) \big) \Big] + \frac{m}{3} \ell^2 \ddot{\sigma}_n$$

$$+ m_{pL} \ell^2 \sum_{i=1}^{N} \Big[-\ddot{\xi}_i \, c\sigma_i s\sigma_n s(\xi_n - \xi_i) + \ddot{\sigma}_i \big(c\sigma_i c\sigma_n + s\sigma_i s\sigma_n c(\xi_n - \xi_i) \big) \Big]$$

$$+ M_S \Bigg\langle \ell \sum_{i=1}^{N} \Big\{ \ddot{\xi}_i \, c\sigma_i \big[s\xi_n (s\phi s\theta c\psi - c\phi s\psi) + c\xi_n (-s\phi c\theta) \big]$$

$$+ \ddot{\sigma}_i \big[c\sigma_n (s\phi s\theta s\psi + c\phi c\psi) + s\sigma_n c\xi_n (s\phi s\theta c\psi - c\phi s\psi) + s\sigma_n s\xi_n (s\phi c\theta) \big] \Big\}$$

$$+ \big[R_{jm} (-\ddot{\psi} c\theta c\phi + \ddot{\theta} s\phi) - R_{km} (-\ddot{\psi} s\theta + \ddot{\phi}) \big] \Bigg\rangle \Bigg\langle \ell \big[c\sigma_n (s\phi s\theta s\psi + c\phi c\psi)$$

$$+ s\sigma_n c\xi_n (s\phi s\theta c\psi - c\phi s\psi) + s\sigma_n s\xi_n (s\phi c\theta) \big] \Bigg\rangle$$

$$+ M_L \Bigg\langle \ell \sum_{i=1}^{N} \Big\{ \ddot{\xi}_i \, c\sigma_n \big[s\xi_n (c\theta c\psi) + c\xi_n (s\theta) \big] + \ddot{\sigma}_i \big[c\sigma_n (c\theta s\psi) + s\sigma_n c\xi_n (c\theta c\psi)$$

$$- s\sigma_n s\xi_n (s\theta) \big] \Big\} + \big[R_{km} (\ddot{\psi} s\phi c\theta + \ddot{\theta} c\phi) \big] \Bigg\rangle \Bigg\langle \ell \big[c\sigma_n (c\theta s\psi) + s\sigma_n c\xi_n (c\theta c\psi)$$

$$- s\sigma_n s\xi_n (s\theta) \big] \Bigg\rangle + M_V \Bigg\langle \ell \sum_{i=1}^{N} \Big\{ \ddot{\xi}_i \, c\sigma_n \big[s\xi_n (-c\phi s\theta c\psi - s\phi s\psi) + c\xi_n (c\phi c\theta) \big]$$

$$+ \ddot{\sigma}_i \big[c\sigma_n (-c\phi s\theta s\psi + s\phi c\psi) + s\sigma_n c\xi_n (-c\phi s\theta c\psi - s\phi s\psi) - s\sigma_n s\xi_n (c\phi c\theta) \big] \Big\}$$

$$+[-R_{jm}(\ddot{\psi}\, s\phi\, c\theta + \ddot{\theta}\, c\phi)]\rangle\langle \ell[c\sigma_n(-c\phi\, s\theta\, s\psi + s\phi\, c\psi)$$

$$+ s\sigma_n\, c\beta_n(-c\phi\, s\theta\, c\psi - s\phi\, s\psi) - s\sigma_n\, s\beta_n(c\phi\, c\theta)]\rangle = F_{\sigma_n} \qquad (108)$$

6. Linearized Inertia Terms

Equations (73), (80), (86), (97), and (108) are the equations of motion for a tethered balloon in three dimensional space. In the derivation of these equations, it was assumed that the angular velocities were small, and consequently, products of angular velocities were neglected. Now consider the system in equilibrium under the influence of a steady wind profile blowing in the negative $\overline{Y}$ direction. Under this condition the balloon yaw and roll angles and the link yaw angles will be zero. The balloon's pitch angle and the links' pitch angles will be some finite value. If the excursion from equilibrium is small, the angles ψ, ϕ, and σ_n will be small.

$$\left.\begin{aligned} s\psi = \psi \quad , \quad s\phi = \phi \quad , \quad s\sigma_n = \sigma_n \\ c\psi = c\phi = c\sigma_n = 1 \end{aligned}\right\} \qquad (109)$$

Furthermore, products of the angles ψ, ϕ, and σ_n with themselves or with any accelerations are of second order and neglected. With these assumptions, the equations of motion are reduced to the following form:

$$M_s\left[\ell\sum_{i=1}^{N}\ddot{\sigma}_i - R_{jm}\ddot{\psi}\, c\theta + R_{km}(\ddot{\psi}\, s\theta - \ddot{\phi})\right][-R_{jm}\, c\theta + R_{km}\, s\theta]$$

$$+\ddot{\psi}\left[c^2\theta\, I_{zB} + s^2\theta\, I_{yB} - s2\theta\, I_{yzB}\right] + \ddot{\phi}\left[-I_{yB}\, s\theta + I_{yzB}\, c\theta\right] = F_{\psi} \qquad (110)$$

$$M_L[\ell\sum_{i=1}^{N}\ddot{\xi}_i(s\xi_i c\theta + c\xi_i s\theta) + R_{km}\ddot{\theta}][R_{km}]$$

$$+M_V[\ell\sum_{i=1}^{N}-\ddot{\xi}_i(s\xi_i s\theta - c\xi_i c\theta) - R_{jm}\ddot{\theta}][-R_{jm}] + \ddot{\theta}[I_{x\theta}] = F_\theta \qquad (111)$$

$$M_S[\ell\sum_{i=1}^{N}\ddot{\sigma}_i - R_{jm}\ddot{\psi}c\theta + R_{km}(\ddot{\psi}s\theta - \ddot{\phi})][-R_{km}] + \ddot{\phi}[I_{y\theta}]$$

$$+\ddot{\psi}[-I_{y\theta}s\theta + I_{y z\theta}c\theta] = F_\phi \qquad (112)$$

$$\sum_{n=n+1}^{N} m\ell^2[\sum_{i=1}^{n-1}\ddot{\xi}_i c(\xi_n - \xi_i) + \tfrac{1}{2}\ddot{\xi}_n c(\xi_n - \xi_n)] + \tfrac{m}{2}\ell^2\sum_{i=1}^{n-1}\ddot{\xi}_i c(\xi_n - \xi_i)$$

$$+\tfrac{m}{3}\ell^2\ddot{\xi}_n + m_{pL}\ell^2\sum_{i=1}^{N}\ddot{\xi}_i c(\xi_n - \xi_i) + M_L[\ell\sum_{i=1}^{N}\ddot{\xi}_i(s\xi_i c\theta + c\xi_i s\theta)$$

$$+R_{km}\ddot{\theta}][\ell(s\xi_n c\theta + c\xi_n s\theta)] + M_V[\ell\sum_{i=1}^{N}\ddot{\xi}_i(-s\xi_i s\theta + c\xi_i c\theta) \qquad (113)$$

$$-R_{jm}\ddot{\theta}][\ell(-s\xi_n s\theta + c\xi_n c\theta)] = F_{\xi_n}$$

$$\sum_{m=n+1}^{N} m\ell^2[\sum_{i=1}^{m-1}\ddot{\sigma}_i + \tfrac{1}{2}\ddot{\sigma}_m] + \tfrac{m}{2}\ell^2\sum_{i=1}^{n-1}\ddot{\sigma}_i + \tfrac{m}{3}\ell^2\ddot{\sigma}_n + m_{pL}\ell^2\sum_{i=1}^{N}\ddot{\sigma}_i$$

$$+M_S[\ell\sum_{i=1}^{N}\ddot{\sigma}_i - R_{jm}\ddot{\psi}c\theta + R_{km}(\ddot{\psi}s\theta - \ddot{\phi})][\ell] = F_{\sigma_n} \qquad (114)$$

Now that the equations are linearized they are uncoupled in the pitch plane and lateral plane accelerations. The two equations of motion for longitudinal dynamics are Equations (111) and (113).

$$M_L\ell R_{km}\sum_{i=1}^{N}\ddot{\xi}_i s(\xi_i+\theta) - M_V\ell R_{jm}\sum_{i=1}^{N}\ddot{\xi}_i c(\xi_i+\theta)$$

$$+[I_{x\theta} + M_L R_{km}^2 + M_V R_{jm}^2]\ddot{\theta} = F_\theta \qquad (115)$$

$$\sum_{n=\Lambda+1}^{N} m\ell^2 \sum_{i=1}^{n-1} \ddot{\xi}_i\, c(\xi_n-\xi_i) + \frac{m}{3}\ell^2 \ddot{\xi}_n + M_{pL}\ell^2 \sum_{i=1}^{N} \ddot{\xi}_i\, c(\xi_n-\xi_i)$$

$$+M_L \ell^2 s(\xi_n+\theta)\sum_{i=1}^{N} \ddot{\xi}_i\, s(\xi_i+\theta) + M_V \ell^2 c(\xi_n+\theta)\sum_{i=1}^{N} \ddot{\xi}_i\, c(\xi_i+\theta)$$

$$+\frac{m}{2}\ell^2\left[\sum_{n=\Lambda+1}^{N} \ddot{\xi}_n\, c(\xi_i-\xi_n) + \sum_{i=1}^{n-1} \ddot{\xi}_i\, c(\xi_n-\xi_i)\right]$$

$$+\left[M_L \ell R_{km}\, s(\xi_n+\theta) - M_V \ell R_{jm}\, c(\xi_n+\theta)\right]\ddot{\theta} = F_{\xi_n} \qquad (116)$$

The three equations of motion for lateral dynamics are Equations (110), (112) and (114).

$$M_S \ell (R_{km}\, s\theta - R_{jm}\, c\theta)\sum_{i=1}^{N} \ddot{\sigma}_i + \left[I_{zB} c^2\theta + I_{yB} s^2\theta - I_{yzB} s2\theta + M_S (R_{km}\, s\theta\right.$$

$$\left.-R_{jm}\, c\theta)^2\right]\ddot{\psi} + \left[I_{yzB} c\theta - I_{yB} s\theta + M_S R_{km}(R_{jm} c\theta - R_{km} s\theta)\right]\ddot{\phi} = F_\psi \qquad (117)$$

$$-M_S \ell R_{km}\sum_{i=1}^{N} \ddot{\sigma}_i + \left[I_{yzB} c\theta - I_{yB} s\theta + M_S R_{km}(R_{jm} c\theta - R_{km} s\theta)\right]\ddot{\psi}$$

$$+\left[I_{yB} + M_S R_{km}^2\right]\ddot{\phi} = F_\phi \qquad (118)$$

$$\sum_{n=\Lambda+1}^{N} m\ell^2 \sum_{i=1}^{n-1} \ddot{\sigma}_i + \frac{m}{3}\ell^2 \ddot{\sigma}_n + M_{pL}\ell^2 \sum_{i=1}^{N} \ddot{\sigma}_i + M_S \ell^2 \sum_{i=1}^{N} \ddot{\sigma}_i + \frac{m}{2}\ell^2\left[\sum_{n=\Lambda+1}^{N} \ddot{\sigma}_n\right.$$

$$\left.+\sum_{i=1}^{n-1} \ddot{\sigma}_i\right] + M_S \ell\left[R_{km}\, s\theta - R_{jm}\, c\theta\right]\ddot{\psi} + \left[-M_S \ell R_{km}\right]\ddot{\phi} = F_{\sigma_n} \qquad (119)$$

Note that the lateral equations (117), (118) and (119) are still dependent on θ. If the number of links is specified, the inertial terms in the equation can be

written out explicitly. To do this, set N = 3.

The four equations involving longitudinal motion are:

$$\{ I_{x\theta} + M_L R_{km}^2 + M_V R_{jm}^2 \} \ddot{\theta}$$

$$+\{ \ell [M_L R_{km} s(\xi_1+\theta) - M_V R_{jm} c(\xi_1+\theta)] \} \ddot{\xi}_1$$

$$+\{ \ell [M_L R_{km} s(\xi_2+\theta) - M_V R_{jm} c(\xi_2+\theta)] \} \ddot{\xi}_2$$

$$+\{ \ell [M_L R_{km} s(\xi_3+\theta) - M_V R_{jm} c(\xi_3+\theta)] \} \ddot{\xi}_3 = F_\theta \qquad (120)$$

$$\{ \ell [M_L R_{km} s(\xi_1+\theta) - M_V R_{jm} c(\xi_1+\theta)] \} \ddot{\theta}$$

$$+\{ \ell^2 [\tfrac{7m}{3} + m_{pL} + M_L s^2(\xi_1+\theta) + M_V c^2(\xi_1+\theta)] \} \ddot{\xi}_1$$

$$+\{ \ell^2 [(\tfrac{3m}{2} + m_{pL}) c(\xi_1-\xi_2) + M_L s(\xi_1+\theta) s(\xi_2+\theta) + M_V c(\xi_1+\theta) c(\xi_2+\theta)] \} \ddot{\xi}_2$$

$$+\{ \ell^2 [(\tfrac{m}{2} + m_{pL}) c(\xi_1-\xi_3) + M_L s(\xi_1+\theta) s(\xi_3+\theta) + M_V c(\xi_1+\theta) c(\xi_3+\theta)] \} \ddot{\xi}_3 = F_{\xi_1} \qquad (121)$$

$$\{ \ell [M_L R_{km} s(\xi_2+\theta) - M_V R_{jm} c(\xi_2+\theta)] \} \ddot{\theta}$$

$$+\{ \ell^2 [(\tfrac{3m}{2} + m_{pL}) c(\xi_1-\xi_2) + M_L s(\xi_1+\theta) s(\xi_2+\theta) + M_V c(\xi_1+\theta) c(\xi_2+\theta)] \} \ddot{\xi}_1$$

$$+\{ \ell^2 [\tfrac{4m}{3} + m_{pL} + M_L s^2(\xi_2+\theta) + M_V c^2(\xi_2+\theta)] \} \ddot{\xi}_2$$

$$+\{ \ell^2 [(\tfrac{m}{2} + m_{pL}) c(\xi_2-\xi_3) + M_L s(\xi_2+\theta) s(\xi_3+\theta) + M_V c(\xi_2+\theta) c(\xi_3+\theta)] \} \ddot{\xi}_3 = F_{\xi_2} \qquad (122)$$

$$\{\ell[M_L R_{km} S(\xi_3+\theta) - M_V R_{jm} C(\xi_3+\theta)]\}\ddot{\theta}$$

$$+\{\ell^2[(\tfrac{m}{2}+m_{pL})C(\xi_1-\xi_3)+M_L S(\xi_1+\theta)S(\xi_3+\theta)+M_V C(\xi_1+\theta)C(\xi_3+\theta)]\}\ddot{\xi}_1$$

$$+\{\ell^2[(\tfrac{m}{2}+m_{pL})C(\xi_2-\xi_3)+M_L S(\xi_2+\theta)S(\xi_3+\theta)+M_V C(\xi_2+\theta)C(\xi_3+\theta)]\}\ddot{\xi}_2$$

$$+\{\ell^2[\tfrac{m}{3}+m_{pL}+M_L S^2(\xi_3+\theta)+M_V C^2(\xi_3+\theta)]\}\ddot{\xi}_3 = F_{\xi_3} \qquad (123)$$

The five equations involving lateral motion are:

$$\{I_{zB}C^2\theta + I_{yB}S^2\theta - I_{yzB}S2\theta + M_s(R_{km}S\theta - R_{jm}C\theta)^2\}\ddot{\psi}$$

$$+\{I_{yzB}C\theta - I_{yB}S\theta + M_s R_{km}(R_{jm}C\theta - R_{km}S\theta)\}\ddot{\phi}$$

$$+\{\ell M_s[R_{km}S\theta - R_{jm}C\theta]\}\ddot{\sigma}_1 + \{\ell M_s[R_{km}S\theta - R_{jm}C\theta]\}\ddot{\sigma}_2$$

$$+\{\ell M_s[R_{km}S\theta - R_{jm}C\theta]\}\ddot{\sigma}_3 = F_\psi \qquad (124)$$

$$\{I_{yzB}C\theta - I_{yB}S\theta + M_s R_{km}(R_{jm}C\theta - R_{km}S\theta)\}\ddot{\psi}$$

$$+\{I_{yB} + M_s R_{km}^2\}\ddot{\phi} + \{-\ell M_s R_{km}\}\ddot{\sigma}_1$$

$$+\{-\ell M_s R_{km}\}\ddot{\sigma}_2 + \{-\ell M_s R_{km}\}\ddot{\sigma}_3 = F_\phi \qquad (125)$$

$$\{\ell M_s[R_{km}S\theta - R_{jm}C\theta]\}\ddot{\psi} + \{-\ell M_s R_{km}\}\ddot{\phi}$$
$$+\{\ell^2[\tfrac{7m}{3} + m_{pL} + M_s]\}\ddot{\sigma}_1 + \{\ell^2[\tfrac{3m}{2} + m_{pL} + M_s]\}\ddot{\sigma}_2$$
$$+\{\ell^2[\tfrac{m}{2} + m_{pL} + M_s]\}\ddot{\sigma}_3 = F_{\sigma_1} \qquad (126)$$

$$\{\ell M_s[R_{km}S\theta - R_{jm}C\theta]\}\ddot{\psi} + \{-\ell M_s R_{km}\}\ddot{\phi}$$
$$+\{\ell^2[\tfrac{3m}{2} + m_{pL} + M_s]\}\ddot{\sigma}_1 + \{\ell^2[\tfrac{4m}{3} + m_{pL} + M_s]\}\ddot{\sigma}_2$$
$$+\{\ell^2[\tfrac{m}{2} + m_{pL} + M_s]\}\ddot{\sigma}_3 = F_{\sigma_2} \qquad (127)$$

$$\{\ell M_s[R_{km}S\theta - R_{jm}C\theta]\}\ddot{\psi} + \{-\ell M_s R_{km}\}\ddot{\phi}$$
$$+\{\ell^2[\tfrac{m}{2} + m_{pL} + M_s]\}\ddot{\sigma}_1 + \{\ell^2[\tfrac{m}{2} + m_{pL} + M_s]\}\ddot{\sigma}_2$$
$$+\{\ell^2[\tfrac{m}{3} + m_{pL} + M_s]\}\ddot{\sigma}_3 = F_{\sigma_3} \qquad (128)$$

Again notice that the lateral equations are dependent upon θ. It will be assumed that θ remains constant when working with the lateral equations.

SECTION III

GENERALIZED FORCES IN THE LONGITUDINAL PLANE

1. General

An expression for the generalized force can be written as:

$$Q_i = \sum_j \vec{F}_j \cdot \frac{\partial \vec{V}_j}{\partial \dot{q}_i} + M_i \quad (*) \qquad (129)$$

where $\dot{q}_i = \dot{\theta}, \dot{\xi}_n$

M_i = aerodynamic moment acting on balloon

$\vec{F}_j$ = applied forces acting on system

$\vec{V}_j$ = velocity of system at point of applied force

The applied forces acting on the system are:

$\vec{F}_B$ = buoyant force acting on balloon at C.B.

$\vec{F}_g$ = gravitational force acting on balloon at c.g.

$\vec{F}_A$ = aerodynamic force acting on balloon at some reference point C.A.

$\vec{F}_{P_i}$ = aerodynamic force acting at c.p. of "i" th link

$\vec{F}_{g_i}$ = gravitational force acting at c.g. of "i"th link

$\vec{F}_{PL}$ = gravitational and aerodynamic forces of payload acting at P_N.

(*) see Reference (7)

Figure 59 shows the applied forces acting on the balloon in the longitudinal plane.

$$\vec{F}_B = L_S \vec{N}_3 \tag{130}$$

$$\vec{F}_g = -W_B \vec{N}_3 \tag{131}$$

$$\vec{F}_A = F_{BVA} \vec{N}_3 - F_{BHA} \vec{N}_2 \tag{132}$$

The following dot products will be necessary.

$$\left.\begin{aligned} \vec{N}_3 \cdot \vec{j}_B &= S\theta \\ \vec{N}_3 \cdot \vec{k}_B &= C\theta \end{aligned}\right\} \tag{133}$$

$$\left.\begin{aligned} \vec{N}_2 \cdot \vec{j}_B &= C\theta \\ \vec{N}_2 \cdot \vec{k}_B &= -S\theta \end{aligned}\right\} \tag{134}$$

The velocities of the points at which these forces are acting are:

$$\vec{V}_B = \sum_{i=1}^{N} l \dot{\xi}_i \vec{e}_i + R_{kB} \dot{\theta} \vec{j}_B - R_{jB} \dot{\theta} \vec{k}_B \tag{135}$$

$$\vec{V}_g = \sum_{i=1}^{N} l \dot{\xi}_i \vec{e}_i + R_{kg} \dot{\theta} \vec{j}_B - R_{jg} \dot{\theta} \vec{k}_B \tag{136}$$

$$\vec{V}_A = \sum_{i=1}^{N} l \dot{\xi}_i \vec{e}_i + R_{kA} \dot{\theta} \vec{j}_B - R_{jA} \dot{\theta} \vec{k}_B \tag{137}$$

It then follows that :

$$\frac{\partial \vec{V}_B}{\partial \dot{\theta}} = R_{kB} \vec{j}_B - R_{jB} \vec{k}_B \quad ; \quad \frac{\partial \vec{V}_B}{\partial \dot{\xi}_n} = l \vec{e}_n \tag{138}$$

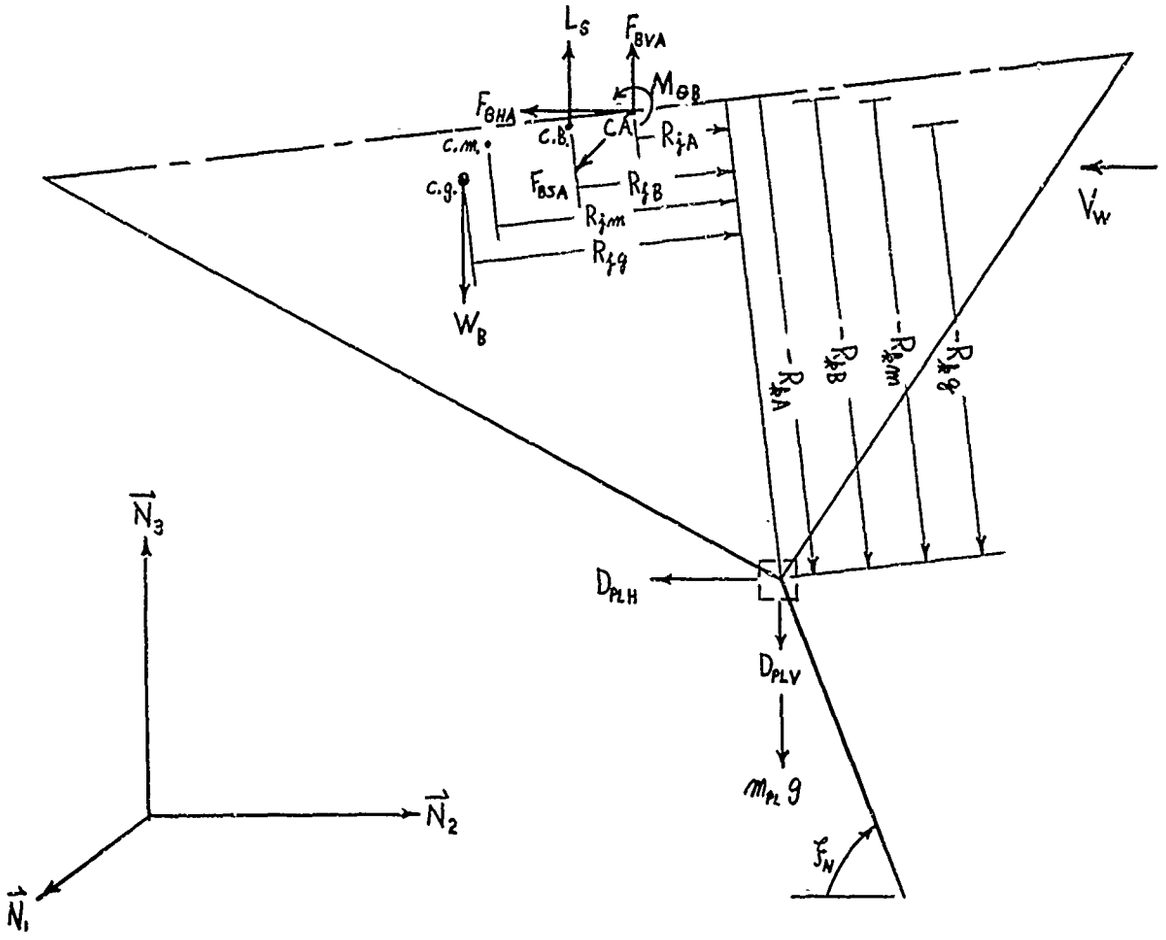

Figure 59 Applied Forces Acting on Balloon

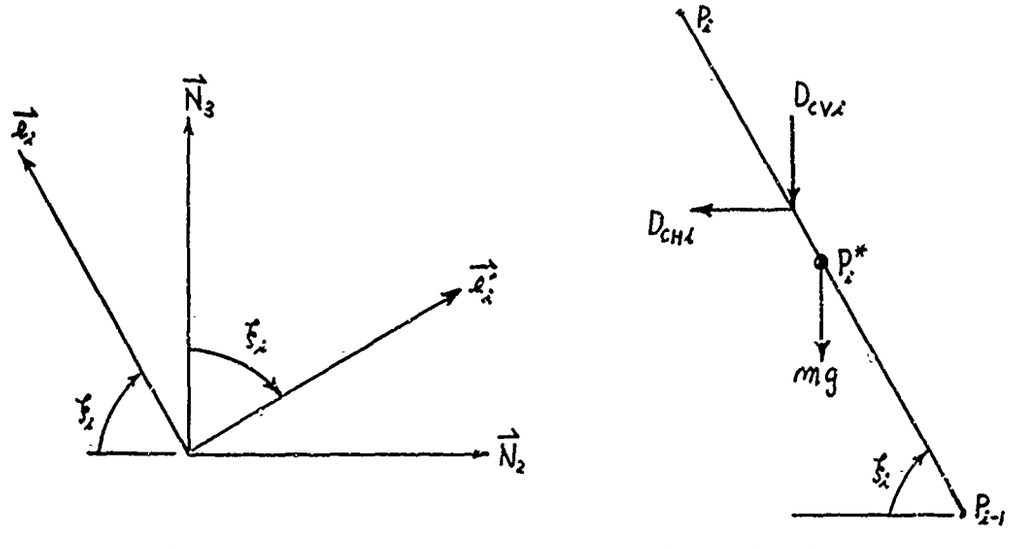

Figure 60 Applied Forces on "i" th Link

$$\frac{\partial \vec{V}_g}{\partial \dot{\theta}} = R_{kg}\,\vec{i}_B - R_{jg}\,\vec{k}_B \qquad ; \quad \frac{\partial \vec{V}_g}{\partial \dot{\xi}_n} = l\,\vec{e}_n \tag{139}$$

$$\frac{\partial \vec{V}_A}{\partial \dot{\theta}} = R_{kA}\,\vec{i}_B - R_{jA}\,\vec{k}_B \qquad ; \quad \frac{\partial \vec{V}_A}{\partial \dot{\xi}_n} = l\,\vec{e}_n \tag{140}$$

Applying Equation (129) to find F_θ:

$$F_\theta = \vec{F}_B \cdot \frac{\partial \vec{V}_B}{\partial \dot{\theta}} + \vec{F}_g \cdot \frac{\partial \vec{V}_g}{\partial \dot{\theta}} + \vec{F}_A \cdot \frac{\partial \vec{V}_A}{\partial \dot{\theta}} + M_{\theta B} \tag{141}$$

Expanding Equation (141) gives:

$$F_\theta = [\,L_S R_{kB} - W_B R_{kg} + F_{BVA} R_{kA} - F_{BHA} R_{jA}\,]\,S\theta$$

$$+ [-L_S R_{jB} + W_B R_{jg} - F_{BVA} R_{jA} - F_{BHA} R_{kA}\,]\,C\theta + M_{\theta B} \tag{142}$$

The generalized force F_{ξ_n} is now calculated.

$$\vec{F}_{PL} = -m_{PL}\,g\,\vec{N}_3 + D_{PLH}\,\vec{N}_2 - D_{PLV}\,\vec{N}_3 \tag{143}$$

$$\vec{F}_{gi} = m_i\,g\,\vec{N}_3 \tag{144}$$

$$\vec{F}_{Pi} = -D_{CHi}\,S^2\xi_i\,\vec{e}_i - D_{CVi}\,C^2\xi_i\,\vec{e}_i \tag{145}$$

The forces in Equation (143) can be seen in Figure 59. The forces in Equations (144) and (145) can be seen in Figure 60.

Shear forces are neglected. The velocities of the points at which these forces act are:

$$\vec{V}_{P_i} = l \sum_{i=1}^{N} \dot{\xi}_i \vec{e}_i' \tag{146}$$

$$\vec{V}_{g_i} = \vec{V}^{P_i^*} = l \sum_{j=1}^{i-1} \dot{\xi}_j \vec{e}_j' + \frac{1}{2} l \dot{\xi}_i \vec{e}_i' \tag{147}$$

$$\vec{V}_{\bar{P}_i} = l \sum_{j=1}^{i-1} \dot{\xi}_j \vec{e}_j' + l C_i \dot{\xi}_i \vec{e}_i' \tag{148}$$

where C_i is the ratio of the distance from P_{i-1} to the c.p. of the "i" th link to the total length of the link. From equations (146), (147), and (148) it follows that:

$$\frac{\partial \vec{V}_{P_i}}{\partial \dot{\xi}_n} = l \vec{e}_n' \tag{149}$$

$$\frac{\partial \vec{V}_{g_i}}{\partial \dot{\xi}_n} = \begin{cases} l \vec{e}_n' & n < i \\ \frac{l}{2} \vec{e}_n' & n = i \\ 0 & n > i \end{cases} \tag{150}$$

$$\frac{\partial \vec{V}_{\bar{P}_i}}{\partial \dot{\xi}_n} = \begin{cases} l \vec{e}_n' & n < i \\ l C_n \vec{e}_i' & n = i \\ 0 & n > i \end{cases} \tag{151}$$

Applying Equation (129) to find F_{θ_n} :

$$F_{\theta_n} = \vec{F}_B \cdot \frac{\partial \vec{V}_B}{\partial \dot{\theta}_n} + \vec{F}_g \cdot \frac{\partial \vec{V}_g}{\partial \dot{\theta}_n} + \vec{F}_A \cdot \frac{\partial \vec{V}_A}{\partial \dot{\theta}_n} + \vec{F}_{PL} \cdot \frac{\partial \vec{V}_{PL}}{\partial \dot{\theta}_n}$$
$$+ \sum_{i=1}^{N} \vec{F}_{g_i} \cdot \frac{\partial \vec{V}_{g_i}}{\partial \dot{\theta}_n} + \sum_{i=1}^{N} \vec{F}_{\bar{P}_i} \cdot \frac{\partial \vec{V}_{\bar{P}_i}}{\partial \dot{\theta}_n} \qquad (152)$$

Simplifying Equation (152):

$$F_{\theta_n} = L_S \ell C\theta_n - W_B \ell C\theta_n + F_{BVA} \ell C\theta_n - F_{BHA} \ell S\theta_n$$
$$- m_{PL} g \ell C\theta_n - D_{PLH} \ell S\theta_n - D_{PLV} \ell C\theta_n$$
$$- mg \frac{\ell}{2} C\theta_n - g\ell C\theta_n \sum_{i=n+1}^{N} m_i - \ell C_n [D_{CHn} S^2\theta_n + D_{CVn} C^2\theta_n]$$
$$- \ell \sum_{i=n+1}^{N} [D_{CHi} S^2\theta_i + D_{CVi} C^2\theta_i] C(\theta_i - \theta_n) \qquad (153)$$

As with the inertia terms the generalized forces are coupled in the displacement coordinate and the first derivative (the aerodynamic terms contain a velocity dependency). If it is assumed that N = 3, the generalized force for each link can be written explicitly.

$$F_{\theta_1} = L_S \ell C\theta_1 - W_B \ell C\theta_1 + F_{BVA} \ell C\theta_1 - F_{BHA} \ell S\theta_1 - m_{PL} g \ell C\theta_1$$
$$- D_{PLH} \ell S\theta - D_{PLV} \ell C\theta_1 - mg \frac{\ell}{2} C\theta_1 - g\ell C\theta_1 [m + m]$$
$$- \ell C_1 [D_{CH1} S^2\theta_1 + D_{CV1} C^2\theta_1] - \ell [(D_{CH2} S^2\theta_2$$
$$+ D_{CV2} C^2\theta_2) C(\theta_2 - \theta_1) + (D_{CH3} S^2\theta_3 + D_{CV3} C^2\theta_3) C(\theta_3 - \theta_1)] \qquad (154)$$

$$F_{\beta_2} = L_S \ell C\beta_2 - W_B \ell C\beta_2 + F_{BVH} \ell C\beta_2 - F_{BHA} \ell S\beta_2 - m_{PL} g \ell C\beta_2$$

$$- D_{PLH} \ell S\beta_2 - D_{PLV} \ell C\beta_2 - mg \frac{\ell}{2} C\beta_2 - mg \ell C\beta_2 - \ell C_2 [D_{CH2} S^2\beta_2$$

$$+ D_{CV2} C^2\beta_2] - \ell [D_{CH2} S^2\beta_3 + D_{CV3} C^2\beta_3] C(\beta_3 - \beta_2) \qquad (155)$$

$$F_{\beta_3} = L_S \ell C\beta_3 - W_B \ell C\beta_3 + F_{BVA} \ell C\beta_3 - F_{BHA} \ell S\beta_3$$

$$- m_{PL} g \ell C\beta_3 - D_{PLH} \ell S\beta_3 - D_{PLV} \ell C\beta_3 - mg \frac{\ell}{2} C\beta_3$$

$$- \ell C_3 [D_{CH3} S^2\beta_3 + D_{CV3} C^2\beta_3] \qquad (156)$$

2. Aerodynamics

The following aerodynamic forces and moments are defined in this section.

F_{BVA}, F_{BHA}, M_{BB}, D_{PLH}, D_{PLV}, D_{CHi}, D_{CVi}

The forces F_{BVA} and F_{BHA} are the sum of the lift and drag components acting on the balloon in the vertical and horizontal directions.

$$LIFTB = q_B S_B \left[C_{L_{\alpha B}} \alpha_B + C_{L_{\dot{\theta} B}} \left(\frac{d_B \dot{\alpha}}{V_{3R}} \right) \right] \qquad (157)$$

$$DRAGB = q_B S_B \left[C_{D_{\alpha B}} \alpha_B + C_{D_{\dot{\theta} B}} \left(\frac{d_B \dot{\theta}}{V_{BR}} \right) \right] \tag{158}$$

The aerodynamic coefficients $C_{L_{\alpha B}}$, $C_{L_{\dot{\theta} B}}$, $C_{D_{\alpha B}}$, $C_{D_{\dot{\theta} B}}$, are generally functions of angle-of-attack (α_B).

$$F_{BHA} = DRAGB(C\gamma_B) + LIFTB(S\gamma_B) \tag{159}$$

$$F_{BVA} = LIFTB(C\gamma_B) - DRAGB(S\gamma_B) \tag{160}$$

The variables q_B , V_{BR} , α_B , and γ_B will be discussed under the wind velocity section.

The aerodynamic pitch moment acting on the balloon is given by:

$$M_{\theta B} = q_B S_B d_B \left[C_{m_{\alpha B}} \alpha_B + C_{m_{\dot{\theta} B}} \left(\frac{d_B \dot{\theta}}{V_{BR}} \right) \right] \tag{161}$$

where $C_{m_{\alpha B}}$ and $C_{m_{\dot{\theta} B}}$ are functions of angle-of-attack.

The terms D_{PLH} and D_{PLV} are aerodynamic drags acting on the payload in the horizontal and vertical directions respectively.

$$D_{PLH} = \frac{1}{2} \rho_{PL} \left[V_{PL_R} \right]^2 S_{PL} C_{D_{PL}} C\gamma_{PL_R} \tag{162}$$

$$D_{PLV} = \frac{1}{2} \rho_{PL} \left[V_{PL_R} \right]^2 S_{PL} C_{D_{PL}} S\gamma_{PL_R} \tag{163}$$

V_{PL_R} and γ_{PL_R} are discussed under the wind velocity section.
$C_{D_{PL}}$ is an input constant.

The terms D_{CHi} and D_{CVi} are the aerodynamic drags acting on the "i" th link in the horizontal and vertical directions respectively.

$$D_{CHi} = \frac{1}{2}\rho_{Ci} S_{Ci} C_{DC} V_{Ci}^2 C\delta_{Ci} = \frac{1}{2}\rho_{Ci} S_{Ci} C_{DC} V_{Ci} (V_{WCi} + \dot{Y}_{Ci}) \tag{164}$$

$$D_{CVi} = \frac{1}{2}\rho_{Ci} S_{Ci} C_{DC} V_{Ci}^2 S\gamma_{Ci} = \frac{1}{2}\rho_{Ci} S_{Ci} C_{DC} V_{Ci} (\dot{Z}_{Ci}) \tag{165}$$

ρ_{Ci} and V_{WCi} are discussed in the wind velocity section.

$\dot{Y}_{Ci}$ and $\dot{Z}_{Ci}$ are discussed in the translational dynamics section. V_{Ci} and γ_{Ci} are the total effective velocity and effective flight path angle of the C.P. of the "i"th link.

3. Translational Dynamics

Although angular coordinates best define the motion of the system, it is necessary to calculate linear coordinates to express the applied forces acting on the system.

a. Tether Dynamics in Longitudinal Plane

The following equations define the linear displacements, velocities, and accelerations of the c.p. of the "r" th link.

$$Y_{Cn} = -\ell \sum_{i=1}^{n-1} C\beta_i - C_n \ell C\beta_n \tag{166}$$

$$Z_{Cn} = \ell \sum_{i=1}^{n-1} S\beta_i + C_n \ell S\beta_n \tag{167}$$

$$\dot{Y}_{Cn} = \ell \sum_{i=1}^{n-1} \dot{\beta}_i S\beta_i + C_n \ell \dot{\beta}_n S\beta_n \tag{168}$$

$$\dot{Z}_{Cn} = \ell \sum_{i=1}^{n-1} \dot{\beta}_i C\beta_i + C_n \ell \dot{\beta}_n C\beta_n \tag{169}$$

$$\ddot{Y}_{cn} = \ell \sum_{i=1}^{n-1} \ddot{\varphi}_i S\varphi_i + \ell \sum_{i=1}^{n-1} \dot{\varphi}_i^2 C\varphi_i + C_n \ell \ddot{\varphi}_n S\varphi_n + C_n \ell \dot{\varphi}_n^2 C\varphi_n \tag{170}$$

$$\ddot{Z}_{cn} = \ell \sum_{i=1}^{n-1} \ddot{\varphi}_i C\varphi_i - \ell \sum_{i=1}^{n-1} \dot{\varphi}_i^2 S\varphi_i + C_n \ell \ddot{\varphi}_n C\varphi_n - C_n \ell \dot{\varphi}_n^2 S\varphi_n \tag{171}$$

b. Payload Dynamics

$$Y_{PL} = -\ell \sum_{i=1}^{N} C\varphi_i \tag{172}$$

$$Z_{PL} = \ell \sum_{i=1}^{N} S\varphi_i \tag{173}$$

$$\dot{Y}_{PL} = \ell \sum_{i=1}^{N} \dot{\varphi}_i S\varphi_i \tag{174}$$

$$\dot{Z}_{PL} = \ell \sum_{i=1}^{N} \dot{\varphi}_i C\varphi_i \tag{175}$$

$$\ddot{Y}_{PL} = \ell \sum_{i=1}^{N} \ddot{\varphi}_i S\varphi_i + \ell \sum_{i=1}^{N} \dot{\varphi}_i^2 C\varphi_i \tag{176}$$

$$\ddot{Z}_{PL} = \ell \sum_{i=1}^{N} \ddot{\varphi}_i C\varphi_i - \ell \sum_{i=1}^{N} \dot{\varphi}_i^2 S\varphi_i \tag{177}$$

c. Balloon Dynamics

$$Y_B = Y_{PL} + [R_{kq} S\theta - R_{jq} C\theta] \tag{178}$$

$$Z_B = Z_{PL} + [-R_{kq} C\theta - R_{jq} S\theta] \tag{179}$$

$$\dot{Y}_B = \dot{Y}_{PL} + [R_{kq} C\theta + R_{jq} S\theta]\dot{\theta} \tag{180}$$

$$\dot{Z}_B = \dot{Z}_{PL} + [R_{kq} S\theta - R_{jq} C\theta]\dot{\theta} \tag{181}$$

$$\ddot{Y}_B = \ddot{Y}_{PL} + [R_{kq} C\theta + R_{jq} S\theta]\ddot{\theta} + [-R_{kq} S\theta + R_{jq} C\theta]\dot{\theta}^2 \tag{182}$$

$$\ddot{Z}_B = \ddot{Z}_{PL} + [R_{kq} S\theta - R_{jq} C\theta]\ddot{\theta} + [R_{kq} C\theta + R_{jq} S\theta]\dot{\theta}^2 \tag{183}$$

4. Wind Velocity

The steady state wind profile for any simulation is assumed to be a function of altitude and acts in the horizontal direction only. A second force in the form of a gust may be incorporated on the balloon. This gust is a function of time and may be applied at any angle (also a function of time). Referring to Figure 61, the effective free stream velocity for the balloon is found in the following manner.

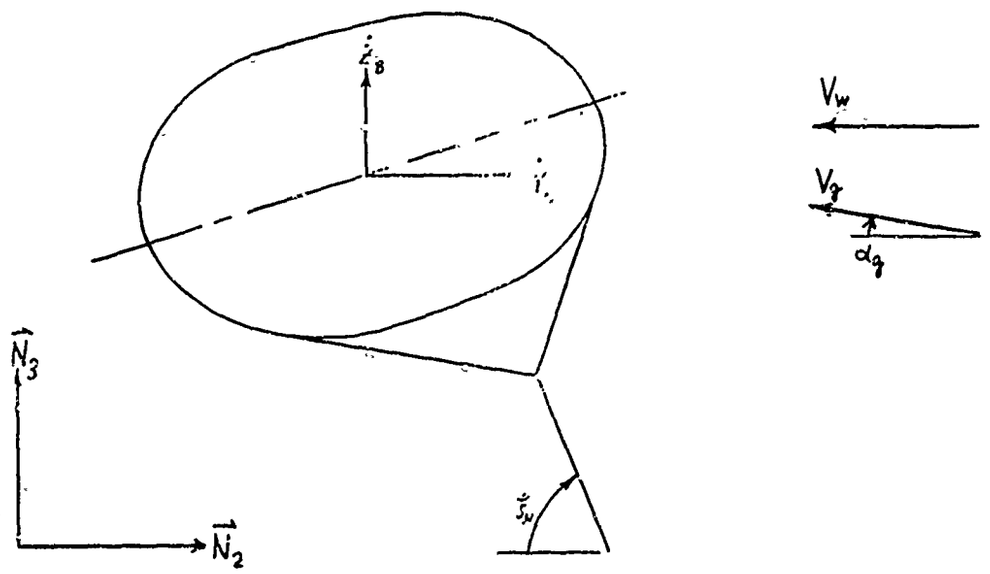

Figure 61

Steady State Wind and Gust Acting on Balloon in Longitudinal Plane

The components of the gust in the vertical and horizontal directions respectively are:

$$V_{gV} = V_g \, S\alpha_g \tag{184}$$

$$V_{gH} = V_g \, C\alpha_g \tag{185}$$

The vertical and horizontal velocities of the balloon relative to the free stream are:

$$\dot{Z}_{BR} = \dot{Z}_B - V_{gV} \tag{186}$$

$$\dot{y}_{BR} = \dot{y}_B + V_w + V_{gH} \tag{187}$$

The velocity, dynamic pressure, flight path angle and angle-of-attack of the balloon are:

$$V_{BR} = \sqrt{\dot{y}_{BR}^2 + \dot{Z}_{BR}^2} \tag{188}$$

$$q_B = \frac{1}{2} \rho_B V_{BR}^2 \tag{189}$$

$$\gamma_B = \tan^{-1}\left[\dot{Z}_{BR} / \dot{y}_{BR}\right] \tag{190}$$

$$\alpha_B = \theta - \gamma_B \tag{191}$$

The relative wind velocity and flight path angle acting on the payload are:

$$V_{PL_R} = \sqrt{(V_w + \dot{y}_{PL})^2 + \dot{Z}_{PL}^2} \tag{192}$$

$$\gamma_{PL} = \tan^{-1}\left[\dot{Z}_{PL} / (V_w + \dot{y}_{PL})\right] \tag{193}$$

The steady state wind (V_W) and the atmospheric density (ρ_a) are considered to be the same for the balloon and the payload.

The wind velocity at the center of pressure of the "i" th link (V_{wci}) is assumed to be the effective wind velocity over the whole link for purposes of calculating the drag on the link. The center of pressure is calculated by finding the dynamic pressure at the bottom and top hinge points of the link and assuming a linear distribution of dynamic pressure over the link as shown in Figure 62.

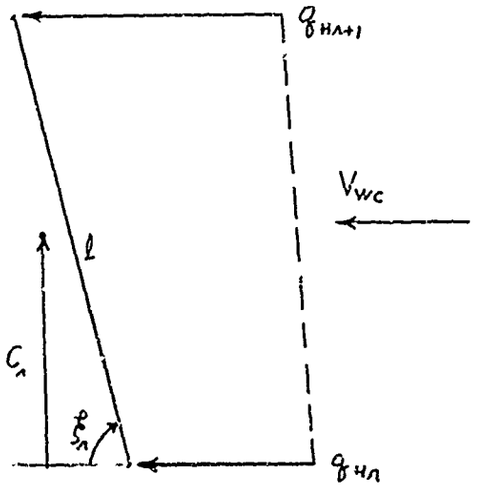

Figure 62. Dynamic Pressure Profile Acting on Link

The dynamic pressure at a hinge due to relative velocity of the hinge is:

$$q_{H\Lambda} = \frac{1}{2} \rho_{H\Lambda} \left\{ \left[V_{w_{H\Lambda}} + \dot{y}_{cm} \right]^2 + \dot{z}_{CH\Lambda}^2 \right\} \tag{194}$$

The dynamic pressure profile presents a trapezoidal distribution of force acting on the link. The centroid of the trapezoid, divided by the vertical length of a link ($l \sin \xi_\Lambda$), is:

$$C_r = \frac{1}{3}\left[\frac{g_{Hr} + 2g_{Hr+1}}{g_{Hr} + g_{Hr+1}}\right] \tag{195}$$

C_r is a non-dimensional center of pressure for the "r" th link. The non-dimensional center of pressure for vertical drag forces is assumed also to be located at C_r.

SECTION IV

LINEARIZED EQUATIONS OF MOTION IN LONGITUDINAL PLANE

1. General

It is now desirable to study the motion of the system when perturbed from its equilibrium position. This perturbation is considered to be small and consequently allows one to ignore higher order effects. For example, if $\delta\dot{\xi}_1$ is a small value, terms involving $\delta\dot{\xi}_1^2$ will be negligible. The four variables θ, ξ_1, ξ_2, ξ_3, and their derivatives are perturbed as follows:

$$\left.\begin{aligned} \theta &= \theta_0 + \delta\theta \quad , \quad \dot{\theta} = \delta\dot{\theta} \quad , \quad \ddot{\theta} = \delta\ddot{\theta} \\ \xi_i &= \xi_{i0} + \delta\xi_i \quad , \quad \dot{\xi}_i = \delta\dot{\xi}_i \quad , \quad \ddot{\xi}_i = \delta\ddot{\xi}_i \end{aligned}\right\} \tag{196}$$

There are several terms containing sines and cosines of combinations of θ and ξ_i. These terms are linearized below.

$$\left.\begin{aligned} S\xi_i &= S\xi_{i0} + \delta\xi_i C\xi_{i0} \\ C\xi_i &= C\xi_{i0} - \delta\xi_i S\xi_{i0} \\ S^2\xi_i &= S^2\xi_{i0} + \delta\xi_i S2\xi_{i0} \\ C^2\xi_i &= C^2\xi_{i0} - \delta\xi_i S2\xi_{i0} \\ S(\theta+\xi_i) &= S(\theta_0+\xi_{i0}) + (\delta\theta+\delta\xi_i)C(\theta_0+\xi_{i0}) \\ C(\theta+\xi_i) &= C(\theta_0+\xi_{i0}) - (\delta\theta+\delta\xi_i)S(\theta_0+\xi_{i0}) \\ C(\xi_i-\xi_j) &= C(\xi_{i0}-\xi_{j0}) + (\delta\xi_j-\delta\xi_i)S(\xi_{i0}-\xi_{j0}) \end{aligned}\right\} \tag{197}$$

2. Inertia Terms

Equations (120) to (123) are the equations of motion to be linearized. If Equations (196) and (197) are substituted in, the results (after cancelling higher order terms) is given. Note: The δ symbol is dropped from the perturbation variable for ease of writing.

$$\{ I_{xo} + M_L R_{km}^2 + M_V R_{jm}^2 \} \ddot{\theta}$$

$$+ \{ \ell [M_L R_{km} S(\xi_{1o} + \theta_o) - M_V R_{jm} C(\xi_{1o} + \theta_o)] \} \ddot{\xi}_1$$

$$+ \{ \ell [M_L R_{km} S(\xi_{2o} + \theta_o) - M_V R_{jm} C(\xi_{2o} + \theta_o)] \} \ddot{\xi}_2$$

$$+ \{ \ell [M_L R_{km} S(\xi_{3o} + \theta_o) - M_V R_{jm} C(\xi_{3o} + \theta_o)] \} \ddot{\xi}_3 = F_\theta \qquad (198)$$

$$\{ \ell [M_L R_{km} S(\xi_{1o} + \theta_o) - M_V R_{jm} C(\xi_{1o} + \theta_o)] \} \ddot{\theta}$$

$$+ \{ \ell^2 [\tfrac{7m}{3} + m_{pL} + M_L S^2(\xi_{1o} + \theta_o) + M_V C^2(\xi_{1o} + \theta_o)] \} \ddot{\xi}_1$$

$$+ \{ \ell^2 [(\tfrac{3m}{2} + m_{pL}) C(\xi_{1o} - \xi_{2o}) + M_L S(\xi_{1o} + \theta_o) S(\xi_{2o} + \theta_o) + M_V C(\xi_{1o} + \theta_o) C(\xi_{2o} + \theta_o)] \} \ddot{\xi}_2$$

$$+ \{ \ell^2 [(\tfrac{m}{2} + m_{pL}) C(\xi_{1o} - \xi_{3o}) + M_L S(\xi_{1o} + \theta_o) S(\xi_{3o} + \theta_o) + M_V C(\xi_{1o} + \theta_o) C(\xi_{3o} + \theta_o)] \} \ddot{\xi}_3 = F_{\xi_1} \qquad (199)$$

$$\{ \ell [M_L R_{km} S(\xi_{2o} + \theta_o) - M_V R_{jm} C(\xi_{2o} + \theta_o)] \} \ddot{\theta}$$

$$+ \{ \ell^2 [(\tfrac{3m}{2} + m_{pL}) C(\xi_{1o} - \xi_{2o}) + M_L S(\xi_{2o} + \theta_o) S(\xi_{1o} + \theta_o) + M_V C(\xi_{2o} + \theta_o) C(\xi_{1o} + \theta_o)] \} \ddot{\xi}_1$$

$$+ \{ \ell^2 [\tfrac{4m}{3} + m_{pL} + M_L S^2(\xi_{2o} + \theta_o) + M_V C^2(\xi_{2o} + \theta_o)] \} \ddot{\xi}_2$$

$$+ \{ \ell^2 [(\tfrac{m}{2} + m_{pL}) C(\xi_{2o} - \xi_{3o}) + M_L S(\xi_{2o} + \theta_o) S(\xi_{3o} + \theta_o) + M_V C(\xi_{2o} + \theta_o) C(\xi_{3o} + \theta_o)] \} \ddot{\xi}_3 = F_{\xi_2} \qquad (200)$$

$$\{\ell[M_L R_{km} S(\xi_{30}+\theta_0) - M_V R_{jm} C(\xi_{30}+\theta_0)]\}\ddot{\theta}$$

$$+\{\ell^2[(\tfrac{m}{2}+M_{PL})C(\xi_{10}-\xi_{30})+M_L S(\xi_{30}+\theta_0)S(\xi_{10}+\theta_0)+M_V C(\xi_{30}+\theta_0)C(\xi_{10}+\theta_0)]\}\ddot{\xi}_1$$

$$+\{\ell^2[(\tfrac{m}{2}+M_{PL})C(\xi_{20}-\xi_{30})+M_L S(\xi_{30}+\theta_0)S(\xi_{30}+\theta_0)+M_V C(\xi_{30}+\theta_0)C(\xi_{20}+\theta_0)]\}\ddot{\xi}_2$$

$$+\{\ell^2[\tfrac{m}{3}+M_{PL}+M_L S^2(\xi_{30}+\theta_0)+M_V C^2(\xi_{30}+\theta_0)]\}\ddot{\xi}_3 = F_{\xi_3} \qquad (201)$$

3. Generalized Forces

Equations (198) to (201) give the coefficients of the second derivatives. It is now necessary to expand F_θ and F_{ξ_i} to find the coefficients of the first derivatives and the generalized coordinates. Linearizing Equation (142):

$$F_\theta = [L_S R_{kB} - W_B R_{kq} + F_{BVA} R_{kA} - F_{BHA} R_{jA}][S\theta_0 + \theta C\theta_0]$$

$$+[-L_S R_{jB} + W_B R_{jq} - F_{BVA} R_{jA} - F_{BHA} R_{kA}][C\theta_0 - \theta S\theta_0] + M_{\theta B} \qquad (202)$$

The variables F_{BVA}, F_{BHA}, and $M_{\theta B}$ must be expanded and linearized. The Equations (157) to (161) can be written as:

$$LIFTB = \tfrac{1}{2}\rho_B V_{BR}^2 S_B\left[C_{L_{\alpha B}}(\alpha_{B0}+\theta) + C_{L_{\dot\theta B}}\left(\frac{d_B}{V_{BR}}\right)\dot\theta\right] \qquad (203)$$

$$DRAGB = \tfrac{1}{2}\rho_B V_{BR}^2 S_B\left[C_{D_{\alpha B}}(\alpha_{B0}+\theta) + C_{D_{\dot\theta B}}\left(\frac{d_B}{V_{BR}}\right)\dot\theta\right] \qquad (204)$$

$$M_{\theta B} = \tfrac{1}{2}\rho_B V_{BR}^2 S_B\left[C_{m_{\alpha B}}(\alpha_{B0}+\theta) + C_{m_{\dot\theta B}}\left(\frac{d_B}{V_{BR}}\right)\dot\theta\right] \qquad (205)$$

$$F_{BHA} = DRAGB \qquad (206)$$

$$F_{BVA} = LIFTB \tag{207}$$

Note: $\gamma_B = 0$

In Equations (203) to (205) the coefficient V_{BR}^2 must be linearized.

From Equation (188) V_{BR}^2 is:

$$V_{BR}^2 = \dot{y}_{BR}^2 + \dot{Z}_{BR}^2 \tag{208}$$

$$V_{BR}^2 = \{\ell[\dot{\xi}_1 S\xi_{10} + \dot{\xi}_2 S\xi_{20} + \dot{\xi}_3 S\xi_{30}] + [R_{kq} C\theta_o + R_{jq} S\theta_o]\dot{\theta} + V_w\}^2 \tag{209}$$

$$V_{BR}^2 = V_w^2 + 2V_w[\ell(\dot{\xi}_1 S\xi_{10} + \dot{\xi}_2 S\xi_{20} + \dot{\xi}_3 S\xi_{30}) + (R_{kq} C\theta_o + R_{jq} S\theta_o)\dot{\theta}] \tag{210}$$

Substituting Equation (210) into (203) and noting that $C_{L_{\alpha B}} \alpha_{Bo} = C_{LB}$;

$$LIFTB = \tfrac{1}{2}\rho_B V_w^2 S_B\left[C_{LB} + C_{L_{\alpha B}}\theta + C_{L_{\dot{\alpha}B}}\left(\frac{\dot{\alpha}_B}{V_w}\right)\dot{\theta}\right]$$

$$+\rho_B V_w S_B[\ell(\dot{\xi}_1 S\xi_{10} + \dot{\xi}_2 S\xi_{20} + \dot{\xi}_3 S\xi_{30}) + (R_{kq} C\theta_o + R_{jq} S\theta_o)\dot{\theta}][C_{LB}] \tag{211}$$

Substituting Equation (210) into (204) gives:

$$DRAGB = \tfrac{1}{2}\rho_B V_w^2 S_B\left[C_{DB} + C_{D_{\alpha B}}\theta + C_{D_{\dot{\alpha}B}}\left(\frac{\dot{\alpha}_B}{V_w}\right)\dot{\theta}\right]$$

$$+\rho_B V_w S_B[\ell(\dot{\xi}_1 S\xi_{10} + \dot{\xi}_2 S\xi_{20} + \dot{\xi}_3 S\xi_{30}) + (R_{kq} C\theta_o + R_{jq} S\theta_o)\dot{\theta}][C_{DB}] \tag{212}$$

Rearranging terms, the variables F_{BVA} , F_{BHA} , and $M_{\theta B}$ are:

$$F_{BVA} = q_B S_B C_{LB} + [q_B S_B C_{L_{\alpha B}}]\theta + S_B\left[q_B \frac{d_B}{V_w} C_{L_{\dot\theta B}} + \rho_B V_w (R_{kq} C\theta_o + R_{jq} S\theta_o) C_{LB}\right]\dot\theta + [\rho_B V_w S_B \ell S \xi_{10} C_{LB}]\dot\xi_1 + [\rho_B V_w S_B \ell S \xi_{20} C_{LB}]\dot\xi_2 + [\rho_B V_w S_B \ell S \xi_{30} C_{LB}]\dot\xi_3 \quad (213)$$

$$F_{BHA} = q_B S_B C_{DB} + [q_B S_B C_{D_{\alpha B}}]\theta + S_B\left[q_B \frac{d_B}{V_w} C_{D_{\dot\theta B}} + \rho_B V_w (R_{kq} C\theta_o + R_{jq} S\theta_o) C_{DB}\right]\dot\theta + [\rho_B V_w S_B \ell S \xi_{10} C_{DB}]\dot\xi_1 + [\rho_B V_w S_B \ell S \xi_{20} C_{DB}]\dot\xi_2 + [\rho_B V_w S_B \ell S \xi_{30} C_{DB}]\dot\xi_3 \quad (214)$$

$$M_{OB} = q_B S_B d_B C_{mB} + [q_B S_B d_B C_{m_{\alpha B}}]\theta + S_B d_B\left[q_B \frac{d_B}{V_w} C_{m_{\dot\theta B}} + \rho_B V_w (R_{kq} C\theta_o + R_{jq} S\theta_o) C_{mB}\right]\dot\theta + [\rho_B V_w S_B d_B \ell S \xi_{10} C_{mB}]\dot\xi_1 + [\rho_B V_w S_B d_B \ell S \xi_{20} C_{mB}]\dot\xi_2 + [\rho_B V_w S_B d_B \ell S \xi_{30} C_{mB}]\dot\xi_3 \quad (215)$$

Substituting Equations (213) to (215) into Equation (202) gives the final linearized form of F_θ .

$$F_\theta = \{[L_S R_{kB} - W_B R_{kq} + q_B S_B (R_{kA} C_{LB} - R_{jA} C_{DB})] S\theta_o + [-L_S R_{jB} + W_B R_{jq} + q_B S_B (-R_{jA} C_{LB} - R_{kA} C_{DB})] C\theta_o + q_B S_B d_B C_{mB}\} + \{[L_S R_{kB} - W_B R_{kq} + q_B S_B (R_{kA} C_{LB} - R_{jA} C_{DB})] C\theta_o - [-L_S R_{jB} + W_B R_{jq}$$

$$+ q_B S_B \left(-R_{jA} C_{L_B} - R_{kA} C_{D_B}\right)\Big] S\theta_o + q_B S_B \left[R_{kA} C_{L_{\alpha B}} - R_{jA} C_{D_{\alpha B}}\right] S\theta_o$$

$$+ q_B S_B \left[-R_{jA} C_{L_{\alpha B}} - R_{kA} C_{D_{\alpha B}}\right] C\theta_o + q_B S_B d_B C_{m_{\alpha B}} \Big\} \theta$$

$$+ \Big\{ q_B S_B \frac{d_B}{V_w} \left[R_{kA}\left(C_{L_{\dot\theta B}} S\theta_o - C_{D_{\dot\theta B}} C\theta_o\right) + R_{jA}\left(-C_{D_{\dot\theta B}} S\theta_o - C_{L_{\dot\theta B}} C\theta_o\right) + d_B C_{m_{\dot\theta B}}\right]$$

$$+ \rho_B V_w S_B \left[R_{kq} C\theta_o + R_{jq} S\theta_o\right]\left[\left(R_{kA} S\theta_o - R_{jA} C\theta_o\right) C_{L_B} - \left(R_{kA} C\theta_o + R_{jA} S\theta_o\right) C_{D_B} + d_B C_{m_B}\right] \Big\} \dot\theta$$

$$+ \rho_B V_w S_B \ell S\xi_{10} \left[R_{kA}\left(C_{L_B} S\theta_o - C_{D_B} C\theta_o\right) - R_{jA}\left(C_{D_B} S\theta_o + C_{L_B} C\theta_o\right) + d_B C_{m_B}\right] \dot\xi_1$$

$$+ \rho_B V_w S_B \ell S\xi_{20} \left[R_{kA}\left(C_{L_B} S\theta_o - C_{D_B} C\theta_o\right) - R_{jA}\left(C_{D_B} S\theta_o + C_{L_B} C\theta_o\right) + d_B C_{m_B}\right] \dot\xi_2$$

$$+ \rho_B V_w S_B \ell S\xi_{30} \left[R_{kA}\left(C_{L_B} S\theta_o - C_{D_B} C\theta_o\right) - R_{jA}\left(C_{D_B} S\theta_o + C_{L_B} C\theta_o\right) + d_B C_{m_B}\right] \dot\xi_3 \qquad (216)$$

Next linearize Equation (154) assuming that the payload drag is zero and that the center of pressure is a constant.

$$F_{\xi_1} = \ell \Big\{ \left[C\xi_{10} - \xi_1 S\xi_{10}\right]\left[L_S - W_B + F_{BVA} - q\left(m_{PL} + \frac{5m}{2}\right)\right]$$

$$+ \left[S\xi_{10} + \xi_1 C\xi_{10}\right]\left[-F_{BHA}\right]$$

$$- C_1 \left[D_{CH1}\left(S^2\xi_{10} + \xi_1 S2\xi_{10}\right) + D_{CV1}\left(C^2\xi_{10} - \xi_1 S2\xi_{10}\right)\right]$$

$$- \left[D_{CH2}\left(S^2\xi_{20} + \xi_2 S2\xi_{20}\right) + D_{CV2}\left(C^2\xi_{20} - \xi_2 S2\xi_{20}\right)\right]\left[C\left(\xi_{20} - \xi_{10}\right) + \left(\xi_1 - \xi_2\right) S\left(\xi_{20} - \xi_{10}\right)\right]$$

$$- \left[D_{CH3}\left(S^2\xi_{30} + \xi_3 S2\xi_{30}\right) + D_{CV3}\left(C^2\xi_{30} - \xi_3 S2\xi_{30}\right)\right]\left[C\left(\xi_{10} - \xi_{10}\right) + \left(\xi_1 - \xi_3\right) S\left(\xi_{30} - \xi_{10}\right)\right] \Big\} \qquad (217)$$

C_1 is given by Equation (112),

$$C_1 = \frac{1}{3}\left[\frac{\rho_{H1} + 2\rho_{H2}}{\rho_{H1} + \rho_{H2}}\right] \tag{218}$$

From Equations (164) and (165):

$$D_{CH_i} = \frac{1}{2}\rho_{C_i}\left[\dot{Y}_{C_i} + V_{WC_i}\right]^2 S_{C_i} C_{DC} \tag{219}$$

$$D_{CV_i} = \frac{1}{2}\rho_{C_i}\dot{Z}_{C_i} V_{WC_i} S_{C_i} C_{DC} \tag{220}$$

From Equations (168) and (169):

$$\dot{Y}_{C_i} = \ell \sum_{j=1}^{i-1} \dot{\rho}_j S\rho_j + C_i \ell \dot{\rho}_i S\rho_i \tag{221}$$

$$\dot{Z}_{C_i} = \ell \sum_{j=1}^{i-1} \dot{\rho}_j C\rho_j + C_i \ell \dot{\rho}_i C\rho_i \tag{222}$$

Linearizing Equation (220) gives:

$$D_{CV_i} = \frac{1}{2}\rho_{C_i} S_{C_i} C_{DC} V_{WC_i} \ell\left[\sum_{j=1}^{i-1} \dot{\rho}_j C\rho_{j0} + C_i \dot{\rho}_i C\rho_{i0}\right] \tag{223}$$

The terms $\left[\dot{Y}_{C_i} + V_{WC_i}\right]^2$ are expanded as follows:

$$\left[\dot{Y}_{C1} + V_{WC1}\right]^2 = 2\left[C_1 \dot{\rho}_1 S\rho_{10}\right]\ell V_{WC1} + V_{WC1}^2 \tag{224}$$

$$\left[\dot{Y}_{C2} + V_{WC2}\right]^2 = 2\left[\dot{\rho}_1 S\rho_{10} + C_2 \dot{\rho}_2 S\rho_{20}\right]\ell V_{WC2} + V_{WC2}^2 \tag{225}$$

$$\left[\dot{Y}_{C3} + V_{WC3}\right]^2 = 2\left[\dot{\rho}_1 S\rho_{10} + \dot{\rho}_2 S\rho_{20} + C_3 \dot{\rho}_3 S\rho_{30}\right]\ell V_{WC3} + V_{WC3}^2 \tag{226}$$

Substituting Equations (224) to (226) into Equation (219) yields D_{cHi} . D_{cVi} comes from expanding Equation (223)

$$\left.\begin{aligned} D_{cH1} &= \tfrac{1}{2}\rho_{c1} S_{c1} C_{Dc}\left[2\left(C_1 \dot{\xi}_1 S\beta_{1c}\right) l V_{wc1} + V_{wc1}^2\right] \\ D_{cV1} &= \tfrac{1}{2}\rho_{c1} S_{c1} C_{Dc} V_{wc1} l\, C_1 \dot{\xi}_1 C\beta_{1c} \end{aligned}\right\} \quad (227)$$

$$\left.\begin{aligned} D_{cH2} &= \tfrac{1}{2}\rho_{c2} S_{c2} C_{Dc}\left[2\left(\dot{\xi}_1 S\beta_{1c} + C_2 \dot{\xi}_2 S\beta_{2c}\right) l V_{wc2} + V_{wc2}^2\right] \\ D_{cV2} &= \tfrac{1}{2}\rho_{c2} S_{c2} C_{Dc} V_{wc2} l\left[\dot{\xi}_1 C\beta_{1c} + C_2 \dot{\xi}_2 C\beta_{2c}\right] \end{aligned}\right\} \quad (228)$$

$$\left.\begin{aligned} D_{cH3} &= \tfrac{1}{2}\rho_{c3} S_{c3} C_{Dc}\left[2\left(\dot{\xi}_1 S\beta_{1c} + \dot{\xi}_2 S\beta_{2c} + C_3 \dot{\xi}_3 S\beta_{3c}\right) l V_{wc3} + V_{wc3}^2\right] \\ D_{cV3} &= \tfrac{1}{2}\rho_{c3} S_{c3} C_{Dc} V_{wc3} l\left[\dot{\xi}_1 C\beta_{1c} + \dot{\xi}_2 C\beta_{2c} + C_3 \dot{\xi}_3 C\beta_{3c}\right] \end{aligned}\right\} \quad (229)$$

Substituting Equations (213), (214), (227), to (229) into Equation (217) and separating terms gives the final linearized form of F_{ξ_1} .

$$\begin{aligned} F_{\xi_1} = l\{ & C\beta_{1c}\left[L_S - W_B - g\left(m_{PL} + \tfrac{5}{2}m\right) + \gamma_B S_B C_{LB}\right] + S\beta_{1c}\left[-\gamma_B S_B C_{DB}\right] \\ & - \tfrac{C_1}{2}\rho_{c1} S_{c1} C_{Dc} V_{wc1}^2 S^2\beta_{1c} - \tfrac{1}{2}\rho_{c2} S_{c2} C_{Dc} V_{wc2}^2 S^2\beta_{2c} C(\beta_{1c} - \beta_{2c}) \\ & - \tfrac{1}{2}\rho_{c3} S_{c3} C_{Dc} V_{wc3}^2 S^2\beta_{3c} C(\beta_{1c} - \beta_{3c})\} \\ & + l\{\gamma_B S_B\left[C\beta_{1c} C_{L_{\alpha B}} - S\beta_{1c} C_{D_{\alpha B}}\right]\}\Theta \end{aligned}$$

$$+\ell\{-S\beta_{10}[L_S - W_B - g(m_{PL}+\tfrac{5}{2}m)+q_B S_B C_{LB}] + C\beta_{10}[-q_B S_B C_{DB}]$$

$$-\tfrac{C_1}{2}\rho_{C1}S_{C1}C_{DC}V_{WC1}^2 S2\beta_{10} - \tfrac{1}{2}\rho_{C2}S_{C2}C_{DC}V_{WC2}^2 S^2\beta_{20} S(\beta_{20}-\beta_{10})$$

$$-\tfrac{1}{2}\rho_{C3}S_{C3}C_{DC}V_{WC3}^2 S^2\beta_{30} S(\beta_{30}-\beta_{10})\}\beta_1$$

$$+\ell\{-\tfrac{1}{2}\rho_{C2}S_{C2}C_{DC}V_{WC2}^2[S2\beta_{20}C(\beta_{10}-\beta_{20}) - S^2\beta_{20}S(\beta_{20}-\beta_{10})]\}\beta_2$$

$$+\ell\{-\tfrac{1}{2}\rho_{C3}S_{C3}C_{DC}V_{WC3}^2[S2\beta_{30}C(\beta_{10}-\beta_{30}) - S^2\beta_{30}S(\beta_{20}-\beta_{10})]\}\beta_3$$

$$+\ell\{q_B S_B \frac{d_B}{V_W}[C_{L\dot\theta B}C\beta_{10} - C_{D\dot\theta B}S\beta_{10}] + S_B\rho_B V_W[R_{kq}C\theta_0 + R_{jq}S\theta_0][C_{LB}C\beta_{10} - C_{DB}S\beta_{10}]\}\dot\theta$$

$$+\ell\{S_B\rho_B V_W \ell S\beta_{10}[C_{LB}C\beta_{10} - C_{DB}S\beta_{10}] - \ell[C_1^2\rho_{C1}S_{C1}C_{DC}V_{WC1}(S^3\beta_{10}+\tfrac{1}{2}C^3\beta_{10})$$

$$+\rho_{C2}S_{C2}C_{DC}V_{WC2}(S^2\beta_{20}S\beta_{10}+\tfrac{1}{2}C^2\beta_{20}C\beta_{10})C(\beta_{10}-\beta_{20})$$

$$+\rho_{C3}S_{C3}C_{DC}V_{WC3}(S^2\beta_{30}S\beta_{10}+\tfrac{1}{2}C^2\beta_{30}C\beta_{10})C(\beta_{10}-\beta_{30})]\}\dot\beta_1$$

$$+\ell\{S_B\rho_B V_W \ell S\beta_{20}[C_{LB}C\beta_{10} - C_{DB}S\beta_{10}] - \ell[C_2\rho_{C2}S_{C2}C_{DC}V_{WC2}(S^3\beta_{20}$$

$$+\tfrac{1}{2}C^3\beta_{20})C(\beta_{10}-\beta_{20}) + \rho_{C3}S_{C3}C_{DC}V_{WC3}(S^2\beta_{30}S\beta_{20}+\tfrac{1}{2}C^2\beta_{30}C\beta_{20})C(\beta_{10}-\beta_{30})]\}\dot\beta_2$$

$$+\ell\{S_B\rho_B V_W \ell S\beta_{30}[C_{LB}C\beta_{10} - C_{DB}S\beta_{10}]$$

$$-\ell[C_3\rho_{C3}S_{C3}C_{DC}V_{WC3}(S^3\beta_{30}+\tfrac{1}{2}C^3\beta_{30})C(\beta_{10}-\beta_{30})]\}\dot\beta_3 \qquad (230)$$

Equation (155) is:

$$F_{\xi_2} = \ell\Big\{\left[C\xi_{20} - \xi_2 S\xi_{20}\right]\left[L_S - W_B + F_{BVA} - g\left(m_{PL} + \tfrac{3}{2}m\right)\right]$$

$$+\left[S\xi_{20} + \xi_2 C\xi_{20}\right]\left[-F_{BHA}\right] - C_2\left[D_{CH2}\left(S^2\xi_{20} + \xi_2\, S2\xi_{20}\right)\right.$$

$$\left.+ D_{CV2}\left(C^2\xi_{20} - \xi_2\, S2\xi_{20}\right)\right] - \left[D_{CH3}\left(S^2\xi_{30} + \xi_3\, S2\xi_{30}\right)\right.$$

$$\left.+ D_{CV3}\left(C^2\xi_{30} - \xi_3\, S2\xi_{30}\right)\right]\left[C(\xi_{20}-\xi_{30}) + (\xi_2 - \xi_3)\,S(\xi_{30}-\xi_{20})\right]\Big\} \qquad (231)$$

Substituting Equations (213), (214), (228) and (229) into Equation (231) and separating terms gives the final linearized form of F_{ξ_2}.

$$F_{\xi_2} = \ell\Big\{C\xi_{20}\left[L_S - W_B - g\left(m_{PL} + \tfrac{3}{2}m\right) + q_B S_B C_{LB}\right] + S\xi_{20}\left[-q_B S_B C_{DB}\right]$$

$$- \tfrac{C_2}{2}\rho_{C2} S_{C2} C_{DC} V_{WC2}^2 S^2\xi_{20} - \tfrac{1}{2}\rho_{C3} S_{C3} C_{DC} V_{WC3}^2 S^2\xi_{30}\, C(\xi_{20}-\xi_{30})\Big\}$$

$$+\ell\left\{q_B S_B\left[C\xi_{20} C_{L_{\alpha B}} - S\xi_{20} C_{D_{\alpha B}}\right]\right\}\theta$$

$$+\ell\Big\{-S\xi_{20}\left[L_S - W_B - g\left(m_{PL} + \tfrac{3}{2}m\right) + q_B S_B C_{LB}\right] + C\xi_{20}\left[-q_B S_B C_{DB}\right]$$

$$- \tfrac{C_2}{2}\rho_{C2} S_{C2} C_{DC} V_{WC2}^2\, S2\xi_{20} - \tfrac{1}{2}\rho_{C3} S_{C3} C_{DC} V_{WC3}^2 S^2\xi_{30}\, S(\xi_{30}-\xi_{20})\Big\}\xi_2$$

$$+\ell\left\{-\tfrac{1}{2}\rho_{C3} S_{C3} C_{DC} V_{WC3}^2\left[S2\xi_{30}\, C(\xi_{20}-\xi_{30}) - S^2\xi_{30}\, S(\xi_{30}-\xi_{20})\right]\right\}\xi_3$$

$$+\ell\left\{q_B S_B \tfrac{d_B}{V_W}\left[C_{L_{\dot\theta B}} C\xi_{20} - C_{D_{\dot\theta B}} S\xi_{20}\right] + S_B \rho_B V_W\left[R_{kig} C\theta_0 + R_{jig} S\theta_0\right]\left[C_{LB} C\xi_{20} - C_{DB} S\xi_{20}\right]\right\}\dot\theta$$

$$+\ell\{S_B\rho_B V_w \ell S\beta_{10}[C_{LB}C\beta_{20} - C_{DB}S\beta_{20}]$$

$$-\ell[C_2\rho_{C2}S_{C2}C_{DC}V_{WC2}(S^2\beta_{20}S\beta_{10} + \tfrac{1}{2}C^2\beta_{20}C\beta_{10})$$

$$+\rho_{C3}S_{C3}C_{DC}V_{WC3}(S^2\beta_{30}S\beta_{10} + \tfrac{1}{2}C^2\beta_{30}C\beta_{10})C(\beta_{20}-\beta_{30})]\}\dot{\beta}_2$$

$$+\ell\{S_B\rho_B V_w \ell S\beta_{20}[C_{LB}C\beta_{20} - C_{DB}S\beta_{20}]$$

$$-\ell[C_2^2\rho_{C2}S_{C2}C_{DC}V_{WC2}(S^3\beta_{20} + \tfrac{1}{2}C^3\beta_{20})$$

$$+\rho_{C3}S_{C3}C_{DC}V_{WC3}(S^2\beta_{30}S\beta_{20} + \tfrac{1}{2}C^2\beta_{30}C\beta_{20})C(\beta_{20}-\beta_{30})]\}\dot{\beta}_2$$

$$+\ell\{S_B\rho_B V_w \ell S\beta_{30}[C_{LB}C\beta_{20} - C_{DB}S\beta_{20}]$$

$$-\ell[C_3\rho_{C3}S_{C3}C_{DC}V_{WC3}(S^3\beta_{30} + \tfrac{1}{2}C^3\beta_{30})C(\beta_{20}-\beta_{30})]\}\dot{\beta}_3 \qquad (232)$$

Equation (156) is:

$$F_{\beta_3} = \ell\{[C\beta_{30} - \beta_3 S\beta_{30}][L_S - W_B + F_{BVA} - g(m_{PL} + \tfrac{m}{2})]$$

$$+[S\beta_{20} + \beta_3 C\beta_{20}][-F_{BHA}]$$

$$-C_3[D_{CH3}(S^2\beta_{30} + \beta_3 S2\beta_{30}) + D_{CV3}(C^2\beta_{30} - \beta_3 S2\beta_{30})]\} \qquad (233)$$

Substituting Equations (213), (214) and (229) into Equation (233) and separating terms gives the final linearized form of F_{β_3}.

$$
\begin{aligned}
F_{\beta_3} = {} & \ell\{ C\beta_{30}[L_S - W_B - g(m_{PL} + \tfrac{m}{2}) + q_B S_B C_{LB}] \\
& + S\beta_{30}[-q_S S_B C_{DB}] - \tfrac{C_3}{2}\rho_{C3} S_{C3} C_{DC} V_{WC3}^2 S^2\beta_{30}\} \\
& + \ell\{ q_B S_B [C\beta_{30} C_{L\alpha B} - S\beta_{30} C_{D\alpha B}]\}\theta \\
& + \ell\{ -S\beta_{30}[L_S - W_B - g(m_{PL} + \tfrac{m}{2}) + q_B S_B C_{LB}] \\
& - C\beta_{30}[q_B S_B C_{DB}] - \tfrac{C_3}{2}\rho_{C3} S_{C3} C_{DC} V_{WC3}^2 S2\beta_{30}\}\beta_3 \\
& + \ell\{ S_B[\tfrac{\dot{\alpha}_B}{V_W} q_B (C_{L\dot{\alpha}B} C\beta_{30} - C_{D\dot{\alpha}B} S\beta_{30}) \\
& + \rho_B V_W (R_{\beta q} C\theta_0 + R_{\beta r} S\theta_0)(C_{LB} C\beta_{30} - C_{DB} S\beta_{30})]\}\dot{\theta} \\
& + \ell\{ S_B \rho_B V_W \ell S\beta_{10}[C_{LB} C\beta_{30} - C_{DB} S\beta_{30}] \\
& - \ell C_3 \rho_{C3} S_{C3} C_{DC} V_{WC3}(S^2\beta_{30} S\beta_{10} + \tfrac{1}{2} C^2\beta_{30} C\beta_{10})\}\dot{\beta}_1 \\
& + \ell\{ S_B \rho_B V_W \ell S\beta_{20}[C_{LB} C\beta_{30} - C_{DB} S\beta_{30}] \\
& - \ell C_3 \rho_{C3} S_{C3} C_{DC} V_{WC3}(S^2\beta_{30} S\beta_{20} + \tfrac{1}{2} C^2\beta_{30} C\beta_{20})\}\dot{\beta}_2 \\
& + \ell\{ S_B \rho_B V_W \ell S\beta_{30}[C_{LB} C\beta_{30} - C_{DB} S\beta_{30}] \\
& - \ell C_3^2 \rho_{C3} S_{C3} C_{DC} V_{WC3}(S^3\beta_{30} + \tfrac{1}{2} C^3\beta_{30})\}\dot{\beta}_3
\end{aligned}
\tag{234}
$$

4. Characteristic Equation

Equations (198) to (201) in conjunction with Equations (216), (230), (232) and (234) form a set of four simultaneous equations of the following form.

$$\alpha_{i1}\ddot{\theta} + \alpha_{i2}\ddot{\beta}_1 + \alpha_{i3}\ddot{\beta}_2 + \alpha_{i4}\ddot{\beta}_3 + \beta_{i1}\dot{\theta} + \beta_{i2}\dot{\beta}_1 + \beta_{i3}\dot{\beta}_2 + \beta_{i4}\dot{\beta}_3$$

$$+ \gamma_{i1}\theta + \gamma_{i2}\beta_1 + \gamma_{i3}\beta_2 + \gamma_{i4}\beta_3 = \delta_i$$

$$i = 1, 2, 3, 4 \qquad (235)$$

The system is assumed to be in equilibrium, $\delta_i = 0$; and all initial conditions are zero $\left(\dot{\theta}(0) = \dot{\beta}_i(0) = \theta(0) = \beta_i(0) = 0\right)$.

Taking the Laplace transform of Equation (235) and writing in matrix notation gives the following equation.

$$\begin{bmatrix} \alpha_{11}S^2+\beta_{11}S+\gamma_{11} & \alpha_{12}S^2+\beta_{12}S+\gamma_{12} & \alpha_{13}S^2+\beta_{13}S+\gamma_{13} \\ \alpha_{21}S^2+\beta_{21}S+\gamma_{21} & \alpha_{22}S^2+\beta_{22}S+\gamma_{22} & \alpha_{23}S^2+\beta_{23}S+\gamma_{23} \\ \alpha_{31}S^2+\beta_{31}S+\gamma_{31} & \alpha_{32}S^2+\beta_{32}S+\gamma_{32} & \alpha_{33}S^2+\beta_{33}S+\gamma_{33} \\ \alpha_{41}S^2+\beta_{41}S+\gamma_{41} & \alpha_{42}S^2+\beta_{42}S+\gamma_{42} & \alpha_{43}S^2+\beta_{43}S+\gamma_{43} \end{bmatrix}$$

$$\begin{bmatrix} \alpha_{14}S^2+\beta_{14}S+\gamma_{14} \\ \alpha_{24}S^2+\beta_{24}S+\gamma_{24} \\ \alpha_{34}S^2+\beta_{34}S+\gamma_{34} \\ \alpha_{44}S^2+\beta_{44}S+\gamma_{44} \end{bmatrix} \begin{Bmatrix} \theta(S) \\ \beta_1(S) \\ \beta_2(S) \\ \beta_3(S) \end{Bmatrix} = \begin{Bmatrix} 0 \\ 0 \\ 0 \\ 0 \end{Bmatrix} \qquad (236)$$

The coefficients α_{ij}, β_{ij}, γ_{ij}, and δ_i are tabulated for easy reference.

$$\alpha_{11} = I_{xB} + M_L R_{km}^2 + M_V R_{jm}^2 \tag{237}$$

$$\alpha_{12} = \ell\left[M_L R_{km} S(\beta_{10}+\theta_0) - M_V R_{jm} C(\beta_{10}+\theta_0)\right] \tag{238}$$

$$\alpha_{13} = \ell\left[M_L R_{km} S(\beta_{20}+\theta_0) - M_V R_{jm} C(\beta_{20}+\theta_0)\right] \tag{239}$$

$$\alpha_{14} = \ell\left[M_L R_{km} S(\beta_{30}+\theta_0) - M_V R_{jm} C(\beta_{30}+\theta_0)\right] \tag{240}$$

$$\alpha_{21} = \ell\left[M_L R_{km} S(\beta_{10}+\theta_0) - M_V R_{jm} C(\beta_{10}+\theta_0)\right] \tag{241}$$

$$\alpha_{22} = \ell^2\left[\frac{7m}{3} + m_{pL} + M_L S^2(\beta_{10}+\theta_0) + M_V C^2(\beta_{10}+\theta_0)\right] \tag{242}$$

$$\alpha_{23} = \ell^2\left[\left(\frac{3m}{2}+m_{pL}\right)C(\beta_{10}-\beta_{20}) + M_L S(\beta_{10}+\theta_0)S(\beta_{20}+\theta_0) + M_V C(\beta_{10}+\theta_0)C(\beta_{20}+\theta_0)\right] \tag{243}$$

$$\alpha_{24} = \ell^2\left[\left(\frac{m}{2}+m_{pL}\right)C(\beta_{10}-\beta_{30}) + M_L S(\beta_{10}+\theta_0)S(\beta_{30}+\theta_0) + M_V C(\beta_{10}+\theta_0)C(\beta_{30}+\theta_0)\right] \tag{244}$$

$$\alpha_{31} = \ell\left[M_L R_{km} S(\beta_{20}+\theta_0) - M_V R_{jm} C(\beta_{20}+\theta_0)\right] \tag{245}$$

$$\alpha_{32} = \ell^2\left[\left(\frac{3m}{2}+m_{pL}\right)C(\beta_{10}-\beta_{20}) + M_L S(\beta_{10}+\theta_0)S(\beta_{20}+\theta_0) + M_V C(\beta_{10}+\theta_0)C(\beta_{20}+\theta_0)\right] \tag{246}$$

$$\alpha_{33} = \ell^2\left[\frac{4m}{3} + m_{pL} + M_L S^2(\beta_{20}+\theta_0) + M_V C^2(\beta_{20}+\theta_0)\right] \tag{247}$$

$$\alpha_{34} = \ell^2\left[\left(\frac{m}{2}+m_{pL}\right)C(\beta_{20}-\beta_{30}) + M_L S(\beta_{20}+\theta_0)S(\beta_{30}+\theta_0) + M_V C(\beta_{20}+\theta_0)C(\beta_{20}+\theta_0)\right] \tag{248}$$

$$\alpha_{41} = \ell\left[M_L R_{km} S(\beta_{30}+\theta_0) - M_V R_{jm} C(\beta_{30}+\theta_0)\right] \tag{249}$$

$$a_{42} = \ell^2\left[\left(\frac{m}{2}+m_{PL}\right)c(\beta_{10}-\beta_{30}) + M_L s(\beta_{10}+\theta_0)\,s(\beta_{30}+\theta_0) + M_V c(\beta_{10}+\theta_0)\,c(\beta_{30}+\theta_0)\right] \quad (250)$$

$$a_{43} = \ell^2\left[\left(\frac{m}{2}+m_{PL}\right)c(\beta_{20}-\beta_{30}) + M_L s(\beta_{20}+\theta_0)\,s(\beta_{30}+\theta_0) + M_V c(\beta_{20}+\theta_0)\,c(\beta_{30}+\theta_0)\right] \quad (251)$$

$$a_{44} = \ell^2\left[\frac{m}{3} + m_{PL} + M_L s^2(\beta_{30}+\theta_0) + M_V c^2(\beta_{30}+\theta_0)\right] \quad (252)$$

$$\beta_{11} = \rho_B S_B \frac{d_B}{V_w}\left[R_{kA}(C_{L\dot\theta B}c\theta_0 - C_{L\dot\theta B}s\theta_0) + R_{jA}(C_{D\dot\theta B}s\theta_0 + C_{L\dot\theta B}c\theta_0) - d_B C_{m\dot\theta B}\right]$$

$$-\rho_B V_w S_B\left[R_{kq}c\theta_0 + R_{jq}s\theta_0\right]\left[R_{kA}(C_{LB}s\theta_0 - C_{DB}c\theta_0) - R_{jA}(C_{DB}s\theta_0 + C_{LB}c\theta_0) + d_B C_{mB}\right] \quad (253)$$

$$\beta_{12} = \rho_B V_w S_B \ell\, s\beta_{10}\left[-R_{kA}(C_{LB}s\theta_0 - C_{DB}c\theta_0) + R_{jA}(C_{DB}s\theta_0 + C_{LB}c\theta_0) - d_B C_{mB}\right] \quad (254)$$

$$\beta_{13} = \rho_B V_w S_B \ell\, s\beta_{20}\left[-R_{kA}(C_{LB}s\theta_0 - C_{DB}c\theta_0) + R_{jA}(C_{DB}s\theta_0 + C_{LB}c\theta_0) - d_B C_{mB}\right] \quad (255)$$

$$\beta_{14} = \rho_B V_w S_B \ell\, s\beta_{30}\left[-R_{kA}(C_{LB}s\theta_0 - C_{DB}c\theta_0) + R_{jA}(C_{DB}s\theta_0 + C_{LB}c\theta_0) - d_B C_{mB}\right] \quad (256)$$

$$\beta_{21} = \ell\,\rho_B S_B \frac{d_B}{V_w}\left[C_{D\dot\theta B}s\beta_{10} - C_{L\dot\theta B}c\beta_{10}\right]$$

$$+\rho_B V_w S_B \ell\left[R_{kq}c\theta_0 + R_{jq}s\theta_0\right]\left[C_{DB}s\beta_{10} - C_{LB}c\beta_{10}\right] \quad (257)$$

$$\beta_{22} = \rho_B V_w S_B \ell^2 s\beta_{10}\left[C_{DB}s\beta_{10} - C_{LB}c\beta_{10}\right] + \ell^2\left[C_1^2\rho_{C1}S_{C1}C_{DC}V_{wC1}\left(s^3\beta_{10} + \tfrac{1}{2}c^3\beta_{10}\right)\right.$$

$$+\rho_{C2}S_{C2}C_{DC}V_{wC2}\left(s^2\beta_{20}s\beta_{10} + \tfrac{1}{2}c^2\beta_{2C}c\beta_{10}\right)c(\beta_{1C}-\beta_{2C})$$

$$\left.+\rho_{C3}S_{C3}C_{DC}V_{wC3}\left(s^2\beta_{30}s\beta_{10} + \tfrac{1}{2}c^2\beta_{3C}c\beta_{10}\right)c(\beta_{10}-\beta_{30})\right] \quad (258)$$

$$\beta_{23} = \rho_B V_w S_B \ell^2 S\varphi_{20}\left[C_{DB} S\varphi_{10} - C_{LB} C\varphi_{10}\right] + \ell^2\left[C_2 \rho_{c2} S_{c2} C_{Dc} V_{wc2}\left(S^3\varphi_{20} + \tfrac{1}{2} C^3\varphi_{20}\right) C(\varphi_{10} - \varphi_{20}) + \rho_{c3} S_{c3} C_{Dc} V_{wc3}\left(S^2\varphi_{30} S\varphi_{20} + \tfrac{1}{3} C^3\varphi_{30} C\varphi_{20}\right) C(\varphi_{10} - \varphi_{30})\right] \quad (259)$$

$$\beta_{24} = \rho_B V_w S_B \ell^2 S\varphi_{30}\left[C_{DB} S\varphi_{10} - C_{LB} C\varphi_{10}\right] + \ell\left[C_3 \rho_{c3} S_{c3} C_{Dc} V_{wc3}\left(S^3\varphi_{30} + \tfrac{1}{2} C^3\varphi_{30}\right) C(\varphi_{10} - \varphi_{30})\right] \quad (260)$$

$$\beta_{31} = \ell S_B\left\{\rho_B \frac{d_B}{V_w}\left[C_{D_{\dot\theta B}} S\varphi_{20} - C_{L_{\dot\theta B}} C\varphi_{20}\right] + \rho_B V_w\left[R_{kq} C\theta_0 + R_{jq} S\theta_0\right]\left[C_{DB} S\varphi_{20} - C_{LB} C\varphi_{20}\right]\right\} \quad (261)$$

$$\beta_{32} = \rho_B V_w S_B \ell^2 S\varphi_{10}\left[C_{DB} S\varphi_{20} - C_{LB} C\varphi_{20}\right] + \ell^2\left[C_2 \rho_{c2} S_{c2} C_{Dc} V_{wc2}\left(S^2\varphi_{20} S\varphi_{10} + \tfrac{1}{2} C^2\varphi_{20} C\varphi_{10}\right) + \rho_{c3} S_{c3} C_{Dc} V_{wc3}\left(S^2\varphi_{30} S\varphi_{10} + \tfrac{1}{2} C^2\varphi_{30} C\varphi_{10}\right) C(\varphi_{20} - \varphi_{30})\right] \quad (262)$$

$$\beta_{33} = \rho_B V_w S_B \ell^2 S\varphi_{20}\left[C_{DB} S\varphi_{20} - C_{LB} C\varphi_{20}\right] + \ell^2\left[C_2 \rho_{c2} S_{c2} C_{Dc} V_{wc2}\left(S^3\varphi_{20} + \tfrac{1}{2} C^3\varphi_{20}\right) + \rho_{c3} S_{c3} C_{Dc} V_{wc3}\left(S^2\varphi_{30} S\varphi_{20} + \tfrac{1}{3} C^2\varphi_{30} C\varphi_{20}\right) C(\varphi_{20} - \varphi_{30})\right] \quad (263)$$

$$\beta_{34} = \rho_B V_w S_B \ell^2 S\varphi_{30}\left[C_{DB} S\varphi_{20} - C_{LB} C\varphi_{20}\right] + \ell^2\left[C_3 \rho_{c3} S_{c3} C_{Dc} V_{wc3}\left(S^3\varphi_{30} + \tfrac{1}{3} C^3\varphi_{30}\right) C(\varphi_{20} - \varphi_{30})\right] \quad (264)$$

$$\beta_{41} = \ell \rho_B S_B \frac{d_B}{V_w}\left[C_{D_{\dot\theta B}} S\varphi_{30} - C_{L_{\dot\theta B}} C\varphi_{30}\right] + \rho_B V_w S_B \ell\left[R_{kq} C\theta_0 + R_{jq} S\theta_0\right]\left[C_{DB} S\varphi_{30} - C_{LB} C\varphi_{30}\right] \quad (265)$$

$$\beta_{u2} = \ell^2 \{ \rho_B V_w S_B S\beta_{10} [C_{DB} S\beta_{2c} - C_{LB} C\beta_{2c}] + [C_3 \rho_{c3} S_{c3} C_{Dc} V_{wc3} (S^2\beta_{3c} S\beta_{2c} + \tfrac{1}{2} C^2 \beta_{3c} C\beta_{2c})] \} \quad (266)$$

$$\beta_{u3} = \ell^2 \{ \rho_B V_w S_B S^2\beta_{2c} [C_{DB} S\beta_{3c} - C_{LB} C\beta_{3c}] + [C_3 \rho_{c3} S_{c3} C_{Dc} V_{wc3} (S^2\beta_{3c} S\beta_{2c} + \tfrac{1}{2} C^2 \beta_{3c} C\beta_{2c})] \} \quad (267)$$

$$\beta_{u4} = \ell^2 \{ \rho_B V_w S_B S\beta_{3c} [C_{DB} S\beta_{3c} - C_{LB} C\beta_{3c}] + [C_3^2 \rho_{c3} S_{c3} C_{Dc} V_{wc3} (S^3\beta_{3c} + \tfrac{1}{2} C^3 \beta_{3c})] \} \quad (268)$$

$$\gamma_{11} = -L_S [R_{kB} C\theta_c + R_{jB} S\theta_c] + W_B [R_{kg} C\theta_c + R_{jg} S\theta_c] - q_B S_B [C_{LB} (R_{kA} C\theta_c + R_{jA} S\theta_c)$$

$$- C_{DB} (- R_{kA} S\theta_c + R_{jA} C\theta_c) + C_{L_{\alpha B}} (R_{kA} S\theta_c - R_{jA} C\theta_c) - C_{D_{\alpha B}} (R_{kA} C\theta_c + R_{jA} S\theta_c) + \ell_B C_{m_{wB}}] \quad (269)$$

$$\gamma_{12} = 0 \quad (270)$$

$$\gamma_{13} = 0 \quad (271)$$

$$\gamma_{14} = 0 \quad (272)$$

$$\gamma_{21} = \ell\, q_B S_B [C_{D_{\alpha B}} S\beta_{10} - C_{L_{\alpha B}} C\beta_{10}] \quad (273)$$

$$\gamma_{22} = \ell \{ S\beta_{10} [L_S - W_B - q (\tfrac{S m}{2} + m_{PL}) + q_B S_B C_{LB}] + C\beta_{10} [q_B S_B C_{DB}]$$

$$+ \tfrac{1}{2} C_1 \rho_{c1} S_{c1} C_{Dc} V_{wc1}^2 S2\beta_{10} + \tfrac{1}{2} \rho_{c2} S_{c2} C_{Dc} V_{wc2}^2 S^2\beta_{2c} S (\beta_{2c} - \beta_{10})$$

$$+ \tfrac{1}{2} \rho_{c3} S_{c3} C_{Dc} V_{wc3}^2 S^2\beta_{3c} S (\beta_{3c} - \beta_{10}) \} \quad (274)$$

$$\gamma_{23} = \tfrac{1}{2} \ell\, \rho_{c2} S_{c2} C_{Dc} V_{wc2}^2 [S2\beta_{2c} C (\beta_{10} - \beta_{2c}) - S^2\beta_{2c} S (\beta_{2c} - \beta_{10})] \quad (275)$$

$$\gamma_{24} = \tfrac{1}{2} \ell \rho_{c3} S_{c3} C_{DC} V_{wc3}^2 \left[S2\varphi_{30} C(\varphi_{10} - \varphi_{30}) - S^2\varphi_{30} S(\varphi_{30} - \varphi_{10}) \right] \quad (276)$$

$$\gamma_{31} = \ell q_B S_B \left[C_{D_{\alpha B}} S\varphi_{20} - C_{L_{\alpha B}} C\varphi_{20} \right] \quad (277)$$

$$\gamma_{32} = 0 \quad (278)$$

$$\gamma_{33} = \ell S\varphi_{20} \left[L_S - W_B - q_j \left(m_{PL} + \tfrac{3m}{2} \right) + q_B S_B C_{LB} \right] + \ell C\varphi_{20} \left[q_B S_B C_{DB} \right]$$
$$+ \tfrac{1}{2} \ell C_2 \rho_{c2} S_{c2} C_{DC} V_{wc2}^2 S2\varphi_{20} + \tfrac{1}{2} \ell \rho_{c3} S_{c3} C_{DC} V_{wc3}^2 S^2\varphi_{30} S(\varphi_{30} - \varphi_{20}) \quad (279)$$

$$\gamma_{34} = \tfrac{1}{2} \ell \rho_{c3} S_{c3} C_{DC} V_{wc3}^2 \left[S2\varphi_{30} C(\varphi_{30} - \varphi_{20}) - S^2\varphi_{30} S(\varphi_{30} - \varphi_{20}) \right] \quad (280)$$

$$\gamma_{41} = \ell q_B S_B \left[C_{D_{\alpha B}} S\varphi_{30} - C_{L_{\alpha B}} C\varphi_{30} \right] \quad (281)$$

$$\gamma_{42} = 0 \quad (282)$$

$$\gamma_{43} = 0 \quad (283)$$

$$\gamma_{44} = \ell S\varphi_{30} \left[L_S - W_B - q_j \left(m_{PL} + \tfrac{m}{2} \right) + q_B S_B C_{LB} \right]$$
$$+ \ell C\varphi_{30} \left[q_B S_B C_{DB} \right] + \tfrac{1}{2} \ell C_3 \rho_{c3} S_{c3} C_{DC} V_{wc3}^2 S2\varphi_{30} \quad (284)$$

$$S_1 = L_S \left(R_{kB} S\theta_0 - R_{jB} C\theta_0 \right) - W_B \left(R_{kg} S\theta_0 - R_{jg} C\theta_0 \right)$$
$$+ q_B S_B \left[C_{LB} \left(R_{kA} S\theta_0 - R_{jA} C\theta_0 \right) - C_{DB} \left(R_{kA} C\theta_0 + R_{jA} S\theta_0 \right) + d_B C_{mB} \right] \quad (285)$$

$$\delta_2 = \ell C \beta_{10} [L_s - W_B - g_0 (\tfrac{5m}{2} + m_{PL}) + g_B S_B C_{LB}] - \ell S \beta_{10} [g_B S_B C_{DB}]$$

$$-\tfrac{1}{2}\ell [C_1 \rho_{c1} S_{c1} C_{Dc} V_{wc1}^2 S \beta_{10} + \rho_{c2} S_{c2} C_{Dc} V_{wc2}^2 S^2 \beta_{20} C(\beta_{10} - \beta_{20})$$

$$+ \rho_{c3} S_{c3} C_{Dc} V_{wc3}^2 S^2 \beta_{30} C(\beta_{10} - \beta_{30})] \qquad (286)$$

$$\delta_3 = \ell C \beta_{20} [L_s - W_B - g_0 (m_{PL} + \tfrac{3m}{2}) + g_B S_B C_{LB}] - \ell S \beta_{20} [g_B S_B C_{DB}]$$

$$-\tfrac{1}{2}\ell [C_2 \rho_{c2} S_{c2} C_{Dc} V_{wc2}^2 S^2 \beta_{20} + \rho_{c3} S_{c3} C_{Dc} V_{wc3}^2 S^2 \beta_{30} C(\beta_{30} - \beta_{20})] \qquad (287)$$

$$\delta_4 = \ell C \beta_{30} [L_s - W_B - g_0 (m_{PL} + \tfrac{m}{2}) + g_B S_B C_{LB}] - \ell S \beta_{30} [g_B S_B C_{DB}]$$

$$-\tfrac{1}{2}\ell [C_3 \rho_{c3} S_{c3} C_{Dc} V_{wc3}^2 S^2 \beta_{30}] \qquad (288)$$

If Equations (285) to (288) are set equal to zero and solved simultaneously, the equilibrium angles (θ_0 , β_{10} , β_{20} , β_{30}) can be found. Then using the quilibrium angles and other given characteristics of the system, α_{ij} , β_{ij} , and γ_{ij} can be solved for. This procedure determines the square matrix in Equation (236). For non-trivial solutions, the determinant of this matrix is set equal to zero and an eighth order characteristic equation is formed. In general, the characteristic equation has the following form:

$$A_0 + A_1 S + A_2 S^2 + \cdots + A_8 S^8 = 0 \qquad (289)$$

The roots of Equation (289) are, in general, four sets of complex conjugates. From these roots, natural frequencies and damping characteristics of the system can be investigated.

SECTION V. GENERALIZED FORCES IN LATERAL PLANE

1. General

The generalized forces can be written as:

$$Q_i = \sum_j \vec{F}_j \cdot \frac{\partial \vec{V}_j}{\partial \dot{\xi}_i} + M_i \tag{290}$$

where $\dot{\xi}_i = \dot{\psi}, \dot{\phi}, \dot{\sigma}_n$

M_i = aerodynamic moment acting on balloon

$\vec{F}_j$ = applied forces acting on system

$\vec{V}_j$ = velocity of system at point of applied force

The applied forces acting on the system are:

$\vec{F}_B$ = buoyant force acting on balloon at C.B.

$\vec{F}_g$ = gravitational force acting on balloon at c.g.

$\vec{F}_A$ = aerodynamic force acting on balloon at some reference point C.A.

$\vec{F}_{Fi}$ = aerodynamic force acting at c.p. of "i"th link

$\vec{F}_{gi}$ = gravitational force acting at c.g. of "i" th link

$\vec{F}_{PL}$ = gravitational and aerodynamic force of payload acting at P_N.

The applied forces acting on the balloon are shown in Figure 59.

$$\vec{F}_B = L_S \vec{N}_3 \tag{291}$$

$$\vec{F}_g = -W_B \vec{N}_3 \tag{292}$$

$$\vec{F}_A = F_{BSn} \vec{N}_1 \tag{293}$$

The velocities of the points at which these forces are acting are:

$$\vec{V}_B = \ell \sum_{i=1}^{N} \dot{\sigma}_i \vec{F}_i + [R_{jB}(-\dot{\psi} c\theta_o c\phi) - R_{kB}(-\dot{\psi} s\theta_o + \dot{\phi})]\vec{i}_B$$

$$+ [R_{kB}(\dot{\psi} s\phi c\theta_o)]\vec{j}_B + [-R_{jB}(\dot{\psi} s\phi c\theta_o)]\vec{k}_B \qquad (294)$$

$$\vec{V}_g = \ell \sum_{i=1}^{N} \dot{\sigma}_i \vec{F}_i + [R_{jg}(-\dot{\psi} c\theta_o c\phi) - R_{kg}(-\dot{\psi} s\theta_o + \dot{\phi})]\vec{i}_B$$

$$+ [R_{kg}(\dot{\psi} s\phi c\theta_o)]\vec{j}_B + [-R_{jg}(\dot{\psi} s\phi c\theta_o)]\vec{k}_B \qquad (295)$$

$$\vec{V}_A = \ell \sum_{i=1}^{N} \dot{\sigma}_i \vec{F}_i + [R_{jA}(-\dot{\psi} c\theta_o c\phi) - R_{kA}(-\dot{\psi} s\theta_o + \dot{\phi})]\vec{i}_B$$

$$+ [R_{kA}(\dot{\psi} s\phi c\theta_o)]\vec{j}_B + [-R_{jA}(\dot{\psi} s\phi c\theta_o)]\vec{k}_B \qquad (296)$$

where R_{jB} , R_{kB} are distances from the C.B. to the bridle apex point measured along the body axes $\vec{j}_B$ and $\vec{k}_B$. R_{jg} , R_{kg} , R_{jA} , R_{kA} have similar definitions.

It then follows:

$$\frac{\partial \vec{V}_B}{\partial \dot{\psi}} = [R_{jB}(-c\theta_o c\phi) - R_{kB}(-s\theta_o)]\vec{i}_B + [R_{kB}(s\phi c\theta_o)]\vec{j}_B + [-R_{jB}(s\phi c\theta_o)]\vec{k}_B \qquad (297)$$

$$\frac{\partial \vec{V}_g}{\partial \dot{\psi}} = [R_{jg}(-c\theta_o c\phi) - R_{kg}(-s\theta_o)]\vec{i}_B + [R_{kg}(s\phi c\theta_o)]\vec{j}_B + [-R_{jg}(s\phi c\theta_o)]\vec{k}_B \qquad (298)$$

$$\frac{\partial \vec{V}_A}{\partial \dot{\psi}} = [R_{jA}(-c\theta_o c\phi) - R_{kA}(-s\theta_o)]\vec{i}_B + [R_{kA}(s\phi c\theta_o)]\vec{j}_B + [-R_{jA}(s\phi c\theta_o)]\vec{k}_B \qquad (299)$$

$$\frac{\partial \vec{V}_B}{\partial \dot{\phi}} = [-R_{kB}]\vec{i}_B \qquad (300)$$

$$\frac{\partial \vec{V}_g}{\partial \dot{\phi}} = [-R_{kg}]\,\vec{i}_3 \tag{301}$$

$$\frac{\partial \vec{V}_A}{\partial \dot{\phi}} = [-R_{kA}]\,\vec{i}_3 \tag{302}$$

$$\frac{\partial \vec{V}_B}{\partial \dot{\sigma}_n} = \ell\,\vec{f}_n' \tag{303}$$

$$\frac{\partial \vec{V}_g}{\partial \dot{\sigma}_n} = \ell\,\vec{f}_n' \tag{304}$$

$$\frac{\partial \vec{V}_A}{\partial \dot{\sigma}_n} = \ell\,\vec{f}_n' \tag{305}$$

Applying Equation (290) to find F_ψ and F_ϕ :

$$F_\psi = \vec{F}_B \cdot \frac{\partial \vec{V}_B}{\partial \dot{\psi}} + \vec{F}_g \cdot \frac{\partial \vec{V}_g}{\partial \dot{\psi}} + \vec{F}_A \cdot \frac{\partial \vec{V}_A}{\partial \dot{\psi}} + M_{\psi B} \tag{306}$$

$$F_\phi = \vec{F}_B \cdot \frac{\partial \vec{V}_B}{\partial \dot{\phi}} + \vec{F}_g \cdot \frac{\partial \vec{V}_g}{\partial \dot{\phi}} + \vec{F}_A \cdot \frac{\partial \vec{V}_A}{\partial \dot{\phi}} + M_{\phi B} \tag{307}$$

Expanding Equation (306):

$$F_\psi = L_S\{[R_{jB}(-c\theta_n c\phi) - R_{kB}(-s\theta_n)][-s\phi c\theta_n] + [R_{kB}(s\phi c\theta_n)][s\theta_n] + [-R_{jB}(s\phi c\theta_n)][c\phi c\theta_n]\}$$

$$-W_B\{[R_{jg}(-c\theta_3 c\phi) - R_{kg}(-s\theta_3)][-s\phi c\theta_n] + [R_{kg}(s\phi c\theta_n)][s\theta_n] + [-R_{jg}(s\phi c\theta_n)][c\phi c\theta_n]\}$$

$$+F_{BSA}\{[R_{jA}(-c\theta_n c\phi) - R_{kA}(-s\theta_n)][s\phi s\theta_n s\psi + c\phi c\psi] + [R_{kA}(s\phi c\theta_n)][c\theta_n s\psi]$$

$$+[-R_{jA}(s\phi c\theta_n)][-c\phi s\theta_n s\psi + s\phi c\psi]\} + M_{\psi B} \tag{308}$$

Expanding Equation (307):

$$F_\phi = L_S\{[-R_{LB}][-S\phi C\theta_0]\} - W_B\{[-R_{Lg}][-S\phi C\theta_0]\}$$

$$+F_{BSA}\{[-R_{LA}][S\phi S\theta_0 S\psi + C\phi C\psi]\} + M_{\phi B} \tag{309}$$

The forces acting on the links are:

$$\vec{F}_{PL} = -m_{PL} g \vec{N}_3 \tag{310}$$

$$\vec{F}_{gi} = -m_i g \vec{N}_3 \tag{311}$$

$$\vec{F}_{Pi} = D_{CSi} C^2 \sigma_i \vec{f}_i' \tag{312}$$

In Equation (310) the drag force on the payload is ignored. The factor $\cos^2\sigma_i$ in Equation (312) takes into account the projected area in the lateral direction and then rotates the lateral drag component into the direction normal to ℓ. Shear forces are neglected. The velocities of the points at which these forces act are:

$$\vec{V}_{PL} = \ell \sum_{i=1}^{N} \dot{\sigma}_i \vec{f}_i' \tag{313}$$

$$\vec{V}_{gi} = \vec{V}^{P_i} = \ell \sum_{j=1}^{i-1} \dot{\sigma}_j \vec{f}_j' + \tfrac{1}{2}\ell \dot{\sigma}_i \vec{f}_i' \tag{314}$$

$$\vec{V}_{Pi} = \ell \sum_{j=1}^{i-1} \dot{\sigma}_j \vec{f}_j' + \ell C_i \dot{\sigma}_i \vec{f}_i' \tag{315}$$

where C_i is the ratio of the distance from P_{i-1} to the c.p. of the "i" th link to the total length of the link.

From Equations (313), (314) and (315) it follows:

$$\frac{\partial \vec{V}_{PL}}{\partial \dot{\sigma}_n} = \ell \vec{f}_n' \tag{316}$$

$$\frac{\partial \vec{V}_{qi}}{\partial \dot{\sigma}_n} = \begin{cases} \ell \vec{f}_n & n < i \\ \frac{1}{2}\ell \vec{f}_n & n = i \\ 0 & n > i \end{cases} \tag{317}$$

$$\frac{\partial \vec{V}_{Pi}}{\partial \dot{\sigma}_n} = \begin{cases} \ell \vec{f}_n & n < i \\ \ell C_n \vec{f}_n & n = i \\ 0 & n > i \end{cases} \tag{318}$$

Applying Equation (290) to find F_{σ_n} :

$$F_{\sigma_n} = \vec{F}_B \cdot \frac{\partial \vec{V}_B}{\partial \dot{\sigma}_n} + \vec{F}_g \cdot \frac{\partial \vec{V}_g}{\partial \dot{\sigma}_n} + \vec{F}_n \cdot \frac{\partial \vec{V}_n}{\partial \dot{\sigma}_n} + \vec{F}_{PL} \cdot \frac{\partial \vec{V}_{PL}}{\partial \dot{\sigma}_n}$$
$$+ \sum_{i=1}^{N} \vec{F}_{gi} \cdot \frac{\partial \vec{V}_{gi}}{\partial \dot{\sigma}_n} + \sum_{i=1}^{N} \vec{F}_{Pi} \cdot \frac{\partial \vec{V}_{Pi}}{\partial \dot{\sigma}_n} \tag{319}$$

Simplifying Equation (319):

$$F_{\sigma_n} = L_3 \ell [-S\sigma_n S\xi_{n0}] - W_B \ell [-S\sigma_n S\xi_{n0}] + F_{BSH} \ell [C\sigma_n]$$
$$- m_{PL} g \ell [-S\sigma_n S\xi_{n0}] - \frac{m_n}{2} g \ell [-S\sigma_n S\xi_{n0}]$$
$$- \sum_{i=n+1}^{N} m_i g \ell [-S\sigma_n S\xi_{n0}] + D_{csn} C^2\sigma_n \ell C_n$$
$$+ \sum_{i=n+1}^{N} D_{csi} C^2\sigma_i \ell [C\sigma_i C\sigma_n + S\sigma_i C\xi_{i0} S\sigma_n C\xi_{n0} + S\sigma_i S\xi_{i0} S\sigma_n S\xi_{n0}] \tag{320}$$

Assuming N = 3, the generalized force for each link is:

$$F_{\sigma_1} = [L_S - W_B - (m_{PL} + \tfrac{5}{2}m)g][-\ell S\sigma_1 S\beta_{10}] + [F_{BSA}][\ell C\sigma_1] + [D_{cs1}][\ell C_1 C^2\sigma_1]$$

$$+ [D_{cs2}][\ell C^2\sigma_2 (C\sigma_2 C\sigma_1 + S\sigma_2 C\beta_{20} S\sigma_1 C\beta_{10} + S\sigma_2 S\beta_{20} S\sigma_1 S\beta_{10}]$$

$$+ [D_{cs3}][\ell C^2\sigma_3 (C\sigma_3 C\sigma_1 + S\sigma_3 C\beta_{30} S\sigma_1 C\beta_{10} + S\sigma_3 S\beta_{30} S\sigma_1 S\beta_{10})] \quad (321)$$

$$F_{\sigma_2} = [L_S - W_B - (m_{PL} + \tfrac{3}{2}m)g][-\ell S\sigma_2 S\beta_{20}] + [F_{BSA}][\ell C\sigma_2] + [D_{cs2}][\ell C_2 C^2\sigma_2]$$

$$+ [D_{cs3}][\ell C^2\sigma_3 (C\sigma_3 C\sigma_2 + S\sigma_3 C\beta_{30} S\sigma_2 C\beta_{20} + S\sigma_3 S\beta_{30} S\sigma_2 S\beta_{20})] \quad (322)$$

$$F_{\sigma_3} = [L_S - W_B - (m_{PL} + \tfrac{m}{2})g][-\ell S\sigma_3 S\beta_{30}]$$

$$+ [F_{BSA}][\ell C\sigma_3] + [D_{cs3}][\ell C_3 C^2\sigma_3] \quad (323)$$

2. Aerodynamics

The side force F_{BSA} is defined as:

$$F_{BSA} = q_B S_B \left[C_{Y_\psi} \psi + C_{Y_{\dot\psi}} \left(\frac{d_B}{V_{BR}}\right)\dot\psi + C_{Y_{\dot\phi}} \left(\frac{d_B}{V_{BR}}\right)\dot\phi + C_{Y_w} \left(\frac{\dot X_{BR}}{V_{BR}}\right)\right] \quad (324)$$

The aerodynamic yaw moment acting on the balloon is:

$$M_{\psi B} = q_B S_B d_B \left[C_{m_\psi} \psi + C_{m_{\dot\psi}} \left(\frac{d_B}{V_{BR}}\right)\dot\psi + C_{m_{\dot\phi}} \left(\frac{d_B}{V_{BR}}\right)\dot\phi + C_{m_w} \left(\frac{\dot X_{BR}}{V_{BR}}\right)\right] \quad (325)$$

The aerodynamic roll moment acting on the balloon is:

$$M_{\phi B} = q_B S_B d_B \left[C_{\ell_\psi} \psi + C_{\ell_{\dot\psi}} \left(\frac{d_B}{V_{BR}}\right)\dot\psi + C_{\ell_{\dot\phi}} \left(\frac{d_B}{V_{BR}}\right)\dot\phi + C_{\ell_w} \left(\frac{\dot X_{BR}}{V_{BR}}\right)\right] \quad (326)$$

The terms D_{csi} are aerodynamic drags acting on the "i" th link in the side direction.

$$D_{csi} = -\frac{1}{2} \rho_{ci} [V_{ci}]^2 S_{ci} C_{Dc} S\Gamma_{ci} = -\frac{1}{2} \rho_{ci} S_{ci} C_{Dc} V_{ci} \dot{X}_{ci} \tag{327}$$

where $\dot{X}_{ci}$ and Γ_{ci} are the side velocity and effective flight path angle of the C.P. of the "i"th link in the horizontal plane.

3. Translational Dynamics

a. Tether Dynamics

The following equations define the linear displacements and velocities of the c.p. of the "r" th link

$$X_{cn} = \ell \sum_{i=1}^{n-1} S\sigma_i + C_n \ell S\sigma_n \tag{328}$$

$$Y_{cn} = -\ell \sum_{i=1}^{n-1} C\sigma_i C\beta_{i0} - C_n \ell C\sigma_n C\beta_{n0} \tag{329}$$

$$Z_{cn} = \ell \sum_{i=1}^{n-1} C\sigma_i S\beta_{i0} + C_n \ell C\sigma_n S\beta_{n0} \tag{330}$$

$$\dot{X}_{cn} = \ell \sum_{i=1}^{n-1} \dot{\sigma}_i C\sigma_i + C_n \ell \dot{\sigma}_n C\sigma_n \tag{331}$$

$$\dot{Y}_{cn} = \ell \sum_{i=1}^{n-1} \dot{\sigma}_i S\sigma_i C\beta_{i0} + C_n \ell \dot{\sigma}_n S\sigma_n C\beta_{n0} \tag{332}$$

$$\dot{Z}_{cn} = -\ell \sum_{i=1}^{n-1} \dot{\sigma}_i S\sigma_i S\beta_{i0} - C_n \ell \dot{\sigma}_n S\sigma_n S\beta_{n0} \tag{333}$$

b. Payload Dynamics

$$X_{PL} = \ell \sum_{i=1}^{N} S\sigma_i \tag{334}$$

$$Y_{PL} = -\ell \sum_{i=1}^{N} C\sigma_i \, C\xi_{i0} \tag{335}$$

$$Z_{PL} = \ell \sum_{i=1}^{N} C\sigma_i \, S\xi_{i0} \tag{336}$$

$$\dot{X}_{PL} = \ell \sum_{i=1}^{N} \dot{\sigma}_i \, C\sigma_i \tag{337}$$

$$\dot{Y}_{PL} = \ell \sum_{i=1}^{N} \dot{\sigma}_i \, S\sigma_i \, C\xi_{i0} \tag{338}$$

$$\dot{Z}_{PL} = -\ell \sum_{i=1}^{N} \dot{\sigma}_i \, S\sigma_i \, S\xi_{i0} \tag{339}$$

c. Balloon Dynamics

$$X_B = X_{PL} - (R_{jg}\,\vec{j}_B + R_{kg}\,\vec{k}_B)\cdot\vec{N}_1 \tag{340}$$

$$X_B = X_{PL} - R_{jg}\,(C\theta_0 S\psi) - R_{kg}\,(-C\phi S\theta_0 S\psi + S\phi C\psi) \tag{341}$$

$$Y_B = Y_{PL} - (R_{jg}\,\vec{j}_B + R_{kg}\,\vec{k}_B)\cdot\vec{N}_2 \tag{342}$$

$$Y_B = Y_{PL} - R_{jg}\,(C\theta_0 C\psi) - R_{kg}\,(-C\phi S\theta_0 C\psi - S\phi S\psi) \tag{343}$$

$$Z_B = Z_{PL} - (R_{jg}\,\vec{j}_B + R_{kg}\,\vec{k}_B)\cdot\vec{N}_3 \tag{344}$$

$$Z_B = Z_{PL} - R_{jg}\,(S\theta_0) - R_{kg}\,(C\phi C\theta_0) \tag{345}$$

$$\dot{X}_B = \dot{X}_{PL} - R_{jg}\,\dot{\psi}(C\theta_0 C\psi) - R_{kg}\,(\dot{\phi}S\phi S\theta_0 S\psi - \dot{\psi}C\phi S\theta_0 C\psi + \dot{\phi}C\phi C\psi - \dot{\psi}S\phi S\psi) \tag{346}$$

$$\dot{X}_B = \dot{X}_{PL} + \dot{\psi}\left[-R_{jg}\left(c\theta_o c\psi\right) + R_{kg}\left(c\phi s\theta_o c\psi + s\phi s\psi\right)\right] - \dot{\phi}\left[R_{kg}\left(s\phi s\theta_o s\psi + c\phi c\psi\right)\right] \quad (347)$$

$$\dot{Y}_B = \dot{Y}_{PL} + R_{jg}\,\dot{\psi}\left(c\theta_o s\psi\right) + R_{kg}\left(-\dot{\phi}\, s\phi s\theta_o c\psi - \dot{\psi} c\phi s\theta_o s\psi + \dot{\phi} c\phi s\psi + \dot{\psi} s\phi c\psi\right) \quad (348)$$

$$\dot{Y}_B = \dot{Y}_{PL} + \dot{\psi}\left[R_{jg}\left(c\theta_o s\psi\right) + R_{kg}\left(s\phi c\psi - c\phi s\theta_o s\psi\right)\right] + \dot{\phi}\left[R_{kg}\left(c\phi s\psi - s\phi s\theta_o c\psi\right)\right] \quad (349)$$

$$\dot{Z}_B = \dot{Z}_{PL} + \dot{\phi}\left[R_{kg}\left(s\phi\, c\theta_o\right)\right] \quad (350)$$

4. Wind Velocity

A steady state wind profile is assumed to be a function of altitude and acts in the $-\vec{N}_2$ direction only. This wind establishes the equilibrium condition in the longitudinal plane. A side gust in the $\bar{X}\ \bar{Z}$ plane may be applied at any angle. Referring to Figure 63, the effective free stream velocity for the balloon is found in the following manner.

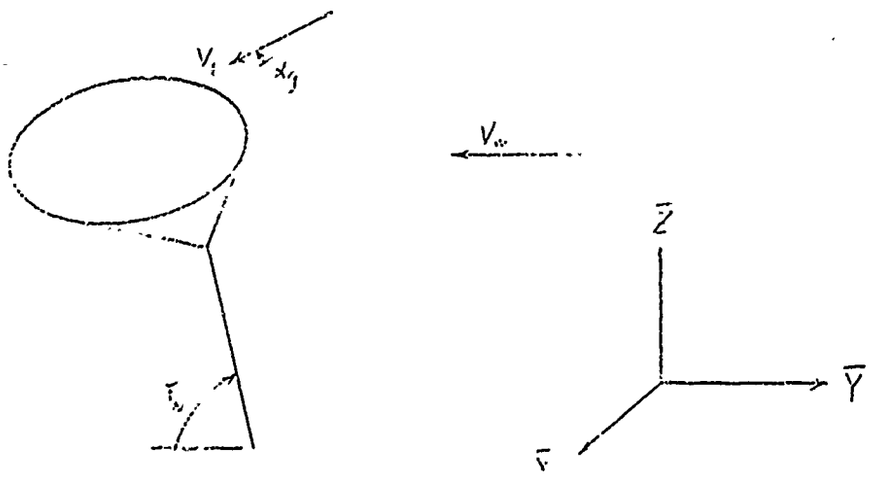

Figure 63- Steady State Wind and Gust Acting on Balloon in Lateral Plane

The components of the gust in the vertical and side directions respectively are:

$$V_{gV} = V_g \, S\alpha_g \tag{351}$$

$$V_{gS} = V_g \, C\alpha_g \tag{352}$$

The vertical, horizontal, and side velocities of the balloon relative to the free stream are:

$$\dot{X}_{BR} = \dot{X}_B - V_{gS} \tag{353}$$

$$\dot{Y}_{BR} = \dot{Y}_B + V_W \tag{354}$$

$$\dot{Z}_{BR} = \dot{Z}_B - V_{gV} \tag{355}$$

The relative velocity, dynamic pressure, lateral plane flight path angle, and sideslip angle are:

$$V_{BR} = \left[\dot{X}_{BR}^2 + \dot{Y}_{BR}^2 + \dot{Z}_{BR}^2 \right]^{1/2} \tag{356}$$

$$q_B = \tfrac{1}{2} \rho_B V_{BR}^2 \tag{357}$$

$$\Gamma_B = \tan^{-1}\left[\dot{X}_{BR} / \dot{Y}_{BR} \right] \tag{358}$$

$$-\beta = \psi - \Gamma_B \tag{359}$$

The drag on the payload will be neglected.

The relative velocity at the c.p. of the "i" th link is assumed to be the effective wind velocity over the whole link for purposes of calculating side drag on the link. The c.p. is located by finding the dynamic pressure at the bottom and top hinge points of the link and assuming a linear distribution of dynamic pressure over the whole link. The procedure is similar to the longitudinal case shown in Figure 62. The dynamic pressure at a hinge point due to a relative velocity of the hinge is:

$$q_{Hn} = \frac{1}{2}\rho_{Hn}\left\{\left[\dot{X}_{cHn}\right]^2 + \left[V_{WHn}\right]^2\right\} \tag{360}$$

The centroid of the trapezoidal distribution of force acting on the "r" th link divided by the vertical length of a link ($\ell \sin\delta_n \cos\sigma_n$) is:

$$C_n = \frac{1}{3}\left[\frac{q_{Hn} + 2q_{Hn+1}}{q_{Hn} + q_{Hn+1}}\right] \tag{361}$$

SECTION VI

LINEARIZED EQUATIONS OF MOTION IN LATERAL PLANE

1. General

In order to separate the inertia terms in the equation of motion, it was assumed that the yaw angles of the links and the yaw and roll angles of the balloon were small and that all angular rates were small. However, the pitch angles of the links and the pitch angle of the balloon have a finite value in equilibrium (ξ_{i0} , θ_0). When working with the lateral equations it is necessary to hold all pitch angles constant when linearizing the equations of motion. The other variables are perturbed as follows:

$$\left.\begin{array}{lll} \psi = \delta\psi & \dot{\psi} = \delta\dot{\psi} & \ddot{\psi} = \delta\ddot{\psi} \\ \phi = \delta\phi & \dot{\phi} = \delta\dot{\phi} & \ddot{\phi} = \delta\ddot{\phi} \\ \sigma_i = \delta\sigma_i & \dot{\sigma}_i = \delta\dot{\sigma}_i & \ddot{\sigma}_i = \delta\ddot{\sigma}_i \end{array}\right\} \qquad (362)$$

2. Inertia Terms

Equations (124) to (128) are the equations of motion to be linearized. The inertia terms are already in a linearized form but will be rewritten for completeness. Note, the δ symbol is dropped for ease of writing.

$$\begin{aligned} &\{I_{zB}C^2\theta_0 + I_{yB}S^2\theta_0 - I_{yzB}S2\theta_0 + M_s(R_{km}S\theta_0 - R_{jm}C\theta_0)^2\}\ddot{\psi} \\ &+\{I_{yzB}C\theta_0 - I_{yB}S\theta_0 + M_s R_{km}(R_{jm}C\theta_0 - R_{km}S\theta_0)\}\ddot{\phi} \\ &+\{\ell M_s[R_{km}S\theta_0 - R_{jm}C\theta_0]\}\ddot{\sigma}_1 + \{\ell M_s[R_{km}S\theta_0 - R_{jm}C\theta_0]\}\ddot{\sigma}_2 \\ &+\{\ell M_s[R_{km}S\theta_0 - R_{jm}C\theta_0]\}\ddot{\sigma}_3 = F_\psi \end{aligned} \qquad (363)$$

$$\{I_{yzB}\,C\theta_o - I_{yB}\,S\theta_o + M_S R_{km}(R_{jm}C\theta_o - R_{km}S\theta_o)\}\ddot{\psi}$$

$$+\{I_{yB} + M_S R_{km}^2\}\ddot{\phi} + \{-\ell M_S R_{km}\}\ddot{\sigma_1}$$

$$+\{-\ell M_S R_{km}\}\ddot{\sigma_2} + \{-\ell M_S R_{km}\}\ddot{\sigma_3} = F_\phi \qquad (364)$$

$$\{\ell M_S[R_{km}S\theta_o - R_{jm}C\theta_o]\}\ddot{\psi} + \{-\ell M_S R_{km}\}\ddot{\phi}$$

$$+\{\ell^2[\tfrac{7m}{3} + m_{PL} + M_S]\}\ddot{\sigma_1} + \{\ell^2[\tfrac{3m}{2} + m_{PL} + M_S]\}\ddot{\sigma_2}$$

$$+\{\ell^2[\tfrac{m}{2} + m_{PL} + M_S]\}\ddot{\sigma_3} = F_{\sigma_1} \qquad (365)$$

$$\{\ell M_S[R_{km}S\theta_o - R_{jm}C\theta_o]\}\ddot{\psi} + \{-\ell M_S R_{km}\}\ddot{\phi}$$

$$+\{\ell^2[\tfrac{3m}{2} + m_{PL} + M_S]\}\ddot{\sigma_1} + \{\ell^2[\tfrac{4m}{3} + m_{PL} + M_S]\}\ddot{\sigma_2}$$

$$+\{\ell^2[\tfrac{m}{2} + m_{PL} + M_S]\}\ddot{\sigma_3} = F_{\sigma_2} \qquad (366)$$

$$\{\ell M_S[R_{km}S\theta_o - R_{jm}C\theta_o]\}\ddot{\psi} + \{-\ell M_S R_{km}\}\ddot{\phi}$$

$$+\{\ell^2[\tfrac{m}{2} + m_{PL} + M_S]\}\ddot{\sigma_1} + \{\ell^2[\tfrac{m}{2} + m_{PL} + M_S]\}\ddot{\sigma_2}$$

$$+\{\ell^2[\tfrac{m}{3} + m_{PL} + M_S]\}\ddot{\sigma_3} = F_{\sigma_3} \qquad (367)$$

3. Generalized Forces

Equations (363) to (367) give the coefficients of the second derivatives. To find the coefficients of the first derivatives and the dependent variables, the generalized forces (F_ψ , F_ϕ , F_{σ_n}) must be expanded. First linearize Equation (308).

$$F_\psi = F_{BSA}\{R_{jA}[-C\theta_o] + R_{kA}[S\theta_o]\} + M_{\psi B} \tag{368}$$

The variables F_{BSA} and $M_{\psi B}$ must be linearized. From Equation (324) and (347):

$$F_{BSA} = \tfrac{1}{2}\rho_B V_{BR}^2 S_B\left\{C_{Y_\psi}\psi + C_{Y_{\dot\psi}}\left(\frac{d_B}{V_{BR}}\right)\dot\psi + C_{Y_{\dot\phi}}\left(\frac{d_B}{V_{BR}}\right)\dot\phi\right.$$

$$\left. + C_{Y_w}\left[\ell(\dot\sigma_1+\dot\sigma_2+\dot\sigma_3) + (-R_{jq}C\theta_o + R_{kq}S\theta_o)\dot\psi + (-R_{kq})\dot\phi\right]/V_{BR}\right\} \tag{369}$$

where $V_{BR}^2 = \dot X_{BR}^2 + \dot Y_{BR}^2 + \dot Z_{BR}^2$ (370)

If the gust velocity is zero, $\dot X_{BR} = \dot Z_{BR} = 0$.
Also $\dot y_B = 0$.

Therefore $V_{BR}^2 = V_w^2$. (371)

Rewriting Equation (369):

$$F_{BSA} = \tfrac{1}{2}\rho_B V_w^2 S_B\left\{C_{Y_\psi}\psi + \left[C_{Y_{\dot\psi}}\left(\frac{d_B}{V_w}\right) + C_{Y_w}\left(\frac{-R_{jq}C\theta_o + R_{kq}S\theta_o}{V_w}\right)\right]\dot\psi\right.$$

$$\left. + \left[C_{Y_{\dot\phi}}\left(\frac{d_B}{V_w}\right) + C_{Y_w}\left(\frac{-R_{kq}}{V_w}\right)\right]\dot\phi + \left[C_{Y_w}\frac{\ell}{V_w}\right][\dot\sigma_1+\dot\sigma_2+\dot\sigma_3]\right\} \tag{372}$$

From Equation (325), the linearized form of $M_{\psi B}$ is:

$$M_{\psi B} = \frac{1}{2}\rho_B V_w^2 S_B d_B \left\{ C_{m_\psi}\psi + \left[C_{m_{\dot\psi}}\left(\frac{d_B}{V_w}\right) + C_{m_w}\left(\frac{-R_{jq}C\theta_o + R_{kq}S\theta_o}{V_w}\right)\right]\dot\psi \right.$$

$$\left. + \left[C_{m_{\dot\phi}}\left(\frac{d_B}{V_w}\right) + C_{m_w}\left(\frac{-R_{kq}}{V_w}\right)\right]\dot\phi + \left[C_{m_w}\frac{\ell}{V_w}\right]\left[\dot\sigma_1 + \dot\sigma_2 + \dot\sigma_3\right]\right\} \qquad (373)$$

In like manner Equation (326) is also linearized to give $M_{\phi B}$.

$$M_{\phi B} = \frac{1}{2}\rho_B V_w^2 S_B d_B \left\{ C_{\ell_\psi}\psi + \left[C_{\ell_{\dot\psi}}\left(\frac{d_B}{V_w}\right) + C_{\ell_w}\left(\frac{-R_{jq}C\theta_o + R_{kq}S\theta_o}{V_w}\right)\right]\dot\psi \right.$$

$$\left. + \left[C_{\ell_{\dot\phi}}\left(\frac{d_B}{V_w}\right) + C_{\ell_w}\left(\frac{-R_{kq}}{V_w}\right)\right]\dot\phi + \left[C_{\ell_w}\frac{\ell}{V_w}\right]\left[\dot\sigma_1 + \dot\sigma_2 + \dot\sigma_3\right]\right\} \qquad (374)$$

Substituting Equations (372) and (373) into (368) gives the linearized form F_ψ.

$$F_\psi = \frac{1}{2}\rho_B V_w^2 S_B \left\{ C_{Y_\psi}\left[-R_{jn}C\theta_o + R_{kn}S\theta_o\right] + C_{n_\psi} d_B \right\}\psi$$

$$+\frac{1}{2}\rho_B V_w S_B \left\{ \left[C_{Y_{\dot\psi}} d_B + C_{Y_w}\left(-R_{jq}C\theta_o + R_{kq}S\theta_o\right)\right]\left[-R_{jn}C\theta_o + R_{kn}S\theta_o\right] \right.$$

$$\left. + d_B\left[C_{n_{\dot\psi}} d_B + C_{n_w}\left(-R_{jq}C\theta_o + R_{kq}S\theta_o\right)\right]\right\}\dot\psi$$

$$+\frac{1}{2}\rho_B V_w S_B \left\{ \left[C_{Y_{\dot\phi}} d_B + C_{Y_w}\left(-R_{kq}\right)\right]\left[-R_{jn}C\theta_o + R_{kn}S\theta_o\right] + d_B\left[C_{m_{\dot\phi}} d_B + C_{m_w}\left(-R_{kq}\right)\right]\right\}\dot\phi$$

$$+\frac{1}{2}\rho_B V_w S_B \ell \left\{ \left[C_{Y_w}\left(-R_{jn}C\theta_o + R_{kn}S\theta_o\right) + C_{n_w} d_B\right]\right\}\dot\sigma_1$$

$$+\frac{1}{2}\rho_B V_w S_B \ell \left\{ \left[C_{Y_w}\left(-R_{jn}C\theta_o + R_{kn}S\theta_o\right) + C_{n_w} d_B\right]\right\}\dot\sigma_2$$

$$+\frac{1}{2}\rho_B V_w S_B \ell \left\{ \left[C_{Y_w}\left(-R_{jn}C\theta_o + R_{kn}S\theta_o\right) + C_{n_w} d_B\right]\right\}\dot\sigma_3 \qquad (375)$$

Next linearize Equation (309).

$$F_\phi = L_S\{R_{kB}\,C\theta_o\}\phi - W_B\{R_{kg}\,C\theta_o\}\phi + F_{BSA}\{-R_{kA}\,S\theta_o\} + M_{\phi B} \tag{376}$$

Substituting Equations (372) and (374) into (376) gives the linearized form of F_ϕ.

$$\begin{aligned}
F_\phi = {} & \tfrac{1}{2}\rho_B V_W^2 S_B\{C_{Y_\psi}[-R_{kA}\,S\theta_o] + C_{\ell_\psi} d_B\}\psi \\
& + C\theta_o\{L_S R_{kB} - W_B R_{kg}\}\phi \\
& + \tfrac{1}{2}\rho_B V_W S_B\{[C_{Y_{\dot\psi}} d_B + C_{Y_r}(-R_{jg}\,C\theta_o + R_{kg}\,S\theta_o)][-R_{kA}\,S\theta_o] \\
& + d_B[C_{\ell_{\dot\psi}} d_B + C_{\ell_r}(-R_{jg}\,C\theta_o + R_{kg}\,S\theta_o)]\}\dot\psi \\
& + \tfrac{1}{2}\rho_B V_W S_B\{[C_{Y_{\dot\phi}} d_B + C_{Y_r}(-R_{kg})][-R_{kA}\,S\theta_o] + d_B[C_{\ell_{\dot\phi}} d_B + C_{\ell_r}(-R_{kg})]\}\dot\phi \\
& + \tfrac{1}{2}\rho_B V_W S_B \ell\{C_{Y_r}[-R_{kA}\,S\theta_o] + C_{\ell_r} d_B\}\dot\sigma_1 \\
& + \tfrac{1}{2}\rho_B V_W S_B \ell\{C_{Y_r}[-R_{kA}\,S\theta_o] + C_{\ell_r} d_B\}\dot\sigma_2 \\
& + \tfrac{1}{2}\rho_B V_W S_B \ell\{C_{Y_r}[-R_{kA}\,S\theta_o] + C_{\ell_r} d_B\}\dot\sigma_3
\end{aligned} \tag{377}$$

Linearizing the generalized force on the first links gives:

$$\begin{aligned}
F_{\sigma_i} = {} & [L_S - W_B - (m_{PL} + \tfrac{5m}{2})g][-\ell\,S\beta_{io}]\dot\sigma_i + F_{BSA}\,\ell \\
& + D_{cs1}\,\ell\,C_i + D_{cs2}\,\ell + D_{cs3}\,\ell
\end{aligned} \tag{378}$$

where: $D_{cs_i} = -\frac{1}{2} \rho_{c_i} S_{c_i} C_{Dc} V_{c_i} \dot{X}_{c_i}$ (379)

$$V_{c_i} = \left[\left(V_{wc_i} + \dot{Y}_{c_i} \right)^2 + \dot{X}_{c_i}^2 + \dot{Z}_{c_i}^2 \right]^{1/2} \quad (380)$$

Neglecting 2nd order terms in Equation (380), V_{c_i} is written:

$$V_{c_i} = \left[V_{wc_i}^2 + 2 V_{wc_i} \dot{Y}_{c_i} \right]^{1/2} \quad (381)$$

Substituting Equation (381) into (379) gives:

$$D_{cs_i} = -\frac{1}{2} \rho_{c_i} S_{c_i} C_{Dc} V_{wc_i} \dot{X}_{c_i} \quad (382)$$

where $\dot{X}_{c_i}$ is given by Equation (331)

$$\dot{X}_{c_i} = \ell \sum_{j=1}^{i-1} \dot{\sigma}_j + C_i \ell \dot{\sigma}_i \quad (383)$$

Substituting Equation (383) into (382) yields:

$$D_{cs_1} = -\frac{1}{2} \rho_{c_1} S_{c_1} C_{Dc} V_{wc_1} \ell C_1 \dot{\sigma}_1 \quad (384)$$

$$D_{cs_2} = -\frac{1}{2} \rho_{c_2} S_{c_2} C_{Dc} V_{wc_2} \ell \left[\dot{\sigma}_1 + C_2 \dot{\sigma}_2 \right] \quad (385)$$

$$D_{cs_3} = -\frac{1}{2} \rho_{c_3} S_{c_3} C_{Dc} V_{wc_3} \ell \left[\dot{\sigma}_1 + \dot{\sigma}_2 + C_3 \dot{\sigma}_3 \right] \quad (386)$$

The final linearized form of F_{σ_1} is:

$$F_{\sigma_1} = \left\{ \tfrac{1}{2} \rho_B V_w^2 S_B \ell C_{Y_\psi} \right\} \psi + \left\{ \left[W_B - L_S + \left(m_{pl} + \tfrac{5}{2} m \right) g \right] \left[\ell S \beta_w \right] \right\} \sigma_1$$

$$+ \left\{ \tfrac{1}{2} \rho_B V_w S_B \ell \left[C_{Y_{\dot\psi}} \alpha_B + C_{Y_w} \left(-R_{jj} C\theta_0 + R_{kj} S\theta_0 \right) \right] \right\} \dot\psi$$

$$+ \left\{ \tfrac{1}{2} \rho_B V_w S_B \ell \left[C_{Y_{\dot\phi}} \alpha_B + C_{Y_v} \left(-R_{kj} \right) \right] \right\} \dot\phi$$

$$+ \left\{ \tfrac{1}{2} \rho_B V_w S_B \ell^2 C_{Y_r} - \tfrac{1}{2} \rho_{c_1} S_{c_1} C_{Dc} V_{wc_1} \ell^2 C_1^2 \right.$$

$$-\tfrac{1}{2}\rho_{c2}S_{c2}C_{Dc}V_{wc2}\ell^2-\tfrac{1}{2}\rho_{c3}S_{c3}C_{Dc}V_{wc3}\ell^2\}\dot{\sigma}_1$$

$$+\{\tfrac{1}{2}\rho_B V_w S_B\ell^2 C_{Y_v}-\tfrac{1}{2}\rho_{c2}S_{c2}C_{Dc}V_{wc2}\ell^2 C_2-\tfrac{1}{2}\rho_{c3}S_{c3}C_{Dc}V_{wc3}\ell^2\}\dot{\sigma}_2$$

$$+\{\tfrac{1}{2}\rho_B V_w S_B\ell^2 C_{Y_w}-\tfrac{1}{2}\rho_{c3}S_{c3}C_{Dc}V_{wc3}\ell^2 C_3\}\dot{\sigma}_3 \qquad (387)$$

For the second link:

$$F_{\sigma_2}=[L_S-W_B-(m_{PL}+\tfrac{3m}{2})g][-\ell S\beta_{20}]\sigma_2+[F_{BSn}]\ell$$

$$+[D_{cs2}]\ell C_2+[D_{cs3}]\ell \qquad (388)$$

Substituting Equations (372), (385) and (386) into (388) gives:

$$F_{\sigma_2}=\{\tfrac{1}{2}\rho_B V_w^2 S_B\ell C_{Y_\psi}\}\psi+\{[W_B-L_S+(m_{PL}+\tfrac{3m}{2})g][\ell S\beta_{20}]\}\sigma_2$$

$$+\{\tfrac{1}{2}\rho_B V_w S_B\ell[C_{Y_{\dot\psi}}d_B+C_{Y_v}(-R_{jg}C\theta_0+R_{kg}S\theta_0)]\}\dot\psi$$

$$+\{\tfrac{1}{2}\rho_B V_w S_B\ell[C_{Y_{\dot\phi}}d_B+C_{Y_v}(-R_{kg})]\}\dot\phi$$

$$+\{\tfrac{1}{2}\rho_B V_w S_B\ell^2 C_{Y_v}-\tfrac{1}{2}\rho_{c2}S_{c2}C_{Dc}V_{wc2}\ell^2 C_2-\tfrac{1}{2}\rho_{c3}S_{c3}C_{Dc}V_{wc3}\ell^2\}\dot{\sigma}_1$$

$$+\{\tfrac{1}{2}\rho_B V_w S_B\ell^2 C_{Y_v}-\tfrac{1}{2}\rho_{c2}S_{c2}C_{Dc}V_{wc2}\ell^2 C_2^2-\tfrac{1}{2}\rho_{c3}S_{c3}C_{Dc}V_{wc3}\ell^2\}\dot{\sigma}_2$$

$$+\{\tfrac{1}{2}\rho_B V_w S_B\ell^2 C_{Y_v}-\tfrac{1}{2}\rho_{c3}S_{c3}C_{Dc}V_{wc3}\ell^2 C_3\}\dot{\sigma}_3 \qquad (389)$$

For the third link:

$$F_{\sigma_3} = \left[L_S - W_B - \left(m_{P_2} + \frac{m_3}{2} \right) g \right] \left[-\ell S \beta_{3_0} \right] \sigma_3 + \left[F_{BSA} \right] \ell + \left[D_{CS3} \right] \ell C_3 \qquad (390)$$

Substituting Equations (372) and (386) into (390) yields:

$$\begin{aligned} F_{\sigma_3} = & \left\{ \tfrac{1}{2} \rho_B V_W^2 S_B \ell C_{Y_\psi} \right\} \psi + \left\{ \left[W_B - L_S + \left(m_{P_2} + \frac{m_3}{2} \right) g \right] \left[\ell S \beta_{3_0} \right] \right\} \sigma_3 \\ & + \left\{ \tfrac{1}{2} \rho_B V_W S_B \ell \left[C_{Y_{\dot\psi}} \alpha_B + C_{Y_{\dot\alpha}} \left(-R_{jg} C\theta_0 + R_{kg} S\theta_0 \right) \right] \right\} \dot\psi \\ & + \left\{ \tfrac{1}{2} \rho_B V_W S_B \ell \left[C_{Y_{\dot\beta}} \alpha_B + C_{Y_{\dot\alpha}} \left(-R_{kg} \right) \right] \right\} \dot\phi \\ & + \left\{ \tfrac{1}{2} \rho_B V_W S_B \ell^2 C_{Y_{\dot\sigma}} - \tfrac{1}{2} \rho_{C3} S_{C3} C_{DC} V_{WC3} \ell^2 C_3 \right\} \dot\sigma_1 \\ & + \left\{ \tfrac{1}{2} \rho_B V_W S_B \ell^2 C_{Y_{\dot\sigma}} - \tfrac{1}{2} \rho_{C3} S_{C3} C_{DC} V_{WC3} \ell^2 C_3 \right\} \dot\sigma_2 \\ & + \left\{ \tfrac{1}{2} \rho_B V_W S_B \ell^2 C_{Y_{\dot\sigma}} - \tfrac{1}{2} \rho_{C3} S_{C3} C_{DC} V_{WC3} \ell^2 C_3^2 \right\} \dot\sigma_3 \end{aligned} \qquad (391)$$

4. Characteristic Equation

Equations (363) to (367) in conjunction with Equation (375), (377), (387), (389), and (391) form a set of five simultaneous differential equations of the following form:

$$\begin{aligned} & \alpha_{i1} \ddot\psi + \alpha_{i2} \ddot\phi + \alpha_{i3} \ddot\sigma_1 + \alpha_{i4} \ddot\sigma_2 + \alpha_{i5} \ddot\sigma_3 + \beta_{i1} \dot\psi + \beta_{i2} \dot\phi + \beta_{i3} \dot\sigma_1 \\ & + \beta_{i4} \dot\sigma_2 + \beta_{i5} \dot\sigma_3 + \delta_{i1} \psi + \gamma_{i2} \phi + \gamma_{i3} \sigma_1 + \gamma_{i4} \sigma_2 + \gamma_{i5} \sigma_3 = 0 \\ & i = 1, 2, 3, 4, 5 \end{aligned} \qquad (392)$$

If the initial conditions are all zero ($\dot{\psi}(0) = \dot{\phi}(0) = \dot{\sigma}_1(0) = \psi(0) = \phi(0) = \sigma_1(0) = 0$) , the equations (392) are easily Laplace transformed. In matrix notation they can be written as follows:

$$\begin{bmatrix} \alpha_{11}S^2+\beta_{11}S+\gamma_{11} & \alpha_{12}S^2+\beta_{12}S+\gamma_{12} & \alpha_{13}S^2+\beta_{13}S+\gamma_{13} \\ \alpha_{21}S^2+\beta_{21}S+\gamma_{21} & \alpha_{22}S^2+\beta_{22}S+\gamma_{22} & \alpha_{23}S^2+\beta_{23}S+\gamma_{23} \\ \alpha_{31}S^2+\beta_{31}S+\gamma_{31} & \alpha_{32}S^2+\beta_{32}S+\gamma_{32} & \alpha_{33}S^2+\beta_{33}S+\gamma_{33} \\ \alpha_{41}S^2+\beta_{41}S+\gamma_{41} & \alpha_{42}S^2+\beta_{42}S+\gamma_{42} & \alpha_{43}S^2+\beta_{43}S+\gamma_{43} \\ \alpha_{51}S^2+\beta_{51}S+\gamma_{51} & \alpha_{52}S^2+\beta_{52}S+\gamma_{52} & \alpha_{53}S^2+\beta_{53}S+\gamma_{53} \end{bmatrix}$$

$$\begin{bmatrix} \alpha_{14}S^2+\beta_{14}S+\gamma_{14} & \alpha_{15}S^2+\beta_{15}S+\gamma_{15} \\ \alpha_{24}S^2+\beta_{24}S+\gamma_{24} & \alpha_{25}S^2+\beta_{25}S+\gamma_{25} \\ \alpha_{34}S^2+\beta_{34}S+\gamma_{34} & \alpha_{35}S^2+\beta_{35}S+\gamma_{35} \\ \alpha_{44}S^2+\beta_{44}S+\gamma_{44} & \alpha_{45}S^2+\beta_{45}S+\gamma_{45} \\ \alpha_{54}S^2+\beta_{54}S+\gamma_{54} & \alpha_{55}S^2+\beta_{55}S+\gamma_{55} \end{bmatrix} \begin{Bmatrix} \psi(S) \\ \phi(S) \\ \sigma_1(S) \\ \sigma_2(S) \\ \sigma_3(S) \end{Bmatrix} = \begin{Bmatrix} 0 \\ 0 \\ 0 \\ 0 \\ 0 \end{Bmatrix} \tag{393}$$

The coefficients α_{ij} , β_{ij} , γ_{ij} , are tabulated for easy reference.

$$\alpha_{11} = I_{zB}C^2\theta_0 + I_{yB}S^2\theta_0 - I_{yzB}S2\theta_0 + M_S(R_{km}S\theta_0 - R_{jm}C\theta_0)^2 \tag{394}$$

$$\alpha_{12} = I_{yzB}C\theta_0 - I_{yB}S\theta_0 + M_S R_{km}(R_{jm}C\theta_0 - R_{km}S\theta_0) \tag{395}$$

$$\alpha_{13} = \ell M_S(R_{km}S\theta_0 - R_{jm}C\theta_0) \tag{396}$$

$$a_{14} = \ell M_s (R_{km} S\theta_o - R_{jm} C\theta_o) \tag{397}$$

$$a_{15} = \ell M_s (R_{km} S\theta_o - R_{jm} C\theta_o) \tag{398}$$

$$a_{21} = I_{YZB} C\theta_o - I_{YB} S\theta_o + M_s R_{km} (R_{jm} C\theta_o - R_{km} S\theta_o) \tag{399}$$

$$a_{22} = I_{YB} + M_s R_{km}^2 \tag{400}$$

$$a_{23} = -\ell M_s R_{km} \tag{401}$$

$$a_{24} = -\ell M_s R_{km} \tag{402}$$

$$a_{25} = -\ell M_s R_{km} \tag{403}$$

$$a_{31} = \ell M_s (R_{km} S\theta_o - R_{jm} C\theta_o) \tag{404}$$

$$a_{32} = -\ell M_s R_{km} \tag{405}$$

$$a_{33} = \ell^2 \left(\frac{7m}{3} + m_{pl} + M_s \right) \tag{406}$$

$$a_{34} = \ell^2 \left(\frac{3m}{2} + m_{pl} + M_s \right) \tag{407}$$

$$a_{35} = \ell^2 \left(\frac{m}{2} + m_{pl} + M_s \right) \tag{408}$$

$$a_{41} = \ell M_s (R_{km} S\theta_o - R_{jm} C\theta_o) \tag{409}$$

$$\alpha_{42} = -\ell M_S R_{km} \tag{410}$$

$$\alpha_{43} = \ell^2 \left(\frac{3m}{2} + m_{PL} + M_S \right) \tag{411}$$

$$\alpha_{44} = \ell^2 \left(\frac{4m}{3} + m_{PL} + M_S \right) \tag{412}$$

$$\alpha_{45} = \ell^2 \left(\frac{m}{2} + m_{PL} + M_S \right) \tag{413}$$

$$\alpha_{51} = \ell M_S \left(R_{km} S\theta_o - R_{jm} C\theta_o \right) \tag{414}$$

$$\alpha_{52} = -\ell M_S R_{km} \tag{415}$$

$$\alpha_{53} = \ell^2 \left(\frac{m}{2} + m_{PL} + M_S \right) \tag{416}$$

$$\alpha_{54} = \ell^2 \left(\frac{m}{2} + m_{PL} + M_S \right) \tag{417}$$

$$\alpha_{55} = \ell^2 \left(\frac{m}{3} + m_{PL} + M_S \right) \tag{418}$$

$$\beta_{11} = -\frac{1}{2} \rho_B V_W S_B \left\{ \left[C_{Y_\dot{\beta}} \dot{\alpha}_B + C_{Y_r} \left(-R_{jg} C\theta_o + R_{kg} S\theta_o \right) \right] \left[-R_{jA} C\theta_o + R_{kA} S\theta_o \right] \right.$$

$$\left. + d_B \left[C_{m_\dot{\beta}} \dot{\alpha}_B + C_{m_r} \left(-R_{jg} C\theta_o + R_{kg} S\theta_o \right) \right] \right\} \tag{419}$$

$$\beta_{12} = -\frac{1}{2} \rho_B V_W S_B \left[\left(C_{Y_\dot{\beta}} d_B - C_{Y_r} R_{kg} \right) \left(-R_{jA} C\theta_o + R_{kA} S\theta_o \right) + d_B \left(C_{m_\dot{\beta}} d_B - C_{m_r} R_{kg} \right) \right] \tag{420}$$

$$\beta_{13} = -\frac{1}{2} \rho_B V_W S_B \ell \left[C_{Y_r} \left(-R_{jA} C\theta_o + R_{kA} S\theta_o \right) + C_{m_r} d_B \right] \tag{421}$$

$$\beta_{14} = -\frac{1}{2}\rho_B V_w S_B \ell \left[C_{Y_v} \left(-R_{jA} C\theta_o + R_{kA} S\theta_o \right) + C_{m_v} d_B \right] \tag{422}$$

$$\beta_{15} = -\frac{1}{2}\rho_B V_w S_B \ell \left[C_{Y_v} \left(-R_{jA} C\theta_o + R_{kA} S\theta_o \right) + C_{m_v} d_B \right] \tag{423}$$

$$\beta_{21} = -\frac{1}{2}\rho_B V_w S_B \left\{ \left[C_{Y_{\dot\psi}} d_B + C_{Y_v} \left(-R_{jq} C\theta_o + R_{kq} S\theta_o \right) \right] \left[-R_{kA} S\theta_o \right] \right.$$

$$\left. + d_B \left[C_{\ell_{\dot\psi}} d_B + C_{\ell_v} \left(-R_{jq} C\theta_o + R_{kq} S\theta_o \right) \right] \right\} \tag{424}$$

$$\beta_{22} = -\frac{1}{2}\rho_B V_w S_B \left[\left(C_{Y_{\dot\phi}} d_B - C_{Y_v} R_{kB} \right) \left(-R_{kA} S\theta_o \right) + d_B \left(C_{\ell_{\dot\phi}} d_B - C_{\ell_v} R_{kB} \right) \right] \tag{425}$$

$$\beta_{23} = -\frac{1}{2}\rho_B V_w S_B \ell \left[C_{Y_v} \left(-R_{kA} S\theta_o \right) + C_{\ell_v} d_B \right] \tag{426}$$

$$\beta_{24} = -\frac{1}{2}\rho_B V_w S_B \ell \left[C_{Y_v} \left(-R_{kA} S\theta_o \right) + C_{\ell_v} d_B \right] \tag{427}$$

$$\beta_{25} = -\frac{1}{2}\rho_B V_w S_B \ell \left[C_{Y_v} \left(-R_{kA} S\theta_o \right) + C_{\ell_v} d_B \right] \tag{428}$$

$$\beta_{31} = -\frac{1}{2}\rho_B V_w S_B \ell \left[C_{Y_{\dot\psi}} d_B + C_{Y_v} \left(-R_{jq} C\theta_o + R_{kq} S\theta_o \right) \right] \tag{429}$$

$$\beta_{32} = -\frac{1}{2}\rho_B V_w S_B \ell \left[C_{Y_{\dot\phi}} d_B - C_{Y_v} R_{kq} \right] \tag{430}$$

$$\beta_{33} = -\frac{1}{2}\rho_B V_w S_B \ell^2 C_{Y_v} + \frac{1}{2}\rho_{c1} S_{c1} C_{Dc} V_{wc1} \ell^2 C_1^2 + \frac{1}{2}\rho_{c2} S_{c2} C_{Dc} V_{wc2} \ell^2 \tag{431}$$

$$+ \frac{1}{2}\rho_{c3} S_{c3} C_{Dc} V_{wc3} \ell^2 \tag{432}$$

$$\beta_{34} = -\frac{1}{2}\rho_B V_w S_B \ell^2 C_{Y_v} + \frac{1}{2}\rho_{c2} S_{c2} C_{Dc} V_{wc2} \ell^2 C_2 + \frac{1}{2}\rho_{c3} S_{c3} C_{Dc} V_{wc3} \ell^2 \tag{433}$$

$$\beta_{35} = -\frac{1}{2}\rho_B V_w S_B \ell^2 C_{Y_v} + \frac{1}{2}\rho_{c3} S_{c3} C_{Dc} V_{wc3} \ell^2 C_3$$

$$\beta_{41} = -\tfrac{1}{2}\rho_B V_w S_B \ell \left[C_{Y_{\dot\psi}} \alpha_B + C_{Y_w}(-R_{jq}\, C\theta_o + R_{kq}\, S\theta_o) \right] \quad (434)$$

$$\beta_{42} = -\tfrac{1}{2}\rho_B V_w S_B \ell \left[C_{Y_{\dot\phi}} \alpha_B - C_{Y_w} R_{kq} \right] \quad (435)$$

$$\beta_{43} = -\tfrac{1}{2}\rho_B V_w S_B \ell \left[C_{Y_w} \ell \right] + \tfrac{1}{2}\rho_{c2} S_{c2} C_{Dc} V_{wc2} \ell^2 C_2 + \tfrac{1}{2}\rho_{c3} S_{c3} C_{Dc} V_{wc3} \ell^2 \quad (436)$$

$$\beta_{44} = -\tfrac{1}{2}\rho_B V_w S_B \ell \left[C_{Y_w} \ell \right] + \tfrac{1}{2}\rho_{c2} S_{c2} C_{Dc} V_{wc2} \ell^2 C_2^2 + \tfrac{1}{2}\rho_{c3} S_{c3} C_{Dc} V_{wc3} \ell^2 \quad (437)$$

$$\beta_{45} = -\tfrac{1}{2}\rho_B V_w S_B \ell \left[C_{Y_w} \ell \right] + \tfrac{1}{2}\rho_{c3} S_{c3} C_{Dc} V_{wc3} \ell^2 C_3 \quad (438)$$

$$\beta_{51} = -\tfrac{1}{2}\rho_B V_w S_B \ell \left[C_{Y_{\dot\psi}} \alpha_B + C_{Y_w}(-R_{jq}\, C\theta_o + R_{kq}\, S\theta_o) \right] \quad (439)$$

$$\beta_{52} = -\tfrac{1}{2}\rho_B V_w S_B \ell \left[C_{Y_{\dot\phi}} \alpha_B - C_{Y_w} R_{kq} \right] \quad (440)$$

$$\beta_{53} = -\tfrac{1}{2}\rho_B V_w S_B \ell \left[C_{Y_w} \ell \right] + \tfrac{1}{2}\rho_{c3} S_{c3} C_{Dc} V_{wc3} \ell^2 C_3 \quad (441)$$

$$\beta_{54} = -\tfrac{1}{2}\rho_B V_w S_B \ell \left[C_{Y_w} \ell \right] + \tfrac{1}{2}\rho_{c3} S_{c3} C_{Dc} V_{wc3} \ell^2 C_3 \quad (442)$$

$$\beta_{55} = -\tfrac{1}{2}\rho_B V_w S_B \ell \left[C_{Y_w} \ell \right] + \tfrac{1}{2}\rho_{c3} S_{c3} C_{Dc} V_{wc3} \ell^2 C_3^2 \quad (443)$$

$$\gamma_{11} = -\tfrac{1}{2}\rho_B V_w^2 S_B \left[C_{Y_\psi}(-R_{jA}\, C\theta_o + R_{kA}\, S\theta_o) + C_{n_\psi} \alpha_B \right] \quad (444)$$

$$\gamma_{12} = \gamma_{13} = \gamma_{14} = \gamma_{15} = 0 \quad (445)$$

$$\gamma_{21} = -\tfrac{1}{2}\rho_B V_w^2 S_B \left[C_{Y_\psi}(-R_{kA}\, S\theta_o) + C_{\ell_\psi} \alpha_B \right] \quad (446)$$

$$\gamma_{22} = (W_B R_{kg} - L_S R_{kB}) C\theta_c \tag{447}$$

$$\gamma_{23} = \gamma_{24} = \gamma_{25} = 0 \tag{448}$$

$$\gamma_{31} = -\tfrac{1}{2} \rho_B V_w^2 S_B \ell C_{Y_\psi} \tag{449}$$

$$\gamma_{32} = 0 \tag{450}$$

$$\gamma_{33} = [L_S - W_B - (m_{PL} + \tfrac{5m}{2}) g] [\ell S \rho_{3c}] \tag{451}$$

$$\gamma_{34} = \gamma_{35} = 0 \tag{452}$$

$$\gamma_{41} = -\tfrac{1}{2} \rho_B V_w^2 S_B \ell C_{Y_\psi} \tag{453}$$

$$\gamma_{42} = \gamma_{43} = 0 \tag{454}$$

$$\gamma_{44} = [L_S - W_B - (m_{PL} + \tfrac{3m}{2}) g] [\ell S \rho_{3c}] \tag{455}$$

$$\gamma_{45} = 0 \tag{456}$$

$$\gamma_{51} = -\tfrac{1}{2} \rho_B V_w^2 S_B \ell C_{Y_\psi} \tag{457}$$

$$\gamma_{52} = \gamma_{53} = \gamma_{54} = 0 \tag{458}$$

$$\gamma_{55} = [L_S - W_B - (m_{PL} + \tfrac{m}{2}) g] [\ell S \rho_{3c}] \tag{459}$$

The equilibrium angles θ_v , ξ_{i0} are found from the longitudinal stability analysis using Equations (285) to (288)..

In a manner similar to the longitudinal equations a tenth order characteristic equation is formed. The roots of this characteristic equation give stability information about the system in the lateral degrees of freedom.

A P P E N D I X B

COMPUTER PROGRAM

COMPUTER PROGRAM NOMENCLATURE

The following is a list of variables used in the computer programs with a brief description of each. The notation is displayed in two forms;

(1) as it appears in the computer programs

(2) as used throughout the discussion of this report.

Some of the variables in the computer programs are simply combinations of other variables or dummy variables; these are not defined in the nomenclature. Also, there are many variables used in the report that are defined when introduced, and are not included in the nomenclature. It should also be noted that some dimensioned variables appear in both computer programs but, because of the different number of equations involved, they are dimensioned differently in the two programs.

Fortran	Standard	Description	Units
A(5,5,11)		A triply-dimensioned array which contains the matrix to be evaluated	
AALP(5,5)	α_{ij}	Coefficients of second derivatives in linear equations of motion	slug-ft^2
AALPA(8)		Angle-of-attack array used for interpolation of balloon's aerodynamic coefficients	rad
AALPD(8)		Angle-of-attack array used for interpolation of balloon's aerodynamic coefficients	deg
AALT(8)		Altitude array used for interpolation of wind velocity	ft
ALP	α	Balloon angle-of-attack	rad
ALPSL		Ratio of two angle-of-attack differences used for interpolation of balloon aerodynamic coefficients	
ALTSL		Ratio of two altitude differences used for interpolation of wind velocity	
BBET(5,5)	β_{ij}	Coefficients of first derivatives in linear equations of motion	slug-ft^2/sec
C(3)	c_i	Non-dimensional center-of-pressure of "i"th link	
CCDB(8)		Balloon drag coefficient array corresponding to AALPD(8)	
CCLB(8)		Balloon lift coefficient array corresponding to AALPD(8)	
CCMB(8)		Balloon moment coefficient array corresponding to AALPD(8)	

Fortran	Standard	Description	Units
CDAB	$C_{D_{\alpha_B}}$	$\frac{\partial C_{DB}}{\partial \alpha}$	rad^{-1}
CDTDB	$C_{D_{\dot{\theta}_B}}$	Balloon drag coefficient due to pitch velocity	rad^{-1}
CDB	C_{DB}	Balloon drag coefficient at "α_T"	
CDC	C_{DC}	Tether drag coefficient	
CDC1	C_{DC1}	Constant used to correct balloon drag coefficient for different size tails	
CDC2	C_{DC2}	Constant used to correct balloon drag coefficient for different size tails	
CLAB	$C_{L_{\alpha_B}}$	$\frac{\partial C_{LB}}{\partial \alpha}$	rad^{-1}
CLTDB	$C_{L_{\dot{\theta}_B}}$	Balloon lift coefficient due to pitch velocity	rad^{-1}
CLB	C_{LB}	Balloon lift coefficient at "α_T"	
CLC	C_{LC}	Constant used to correct balloon lift coefficient for different size tails	
CLPHDB	$C_{\ell_{\dot{\beta}_B}}$	Balloon rolling moment coefficient due to rolling velocity	rad^{-1}
CLPSB	$C_{\ell_{\psi_B}}$	Balloon rolling moment coefficient due to yaw angle	rad^{-1}
CLPSDB	$C_{\ell_{\dot{\psi}_B}}$	Balloon rolling moment coefficient due to yaw velocity	rad^{-1}
CLVB	$C_{\ell_{V_B}}$	Balloon rolling moment coefficient due to lateral velocity	
CMAB	$C_{m_{\alpha_B}}$	$\frac{\partial C_{mB}}{\partial \alpha}$	rad^{-1}

Fortran	Standard	Description	Units
CMTDB	$C_{m_{\dot{\theta}B}}$	Balloon pitching moment coefficient due to pitching velocity	rad^{-1}
CMB	C_{mB}	Balloon pitching moment coefficient at "α_T"	
CMC	C_{mC}	Constant used to correct balloon pitching moment coefficient for different tail sizes	
CNPHDB	$C_{n_{\dot{\phi}B}}$	Balloon yawing moment coefficient due to rolling velocity	rad^{-1}
CNPSB	$C_{n_{\psi_B}}$	Balloon yawing moment coefficient due to yaw angle	rad^{-1}
CNPSDB	$C_{n_{\dot{\psi}B}}$	Balloon yawing moment coefficient due to yawing velocity	rad^{-1}
CNVB	$C_{n_{VB}}$	Balloon yawing moment coefficient due to lateral velocity	
COE(11)		Array of coefficients of characteristic equation in ascending order of variable	
COEF(11)		Array of coefficients of characteristic equation in descending order of variable	
COM1(10)		Input array designating title of computer run	
CTHEO	$C\theta_o$	$\cos \theta_o$	
CTHEO2	$C^2\theta_o$	$\cos^2 \theta_o$	
CTPX(3)	$C(\theta+\xi_i)$	$\cos (\theta + \xi_i)$	
CTPX2(3)	$C^2(\theta+\xi_i)$	$\cos^2 (\theta + \xi_i)$	
CX(3)	$C\xi_i$	$\cos \xi_i$	
CXMX(3,3)	$C(\xi_i-\xi_j)$	$\cos (\xi_i - \xi_j)$	

Fortran	Standard	Description	Units
CYPHDB	$C_{Y_{\dot{\phi}B}}$	Balloon side force coefficient due to rolling velocity	rad^{-1}
CYPSB	$C_{Y_{\psi_B}}$	Balloon side force coefficient due to yaw angle	rad^{-1}
CYPSDB	$C_{Y_{\dot{\psi}_B}}$	Balloon side force coefficient due to yawing velocity	rad^{-1}
CYVB	$C_{Y_{vB}}$	Balloon side force coefficient due to lateral velocity	
DAMRAT(8)	ζ_i	Damping ratio of "i"th mode	
DB	d_B	Aerodynamic reference length of balloon $(\forall^{1/3})$	ft
DC	d_C	Diameter of Tether	ft
DYPRB	q_B	Dynamic pressure on balloon	lb_f/ft^2
DYPRH(4)	q_{Hi}	Dynamic pressure at "i"th hinge	lb_f/ft^2
EPS		A small number used to test for zero	
F		Any one of the four nonlinear longitudinal equations that must be solved simultaneously	$ft\text{-}lb_f$
FREQD(8)	ω_{di}	Damped frequency of "i"th mode	rad/sec
FREQN(8)	ω_{ni}	Natural frequency of "i"th mode	rad/sec
G	g	Acceleration of gravity at sea level	ft/sec^2
GGAM(5,5)	γ_{ij}	Coefficients of generalized variables in linear equations of motion	$slug\text{-}ft^2/sec^2$

Fortran	Standard	Description	Units
GGG(8,8)	G_{ij}	Elements of square matrix used to find normal modes	
HHH(8)	H_i	Elements of column matrix used to find normal modes	
IER		Variable checked to see if solution has been found to simultaneous nonlinear equations	
IERR		Variable checked to see if all the roots of the characteristic equations have been found	
IERSW		Variable checked to see if solution has been found for a set of linear algebraic equations	
ISW(8)		Array defining the validity of the roots of the characteristic equation	
IXB	I_{XB}	Pitch moment of inertia of balloon	$slug\text{-}ft^2$
IYB	I_{YB}	Roll moment of inertia of balloon	$slug\text{-}ft^2$
IYZB	I_{YZB}	Product of inertia with respect to the roll and yaw body axes of the balloon	$slug\text{-}ft^2$
IZB	I_{ZB}	Yaw moment of inertia of balloon	$slug\text{-}ft^2$
KK		Variable used to specify first, second, or third call to SYSTEM subroutine	
L	ℓ	Length of one link	ft
LS	L_S	Balloon's static lift, weight of displaced air	lb_f
M	m	Mass of one link	slugs
MAL		Added mass in balloon's longitudinal direction	slugs

Fortran	Standard	Description	Units
MAS		Added mass in balloon's lateral direction	slugs
MAV		Added mass in balloon's vertical direction	slugs
MAX		Maximum number of iterations allowed if the solution to the simultaneous nonlinear equation fails to converge	
ML	M_L	Apparent mass in balloon's longitudinal direction	slugs
MPL	M_{PL}	Mass of payload	slugs
MS	M_S	Apparent mass in balloon's lateral direction	slugs
MV	M_V	Apparent mass in balloon's vertical direction	slugs
N		Number of equations to be solved	
NF		Number of significant figures used when testing for convergency when solving simultaneous nonlinear equations	
NP1		Number of terms in characteristic equation	
N1		Degree of characteristic equation	
RHOB	ρ_B	Air density at Z_B	$slug/ft^3$
RHOC(3)	ρ_{ci}	Air density at Z_{ci}	$slug/ft^3$
RHOCH(4)		Air density at Z_{cHi}	$slug/ft^3$
RJA	R_{jA}	Distance along longitudinal axis of balloon from aerodynamic reference center to bridle apex (positive toward the nose)	ft
RJB	R_{jB}	Distance along longitudinal axis of balloon from center of buoyancy to bridle apex (positive toward the nose)	ft

Fortran	Standard	Description	Units
RJG	R_{jg}	Distance along longitudinal axis of balloon from center of gravity to bridle apex (positive toward the nose)	ft
RJM	R_{jm}	Distance along longitudinal axis of balloon from dynamic mass center to bridle apex (positive toward the nose)	ft
RKA	R_{kA}	Distance along vertical axis of balloon from aerodynamic reference center to bridle apex (positive up)	ft
RKB	R_{kB}	Distance along vertical axis of balloon from center of buoyancy to bridle apex (positive up)	ft
RKG	R_{kg}	Distance along vertical axis of balloon from center of gravity to bridle apex (positive up)	ft
RKM	R_{km}	Distance along vertical axis of balloon from dynamic mass center to bridle apex (positive up)	ft
ROOTI(8)		Imaginary part of "i"th root of characteristic equation	
ROOTR(8)		Real part of "i"th root of characteristic equation	
SB	S_B	Aerodynamic reference area of balloon ($\forall^{2/3}$)	ft^2
SC(3)	S_{ci}	Aerodynamic reference area of "i"th link = $(\ell)\cdot(d_c)$	ft^2
STHEO	$3\theta_o$	$\sin \theta_o$	
STHEO2	$S^2\theta_o$	$\sin^2 \theta_o$	
STPX(3)	$S(\theta+\xi_i)$	$\sin (\theta + \xi_i)$	
STPX2(3)	$S^2(\theta+\xi_i)$	$\sin^2 (\theta + \xi_i)$	

Fortran	Standard	Description	Units
SX(3)	$S\xi_i$	$\sin \xi_i$	
SXMX(3,3)	$S(\xi_i-\xi_j)$	$\sin (\xi_i - \xi_j)$	
SX2(3)	$S^2 \xi_i$	$\sin^2 \xi_i$	
S2THEO	$S2\theta_o$	$\sin 2\theta_o$	
S2X(3)	$S2 \xi_i$	$\sin 2 \xi_i$	
TETH		Total length of tether	ft
THAMP(8)		Time to half or double amplitude of "i"th mode	sec
THEO	θ_o	Pitch angle of balloon	rad
THEODE	θ_o	Pitch angle of balloon	deg
VBR	V_{BR}	Relative velocity between balloon and air	ft/sec
VECTD(4)		Direction angle of "i"th complex element of mode	
VECTI(4)		Imaginary part of "i"th complex element of mode	
VECTM(4)		Magnitude of "i"th complex element of mode	
VECTR(4)		Real part of "i"th complex element of mode	
VVW(8)		Velocity array used for interpolation of steady state wind velocities corresponding to AALT(8)	ft/sec
VW	V_w	Steady state wind velocity at Z_B	ft/sec
VWC(3)	V_{wci}	Steady state wind velocity at Z_{ci}	ft/sec
VWH(4)		Steady state wind velocity at "i"th hinge	ft/sec
WB	W_B	Total weight of balloon harness	lbs

Fortran	Standard	Description	Units
WTC		Weight of tether	lbs
XIO(3)	ξ_{io}	Pitch equilibrium angle of "i"th link	rad
XIODE(3)	ξ_{io}	Pitch equilibrium angle of "i"th link	deg
YB	Y_B	Down-range distance of balloon from winch in longitudinal plane	ft
ZB	Z_B	Altitude of balloon	ft
ZC(3)	Z_{Ci}	Altitude of center-of-pressure of "i"th link	ft
ZCH(4)	Z_{CH_i}	Altitude of "i"th hinge	ft

INPUTS

All inputs are read in under format F10.0 except COM1. Its format is 10A4. The following is a list of all variables needed. The variables are defined in the nomenclature.

(a) Longitudinal Stability Program

1st READ:	AALT, VVW	2 cards
2nd READ:	AALPD, CCMB, CCLB, CCDB	4 cards
3rd READ:	CMC, CDC1, CDC2, CLC	1 card
4th READ:	WB, LS, MPL, WTC, IXB, MAL, MAV	1 card
5th READ:	SB, DB, CDC, DC, TETH, CMTDB, CLTDB	1 card
6th READ:	COM1	1 card
7th READ:	RJM, RKM, RJA, RKA, RJG, RKG, RJB, RKB	1 card
8th READ:	THEO, XIO(1), XIO(2), XIO(3)	1 card

The input READ cards are arranged such that data from the 1st, 2nd and 3rd READ are read-in only once. Data from the 4th to 8th READ are read-in with each change of conditions to be analyzed. If no new runs are necessary, a card with a 1. in the first two columns should be read-in in place of

the 4th READ. The READ cards can be easily rearranged by the program user for his own convenience.

Note: The input on the 8th READ is a guess; the program will iterate to find correct values.

(b) Lateral Stability Program

1st READ:	AALT, VVW	2 cards
2nd READ:	WB, LS, MPL, WTC, IZB, IYB, IYZB, MAS	1 card
3rd READ:	THEODE, XIODE(1), XIODE(2), XIODE(3)	1 card
4th READ:	COM1	1 card
5th READ:	RJM, RKM, RJA, RKA, RJG, RKG,RKB	1 card
6th READ:	SB, DB, TETH, DC, CDC	1 card
7th READ:	CYPSDB, CYPHDB, CNPSDB, CNPHDB, CLPSDB, CLPHDB	1 card
8th READ:	CYPSB, CNPSB, CLPSB, CYVB, CNVB, CLVB	1 card

The input READ cards are arranged such that data from the first card are read-in only once. Data from the 2nd to 8th card are read-in with each change of condition to be analyzed. If no new runs are necessary, a card with a 1. in the first two columns should be read-in in place of the 2nd READ. Inputs on the 3rd card are obtained from the longitudinal program.

OUTPUTS

The following information is printed out for each condition. All variables are defined in the nomenclature.

(a) Longitudinal Stability Program

(1) COM1

(2) AALT, VVW

(3) AALPD, CCMB, CCLB, CCDB

(4) Iterative values of longitudinal equilibrium angles

(5) Final values of longitudinal equilibrium angles

(6) RJM, RKM, CMB, CMAB, CMTDB, LS, MPL, TETH, IXB, RJA, RKA, CLB, CLAB, CLTDB, WB, SB, DC, MAL, RJG, RKG, CDB, CDAB, CDTDB, WTC, DB, CDC, MAV, RJB, RKB, YB, ZB, DYPRB

(7) AALP(4,4), BBET(4,4), GGAM(4,4)

(8) COE(I); I = 1, 9

(9) ROOTR(I), ROOTI(I), FREQN(I), FREQD(I), DAMRAT(I), THAMP(I); I = 1, 8

(10) VECTR(I), VECTI(I), VECTM(I), VECTD(I); I = 1, 3

(b) Lateral Stability Program

(1) COM1

(2) AALT, VVW

(3) RJM, RKM, CNPSB, CNPSDB, CNPHDB, CNVB, LS, MPL, IZB, TETH, XIODE(1), YB, RJA, RKA, CLPSB, CLPSDB, CLPHDB, CLVB, WB, SB, IYB, MAS, XIODE(2) ZB, RJG, RKG, CYPSB, CYPSDB, CYPHDB, CYVB, WTC, DB, IYZB, THEODE, XIODE(3), DYPRB, RKB, DC, CDC

(4) AALP(5,5) BBET(5,5), GGAM(5,5)

(5) COE(I); I = 1, 11

(6) ROOTR(I), ROOTI(I), FREQN(I), FREQD(I), DAMRAT(I), THAMP(I); I - 1, 10

(7) VECTR(I), VECTI(I), VECTM(I), VECTD(I); I = 1, 4

FORTRAN IV PROGRAM DESCRIPTION

A listing of both programs may be found at the end of Appendix B. A description of the main programs and subroutines is given here.

(a) Longitudinal Stability Program

(1) Main Program

i) Read inputs

ii) Initialize and define certain variables

iii) Calculate equilibrium angles of balloon and links

iv) Write all conditions that define the configuration being analyzed.

v) Calculate α_{ij}, β_{ij}, γ_{ij}

vi) Expand determinant whose elements are quadratic terms so that the characteristic polynominal is formed

vii) Find roots of characteristic equation

viii) Write out roots of characteristic equation, and natural frequency, damped frequency, damping ratio, and time to half or double amplitude for each root.

ix) Calculate mode shape for each root of characteristic equation. The mode shape is complex and can be defined as a magnitude and a direction angle if $\theta = 1 + 0i$

x) Write out variables defining mode shape for each root of characteristic equation

(2) Subroutine EQUIL

i) Calculate aerodynamic coefficients of balloon

ii) Calculate center-of-pressure of each link

iii) Calculate dynamic pressure acting on balloon

iv) Calculate steady state wind velocity acting at center-of-pressure of each link

(3) Subroutine CROUT

Solve a set of linear algebraic equations so that the mode shapes can be obtained.

(5) Subroutine POLMAT

Expand a determinant whose elements are polynominals so that the characteristic plynominal can be obtained.

(6) Subroutine MULLER

Determine the real and complex roots of the characteristic equation.

(b) Lateral Stability Program

The Lateral Stability Program is similar to the Longitudinal Stability Program except that the equilibrium angles do not have to be found. This eliminates the Subroutines EQUIL and SYSTEM.

SAMPLE INPUTS AND OUTPUTS

The following pages show the input and output data for the nominal computer runs in both the longitudinal case and the lateral case.

INPUT DATA FOR LONGITUDINAL STABILITY COMPUTER RUN

```
          5000.     10000.    20000.    25000.
16.9      52.3      67.5      91.1      99.9
-5.                 5.        10.       12.       15.       20.       25.
.0137     .0103     -.0005    .0044     .005      -.0075    -.041     -.078
-.11      .0063     .1368     .2514     .2991     .371      .51       .62
.11       .0764     .0865     .1133     .1279     .1527     .22       .3
0.        0.        0.        0.
2157.     3942.     31.06     708.      116000.   15.7      110.
1533.     39.15     1.1       .0342     12639.    -2.01     1.68
BJ  60K CU. FT.  NOMINAL
19.6      -44.6     6.7       -46.      23.7      -42.3     12.6      -45.4
8.5       45.       55.       65.
1.
```

INPUT DATA FOR LATERAL STABILITY COMPUTER RUN

```
          5000.     10000.    20000.    25000.
16.9      52.3      67.5      91.1      99.9
2157.     3942.     31.06     708.      119000.   26000.    12500.    115.
8.50      41.65     51.53     65.47
BJ 60K CU. FT. NOMINAL
20.5      -42.6     6.7       -46.      23.7      -42.3     -45.4
1533.     39.15     12639.
1.79      .142      -2.31     -.122     -.347     -.327
2.08      -.105     -.351     -2.08     +.105     +.351
1.
```

STABILITY ANALYSIS OF A TETHERED BALLOON IN THE LONGITUDINAL PLANE BJ 60K CU. FT. NOMINAL

ALTITUDE PROFILE	0.0	5000.0	10000.0	20000.0	25000.0	0.0	0.0	0.0
WIND VELOCITY PROFILE	16.9	52.3	67.5	91.1	99.9	0.0	0.0	0.0
ANGLE-OF-ATTACK(DEG)	-5.0000	0.0	5.0000	10.0000	12.0000	15.0000	20.0000	25.0000
MOMENT COEFFICIENT	0.0137	0.0103	-0.0005	0.0044	0.0050	-0.0075	-0.0410	-0.0780
LIFT COEFFICIENT	-0.1100	0.0063	0.1368	0.2514	0.2991	0.3710	0.5100	0.6200
DRAG COEFFICIENT	0.1100	0.0764	0.0865	0.1133	0.1279	0.1527	0.2200	0.3000

THETA	XIO(1)	XIO(2)	XIO(3)
8.50000	44.99998	54.99998	64.99997
8.50764	41.72441	51.53526	65.46983
8.50306	41.64674	51.52979	65.46829
8.50303	41.64664	51.52968	65.46825
FINAL SOLUTION			
8.50303	41.64662	51.52969	65.46825

RJM	RKM	CMB	CMAB	CMTDB	LS	MPL	TETH	IXB
RJA	RKA	CLB	CLAB	CLTDB	WB	SB	DC	MAL
RJG	RKG	CDB	CDAB	CDTDB	WTC	DB	CDC	MAV
RJB	RKB	RANGE	ALTITUDE	DYPRB				
19.6000	-44.6000	0.0029	0.0561	-2.0100	3942.	31.06	12639.	116000.
6.7000	-46.0000	0.2171	1.3132	1.6800	2157.0	1533.0	0.0342	15.70
23.7000	-42.3000	0.1053	0.3071	0.3282	708.0	39.150	1.100	110.000
12.600	-45.400	-7548.1	9969.2	0.399E 01				

ALPHA(I,J)

0.35E 06	-0.21E 08	-0.21E 08	-0.19E 08
-0.21E 08	0.30E 10	0.27E 10	0.22E 10
-0.21E 08	0.27E 10	0.26E 10	0.23E 10
-0.19E 08	0.22E 10	0.23E 10	0.22E 10

BETA(I,J)

0.32E 06	-0.96E 06	-0.11E 07	-0.13E 07
-0.13E 08	0.18E 09	0.70E 08	-0.15E 09
-0.10E 08	0.17E 09	0.14E 09	-0.25E 08
-0.61E 07	0.12E 09	0.13E 09	0.86E 08

GAMMA(I,J)

0.17E 06	0.0	0.0	0.0
-0.20E 08	0.76E 07	0.15E 07	0.85E 06
-0.15E 08	0.0	0.89E 07	0.13E 07
-0.69E 07	0.0	0.0	0.97E 07

COEFFICIENTS OF CHARACTERISTIC EQUATION IN ASCENDING ORDER

0.1090 27 0.1510 28 0.949D 29 0.145D 31 0.664D 31 0.179D 32 0.277D 32 0.266D 32 0.111D 32

ALL ROOTS HAVE BEEN ACCURATELY DETERMINED

ROOTS OF CHARACTERISTIC EQUATION REAL	IMAGINARY	NATURAL FREQUENCY	STABILITY PARAMETERS DAMPED FREQUENCY	DAMPING RATIO	TIME TO HALF OR DOUBLE AMPLITUDE
0.1289D-02	0.3474D-01	0.3476D-01	0.3474D-01	-0.3708D-01	-0.5378D 03
0.1289D-02	-0.3474D-01	0.3476D-01	0.3474D-01	-0.3708D-01	-0.5378D 03
-0.9524D-01	0.2472D-22	0.9524D-01	0.2472D-22	0.1000D 01	0.7278D 01
-0.2984D 00	-0.3461D 00	0.4570D 00	0.3461D 00	0.6530D 00	0.2323D 01
-0.2984D 00	0.3461D 00	0.4570D 00	0.3461D 00	0.6530D 00	0.2323D 01
-0.3150D 00	-0.5312D 00	0.6176D 00	0.5312D 00	0.5101D 00	0.2201D 01
-0.3150D 00	0.5312D 00	0.6176D 00	0.5312D 00	0.5101D 00	0.2201D 01
-0.1077D 01	0.1374D-23	0.1077D 01	0.1374D-23	0.1000D 01	0.6437D 00

MODE SHAPES

EIGENVECTORS

REAL	IMAGINARY	MAGNITUDE	DIRECTION ANGLE
0.3981E 00	-0.2105E 01	0.2142E 01	0.2807E 03
-0.6719E 00	-0.1072E 01	0.1265E 01	0.2379E 03
-0.1241E 01	-0.3185E 00	0.1282E 01	0.1944E 03
0.3981E 00	0.2105E 01	0.2142E 01	0.7929E 02
-0.6719E 00	0.1072E 01	0.1265E 01	0.1221E 03
-0.1241E 01	0.3185E 00	0.1282E 01	0.1656E 03
0.8883E 00	-0.6509E-21	0.8883E 00	0.3600E 03
0.8002E 00	-0.1098E-21	0.8002E 00	0.3600E 03
-0.3636E 00	0.7629E-21	0.3636E 00	0.1800E 03
-0.1264E 00	-0.3748E-01	0.1319E 00	0.1965E 03
0.7975E-01	-0.9819E-02	0.8036E-01	0.3530E 03
0.4492E-01	0.3724E-01	0.5835E-01	0.3966E 02
-0.1264E 00	0.3748E-01	0.1319E 00	0.1635E 03
0.7975E-01	0.9819E-02	0.8036E-01	0.7019E 01
0.4492E-01	-0.3724E-01	0.5835E-01	0.3203E 03
0.7368E-01	0.1246E-01	0.7473E-01	0.9598E 01
-0.2116E 00	-0.2778E-01	0.2135E 00	0.1875E 03
0.1436E 00	0.1866E-01	0.1448E 00	0.7404E 01
0.7368E-01	-0.1246E-01	0.7473E-01	0.3504E 03
-0.2116E 00	0.2778E-01	0.2135E 00	0.1725E 03
0.1436E 00	-0.1866E-01	0.1448E 00	0.3526E 03
0.3337E-02	0.1985E-25	0.3337E-02	0.3409E-21
0.1230E-01	0.3464E-25	0.1230E-01	0.1614E-21
-0.6611E-02	-0.4991E-25	0.6611E-02	0.1800E 03

STABILITY ANALYSIS OF A TETHERED BALLOON IN THE LATERAL PLANE 8J 60K CU. FT. NOMINAL

ALTITUDE PROFILE			0.0	5000.0	10000.0	20000.0	25000.0	0.0	0.0	0.0	
WIND VELOCITY PROFILE			15.9	52.3	67.5	91.3	99.9	0.0	0.0	0.0	
RJM	RKM	CNPSB	CNPSDB	CNPHDB	CNVB	LS	MPL	IZB	TETH	XIO(1)	RANGE
RJA	RKA	CLPSB	CLPSDB	CLPHDB	CLVB	WB	SB	IYB	MAS	XIO(2)	ALTITUDE
RJG	RKG	CYPSB	CYPSDB	CYPHDB	CYVB	WTC	DB	IYZB	THEO	XIO(3)	DYPRB
	RKB	DC	CDC								
20.5000	-42.6000	-0.1050	-2.3100	-0.1220	0.1050	3942.0	31.1	119000.0	12639.0	41.650	-7547.8
6.7000	-46.0000	-0.3510	-0.3470	-0.3270	0.3510	2157.0	1533.0	26000.0	115.0	51.530	9969.4
23.7000	-42.3000	2.0800	1.7900	0.1420	-2.0800	708.0	39.1	12500.0	8.500	65.470	3.992
	-45.4000	0.0342	1.1000								

ALPHA(I,J)

0.24E 06	-0.20E 06	-0.20E 08	-0.20E 08	-0.20E 08
-0.20E 06	0.36E 06	0.33E 08	0.33E 08	0.33E 08
-0.20E 08	0.33E 08	0.41E 10	0.40E 10	0.38E 10
-0.20E 08	0.33E 08	0.40E 10	0.40E 10	0.38E 10
-0.20E 08	0.33E 08	0.38E 10	0.38E 10	0.38E 10

BETA(I,J)

0.49E 06	-0.99E 05	-0.12E 08	-0.12E 08	-0.12E 08
0.39E 04	0.44E 05	0.15E 06	0.15E 06	0.15E 06
-0.50E 08	0.32E 08	0.37E 10	0.36E 10	0.34E 10
-0.50E 08	0.32E 08	0.36E 10	0.36E 10	0.34E 10
-0.50E 08	0.32E 08	0.34E 10	0.34E 10	0.34E 10

GAMMA(I,J)

0.20E 06	0.0	0.0	0.0	0.0
-0.25E 04	0.87E 05	0.0	0.0	0.0
-0.54E 08	0.0	0.55E 06	0.0	0.0
-0.54E 08	0.0	0.0	0.14E 07	0.0
-0.54E 08	0.0	0.0	0.0	0.26E 07

COEFFICIENTS OF CHARACTERISTIC EQUATION IN ASCENDING ORDER

0.340D 29 0.267D 32 0.116D 34 0.352D 35 0.344D 36 0.132D 37 0.259D 37 0.328D 37 0.286D 37 0.143D 37 0.262D 36

ALL ROOTS HAVE BEEN ACCURATELY DETERMINED

ROOTS OF CHARACTERISTIC EQUATION REAL	IMAGINARY	NATURAL FREQUENCY	STABILITY PARAMETERS DAMPED FREQUENCY	DAMPING RATIO	TIME TO HALF OR DOUBLE AMPLITUDE
-0.1633D-01	0.2751D-01	0.3200D-01	0.2751D-01	0.5105D 00	0.4244D 02
-0.1633D-01	-0.2751D-01	0.3200D-01	0.2751D-01	0.5105D 00	0.4244D 02
-0.1348D-02	-0.1292D-26	0.1348D-02	0.1292D-26	0.1000D 01	0.5143D 03
-0.3630D 00	-0.5369D-14	0.3630D 00	0.5369D-14	0.1000D 01	0.1910D 01
-0.1577D 00	0.1799D-16	0.1577D 00	0.1799D-16	0.1000D 01	0.4395D 01
-0.8151D 00	-0.1246D-15	0.8151D 00	0.1246D-15	0.1000D 01	0.8504D 00
-0.1777D 00	0.8387D 00	0.8573D 00	0.8387D 00	0.2073D 00	0.3900D 01
-0.1777D 00	-0.8387D 00	0.8573D 00	0.8387D 00	0.2073D 00	0.3900D 01
-0.1010D 01	0.1625D-23	0.1010D 01	0.1625D-23	0.1000D 01	0.6860D 00
-0.2716D 01	0.4598D-22	0.2716D 01	0.4598D-22	0.1000D 01	0.2552D 00

EIGENVECTOR

REAL	IMAGINARY	MAGNITUDE	DIRECTION ANGLE
0.9974E-01	-0.1678E 00	0.1952E 00	0.3007E 03
0.3972E-01	0.3393E 00	0.3416E 00	0.8332E 02
-0.3197E 00	-0.2863E 00	0.4292E 00	0.2219E 03
0.3753E-01	-0.4817E 00	0.4832E 00	0.2745E 03
0.9974E-01	0.1678E 00	0.1952E 00	0.5927E 02
0.3972E-01	-0.3393E 00	0.3416E 00	0.2767E 03
-0.3197E 00	0.2863E 00	0.4292E 00	0.1381E 03
0.3753E-01	0.4817E 00	0.4832E 00	0.8555E 02
0.8215E-02	0.9448E-26	0.8215E-02	0.6590E-22
-0.8861E 01	0.7635E-23	0.8861E 01	0.1800E 03
-0.2509E 01	0.2997E-23	0.2509E 01	0.1800E 03
-0.4865E 00	0.1675E-23	0.4865E 00	0.1800E 03
0.1576E 01	0.4253E-12	0.1576E 01	0.1546E-10
0.2016E 01	-0.4581E-12	0.2016E 01	0.3600E 03
-0.3593E 01	0.8323E-12	0.3593E 01	0.1800E 03
0.1541E 01	-0.3852E-12	0.1541E 01	0.3600E 03
0.9267E 00	0.1781E-16	0.9267E 00	0.1101E-14
0.1220E 01	-0.7378E-15	0.1220E 01	0.3600E 03
-0.2271E 01	0.1406E-14	0.2271E 01	0.1800E 03
0.9567E 00	-0.6916E-15	0.9567E 00	0.3600E 03
-0.2313E 02	0.5125E-13	0.2313E 02	0.1800E 03
-0.3451E 00	0.7476E-15	0.3451E 00	0.1800E 03
0.1470E 00	-0.5303E-15	0.1470E 00	0.3600E 03
0.5130E 00	-0.9241E-15	0.5130E 00	0.3600E 03
-0.2840E 01	-0.8668E 01	0.9121E 01	0.2519E 03
0.1526E-01	0.4866E-02	0.1602E-01	0.1768E 02
-0.4131E-01	-0.2918E-01	0.5058E-01	0.2152E 03
0.5290E-01	0.8767E-01	0.1024E 00	0.5889E 02
-0.2840E 01	0.8668E 01	0.9121E 01	0.1081E 03
0.1526E-01	-0.4866E-02	0.1602E-01	0.3423E 03
-0.4131E-01	0.2918E-01	0.5058E-01	0.1448E 03
0.5290E-01	-0.8767E-01	0.1024E 00	0.3011E 03
0.6074E 02	-0.1483E-18	0.6074E 02	0.3600E 03
-0.7338E 01	0.1661E-19	0.7338E 01	0.1800E 03
-0.6088E 01	0.1388E-19	0.6088E 01	0.1800E 03
0.1269E 02	-0.2868E-19	0.1269E 02	0.3600E 03
0.9884E 00	-0.5543E-23	0.9884E 00	0.3600E 03
-0.6863E-04	0.4583E-26	0.6863E-04	0.1800E 03
0.5973E-03	-0.2846E-25	0.5973E-03	0.3600E 03
-0.5087E-02	0.8084E-25	0.5087E-02	0.1800E 03

```
      REAL ML,MV,MAL,MAV,M,L,L2,LS,IXB,MPL
      DIMENSION MAT(4,4),ISW(8),XIODE(3),AALP(4,4),BBET(4,4),GGAM(4,4)
      DIMENSION VECTR(3),VECTI(3),VECTM(3),VECTD(3)
      DOUBLE PRECISION GGG(6,6),HHH(6)
      DOUBLE PRECISION A(4,4,9),COE(9),COEF(9),ROOTR(8),ROOTI(8)
     1,FREQN(8),FREQD(8),DAMRAT(8),THAMP(8)
      COMMON THEO,XIO(3)
      COMMON ALP,CDB,CLB,CMB,VW,STHEO,CTHEO,RKG,RJG,
     1OB,L,LS,WB,DYPRB,SB,MPL,CDC,CDAB,CLAB,CMAB,VBR,RHOB
      COMMON C(3),CXMX(3,3),AALPA(8),CCDB(8),CCLB(8),CCMB(8),
     1SC(3),RHOC(3),VWC(3),SX(3),CX(3),DYPRH(4),RHOCH(4),ZC(3),XDEG(4),
     2ZCH(4),VWH(4),AALT(8),VVW(8),M,AALPD(8),SXMX(3,3),STPX(3),
     3CTPX(3),SX2(3),S2X(3),STPX2(3),CTPX2(3),CX2(3),CX3(3),SX3(3)
      DIMENSION CC(4,5),LOOK(4,4),L1(7),XX(4),COM1(10),CCLBP(8)
      EQUIVALENCE(L1(1),N),(L1(2),NF),(L1(3),MAX),(L1(4),KK),(L1(5),J),
     1(L1(6),IER),(L1(7),MA),(XX(1),THEO)
    1 FORMAT(8F10.0)
    2 FORMAT(10A4)
   37 FORMAT(15X,'ALPHA(I,J)',35X,'BETA(I,J)',35X,'GAMMA(I,J)'/)
   38 FORMAT(/8X,'ROOTS OF CHARACTERISTIC EQUATION',25X,'STABILITY PARAM
     1ETERS',23X,'TIME TO HALF OR'/12X,'REAL',10X,'IMAGINARY',10X,'NATUR
     2AL FREQUENCY',5X,'DAMPED FREQUENCY',5X,'DAMPING RATIO',7X,
     3'DOUBLE AMPLITUDE'/)
   42 FORMAT(/10X,'COEFFICIENTS OF CHARACTERISTIC EQUATION IN ASCENDING
     1ORDER')
   43 FORMAT(5X,'ALL ROOTS HAVE BEEN ACCURATELY DETERMINED')
   44 FORMAT(//5X,'DEGREE OF POLYNOMIAL IS LESS THAN EIGHT'//)
   45 FORMAT(//5X,'DEGREE OF POLYNOMIAL IS LESS THAN ONE'//)
   46 FORMAT(//5X,'ROOT NOT ACCURATELY FOUND',5X,8I4//)
   47 FORMAT(10X,8(D11.4,3X,D11.4,12X,D11.4,11X,D11.4,9X,D11.4,10X,
     1D11.4/10X))
   48 FORMAT(/5X,9(2X,E10.3)//)
   49 FORMAT(1X,4(4(E9.2,1X),4X,4(E9.2,1X),4X,4(E9.2,1X)/1X))
   51 FORMAT(10X,4(F10.5,2X))
   52 FORMAT(2X,'FINAL SOLUTION'/10X,4(F10.5,2X)/)
   53 FORMAT(//10X,'NO SOLUTION')
   54 FORMAT(//10X,'SINGULAR MATRIX')
   55 FORMAT(//10X,'INCONSISTENT VALUE OF N',5X,'N=',I4)
  135 FORMAT(5X,'ANGLE-OF-ATTACK(DEG)',6X,8F10.4/5X,'MOMENT COEFFICIENT'
     1,8X,8F10.4/5X,'LIFT COEFFICIENT',10X,8F10.4/5X,'DRAG COEFFICIENT'
     2,10X,8F10.4/)
  136 FORMAT(13X,'THETA',7X,'XIO(1)',6X,'XIO(2)',6X,'XIO(3)'/)
  137 FORMAT(5X,5(F9.4,1X),F8.0,2X,F8.2,2X,2(F8.0,2X)/5X,5(F9.4,1X),
     12(F8.1,2X),F8.4,2X,F8.2/5X,5(F9.4,1X),F8.1,2X,3(F8.3,2X)/5X,
     22(F8.3,2X),2(F8.1,2X),E10.3/)
  138 FORMAT(8X,'RJM',7X,'RKM',7X,'CMB',7X,'CMAB',6X,'CMTDB',5X,'LS',
     18X,'MPL',7X,'TETH',6X,'IXB'/8X,'RJA',7X,'RKA',7X,'CLB',7X,'CLAB'
     2,6X,'CLTDB',5X,'WB',8X,'SB',8X,'DC',8X,'MAL'/8X,'RJG',7X,'RKG',
     37X,'CDB',7X,'CDAB',6X,'CDTDB',5X,'WTC',7X,'DB',8X,'CDC',7X,
     4'MAV'/8X,'RJB',7X,'RKB',7X,'RANGE',5X,'ALTITUDE',2X,'DYPRB'/)
  139 FORMAT(5X,'ALTITUDE PROFILE',10X,8F10.1/5X,'WIND VELOCITY PROFILE'
     1,5X,8F10.1/)
```

```
  140 FORMAT(1H1,20X,'STABILITY ANALYSIS OF A TETHERED BALLOON IN THE LO
     1NGITUDINAL PLANE',5X,10A4//)
  250 FORMAT(3(/10X,4(E11.4,4X)))
  251 FORMAT(1H1//30X,'MODE SHAPES'//17X,'EIGENVECTORS'/12X,'REAL',
     19X,'IMAGINARY',6X,'MAGNITUDE'6X,'DIRECTION ANGLE'/)
      CALL MASK(0)
      G=32.17
      READ(1,1) AALT,VVW
      READ(1,1) AALPD,CCMB,CCLB,CCDB
      READ(1,1) CMC,CDC1,CDC2,CLC
      DO 12 I=1,8
   12 AALPA(I)=AALPD(I)/57.2958
      DO 13 I=1,8
      CCMB(I)=CCMB(I)+CMC*AALPA(I)
      CCLBP(I)=CCLB(I)
      CCLB(I)=CCLB(I)+CLC*AALPA(I)
   13 CCDB(I)=CCDB(I)+CDC1*CCLBP(I)**2+CDC2*CCLB(I)**2
   99 READ(1,1) WB,LS,MPL,WTC,IXB,MAL,MAV
      IF(WB.EQ.1.) CALL EXIT
      READ(1,1) SB,DB,CDC,DC,TETH,CMTDB,CLTDB
      READ(1,2) COM1
      READ(1,1) RJM,RKM,RJA,RKA,RJG,RKG,RJB,RKB
      READ(1,1) THEC,(XIO(I),I=1,3)
      THEO=THEO/57.2958
      DO 6 I=1,3
    6 XIO(I)=XIO(I)/57.2958
      L=TETH/3.
      DO 11 I=1,3
   11 SC(I)=L*DC
      M=WTC/(3.*G)
      WRITE(3,140) COM1
      WRITE(3,139) AALT,VVW
      WRITE(3,135) AALPD,CCMB,CCLB,CCDB
      WRITE(3,136)
      DO 4 I=1,4
    4 XDEG(I)=XX(I)*57.2958
      WRITE(3,51)(XDEG(I),I=1,4)
    5 MAX=30
      NF=5
      N=4
      MA=N
      KK=1
      GO TO 50
   10 CALL EQUIL
      F=LS*(RKB*STHEC-RJB*CTHEO)-WB*(RKG*STHEO-RJG*CTHEO)+DYPRB*SB*(
     1CLB*(RKA*STHEO-RJA*CTHEC)-CDB*(RKA*CTHEO+RJA*STHEO)+DB*CMB)
      GO TO 41
   20 CALL EQUIL
      F=L*(CX(1)*(LS-WB-G*(MPL+2.5*M)
     1+DYPRB*SB*CLB)-SX(1)*DYPRB*SB*CDB-.5*(C(1)*RHOC(1)*SC(1)
     2*CDC*(VWC(1)*SX(1))**2+RHOC(2)*SC(2)*CDC*(VWC(2)*SX(2))**2*COS(
     3XIO(2)-XIO(1))+RHOC(3)*SC(3)*CDC*(VWC(3)*SX(3))**2*COS(XIO(3)-
```

```
      4XIO(1))))
       GO TO 41
   30 CALL EQUIL
       F=L*(CX(2)*(LS-WB-G*(MPL+1.5*M)+DYPRB*SB*
      1CLB)-SX(2)*DYPRB*SB*CDB-.5*(C(2)*RHOC(2)*SC(2)*CDC*
      2(VWC(2)*SX(2))**2+RHOC(3)*SC(3)*CDC*(VWC(3)*SX(3))**2*COS(
      3XIO(3)-XIO(2))))
       GO TO 41
   40 CALL EQUIL
       F=L*(CX(3)*(LS-WB-G*(MPL+.5*M)+DYPRB*SB*CLB)
      1-SX(3)*DYPRB*SB*CDB-.5*C(3)*RHOC(3)*SC(3)*CDC*(VWC(3)*SX(3))**2)
   41 KK=2
   50 CALL SYSTEM(L1,XX,CC,LOOK,F)
       GO TO (10,20,30,40,60,70),J
   60 DO 61 I=1,4
   61 XDEG(I)=XX(I)*57.2958
       WRITE(3,51)(XDEG(I),I=1,4)
       KK=3
       GO TO 50
   70 IF(IER-1) 80,100,110
   80 THEODE=THEO*57.2958
       DO 81 I=1,3
   81 XIODE(I)=XIO(I)*57.2958
       WRITE(3,52) THEODE,XIODE
       CALL EQUIL
       YB=-L*(CX(1)+CX(2)+CX(3))+RKG*STHEO-RJG*CTHEO
       ZB=L*(SX(1)+SX(2)+SX(3))-RKG*CTHEO-RJG*STHEO
C      IF WINCH IS AT 5000. FT.
C      ZB=L*(SX(1)+SX(2)+SX(3))-RKG*CTHEO-RJG*STHEO+5000.
       WRITE(3,138)
       CDTDB=.9*CLB*CLTDB
       WRITE(3,137) RJM,RKM,CMB,CMAB,CMTDB,LS,MPL,TETH,IXB,RJA,RKA,
      1CLB,CLAB,CLTDB,WB,SB,DC,MAL,RJG,RKG,CDB,CDAB,CDTDB,WTC,DB,CDC,
      2MAV,RJB,RKB,YB,ZB,DYPRB
       SXMX(2,1)=SIN(XIO(2)-XIO(1))
       SXMX(3,1)=SIN(XIO(3)-XIO(1))
       SXMX(3,2)=SIN(XIO(3)-XIO(2))
       CXMX(2,1)=COS(XIO(2)-XIO(1))
       CXMX(3,1)=COS(XIO(3)-XIO(1))
       CXMX(3,2)=COS(XIO(3)-XIO(2))
       DO 900 I=1,3
       STPX(I)=SIN(THEO+XIO(I))
       CTPX(I)=COS(THEO+XIO(I))
       SX2(I)=SX(I)**2
       CX2(I)=CX(I)**2
       SX3(I)=SX(I)*SX2(I)
       CX3(I)=CX(I)*CX2(I)
       S2X(I)=2.*SX(I)*CX(I)
       STPX2(I)=STPX(I)**2
  900 CTPX2(I)=CTPX(I)**2
       QSB=DYPRB*SB
       QSBL=QSB*L
```

```
      QSDB=QSB*DB
      L2=L**2
      ML=MAL+WB/32.17
      MV=MAV+WB/32.17
      RG=RKG*CTHEO+RJG*STHEO
      B11=RKA*(CLB*STHEO-CDB*CTHEO)-RJA*(CDB*STHEO+CLB*CTHEO)+DB*CMB
      B21=(CDB*SX(1)+CLB*CX(1))
      B22=(CDB*SX(2)+CLB*CX(2))
      B23=(CDB*SX(3)+CLB*CX(3))
      B31=RHOC(1)*SC(1)*VWC(1)*CDC
      B32=RHOC(2)*SC(2)*VWC(2)*CDC
      B33=RHOC(3)*SC(3)*VWC(3)*CDC
      RVS=RHOB*VW*SB
      RVSL=RVS*L
      RVSL2=RVSL*L
      RVSL21=RVSL2*SX(1)
      RVSL22=RVSL2*SX(2)
      RVSL23=RVSL2*SX(3)
      RVSLRG=RVSL*RG
      FAC1=QSDB/VW
      FAC2=FAC1*L
      AALP(1,1)=IXB+ML*RKM**2+MV*RJM**2
      AALP(1,2)=L*(ML*RKM*STPX(1)-MV*RJM*CTPX(1))
      AALP(1,3)=L*(ML*RKM*STPX(2)-MV*RJM*CTPX(2))
      AALP(1,4)=L*(ML*RKM*STPX(3)-MV*RJM*CTPX(3))
      AALP(2,1)=AALP(1,2)
      AALP(2,2)=L2*(7.*M/3.+MPL+MV*CTPX2(1)+ML*STPX2(1))
      AALP(2,3)=L2*((3.*M/2.+MPL)*CXMX(2,1)+MV*CTPX(1)*CTPX(2)
     1+ML*STPX(1)*STPX(2))
      AALP(2,4)=L2*((M/2.+MPL)*CXMX(3,1)+MV*CTPX(1)*CTPX(3)
     1+ML*STPX(1)*STPX(3))
      AALP(3,1)=AALP(1,3)
      AALP(3,2)=AALP(2,3)
      AALP(3,3)=L2*(4.*M/3.+MPL+MV*CTPX2(2)+ML*STPX2(2))
      AALP(3,4)=L2*((M/2.+MPL)*CXMX(3,2)+MV*CTPX(2)*CTPX(3)
     1+ML*STPX(2)*STPX(3))
      AALP(4,1)=AALP(1,4)
      AALP(4,2)=AALP(2,4)
      AALP(4,3)=AALP(3,4)
      AALP(4,4)=L2*(M/3.+MPL+MV*CTPX2(3)+ML*STPX2(3))
      BBET(1,1)=FAC1*(RKA*(CDTDB*CTHEO-CLTDB*STHEO)+RJA*(CDTDB*STHEO
     1+CLTDB*CTHEO)-DB*CMTDB)-RVS*RG*B11
      BBET(1,2)=-RVSL*SX(1)*B11
      BBET(1,3)=-RVSL*SX(2)*B11
      BBET(1,4)=-RVSL*SX(3)*B11
      BBET(2,1)=FAC2*(CDTDB*SX(1)-CLTDB*CX(1))+RVSLRG*B21
      BBET(2,2)=RVSL21*B21+L2*(C(1)**2*B31*(SX3(1)+.5*CX3(1))
     1+B32*(SX2(2)*SX(1)+.5*CX2(2)*CX(1))*CXMX(2,1)
     2+B33*(SX2(3)*SX(1)+.5*CX2(3)*CX(1))*CXMX(3,1))
      BBET(2,3)=RVSL22*B21+L2*(C(2)*B32*(SX3(2)+.5*CX3(2))*CXMX(2,1)
     1+B33*(SX2(3)*SX(2)+.5*CX2(3)*CX(2))*CXMX(3,1))
      BBET(2,4)=RVSL23*B21+L2*C(3)*B33*(SX3(3)+.5*CX3(3))*CXMX(3,1)
```

```
      BBET(3,1)=FAC2*(CDTDB*SX(2)-CLTDB*CX(2))+RVSLRG*B22
      BBET(3,2)=RVSL21*B22+L2*(C(2)*B32*(SX2(2)+SX(1)+.5*CX2(2)*CX(1))
     1+B33*(SX2(3)*SX(1)+.5*CX2(3)*CX(1))*CXMX(3,2))
      BBET(3,3)=RVSL22*B22+L2*(C(2)**2*B32*(SX3(2)+.5*CX3(2))
     1+B33*(SX2(3)*SX(2)+.5*CX2(3)*CX(2))*CXMX(3,2))
      BBET(3,4)=RVSL23*B22+L2*C(3)*B33*(SX3(3)+.5*CX3(3))*CXMX(3,2)
      BBET(4,1)=FAC2*(CDTDB*SX(3)-CLTDB*CX(3))+RVSLRG*B23
      BBET(4,2)=RVSL21*B23+L2*C(3)*B33*(SX2(3)*SX(1)+.5*CX2(3)*CX(1))
      BBET(4,3)=RVSL22*B23+L2*C(3)*B33*(SX2(3)*SX(2)+.5*CX2(3)*CX(2))
      BBET(4,4)=RVSL23*B23+L2*C(3)**2*B33*(SX3(3)+.5*CX3(3))
      GGAM(1,1)=-LS*(RKB*CTHEO+RJB*STHEO)+WB*(RKG*CTHEO+RJG*STHEO)
     1-QSB*(CLB*(RKA*CTHEO+RJA*STHEO)-CDB*(-RKA*STHEO+RJA*CTHEO)
     2+CLAB*(RKA*STHEO-RJA*CTHEO)-CDAB*(RKA*CTHEO+RJA*STHEO)+DB*CMAB)
      GGAM(1,2)=0.
      GGAM(1,3)=0.
      GGAM(1,4)=0.
      GGAM(2,1)=QSBL*(CDAB*SX(1)-CLAB*CX(1))
      GGAM(2,2)=L*SX(1)*(LS-WB-G*(MPL+5.*M/2.)
     1+QSB*CLB)+QSBL*CX(1)*CDB+.5*L*(C(1)*B31*VWC(1)*S2X(1)
     2+B32*VWC(2)*SX2(2)*SXMX(2,1)+B33*VWC(3)*SX2(3)*SXMX(3,1))
      GGAM(2,3)=.5*L*B32*VWC(2)*(S2X(2)*CXMX(2,1)-SX2(2)*SXMX(2,1))
      GGAM(2,4)=.5*L*B33*VWC(3)*(S2X(3)*CXMX(3,1)-SX2(3)*SXMX(3,1))
      GGAM(3,1)=QSBL*(CDAB*SX(2)-CLAB*CX(2))
      GGAM(3,2)=0.
      GGAM(3,3)=L*SX(2)*(LS-WB-G*(MPL+3.*M/2.)
     1+QSB*CLB)+QSBL*CX(2)*CDB+.5*L*(C(2)*B32*VWC(2)*S2X(2)
     2+B33*VWC(3)*SX2(3)*SXMX(3,2))
      GGAM(3,4)=.5*L*B33*VWC(3)*(S2X(3)*CXMX(3,2)-SX2(3)*SXMX(3,2))
      GGAM(4,1)=QSBL*(CDAB*SX(3)-CLAB*CX(3))
      GGAM(4,2)=0.
      GGAM(4,3)=0.
      GGAM(4,4)=L*SX(3)*(LS-WB-G*(MPL+M/2.)+QSB*CLB)
     1+QSBL*CX(3)*CDB+.5*L*C(3)*B33*VWC(3)*S2X(3)
      WRITE(3,37)
      WRITE(3,49)(((AALP(I,J),J=1,4),(BBET(I,J),J=1,4),(GGAM(I,J),J=1,4)
     1),I=1,4)
      K=1
      DO 101 J=1,4
      DO 101 I=1,4
  101 A(I,J,K)=GGAM(I,J)
      K=2
      DO 102 J=1,4
      DO 102 I=1,4
  102 A(I,J,K)=BBET(I,J)
      K=3
      DO 103 J=1,4
      DO 103 I=1,4
  103 A(I,J,K)=AALP(I,J)
      DO 104 K=4,9
      DO 104 J=1,4
      DO 104 I=1,4
  104 A(I,J,K)=0.
```

```
      EPS=1.E-09
      N=2
      NCOL=4
      CALL POLMAT(A,NCOL,N,EPS,COE,NP1,MAT)
      WRITE(3,42)
      WRITE(3,48)(COE(I),I=1,NP1)
      DO 106 I=1,9
  106 COEF(I)=COE(10-I)
      N1=8
      CALL MULLER(COEF,N1,ROOTR,ROOTI,ISW,IERR)
      IF(IERR.EQ.0) WRITE(3,43)
      IF(IERR.EQ.1) WRITE(3,46)(ISW(I),I=1,8)
      IF(IERR.EQ.2) WRITE(3,45)
      IF(IERR.EQ.3) WRITE(3,44)
      WRITE(3,38)
      DO 105 I=1,8
      FREQN(I)=DSQRT(ROOTR(I)**2+ROOTI(I)**2)
      FREQD(I)=DABS(ROOTI(I))
      DAMRAT(I)=-ROOTR(I)/FREQN(I)
  105 THAMP(I)=.69315/(DAMRAT(I)*FREQN(I))
      WRITE(3,47)((ROOTR(I),ROOTI(I),FREQN(I),FREQD(I),DAMRAT(I),
     1THAMP(I)),I=1,8)
      WRITE(3,251)
      DO 200 K=1,8
      DO 201 I=1,3
      HHH(I)=-(AALP(I+1,1)*(ROOTR(K)**2-ROOTI(K)**2)+BBET(I+1,1)*ROOTR(K
     1)+GGAM(I+1,1))
      DO 201 J=1,3
  201 GGG(I,J)=AALP(I+1,J+1)*(ROOTR(K)**2-ROOTI(K)**2)+BBET(I+1,J+1)*
     1ROOTR(K)+GGAM(I+1,J+1)
      DO 202 I=4,6
      HHH(I)=-(AALP(I-2,1)*2.*ROOTR(K)*ROOTI(K)+BBET(I-2,1)*ROOTI(K))
      DO 202 J=1,3
  202 GGG(I,J)=AALP(I-2,J+1)*2.*ROOTR(K)*ROOTI(K)+BBET(I-2,J+1)*ROOTI(K)
      DO 203 I=1,3
      DO 203 J=4,6
  203 GGG(I,J)=-GGG(I+3,J-3)
      DO 204 I=4,6
      DO 204 J=4,6
  204 GGG(I,J)=GGG(I-3,J-3)
      N=6
      L=6
      EPS=.10-11
      CALL CROUT(GGG,HHH,N,L,EPS,IERSW)
      DO 205 I=1,3
      VECTR(I)=HHH(I)
      VECTI(I)=HHH(I+3)
      VECTM(I)=SQRT(VECTR(I)**2+VECTI(I)**2)
  205 VECTD(I)=ARGD(VECTI(I),VECTR(I))
  200 WRITE(3,250)((VECTR(I),VECTI(I),VECTM(I),VECTD(I)),I=1,3)
      GO TO 99
  100 WRITE(3,53)
```

```
      GO TO 99
110   IF(IER-2)120,120,130
120   WRITE(3,54)
      CALL EXIT
130   WRITE(3,55) N
      CALL EXIT
      END
```

```
      SUBROUTINE EQUIL
      REAL ML,MV,MAL,MAV,M,L,L2,LS,LXB,MPL
      COMMON THEO,XIO(3)
      COMMON ALP,CDB,CLB,CMB,VW,STHEO,CTHEO,RKG,RJG,
     1DB,L,LS,WB,DYPRB,SB,MPL,CDG,CDAB,CLAB,CMAB,VBR,RHOB
      COMMON C(3),CXMX(3,3),AALPA(8),CCDB(8),CCLB(8),CCMB(8),
     1SC(3),RHOC(3),VWC(3),SX(3),CX(3),DYPRH(4),RHOCH(4),ZC(3),XDEG(4),
     2ZCH(4),VWH(4),AALT(8),VVW(8),M,AALPD(8),SXMX(3,3),STPX(3),
     3CTPX(3),SX2(3),S2X(3),STPX2(3),CTPX2(3),CX2(3),CX3(3),SX3(3)
      ZCH(1)=0.
C     IF WINCH IS AT 5000. FT.
C     ZCH(1)=5000.
      ALP=THEO
      STHEO=SIN(THEO)
      CTHEO=COS(THEO)
      I=2
  300 IF(ALP.LT.AALPA(I)) GO TO 301
      I=I+1
      GO TO 300
  301 ALPSL=(ALP-AALPA(I-1))/(AALPA(I)-AALPA(I-1))
      CDB=CCDB(I-1)+(CCDB(I)-CCDB(I-1))*ALPSL
      CLB=CCLB(I-1)+(CCLB(I)-CCLB(I-1))*ALPSL
      CMB=CCMB(I-1)+(CCMB(I)-CCMB(I-1))*ALPSL
      CDAB=(CCDB(I)-CCDB(I-1))/(AALPA(I)-AALPA(I-1))
      CLAB=(CCLB(I)-CCLB(I-1))/(AALPA(I)-AALPA(I-1))
      CMAB=(CCMB(I)-CCMB(I-1))/(AALPA(I)-AALPA(I-1))
      DO 1 I=1,3
      SX(I)=SIN(XIO(I))
    1 CX(I)=COS(XIO(I))
      DO 2 I=2,4
    2 ZCH(I)=ZCH(I-1)+L*SX(I-1)
      DO 3 I=1,4
      CALL DENS(ZCH(I),PR,RHOCH(I),VS)
      J=2
  200 IF(ZCH(I).LT.AALT(J)) GO TO 201
      J=J+1
      GO TO 200
  201 ALTSL=(ZCH(I)-AALT(J-1))/(AALT(J)-AALT(J-1))
      VWH(I)=VVW(J-1)+(VVW(J)-VVW(J-1))*ALTSL
    3 DYPRH(I)=.5*RHOCH(I)*VWH(I)**2
      DO 4 I=1,3
    4 C(I)=(DYPRH(I)+2.*DYPRH(I+1))/(3.*(DYPRH(I)+DYPRH(I+1)))
      ZB=ZCH(4)-RKG*CTHEO-RJG*STHEO
      CALL DENS(ZB,PR,RHOB,VS)
      I=2
  210 IF(ZB.LT.AALT(I)) GO TO 211
      I=I+1
      GO TO 210
  211 ALTSL=(ZB-AALT(I-1))/(AALT(I)-AALT(I-1))
      VW=VVW(I-1)+(VVW(I)-VVW(I-1))*ALTSL
      VBR=VW
      DYPRB=.5*RHOB*VW**2
```

```
      DO 5 I=1,3
      ZC(1)=L*(C(1)*SX(1))
      ZC(2)=L*(SX(1)+C(2)*SX(2))
      ZC(3)=L*(SX(1)+SX(2)+C(3)*SX(3))
C     IF WINCH IS AT 5000. FT.
C     ZC(1)=L*(C(1)*SX(1))+5000.
C     ZC(2)=L*(SX(1)+C(2)*SX(2))+5000.
C     ZC(3)=L*(SX(1)+SX(2)+C(3)*SX(3))+5000.
      CALL DENS(ZC(I),PR,RHOC(I),VS)
      J=2
  220 IF(ZC(I).LT.AALT(J)) GO TO 221
      J=J+1
      GO TO 220
  221 ALTSL=(ZC(I)-AALT(J-1))/(AALT(J)-AALT(J-1))
    5 VWC(I)=VVW(J-1)+(VVW(J)-VVW(J-1))*ALTSL
      RETURN
      END
```

```
      SUBROUTINE CROUT( A, C, N, LD, EPS, IERSW)
C     LINEAR ALGEBRAIC EQUATIONS - CROUT                                LS220  2
C     DIMENSION  A(6,6) , C(6)
      DOUBLE PRECISION A(6,6),C(6),SUM,EPS,ZERO
      ZERO = 0.0D0
C     DOUBLE PRECISION A,C,SUM,EPS,ZERO                                 LS220  4
C     ZERO = 0.0D0                                                      LS220  5
C     ZERO = 0.                                                         LS220  6
      IERSW=0                                                           LS220  7
      IF(DABS(A(1,1))  - EPS)90,5,5
C     IF(ABS(A(1,1))  - EPS)90,5,5                                      LS220  9
C     IF(DABS(A(1,1))  - EPS)90,5,5                                     LS220  8
    5 IF(N-1)90,10,15                                                   LS220 10
   10 C(1) = C(1)/A(1,1)                                                LS220 11
      RETURN                                                            LS220 12
   15 DO 20 I=2,N                                                       LS220 13
   20 A(1,I)=A(1,I)/A(1,1)                                              LS220 14
      DO 65 I=2,N                                                       LS220 15
      DO 65 J=2,N                                                       LS220 16
      SUM = ZERO                                                        LS220 17
      IF(J  - I) 30,30,25                                               LS220 18
   25 JIN=I-1                                                           LS220 19
      GO TO 35                                                          LS220 20
   30 JIN =J-1                                                          LS220 21
   35 DO 40 K=1,JIN                                                     LS220 22
   40 SUM =SUM+A(I,K)*A(K,J)                                            LS220 23
      IF (J-I)45,45,55                                                  LS220 24
   45 A(I,J) = A(I,J)-SUM                                               LS220 25
      IF(J-I)65,50,90                                                   LS220 26
C  50 IF(DABS(A(I,I))-EPS)90,65,65                                      LS220 27
   50 IF(DABS(A(I,I))-EPS)90,65,65
C  50 IF(ABS(A(I,I))-EPS)90,65,65                                       LS220 28
C  55 IF(DABS(A(I,I))  - EPS)90,60,60                                   LS220 29
   55 IF(DABS(A(I,I))  - EPS)90,60,60
C  55 IF(ABS(A(I,I))  - EPS)90,60,60                                    LS220 30
   60 A(I,J)=(A(I,J)-SUM)/A(I,I)                                        LS220 31
   65 CONTINUE                                                          LS220 32
      C(1) = C(1) / A(1,1)                                              LS220 33
      DO 75  I=2,N                                                      LS220 34
      SUM = ZERO                                                        LS220 35
      JIN =I-1                                                          LS220 36
      DO 70 K=1,JIN                                                     LS220 37
   70 SUM=SUM+A(I,K)*C(K)                                               LS220 38
      C(I)=(C(I)-SUM)/A(I,I)                                            LS220 39
   75 CONTINUE                                                          LS220 40
      JIN =N-1                                                          LS220 41
      DO 85 M=1,JIN                                                     LS220 42
      SUM = ZERO                                                        LS220 43
      L=JIN-M+1                                                         LS220 44
      LL=L+1                                                            LS220 45
      DO 80 K=LL,N                                                      LS220 46
   80 SUM = SUM +A(L,K)*C(K)                                            LS220 47
```

```
 85 C(L) = C(L) -SUM                                              LS220 48
    RETURN                                                        LS220 49
 90 IERSW=1                                                       LS220 50
    RETURN                                                        LS220 51
    END                                                           LS220 52
```

```
C      SUBROUTINE SYSTEM WILL SOLVE A SYSTEM OF SIMULTANEOUS NONLINEAR
C       EQUATIONS
C
C      USER MUST DIMENSION TWO WORK ARRAY C(N,N+1) AND LOOK(N,N)
C      WHERE N IS THE NUMBER OF EQUATIONS PLUS X(N) AND L(7).
C      X(1) THRU X(N) MUST CONTAIN INITIAL GUESSES AND L MUST BE
C      SET UP ACCORDING TO COMMENTS
C      UPON RETURN L(6) = 0 FOR GOOD RESULTS
C                  L(6) = 1  FOR NON CONVERGENCE AFTER L(3) ITERATIONS
C                  L(6) = 2  FOR SINGULAR MATRIX,TRY NEW INITIAL GUESSES
C                  L(6) = 3  N IS GREATER THAN 30 (ROUTINE MUST BE
C                            RECOMPILED WITH LARGER DIMENSIONS OR N IS
C                            LESS THAN OR EQUAL TO ZERO
C      THE USER MUST CODE HIS PROGRAM AS FOLLOWS
C      HE MAY EQUIVALENCE  L(1) TO N,L(2) TO NF, ETC. FOR EASIER CODING
C      OR SET
C
C5     L(1) = N
C      L(2) = NF
C      L(3) = MAX
C      L(7) = MA
C
C      L(4) = 1
C      GO TO 50
C10    F = SOME EXPRFESSION FOR F1(X1,X2,X3,,,XN)
C      GO TO 40
C20    F = SOME EXPRESSION FOR F2(X1,X2,X3,,,XN)
C      GO TO 40
C30    F = SOME EXPRESSION FOR F3(X1,X2,X3,,,XN)
C      GO TO 40
C      ETC,
C40    L(4) = 2
C50    CALL SYSTEM(L,X,C,LOOK,F)
C      J = L(5)
C      GO TO (10,20,30,,,,60,70),J
C6     WRITE(3,60) (X(I),I=1,N)    (PRINT INTERMEDIATE ANSWERS STORED IN X
C      L(4) = 3
C      GO TO 50
C70    IF(L(6)-1)80,90,100
C80    WRITE(3,60)(X(I),I=1,N)  PRINT FINAL ROOTS
C
C90    UP ITERATION MAX BY 100,PRINT,GO TO 5,OR CALL EXIT
C
C100   TRY NEW GUESSES OR PRINT MESSAGE,ANSWERS,CALL EXIT
C
       SUBROUTINE SYSTEM(L,X,C,LOOK,F)
C
C      L(1) = N  THE NUMBER OF EQUATIONS
C      L(2) = NF THE NUMBER OF SIGNIFICANT FIGURES THE USER DESIRES
C      L(3) = MAX THE MAXIMUM NO OF ITERATIONS
C      L(4) = KK  SET BY USER TO INDICATE WHICH ENTRY
C      L(5) = J  SET BY SYSTEM
```

```
C      L(6) = IER SET BY SYSTEM
C           = 0   FOR NORMAL RETURN
C      L(7) = MA  MAX NUMBER OF ROWS IN C(I,J) = MA IN DIMENSION C(MA,XX)
C      X    = VECTOR CONTAINS INITIAL GUESSES AND SOLUTIONS
C      C    = WORK COEFFICIENT ARRAY DIMENSIONED AT LEAST (N,N+1)
C      LOOK = WORK SUBSCRIPT   ARRAY DIMENSIONED AT LEAST (N,N)
C      F    = THE VALUE F(X1,X2,,,XN) ON KTH EQUATION
C
C
       DIMENSION X(1), ISUB(30),PART(30),C(1),LOOK(1),TEMP(30),L(1)
C
C      FOR A DOUBLE PRECISION VERSION THE USER MUST REMOVE THE C
C      IN COL 1 OF THE DOUBLE PRECISION CARD AND COMPLETE THE LIST
C      BELOW
C
C      DOUBLE PRECISION X,PART,C,TEMP,SAVE,HOLD,REL,F,DMAX,FACTOR,TEST
C      THE USER MUST CHANGE ALL ABS TO DABS IN THE FOLLOWING STATEMENTS
C      155,160,230,255,260,300,410
C      THE USER MUST CHANGE ALL LITERALS IN THE FOLLOWING STATEMENTS
C      FROM  X.EXX TO X.DXX,15,20,90,110,160,210,215,245,320,910
       KK=L(4)
       IF(KK-2)10,45,47
  10   JTEST=1
       N = L(1)
       IF(N-30)12,12,500
  12   IF(N-1) 500,13,13
  13   NF = L(2)
       MAX = L(3)
       MA = L(7)
  15   REL = 1.E0
       DO 20 I=1,NF
  20   REL = REL*.1E0
       M = 1
       GO TO 47
  30   L(5) = K
  40   RETURN
C      END OF INITIALIZATION
  45   IF(ISW)150,90,150
  47   DO 48 I=1,N
       IJ = (I-1)*MA+1
  48   LOOK(IJ) = I
       K = 1
       GO TO 80
  60   KMIN = K-1
       JJ = 1
       GO TO 900
  70   CONTINUE
C
C      SET UP PARTIAL DERIVATIVES OF THE KTH FUNCTION.
C
  80   ISW = 0
       GO TO 30
```

```
 90   FACTOR = 1.E-3
      SAVE = F
100   ITALLY = 0
105   I = K
108   JK = (I-1)*MA + K
      ITEMP=LOOK(JK)
      HOLD = X(ITEMP)
      H = FACTOR*HOLD
      IF(H)120,110,120
110   H = 1.E-3
120   X(ITEMP) = HOLD+H
      IF(K-1)140,140,130
130   JJ = 2
      GO TO 900
140   ISW = 1
      GO TO 30
150   PART(ITEMP) = (F-SAVE)/H
      X(ITEMP) = HOLD
      HOLD = PART(ITEMP)
155   IF( ABS(HOLD))160,170,160
160   IF( ABS(SAVE/HOLD)-1.E20)180,180,170
170   ITALLY = ITALLY + 1
180   CONTINUE
      IF(I-N)195,200,200
195   I = I+1
      GO TO 108
200   IF(ITALLY-N+K)220,220,210
210   FACTOR = FACTOR*10.E0
215   IF(FACTOR - .15E0)100,100,490
220   IF(K-N)250,230,230
230   IF( ABS(HOLD))240,490,240
240   IJ = MA*N+K
245   C(IJ) = 0.E0
      KMAX = ITEMP
      GO TO 360
C
C     FIND PARTIAL DERIVATIVE OF LARGEST ABSOLUTE VALUE.
C
250   IJ = (K-1)*MA+K
      KMAX = LOOK(IJ)
255   DMAX = ABS(PART(KMAX))
      KP = K+1
      DO 290 I=KP,N
      IJ = (I-1)*MA+K
      JSUB = LOOK(IJ)
260   TEST = ABS(PART(JSUB))
      IF(TEST-DMAX)280,270,270
270   DMAX = TEST
      IJ = (I-1)*MA+KP
      LOOK(IJ) = KMAX
      KMAX = JSUB
      GO TO 290
```

```
 280  IJ = (I-1)*MA+KP
      LOOK(IJ)=JSUB
 290  CONTINUE
 300  IF( ABS(PART(KMAX)))310,490,310
 310  CONTINUE
C
C     SET UP COEFFICIENTS FOR KTH ROW OF TRIANGULAR LINEAR SYSTEM USED
C     TO BACK-SOLVE FOR THE FIRST K X(I) VALUES.
C
      ISUB(K)=KMAX
      IJ = N*MA+K
 320  C(IJ)=0.E0
      IJ = N*MA+K
      DO 350 I=KP,N
      KJ = (I-1)*MA+KP
      JSUB = LOOK(KJ)
      KJ=(JSUB-1)*MA+K
      C(KJ) = -PART(JSUB)/PART(KMAX)
 350  C(IJ) = C(IJ) + PART(JSUB)*X(JSUB)
 360  IJ = N*MA+K
      C(IJ)=(C(IJ)-SAVE)/PART(KMAX) + X(KMAX)
      IF(K-N)370,380,380
 370  K = K+1
      GO TO 60
 380  CONTINUE
C
C     BACK SUBSTITUTE TO OBTAIN NEXT APPROXIMATION TO X.
C
      IJ = N*MA+N
      X(KMAX) = C(IJ)
      IF(N-1)390,400,390
 390  KMIN = N-1
      JJ = 3
      GO TO 900
 400  IF(M-1)440,440,405
C
C     TEST FOR CONVERGENCE
C
 405  DO 420 I=1,N
 410  IF( ABS((TEMP(I)-X(I))/X(I))-REL) 420,420,430
 420  CONTINUE
      JTEST=JTEST+1
      IF(JTEST-3)440,470,470
 430  JTEST=1
 440  DO 450 I=1,N
 450  TEMP(I)=X(I)
      IF(M-MAX)460,480,480
 460  M=M+1
      L(5)=N+1
      GO TO 40
 470  IER=0
 475  L(5) = N+2
```

```
      L(6) = IER
      GO TO 40
  480 IER = 1
      GO TO 475
  490 IER = 2
      GO TO 475
  500 IER = 3
      GO TO 475
C
C     BACK SUBSTITUTION ROUTINE
C
  900 DO 930 IK = 1,KMIN
      KM = KMIN-IK+2
      KMAX = ISUB(KM-1)
  910 X(KMAX) = 0.E0
      DO 920 J=KM,N
      JK=(J-1)*MA+KM
      JSUB=LOOK(JK)
      JK=(JSUB-1)*MA+KM-1
      X(KMAX)=X(KMAX)+C(JK)*X(JSUB)
  920 CONTINUE
      JK=N*MA+KM-1
      X(KMAX)=X(KMAX)+C(JK)
  930 CONTINUE
      GO TO (70,140,400),JJ
      END
```

```
      SUBROUTINE POLMA(A, NCOL, N, EPS, COE, NP1, MAT)
      DIMENSION A(NCOL,NCOL,1), COE(1), MAT(NCOL,NCOL)
      REAL*8 A, COE, SB, SA
      M=N*NCOL+1
      IF (M .GT. 1) GO TO 102
      NP1 = -1
      RETURN
  102 NP1=N+1
C     FIND DEGREE OF EACH MATRIX ELEMENT
      DO  2  I=1,NCOL                                                   L0210
      DO  2  J=1,NCOL                                                   L0210
      MAT(I,J)=0                                                        L0210
      DO 2 K = 1, NP1
      IF (A(I,J,K) .NE. 0) MAT(I,J) = K
    2 CONTINUE                                                          L0210
C     TRIANGULARIZE THE MATRIX
      DO 112 J1 = 1, NCOL
   10 J9=0                                                            L0210
      DO  3 I=J1,NCOL                                                   L0210
      IF (MAT(I,J1) .EQ. 0) GO TO 3
      J9 = J9 + 1
      J3=I                                                              L0210
    3 CONTINUE                                                          L0210
C     J1 = COLUMN NUMBER
C     J9 = NUMBER OF NON-ZERO ELEMENTS IN THIS COLUMN
C     J3 = LAST NON-ZERO ELEMENT IN THIS COLUMN
C     J4 = TEMPORARY STORAGE FOR INTERCHANGE
C     SA = TEMPORARY STORAGE FOR INTERCHANGE
   11 IF (J9-1) 101, 603, 12
  101 NP1 = 0
      RETURN
C     IF THERE IS ONLY ONE NON-ZERO ELEMENT, EXCHANGE ITS ROW WITH J1
  603 IF (J3 .EQ. J1) GO TO 112
      DO 4 J = J1, NCOL
      J2= MAXO(MAT(J3,J),MAT(J1,J))                                     L0210
      J4=MAT(J3,J)                                                      L0210
      MAT(J3,J)=MAT(J1,J)                                               L0210
      MAT(J1,J)= J4                                                     L0210
      DO  4 K=1,J2                                                      L0210
      SA=A(J3,J,K)                                                      L0210
      A(J3,J,K)=A(J1,J,K)                                               L0210
      A(J1,J,K)=-SA                                                     L0210
    4 CONTINUE                                                          L0210
      GO TO 112                                                         L0210
C     THERE IS MORE THAN ONE NON-ZERO ELEMENT
   12 J3=J1+1                                                           L0210
      DO 111 I=J3,NCOL
   13 IF (MAT(I,J1) .EQ. 0) GO TO 111
      IF (MAT(J1,J1) .EQ. 0) GO TO 14
      IF (MAT(I,J1) .GE. MAT(J1,J1)) GO TO 15
C     ELEMENT I IS OF LOWER ORDER THAN J1, SO INTERCHANGE ROW I WITH J1
   14 DO  6 J= J1,NCOL                                                  L0210
```

```
      J2= MAXO(MAT(J1,J),MAT(I,J))                                      L0210
      J4= MAT(J1,J)                                                     L0210
      MAT(J1,J)=MAT(I,J)                                                L0210
      MAT(I,J)=J4                                                       L0210
      DO 6 K=1,J2                                                       L0210
      SA= A(I,J,K)                                                      L0210
      A(I,J,K)=A(J1,J,K)                                                L0210
      A(J1,J,K)=-SA                                                     L0210
    6 CONTINUE                                                          L0210
      GO TO 13                                                          L0210
C
   15 J7=MAT(I,J1)                                                      L0210
      J5=MAT(J1,J1)                                                     L0210
      J6=J7-J5                                                          L0210
      SB=A(I,J1,J7)/A(J1,J1,J5)                                         L0210
      IF (DABS(SB) .LT. 4.) GO TO 16
      IF (J6 .EQ. 0) GO TO 14
   16 DO 19  J= J1,NCOL                                                 L0210
      J5=MAT(J1,J)                                                      L0210
      DO 19  K=1,J5                                                     L0210
      J7= K+J6                                                          L0210
      IF (J7 .GT. M) GO TO 110
      SA = SB*A(J1,J,K)
      A(I,J,J7) = A(I,J,J7) - SA
      IF (DABS(A(I,J,J7)) .LT. DABS(EPS*SA)) A(I,J,J7) = 0.
   19 CONTINUE                                                          L0210
  110 DO  7 J=J1,NCOL                                                   L0210
      J7= MAXO(MAT(I,J),MAT(J1,J)+J6)                                   L0210
      MAT(I,J)=0                                                        L0210
      DO  7  K=1,J7
      IF (A(I,J,K) .NE. 0.) MAT(I,J) = K
    7 CONTINUE                                                          L0210
  111 CONTINUE                                                          L0210
      GO TO 10                                                          L0210
  112 CONTINUE
C     GET PRODUCT OF DIAGONAL ELEMENTS
      NP1 = MAT(1,1)
      DO 113 K = 1, NP1
  113 COE(K) = A(1,1,K)
      DO 117 I = 2, NCOL
      J2 = MAT(I,I)
      J1 = J2 + NP1 - 1
      DO 114 K = 1, NP1
  114 A(2,1,K) = COE(K)
      DO 115 K = 1, J1
  115 COE(K) = 0.
      DO 116 K = 1, NP1
      DO 116 J = 1, J2
  116 COE(J+K-1) = COE(J+K-1) + A(2,1,K)*A(I,I,J)
  117 NP1 = J1
      RETURN
      END
```

```
      SUBROUTINE MULLER(COE,N1,ROOTR,ROOTI,ISW,IERR)
C     MULLER ROUTINE FOR ZEROES OF POLYNOMIALS WITH REAL COEFFICIENTS
C
C     COE IS THE ARRAY OF POLYNOMIAL COEFFICIENTS ORDERED FROM HIGHEST
C     TO LOWEST POWER OF X
C     N1 IS THE DEGREE OF THE POLYNOMIAL
C     ROOTR IS THE ARRAY OF REAL COMPONENTS OF THE ROOTS
C     ROOTI IS THE ARRAY OF IMAGINARY COMPONENTS OF THE ROOTS
C     ISW IS AN ARRAY DEFINING THE VALIDITY OF THE ROOTS
C             ISW(N) = 0     THE NTH ROOT HAS BEEN STORED IN ROOTR(N) AND
C                            ROOTI(N)
C             ISW(N) = 1     THE NTH ROOT HAS BEEN STORED IN ROOTR(N) AND
C                            ROOTI(N), BUT IT MAY NOT BE VALID
C     IERR IS AN ERROR CODE WHICH HAS THE FOLLOWING SIGNIFICANCE.
C             IERR = 0       ALL ROOTS FOUND CORRECTLY
C             IERR = 1       ONE OR MORE ROOTS MAY BE INVALID.  TEST THE
C                            ISW ARRAY .
C             IERR = 2       POLYNOMIAL DEGREE IS LESS THAN 1
C             IERR = 3       POLYNOMIAL DEGREE IS LESS THAN N1
C
C     FOR A POLYNOMIAL OF DEGREE N1 THE COE ARRAY SHOULD BE DIMENSIONED
C     N1+ 1 IN THE USER PROGRAM.  THE OTHER ARRAYS SHOULD BE DIMENSIONED
C     N1 IN THE USER PROGRAM.
C     THE POLYNOMIAL IS SCALED TO AVOID ARITHMETIC OVERFLOW.  ALL
C     SCALING USES FACTORS OF 16.  TO CHANGE TO FACTORS OF X, SET BASE
C     = X   AND   CONST = LN(X)  IN SUBROUTINE
C     THIS SUBROUTINE USES DOUBLE PRECISION ARITHMETIC. SINGLE PRECISION
C     IS NOT RECOMMENDED.
C
      DIMENSION COE(1), ROOTR(1), ROOTI(1), ISW(1)
      DOUBLE PRECISION COE,TE2,TE3,DIV,TEE7,DE15,TE13,HELL,TEM2,ALP1R,
     1ALP2R,ALP3R,TEST1,ZTAU2,AXR,TE5,TE4,UPP,TEMR,DE16,TE14,BELL,ROOTR,
     2ALP1I,ALP2I,ALP3I,TEST2,AXI,TE6,TE7,TE8,TEMI,TE11,TE15,TAU2,ROOTI,
     3BET1R,BET2R,BET3R,ALP4R,TE1,TEM,TE9,TAU,TE10,TE12,TE16,TEM1,Z1,
     4BET1I,BET2I,BET3I,ALP4I,Z2,O1,O2,FACTOR
C
      BASE = 16.
      CONST = 2.77259
C
      CALL MASK(0)
      IF(N1 - 1) 27,28,28
   27 IERR = 2
      GO TO 193
   28 IERR = 0
      FACTOR = 0.
      N2=N1+1
      N4=0
      I=N1+1
   19 IF(COE(I))9,7,9
    7 N4=N4+1
      ROOTR(N4)=0.
      ROOTI(N4)=0.
```

```
      ISW(N4) = 0
      I=I-1
      IF(N4-N1)19,37,19
    9 CONTINUE                                                        HPRS0012
      IF(COE(1)) 190,192,190
  190 TEMP = DABS(COE(I)/COE(1))
      TEMP = ALOG(TEMP)/CONST/(I-1)
      K2 = TEMP + SIGN(.5,TEMP)
      TEMP = DABS(COE(1))
      TEMP = ALOG(TEMP)/CONST
      K1 = TEMP + SIGN(.5,TEMP)
      DO 191 I = 1,N2
  191 COE(I) = COE(I)/BASE**(K1 + K2*(I-1))
      FACTOR = BASE**K2
      GO TO 10
  192 IERR = 3
  193 DO 194 I = 1,N1
      ROOTR(I) = 0.
      ROOTI(I) = 0.
  194 ISW(I) = 1
      RETURN
   10 AXR=0.8
      AXI=0.
      L=1
      N3=1
      ALP1R=AXR
      ALP1I=AXI
      M=1
      GO TO 99
   11  BET1R=TEMR
      BET1I=TEMI
      AXR=0.85
      ALP2R=AXR
      ALP2I=AXI
      M=2
      GO TO 99
   12 BET2R=TEMR
      BET2I=TEMI
      AXR=0.9
      ALP3R=AXR
      ALP3I=AXI
      M=3
      GO TO 99
   13 BET3R=TEMR
      BET3I=TEMI
   14 TE1=ALP1R-ALP3R
      TE2=ALP1I-ALP3I
      TE5=ALP3R-ALP2R
      TE6=ALP3I-ALP2I
      TEM=TE5*TE5+TE6*TE6
      TE3=(TE1*TE5+TE2*TE6)/TEM
      TE4=(TE2*TE5-TE1*TE6)/TEM
```

```
      TE7=TE3+1.
      TE9=TE3*TE3-TE4*TE4
      TE10=2.*TE3*TE4
      DE15=TE7*BET3R-TE4*BET3I
      DE16=TE7*BET3I+TE4*BET3R
      TE11=TE3*BET2R-TE4*BET2I+BET1R-DE15
      TE12=TE3*BET2I+TE4*BET2R+BET1I-DE16
      TE7=TE9-1.
      TE1=TE9*BET2R-TE10*BET2I
      TE2=TE9*BET2I+TE10*BET2R
      TE13=TE1-BET1R-TE7*BET3R+TE10*BET3I
      TE14=TE2-BET1I-TE7*BET3I-TE10*BET3R
      TE15=DE15*TE3-DE16*TE4
      TE16=DE15*TE4+DE16*TE3
      TE1=TE13*TE13-TE14*TE14-4.*(TE11*TE15-TE12*TE16)
      TE2=2.*TE13*TE14-4.*(TE12*TE15+TE11*TE16)
      TEST1=DABS(TE1)
      TEST2=DABS(TE2)
      IF(TEST1-TEST2) 300,301,301
  300 DIV=TEST2
      UPP=TEST1
      GO TO 303
  301 DIV=TEST1
      UPP=TEST2
      IF(DIV-1.D-70) 999,303,303
  999 DIV= 1.D-70
  303 TEM=DIV*DSQRT(1.+(UPP/DIV)*(UPP/DIV))
      IF(TE1)113,113,112
  113 TE4=DSQRT(.5*(TEM-TE1))
      TE3=.5*TE2/TE4
      GO TO 111                                                    HPRS0064
  112 TE3=DSQRT(.5*(TEM+TE1))
      IF(TE2)110,200,200
  110 TE3=-TE3
  200 TE4=.5*TE2/TE3
  111 TE7=TE13+TE3
      TE8=TE14+TE4
      TE9=TE13-TE3
      TE10=TE14-TE4
      TE1=2.*TE15
      TE2=2.*TE16
      IF(TE7*TE7+TE8*TE8-TE9*TE9-TE10*TE10)204,204,205
  204 TE7=TE9
      TE8=TE10
  205 TEM=TE7*TE7+TE8*TE8
      IF(TEM -1.D-70) 998,997,997
  998 TEM= 1.D-70
  997 TE3=(TE1*TE7 + TE2 *TE8)/TEM
      TE4=(TE2*TE7-TE1*TE8)/TEM
      AXR=ALP3R+TE3*TE5-TE4*TE6
      AXI=ALP3I+TE3*TE6+TE4*TE5
      ALP4R=AXR
```

```
      ALP4I=AXI
      M=4
      GO TO 99                                                    HPRS0086
   15 N6=1
   38 01=DABS(HELL)+DABS(BELL)
      TE7=DABS(ALP3R-AXR)+DABS(ALP3I-AXI)
      TEE7=   DABS(AXR)+DABS(AXI)
C IS THE FUNCTION VALUE NEAR ZERO ?
      IF(01   -1.D-20                  )161,161,      16
C IS THE ROOT SMALL ?
161   IF(TEE7-1.0D-03)162,16,16
C IS THE CURRENT ESTIMATE FOR THE ROOT ESSENTIALLY
C THE SAME AS THE PREVIOUS ESTIMATE ?
162   IF(TE7-1.0D-12) 18,17,17
C ARE THE CURRENT AND PREVIOUS ESTIMATES OF THE ROOT ESSENTIALLY
C THE SAME WHEN COMPARED TO THE MAGNITUDE OF THE ROOT ?
16    02=TE7/ TEE7
      IF(02 - 1.E-7)18,18,17
   17 N3=N3+1
      ALP1R=ALP2R
      ALP1I=ALP2I
      ALP2R=ALP3R
      ALP2I=ALP3I
      ALP3R=ALP4R
      ALP3I=ALP4I
      BET1R=BET2R
      BET1I=BET2I
      BET2R=BET3R
      BET2I=BET3I
      BET3R=TEMR
      BET3I=TEMI
      IF(N3-200)14,25,25
   25 ISWT = 1
      GO TO 26
   18 ISWT = 0
   26 N4 = N4 + 1
      ISW(N4) = ISWT
      ROOTR(N4)=ALP4R
      ROOTI(N4)=ALP4I
      N3=0
   41 IF(N4-N1)39,37,37
   37 CONTINUE
      IF(FACTOR) 140,140,138
  138 DO 139 I = 1,N1
      ROOTR(I) = ROOTR(I)*FACTOR
      ROOTI(I) = ROOTI(I)*FACTOR
  139 COE(I) = COE(I)*BASE**(K1+K2*(I-1))
      COE(N2) = COE(N2)*BASE**(K1+K2*N1)
  140 DO 141 I=1,N1
      IF(ISW(I)) 141,141,142
  141 CONTINUE
      IERR = 0
```

```
      GO TO 3001
  142 IERR = 1
 3001 RETURN
   30 IF(DABS(ROOTI(N4)/ROOTR(N4)) - 1.E-5) 10,10,131
  131 IF(ISWT) 31,132,31
  132 GO TO (133,134),L
  133 N4 = N4 + 1
      M4 = N4
      GO TO 135
  134 M4 = N4 - 1
  135 ROOTR(M4) = AXR
      ROOTI(M4) = -AXI
      ISW(M4) = 0
      IF(M4 - N1) 10,37,37
   31 GO TO(32,10),L
   32 AXR=ALP1R
      AXI=-ALP1I
      ALP1I=-ALP1I
      M=5
      GO TO 99                                                    HPRS0117
   33 BET1R=TEMR
      BET1I=TEMI
      AXR=ALP2R
      AXI=-ALP2I
      ALP2I=-ALP2I
      M=6
      GO TO 99                                                    HPRS0124
   34 BET2R=TEMR
      BET2I=TEMI
      AXR=ALP3R
      AXI=-ALP3I
      ALP3I=-ALP3I
      L=2
      M=3
   99 TEMR=COE(1)
      TEMI=0.0
      DO 100 I=1,N1
      TE1=TEMR*AXR-TEMI*AXI
      TEMI=TEMI*AXR+TEMR*AXI
  100 TEMR=      TE1+COE(I+1)
      HELL=TEMR
      BELL=TEMI
   42 IF(N4)102,103,102
  102 DO 101 I=1,N4
      TEM1=AXR-ROOTR(I)
      TEM2=AXI-ROOTI(I)
      TE1=TEM1*TEM1+TEM2*TEM2
      TE2=(TEMR*TEM1+TEMI*TEM2)/TE1
      TEMI=(TEMI*TEM1-TEMR*TEM2)/TE1
  101 TEMR=TE2
  103 GO TO(11,12,13,15,33,34),M
      END                                                         HPRS0149
```

360N-FO-479 3-4 MAINPGM DATE 08/23/71 TIME 11.05.28

```
      REAL MS,MAS,M,L,L2,LS,IYB,IZB,IYZB,MPL,LMS
      DOUBLE PRECISION COE(11),COEF(11),ROOTR(10),ROOTI(10),FREQN(10),
     1FREQD(10),DAMRAT(10),THAMP(10),A(5,5,11)
      DOUBLE PRECISION GGG(8,8),HHH(8)
      DIMENSION VECTR(4),VECTI(4),VECTM(4),VECTD(4)
      DIMENSION MAT(5,5),ISW(10),XIODE(3),XIO(3),AALP(5,5),BBET(5,5),
     1GGAM(5,5),SX(3),AALT(8),VVW(8),COMI(10),CX(3),ZCH(4),RHOCH(4),
     2DYPRH(4),VWH(4),C(3),ZC(3),RHOC(3),VWC(3),SC(3)
    1 FORMAT(8F10.0)
    2 FORMAT(10A4)
   37 FORMAT(25X,'ALPHA(I,J)',45X,'BETA(I,J)'/)
   36 FORMAT(/15X,'GAMMA(I,J)'/)
   38 FORMAT(/8X,'ROOTS OF CHARACTERISTIC EQUATION',25X,'STABILITY PARAM
     1ETERS',23X,'TIME TO HALF OR'/12X,'REAL',10X,'IMAGINARY',10X,'NATUR
     2AL FREQUENCY',5X,'DAMPED FREQUENCY',5X,'DAMPING RATIO',7X,
     3'DOUBLE AMPLITUDE'/)
   39 FORMAT(1X,5(5(E9.2,1X)/1X))
   42 FORMAT(/10X,'COEFFICIENTS OF CHARACTERISTIC EQUATION IN ASCENDING
     1ORDER')
   43 FORMAT(5X,'ALL ROOTS HAVE BEEN ACCURATELY DETERMINED')
   44 FORMAT(//5X,'DEGREE OF POLYNOMINAL IS LESS THAN TEN'//)
   45 FORMAT(//5X,'DEGREE OF POLYNOMINAL IS LESS THAN ONE'//)
   46 FORMAT(//5X,'ROOT NOT ACCURATELY FOUND',5X,10I4//)
   47 FORMAT(10X,10(D11.4,3X,D11.4,12X,D11.4,11X,D11.4,9X,D11.4,10X,
     1D11.4/10X))
   48 FORMAT(/5X,11(1X,E10.3)//)
   49 FORMAT(1X,5(5(E9.2,2X),9X,5(E9.2,2X)/1X))
  137 FORMAT(5X,6(F8.4,2X),4(F9.1,1X),F8.3,2X,F8.1/5X,6(F8.4,2X),
     14(F9.1,1X),F8.3,2X,F8.1/5X,6(F8.4,2X),3(F9.1,1X),3(F8.3,2X)/15X,
     23(F8.4,2X)/)
  138 FORMAT(8X,'RJM',7X,'RKM',7X,'CNPSB',5X,'CNPSDB',4X,'CNPHDB',4X,
     1'CNVB',6X,'LS',8X,'MPL',7X,'IZB',7X,'TETH',6X,'XIO(1)',4X,'RANGE'/
     28X,'RJA',7X,'RKA',7X,'CLPSB',5X,'CLPSDB',4X,'CLPHDB',4X,'CLVB',6X,
     3'WB',8X,'SB',8X,'IYB',7X,'MAS',7X,'XIO(2)',4X,'ALTITUDE'/
     48X,'RJG',7X,'RKG',7X,'CYPSB',5X,'CYPSDB',4X,'CYPHDB',4X,'CYVB',6X,
     5'WTC',7X,'DB',8X,'IYZB',6X,'THEO',6X,'XIO(3)',4X,'DYPRB'/18X,
     6'RKB',7X,'DC',8X,'CDC'/)
  139 FORMAT(5X,'ALTITUDE PROFILE',10X,8F10.1/5X,'WIND VELOCITY PROFILE'
     1,5X,8F10.1/)
  140 FORMAT(1H1,20X,'STABILITY ANALYSIS OF A TETHERED BALLOON IN THE LA
     1TERAL PLANE',5X,10A4//)
  250 FORMAT(4(/10X,4(E11.4,4X)))
  251 FORMAT(1H1//30X,'MODAL ANALYSIS'//17X,'EIGENVECTOR'/12X,'REAL',
     19X,'IMAGINARY',6X,'MAGNITUDE',6X,'DIRECTION ANGLE'/)
      CALL MASK(0)
      G=32.17
      READ(1,1) AALT,VVW
   99 READ(1,1) WB,LS,MPL,WTC,IZB,IYB,IYZB,MAS
      IF(WB.EQ.1.) CALL EXIT
      READ(1,1) THEODE,(XIODE(I),I=1,3)
      READ(1,2) COMI
      READ(1,1) RJM,RKM,RJA,RKA,RJG,RKG,RKB
```

```
      READ(1,1) SB,DB,TETH,DC,CDC
      READ(1,1) CYPSDB,CYPHDB,CNPSDB,CNPHDB,CLPSDB,CLPHDB
      READ(1,1) CYPSB,CNPSB,CLPSB,CYVB,CNVB,CLVB
      THEO=THEODE/57.2958
      L=TETH/3.
      L2=L*L
      DO 6 I=1,3
      SC(I)=L*DC
    6 XIO(I)=XIODE(I)/57.2958
      MS=MAS+WB/32.17
      M=WTC/(3.*G)
      STHEO=SIN(THEO)
      CTHEO=COS(THEO)
      STHEO2=STHEO**2
      CTHEO2=CTHEO**2
      S2THEO=2.*STHEO*CTHEO
      DO 7 I=1,3
      SX(I)=SIN(XIO(I))
    7 CX(I)=COS(XIO(I))
      ZCH(1)=0.
C     IF WINCH IS AT 5000. FT.
C     ZCH(1)=5000.
      DO 300 I=2,4
  300 ZCH(I)=ZCH(I-1)+L*SX(I-1)
      DO 301 I=1,4
      CALL DENS(ZCH(I),PR,RHOCH(I),VS)
      J=2
  310 IF(ZCH(I).LT.AALT(J)) GO TO 311
      J=J+1
      GO TO 310
  311 ALTSL=(ZCH(I)-AALT(J-1))/(AALT(J)-AALT(J-1))
      VWH(I)=VVW(J-1)+(VVW(J)-VVW(J-1))*ALTSL
  301 DYPRH(I)=.5*RHOCH(I)*VWH(I)**2
      DO 302 I=1,3
  302 C(I)=(DYPRH(I)+2.*DYPRH(I+1))/(3.*(DYPRH(I)+DYPRH(I+1)))
      ZC(1)=L*C(1)*SX(1)
      ZC(2)=L*(SX(1)+C(2)*SX(2))
      ZC(3)=L*(SX(1)+SX(2)+C(3)*SX(3))
C     IF WINCH IS AT 5000. FT.
C     ZC(1)=L*C(1)*SX(1)+5000.
C     ZC(2)=L*(SX(1)+C(2)*SX(2))+5000.
C     ZC(3)=L*(SX(1)+SX(2)+C(3)*SX(3))+5000.
      DO 303 I=1,3
      CALL DENS(ZC(I),PR,RHOC(I),VS)
      J=2
  320 IF(ZC(I).LT.AALT(J)) GO TO 321
      J=J+1
      GO TO 320
  321 ALTSL=(ZC(I)-AALT(J-1))/(AALT(J)-AALT(J-1))
  303 VWC(I)=VVW(J-1)+(VVW(J)-VVW(J-1))*ALTSL
      LMS=L*MS
      ZB=L*(SX(1)+SX(2)+SX(3))-RJG*STHEO-RKG*CTHEO
```

```
C       IF WINCH IS AT 5000. FT.
C       ZB=L*(SX(1)+SX(2)+SX(3))-RJG*STHE0-RKG*CTHE0+5000.
        YB=-L*(CX(1)+CX(2)+CX(3))-RJG*CTHE0+RKG*STHE0
        CALL DENS(ZB,PR,RHOB,VS)
        I=2
  210   IF(ZB.LT.AALT(I)) GO TO 211
        I=I+1
        GO TO 210
  211   ALTSL=(ZB-AALT(I-1))/(AALT(I)-AALT(I-1))
        VW=VVW(I-1)+(VVW(I)-VVW(I-1))*ALTSL
        DYPRB=.5*RHOB*VW**2
        WRITE(3,140) COM1
        WRITE(3,139) AALT,VVW
        WRITE(3,138)
        WRITE(3,137) RJM,RKM,CNPSB,CNPSDB,CNPHDB,CNVB,LS,MPL,IZB,TETH,
       1XIODE(1) YB,RJA,RKA,CLPSB,CLPSDB,CLPHDB,CLVB,WB,SB,IYB,MAS,
       2XIODE(2),ZB,RJG,RKG,CYPSB,CYPSDB,CYPHDB,CYVB,WTC,DB,IYZB,THEODE,
       3XIODE(3),DYPRB,RKB,DC,CDC
        A11=RKM*STHE0-RJM*CTHE0
        B11=.5*RHOB*VW*SB
        B12=-RJA*CTHE0+RKA*STHE0
        B13=RKG*STHE0-RJG*CTHE0
        B21=RKA*STHE0
        B31=B11*L
        B32=-.5*RHOC(1)*SC(1)*CDC*VWC(1)*L2
        B33=-.5*RHOC(2)*SC(2)*CDC*VWC(2)*L2
        B34=-.5*RHOC(3)*SC(3)*CDC*VWC(3)*L2
        G11=.5*RHOB*SB*VW**2
        AALP(1,1)=IZB*CTHE02+IYB*STHE02-IYZB*S2THE0+MS*A11**2
        AALP(1,2)=IYZB*CTHE0-IYB*STHE0-MS*RKM*A11
        AALP(1,3)=LMS*A11
        AALP(1,4)=AALP(1,3)
        AALP(1,5)=AALP(1,3)
        AALP(2,1)=AALP(1,2)
        AALP(2,2)=IYB+MS*RKM**2
        AALP(2,3)=-LMS*RKM
        AALP(2,4)=AALP(2,3)
        AALP(2,5)=AALP(2,3)
        AALP(3,1)=AALP(1,3)
        AALP(3,2)=AALP(2,3)
        AALP(3,3)=L2*(7.*M/3.+MPL+MS)
        AALP(3,4)=L2*(3.*M/2.+MPL+MS)
        AALP(3,5)=L2*(M/2.+MPL+MS)
        AALP(4,1)=AALP(1,4)
        AALP(4,2)=AALP(2,4)
        AALP(4,3)=AALP(3,4)
        AALP(4,4)=L2*(4.*M/3.+MPL+MS)
        AALP(4,5)=L2*(M/2.+MPL+MS)
        AALP(5,1)=AALP(1,5)
        AALP(5,2)=AALP(2,5)
        AALP(5,3)=AALP(3,5)
        AALP(5,4)=AALP(4,5)
```

```
      AALP(5,5)=L2*(M/3.+MPL+MS)
      BBET(1,1)=-B11*((CYPSDB*DB+CYVB*B13)*B12+DB*(CNPSDB*DB+CNVB*B13))
      BBET(1,2)=-B11*((CYPHDB*DB-CYVB*RKG)*B12+DB*(CNPHDB*DB-CNVB*RKG))
      BBET(1,3)=-B31*(CYVB*B12+CNVB*DB)
      BBET(1,4)=BBET(1,3)
      BBET(1,5)=BBET(1,3)
      BBET(2,1)=+B11*((CYPSDB*DB+CYVB*B13)*B21-DB*(CLPSDB*DB+CLVB*B13))
      BBET(2,2)=+B11*((CYPHDB*DB-CYVB*RKG)*B21-DB*(CLPHDB*DB-CLVB*RKG))
      BBET(2,3)=-B31*(-CYVB*B21+CLVB*DB)
      BBET(2,4)=BBET(2,3)
      BBET(2,5)=BBET(2,3)
      BBET(3,1)=-B31*(CYPSDB*DB+CYVB*B13)
      BBET(3,2)=-B31*(CYPHDB*DB-CYVB*RKG)
      BBET(3,3)=-(B31*CYVB*L+B32*C(1)**2+B33+B34)
      BBET(3,4)=-(B31*CYVB*L+B33*C(2)+B34)
      BBET(3,5)=-(B31*CYVB*L+B34*C(3))
      BBET(4,1)=BBET(3,1)
      BBET(4,2)=BBET(3,2)
      BBET(4,3)=-(B31*CYVB*L+B33*C(2)+B34)
      BBET(4,4)=-(B31*CYVB*L+B33*C(2)**2+B34)
      BBET(4,5)=-(B31*CYVB*L+B34*C(3))
      BBET(5,1)=BBET(3,1)
      BBET(5,2)=BBET(3,2)
      BBET(5,3)=-(B31*CYVB*L+B34*C(3))
      BBET(5,4)=BBET(5,3)
      BBET(5,5)=-(B31*CYVB*L+B34*C(3)**2)
      GGAM(1,1)=-G11*(CYPSB*B12+CNPSB*DB)
      GGAM(1,2)=0.
      GGAM(1,3)=0.
      GGAM(1,4)=0.
      GGAM(1,5)=0.
      GGAM(2,1)=-G11*(-CYPSB*B21+CLPSB*DB)
      GGAM(2,2)=(WB*RKG-LS*RKB)*CTHEO
      GGAM(2,3)=0.
      GGAM(2,4)=0.
      GGAM(2,5)=0.
      GGAM(3,1)=-G11*L*CYPSB
      GGAM(3,2)=0.
      GGAM(3,3)=(LS-WB-(MPL+5.*M/2.)*G)*L*SX(1)
      GGAM(3,4)=0.
      GGAM(3,5)=0.
      GGAM(4,1)=GGAM(3,1)
      GGAM(4,2)=0.
      GGAM(4,3)=0.
      GGAM(4,4)=(LS-WB-(MPL+3.*M/2.)*G)*L*SX(2)
      GGAM(4,5)=0.
      GGAM(5,1)=GGAM(3,1)
      GGAM(5,2)=0.
      GGAM(5,3)=0.
      GGAM(5,4)=0.
      GGAM(5,5)=(LS-WB-(MPL+M/2.)*G)*L*SX(3)
      WRITE(3,37)
```

```
      WRITE(3,49)(((AALP(I,J),J=1,5),(BBET(I,J),J=1,5)),I=1,5)
      WRITE(3,36)
      WRITE(3,39)(((GGAM(I,J),J=1,5)),I=1,5)
      K=1
      DO 101 J=1,5
      DO 101 I=1,5
  101 A(I,J,K)=GGAM(I,J)
      K=2
      DO 102 J=1,5
      DO 102 I=1,5
  102 A(I,J,K)=BBET(I,J)
      K=3
      DO 103 J=1,5
      DO 103 I=1,5
  103 A(I,J,K)=AALP(I,J)
      DO 104 K=4,11
      DO 104 J=1,5
      DO 104 I=1,5
  104 A(I,J,K)=0.
      EPS=1.E-09
      N=2
      NCOL=5
      CALL POLMAT(A,NCOL,N,EPS,COE,NP1,MAT)
      WRITE(3,42)
      WRITE(3,48)(COE(I),I=1,NP1)
      DO 106 I=1,11
  106 COEF(I)=COE(12-I)
      N1=10
      CALL MULLER(COEF,N1,ROOTR,ROOTI,ISW,IERR)
      IF(IERR.EQ.0) WRITE(3,43)
      IF(IERR.EQ.1) WRITE(3,46)(ISW(I),I=1,10)
      IF(IERR.EQ.2) WRITE(3,45)
      IF(IERR.EQ.3) WRITE(3,44)
      WRITE(3,38)
      DO 105 I=1,10
      FREQN(I)=DSQRT(ROOTR(I)**2+ROOTI(I)**2)
      FREQD(I)=DABS(ROOTI(I))
      DAMRAT(I)=-ROOTR(I)/FREQN(I)
  105 THAMP(I)=.69315/(DAMRAT(I)*FREQN(I))
      WRITE(3,47)((ROOTR(I),ROOTI(I),FREQN(I),FREQD(I),DAMRAT(I),
     1THAMP(I)),I=1,10)
      WRITE(3,251)
      DO 200 K=1,10
      DO 201 I=1,4
      HHH(I)=-(AALP(I+1,1)*(ROOTR(K)**2-ROOTI(K)**2)+BBET(I+1,1)*ROOTR(K
     1)+GGAM(I+1,1))
      DO 201 J=1,4
  201 GGG(I,J)=AALP(I+1,J+1)*(ROOTR(K)**2-ROOTI(K)**2)+BBET(I+1,J+1)*
     1ROOTR(K)+GGAM(I+1,J+1)
      DO 202 I=5,8
      HHH(I)=-(AALP(I-3,1)*2.*ROOTR(K)*ROOTI(K)+BBET(I-3,1)*ROOTI(K))
      DO 202 J=1,4
```

```
202 GGG(I,J)=AALP(I-3,J+1)*2.*ROOTR(K)*ROOTI(K)+BBET(I-3,J+1)*ROOTI(K)
    DO 203 I=1,4
    DO 203 J=5,8
203 GGG(I,J)=-GGG(I+4,J-4)
    DO 204 I=5,8
    DO 204 J=5,8
204 GGG(I,J)=GGG(I-4,J-4)
    N=8
    L=8
    EPS=.1E-11
    CALL CROUT(GGG,HHH,N,L,EPS,IERSW)
    DO 205 I=1,4
    VECTR(I)=HHH(I)
    VECTI(I)=HHH(I+4)
    VECTM(I)=SQRT(VECTR(I)**2+VECTI(I)**2)
205 VECTD(I)=ARGD(VECTI(I),VECTR(I))
200 WRITE(3,250)((VECTR(I),VECTI(I),VECTM(I),VECTD(I)),I=1,4)
    GO TO 99
    END
```

APPENDIX C

ADDITIONAL BALLOON AERODYNAMIC MASS, AND GEOMETRIC CHARACTERISTICS

TABLE OF CONTENTS

LIST OF FIGURES

APPENDIX C
ADDITIONAL BALLOON AERODYNAMIC, MASS AND GEOMETRIC CHARACTERISTICS

1. GENERAL

The static and dynamic aerodynamic force and moment coefficients are described in Reference 1. Coefficients obtained from available wind tunnel data for the three balloon types being investigated are also plotted as a function of angle of attack and angle of sideslip. The numerical values of aerodynamic coefficients used in the stability analysis are given in this Appendix along with some notes as to their development. Reynold's Number changes only affect the skin friction drag and have no effect on the stability derivatives. The drag curves were not corrected for Reynolds Number because the amount of correction is within the test accuracy of the data. This Appendix also provides supplementary mass and geometric data used in the analysis of tethered balloon stability characteristics.

2. AERODYNAMIC CHARACTERISTICS

Table VII shows the aerodynamic coefficients computed according to the methods outlined in Reference 1. These partial derivatives were incorporated in the general equations and the value of the algebraic signs were established to be consistent with the sign convention chosen for the equations of motion developed in Appendix A where forward, up, and to the right are positive and nose-up, nose to the right, and right side down are positive rotations. It should be noted that a change of axis notation has been used between the aerodynamic section of this report as noted in Table VII and the dynamics section in Appendix A. In the dynamics section, pitch rotation is about the X axis which is an axis transverse to the balloon and roll is about the y axis which is along the longitudinal axis of the balloon. The signs for each coefficient for all balloons are the same except that the yawing moment of the BJ balloon with reduced tail size became unstable in yaw about the reference aerodynamic center of moment and those signs reversed.

The force vectors and angles are referenced to the relative wind in the usual manner. The moments are taken about the center of hull volume in the three planes. The reference center for the Vee Balloons is located on the center line between the two hulls.

The force and moment derivatives in the longitudinal case were obtained from the force and moment curves of Figures 5, 6, 11, 15 and 18 of Reference 1. They were entered into the computer memory and referenced where required. Thus the slopes of the curves are the tangents to the curve at that particular angle of attack, and the slope will change when the angle changes.

The data of Figure 18 (Reference 1) was obtained at a center of moment located 0.444L from the nose. These moments were transferred by the method shown in Figure 20 (Reference 1) to the center of the hull volume located at 0.413L. The data of the other balloons are already referenced to the center of hull volume.

The derivatives in Reference 1 for small perturbations in horizontal and vertical velocity are not used in the form derived because they are already indigenous in the equations. Accordingly, those values are not included in Table VII.

Test data on the rotary derivatives of these balloon shapes are non-existent so the values were calculated based on unpublished airship data. Lift and pitching moment vs. pitching velocity were obtained at zero angle of attack. A correction for angle of attack was not attempted because it is believed that the effect is so small that it would not influence the final results of the stability plot. The typical lift and pitching moment curve is generally a straight line for a few degrees either side of zero. The drag due to pitching velocity is based on the induced lift-drag ratio as explained in Reference 1. Since the drag curve is not a straight line, this derivative was made dependent on the lift coefficients as they affect induced drag as shown in Table VII.

The rotary derivatives of the Vee Balloon exhibited a special case. The two hulls overlap only a small amount at the front. Further, there is some interference to flow from one hull to the other. Consequently it seemed logical to assume that the Vee Balloon hull acted exactly in pitch as if it were two separate hulls of half the total volume each. Also each hull is skewed on the axis at 17.5° which affects the velocity of each section. To account for this effect, it was assumed that the length/diameter ratio was multiplied by cos 17.5°.

Table VII. Tethered Balloon Stabi

	Longitudinal Derivatives							
	Lift		Drag		Pitching Moment		Rolling	
	$\partial L/\partial\alpha$	$\partial L/\partial\dot{\theta}$	$\partial D/\partial\alpha$	$\partial D/\partial\dot{\theta}$	$\partial M/\partial\alpha$	$\partial M/\partial\dot{\theta}$	$\partial M_x/\partial\psi = -\partial M_x/\partial\beta$	∂M_x
Multiplier	$q\,V^{2/3}$	$q\frac{V}{V}$	$q\,V^{2/3}$	$q\frac{V}{V}$	$q\,V$	$q\frac{V^{4/3}}{V}$	$q\,V$	$q\frac{}{}$
BJ Balloon with 64% Tail Area (80% of Linear Dimensions)	Slope of C_{LBO} - 0.64α	0.696	Slope of C_{DBO} - $0.1248\,C_{LBO}^2$ + $0.1188\,C_{LB}$	$0.9\,C_L$ $C_L q$	Slope of C_{MBO} + $0.625\,\alpha$	-0.934	-0.193	-0.
BJ Balloon with 90% Linear Tail	Slope of C_{LBO} -0.30α	1.25	Slope of C_{DBO} - $0.125\,C_{LBO}^2$ + $0.123\,C_{LBO}^2$	"	Slope of C_{MBO} + 0.27α	-1.58	-0.26	-0.
BJ Balloon	Slope -Fig.5	1.68	Slope -Fig.6	"	Slope -Fig.18 Corrected	-2.01	-0.351	-0.
BJ Balloon with 144% Tail Area (120% of linear dimensions)	Slope of C_{LBO} +0.49α	2.14	Slope of C_{DBO} - $0.125\,C_{LBO}^2$ + $0.127\,C_{LB}^2$	"	Slope of C_{MBO} -0.405α	-2.62	-0.553	-0.
GAC 1649 with thin fins	Slope-Fig.5	1.49	Slope-Fig. 6	"	Slope-Fig.15	-2.07	-0.374	-0.
Vee Balloon	Slope-Fig.5	2.495	Slope-Fig.6	"	Slope-Fig.11	-2.483	-0.0578	-0.
Vee Balloon with Sym 100% Area Vert. Tails							0	-0.
Vee Balloon 200% Area Vert. Tails on Bottom							-0.135	-0.
Vee Balloon with Sym. 200% Area Vert. Tails							0	-0.
Vee Balloon 300% Area Vert. Tails on Bottom							-0.220	-0.
Vee Balloon with Sym. 300% Area Vert. Tails							0	-0.

Notes: (1) Figure numbers referenced above are located in Reference 1

(2) C_{LBO}, C_{DBO}, C_{MBO} are coefficients of unmodified balloon

(3) C_{LB} is coefficient of balloon wi

(4) Moments are about an aerodynamic center of hull volume

alloon Stability Program

Lateral Derivatives											
Rolling Moment				Yawing Moment				Side Force			
$\partial M_x/\partial\psi$ $\partial M_x/\partial\beta$	$\partial M_x/\partial p$	$\partial M_x/\partial r$	$\partial M_z/\partial v$	$\partial N/\partial\psi$ $= -\partial N/\partial\beta$	$\partial N/\partial p$	$\partial N/\partial r$	$\partial N/\partial v$	$\partial Y/\partial\psi$ $= -\partial Y/\partial\beta$	$\partial Y/\partial p$	$\partial Y/\partial r$	$\partial Y/\partial v$
V	$q\frac{b^{4/3}}{V}$	$q\frac{b^{4/3}}{V}$	$q\frac{b}{V}$	$q\,b$	$q\frac{b^{4/3}}{V}$	$q\frac{b^{4/3}}{V}$	$q\frac{b}{V}$	$q\,b^{2/3}$	$q\frac{b}{V}$	$q\frac{b}{V}$	$q\frac{b^{2/3}}{V}$
193	-0.137	-0.21	0.193	0.239	-0.0714	-1.90	-0.239	1.658	0.0737	1.315	-1.658
26	-0.21	-0.28	0.26	0.08	-0.096	-2.08	-0.08	1.85	0.104	1.55	-1.85
351	-0.327	-0.347	0.351	-0.105 Corr.Slope Fig. 17	-0.122	-2.31	0.105	2.08 Slope Fig. 16	0.142	1.79	-2.08
553	-0.609	-0.484	0.553	-0.498	-0.17	-2.67	0.498	2.645	0.224	2.27	-2.645
374	-0.508	-0.298	0.374	-0.22*	0	-2.07	0.22	1.99 **	0	1.94	-1.9
0578	-0.3758	-0.0212	0.0578	-0.004 Corr. Slope Fig.9	-0.0505	-0 482	0.004	0.857 Slope Fig. 8	0.054	0.439	-0.857
	-0.389	0	0	-0.441	0	-0.784	0.441	1.439	0	0.718	-1.439
135	-0.393	-0.0494	0.135	-0.441	-0.1010	-0.784	0.441	1.439	0.108	0.718	-1.439
	-0.427	0	0	-1.315	0	-1.388	1.315	2.603	0	1.276	-2.603
220	-0.412	-0.0810	0.220	-0.878	-0.1515	-1.086	0.878	2.021	0.162	0.997	-2.021
	-0.461	0	0	-2.189	0	-1.992	2.189	3.767	0	1.834	-3.767

balloon with modified tail

aerodynamic reference center located at the

* Corr. Slope - Fig. 13

** Slope - Fig. 12

BLANK PAGE

The lateral stability was considered separate from the longitudinal case. In the lateral modes, data were available only at zero angle of attack, Figures 8, 9, 12, 13, 16, and 17 (Reference 1). Further the data were available for only a few degrees on either side of 0° yaw. Consequently, the derivatives were taken as the slope of the curves at 0° yaw and pitch. The center of moments of the BJ balloon was shifted from the test position to the center of hull volume in accordance with the method of Figure 19 (Reference 1).

The rotary derivatives in yaw were handled in a manner similar to the rotary derivatives in pitch using the same basic airship information.

Test data for the balloons with changes in tail size were not available. It was assumed therefore that the test data could be modified by subtracting the theoretical effect of an isolated tail of the size measured, and then adding the theoretical effect of an isolated tail of the size of interest. This assumed that the hull and hull-tail interference effects did not change within the limits of the tail size variation. The tails were assumed to be placed on the balloon such that their trailing edges attached to the hulls at the same point as the original tail.

In the interest of space limitation, the detailed mathematics involved in determining the derivatives is not included in this report.

3. ADDITIONAL MASS CHARACTERISTICS

The mass characteristics presented in Reference 1 are supplemented here to include additional data generated for the stability analysis. The apparent mass moment of inertia about the dynamic center which is the sum of the physical and additional mass moment of inertia is plotted for each balloon type at 10,000 feet in Figure 64. The apparent mass moments of inertia for roll, pitch and yaw are respectively I_x, I_y and I_z. The apparent products of inertia for the three balloon types at 10,000 feet are given in Figure 65.

As a given balloon is moved to lower altitudes than the design altitude, the physical mass of the balloon increases by virtue of the denser air in the tails and the air introduced into the ballonets as a result of compression of the lifting gas. In addition, the additional mass increases with the air density increase at lower altitudes. The 60,000 cubic foot BJ balloon designed for

10,000 feet was chosen to explore the effects of change of altitude encountered during launch and retrieval. The mass characteristics developed for this investigation are plotted in Figures 66, 67 and 68 as a function of altitudes.

Physical and added mass characteristics for the BJ and Vee balloon change as tail size changes. These effects were computed and are tabulated in the body of this report as computer input data for the changing tail size investigation. Changing rotational inertia with payload relocation is also tabulated in the body of this report.

In view of the unique configuration of the Vee balloon, special consideration must be given to establishing its additional mass characteristics.

Additional Mass of the Vee-Balloon

The configuration of the Vee balloon is so complex that the evaluation of the added mass is not easy or straight forward. The approach made here is to make an engineering estimate of its value.

Vertical Acceleration:

In this direction the two hulls and the horizontal tail accelerates normal to their axis, or flat plate area in the case of the tail. The added mass of the two hulls is the mass of the displaced volume of air multiplied by a "k" factor based on the fineness ratio of one hull. The added mass of the tail is the mass of air contained in a cylinder where diameter equals the tail chord and whose length equals the tail length.

Longitudinal Acceleration :

In this direction the horizontal and vertical tail effect is zero. The hulls are inclined to the flow and the added mass effect can be handled as if it is the sum of two components, k_1 and k_2 are based on the fineness ratio of one of the hulls. Then the mass of the displaced air of both hulls is multiplied by $(k_1 \cos \theta + k_2 \sin \theta)$, when θ is the half angle between the hulls.

Lateral Acceleration:

In this case the horizontal tail effect is zero, but the vertical tails enter into the computation. The hulls are inclined to the flow.

The hull added mass is the mass of the displaced air of both hulls multiplied by the components of the appropriate k factors based on fineness ratio of one hull. The k factor becomes $(k_1 \sin \theta + k_2 \cos \theta)$.

The added mass of each vertical tail becomes the mass of air contained in a cylinder whose diameter equals the chord and whose length equals the vertical height from the center line of the hull. Correction factors for aspect ratio are obtained from Figure 32 of Reference 1.

Pitching Added Moment of Inertia:

The pitching added mass moment of inertia should be first determined about the center of added mass and later transferred to the dynamic center. In this case the center of added mass in the vertical direction is the governing location.

The moment of inertia contributed by the two hulls are calculated as the moment of inertia along the principle axis and then rotated and transferred to act about the lateral axis thru the added mass center.

The added moment of inertia of the horizontal tail is also computed as the moment of inertia of a cylinder of air about its lateral axis and transferred to the center of added mass. The vertical tail does not contribute to the added moment of inertia about this axis.

Yawing added Mass Moment of Inertia:

The axis of yawing moment of inertia passes thru the center of added mass when undergoing lateral acceleration.

The moment of inertia of the mass of the displaced air of each hull is corrected by the appropriate k factor from Figure 31 of Reference 1 and then it is transferred to the axis.

The moment of inertia due to the vertical tails is the moment of inertia of a cylinder of air with its axis vertical and a diameter equal to the chord of the tail. Its length is the tail height to the center line and the appropriate aspect ratio correction is applied. This is transferred to the axis and added to the moment of inertia of the hulls.

Rolling Added Mass Moment of Inertia:

Rolling of the hulls about their respective center lines produces no added moment of inertia. The main contribution of the hulls is due to the tangential acceleration of the hull section about the roll axis on the center line. This is calculated as a canted ellipsoid utilizing the appropriate k factors.

The vertical tails contribute very little to the roll inertia due to the geometry of their location, and so are neglected.

The horizontal tail contributes the added moment of inertia, modified of the appropriate k factor, of the mass of air contained in a cylinder whose diameter is the chord and rotated about its center chord as an axis.

4. SUSPENSION SYSTEM GEOMETRY

The location of the confluence point of the bridle suspension lines establishes the angle of attack at which the balloom trims. As part of the parametric study of stability characteristics it was of interest to know the effects of trim angles of attack and vertical location of the apex of the bridle. Bridle geometries for the tethered balloon systems of interest were established and variation of angle of attack was computed. The results are plotted in Figures 69 through 76.

5. EFFECT OF INCREMENTS OF OPERATIONAL WIND

For a balloon system designed to fly at altitude in an operational wind the tether length will change as winds are reduced to maintain the flight altitude. This variation for the BJ balloon with Nolaro tether for flight at 10,000 feet is given in Figure 77.

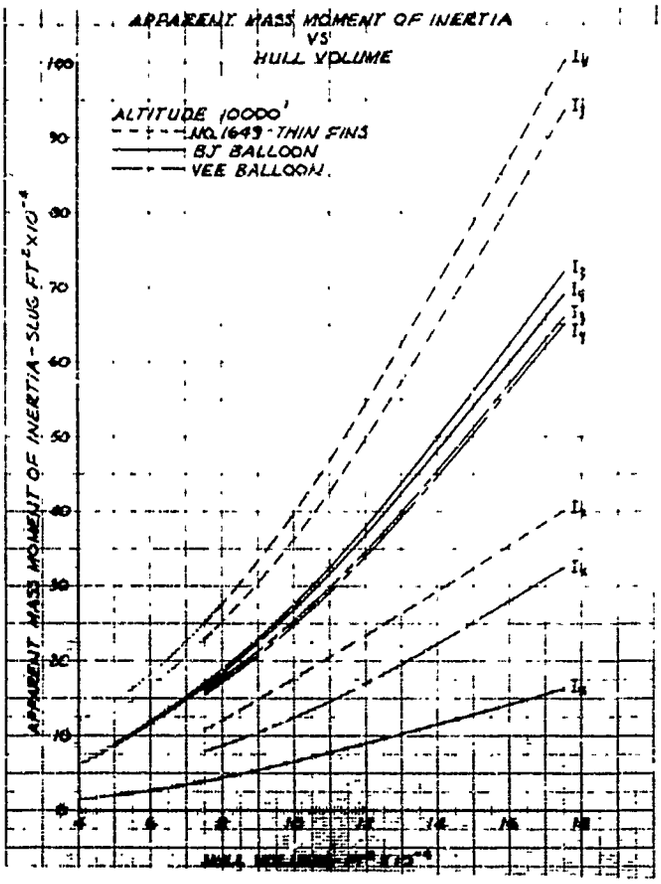

Figure 64

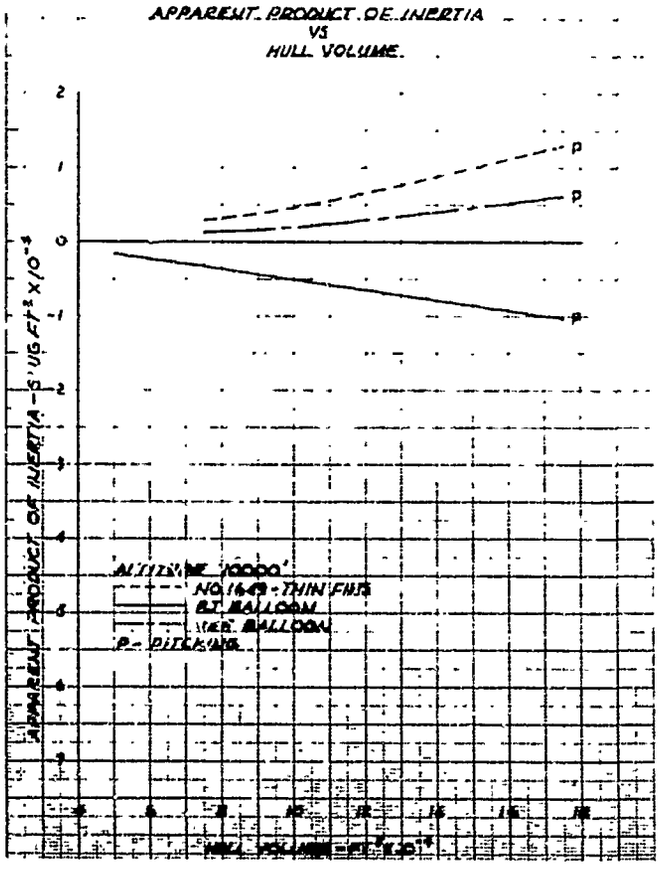

Figure 65

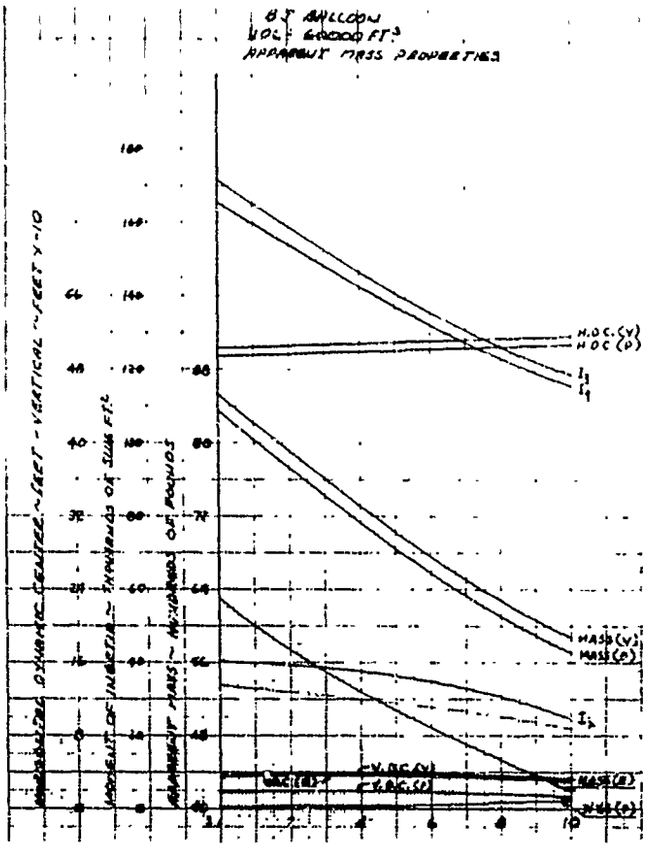

Figure 66

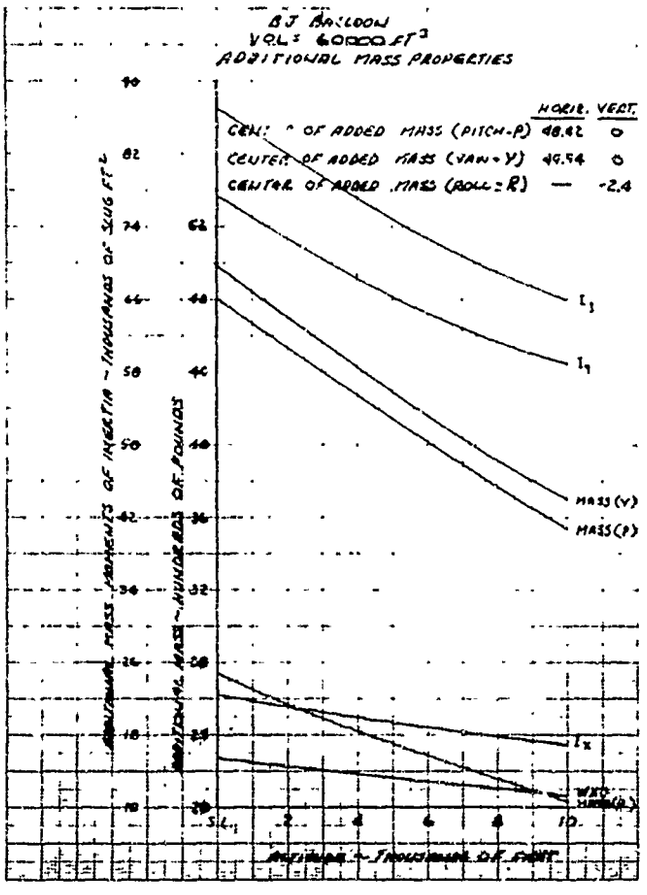

Figure 67

Figure 68

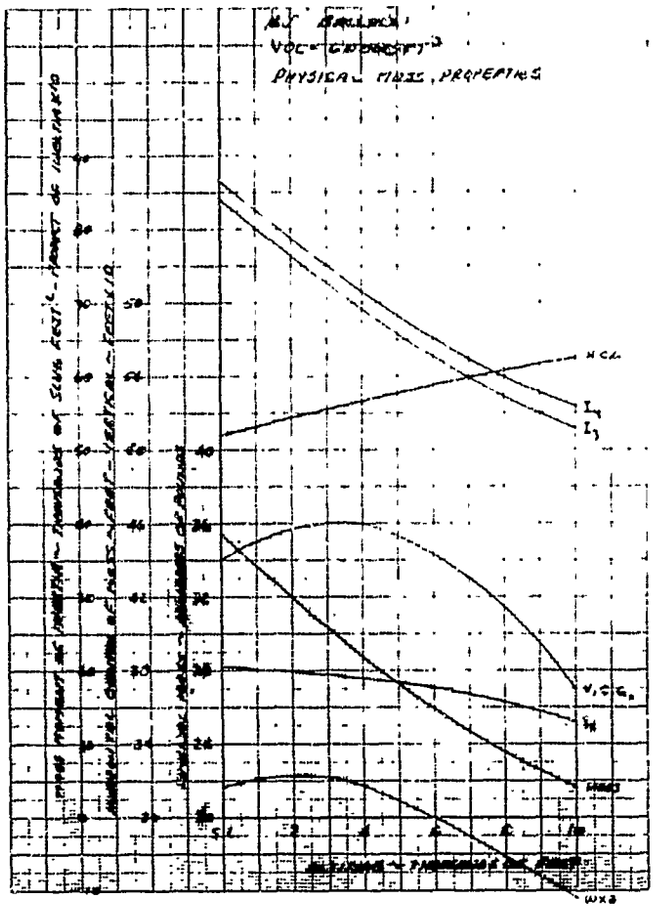

Figure 69

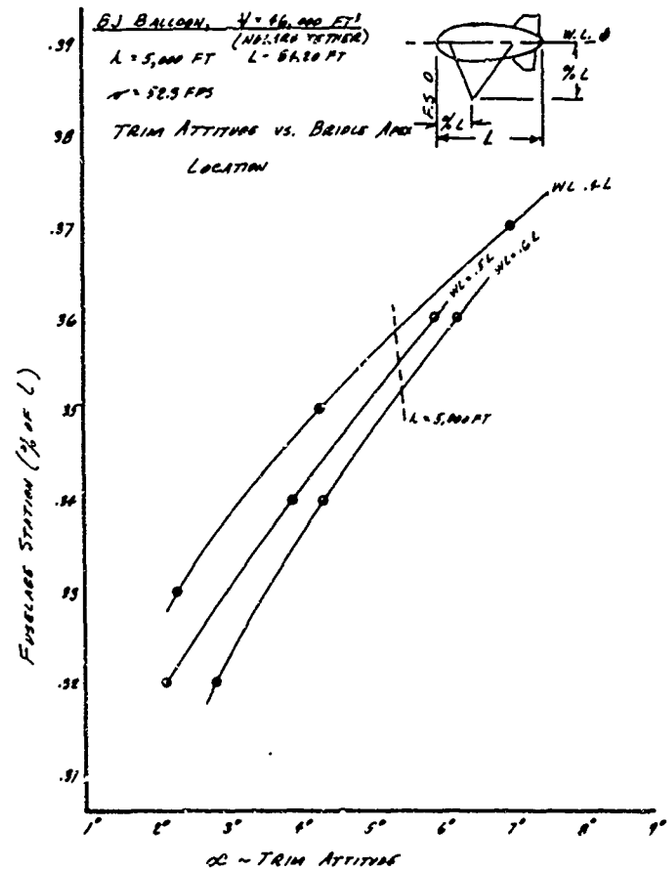

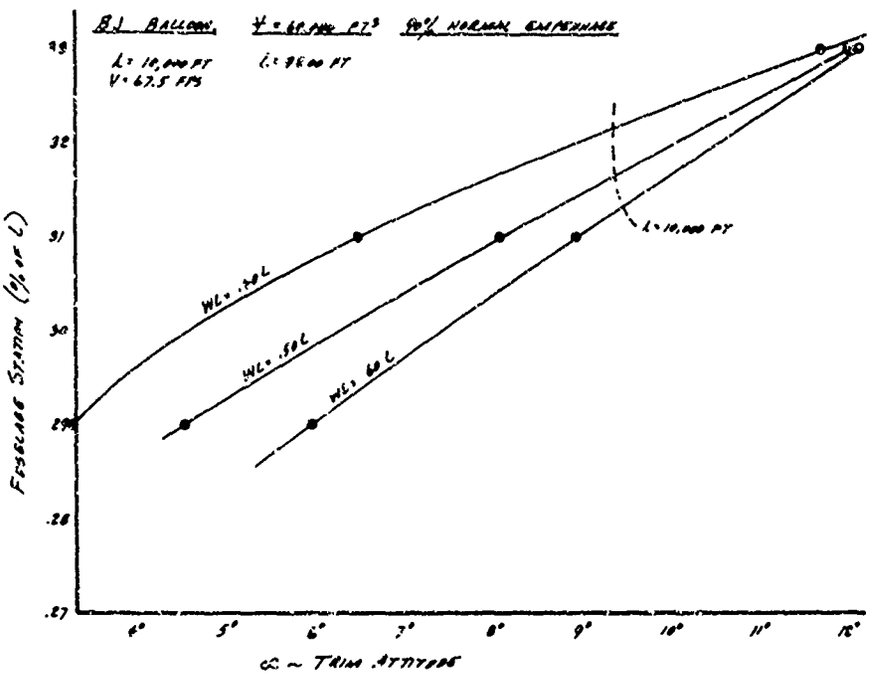

Figure 70

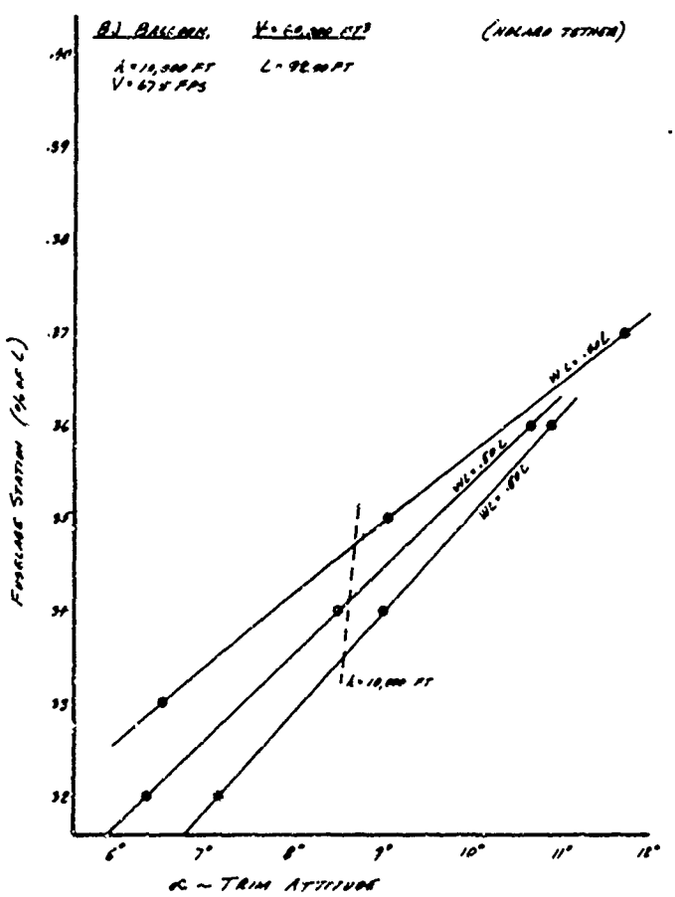

Figure 71

Figure 72

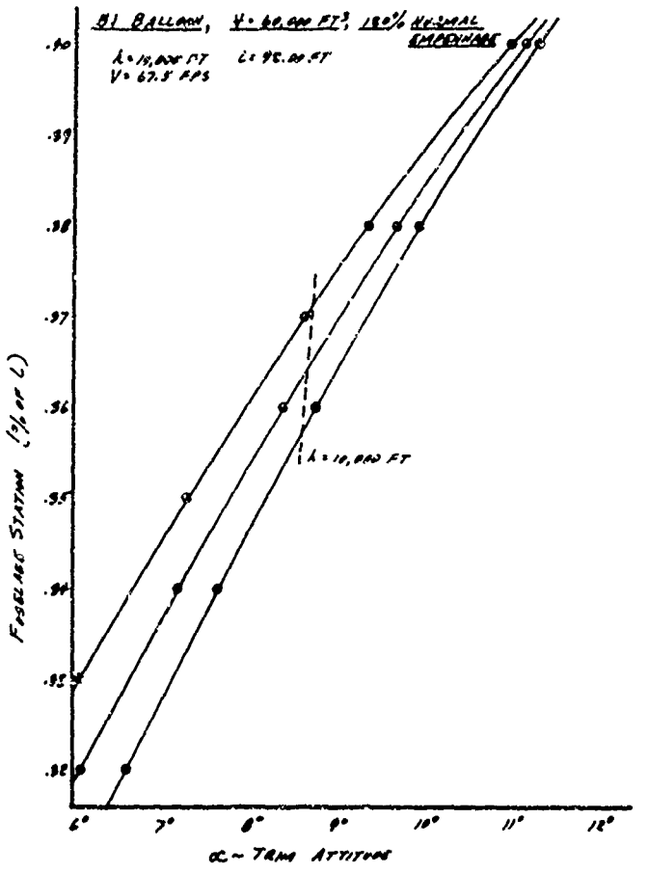

Figure 73

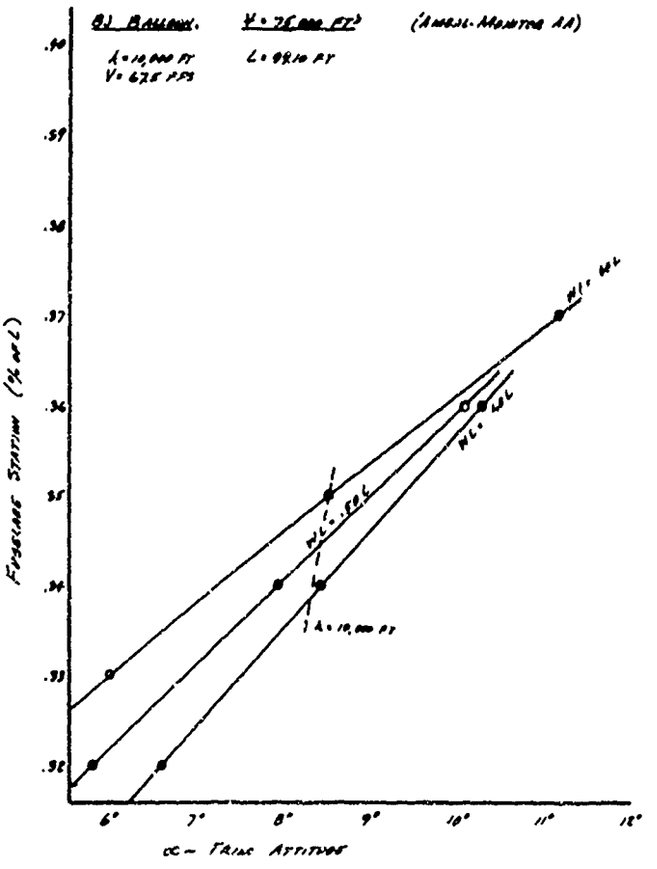

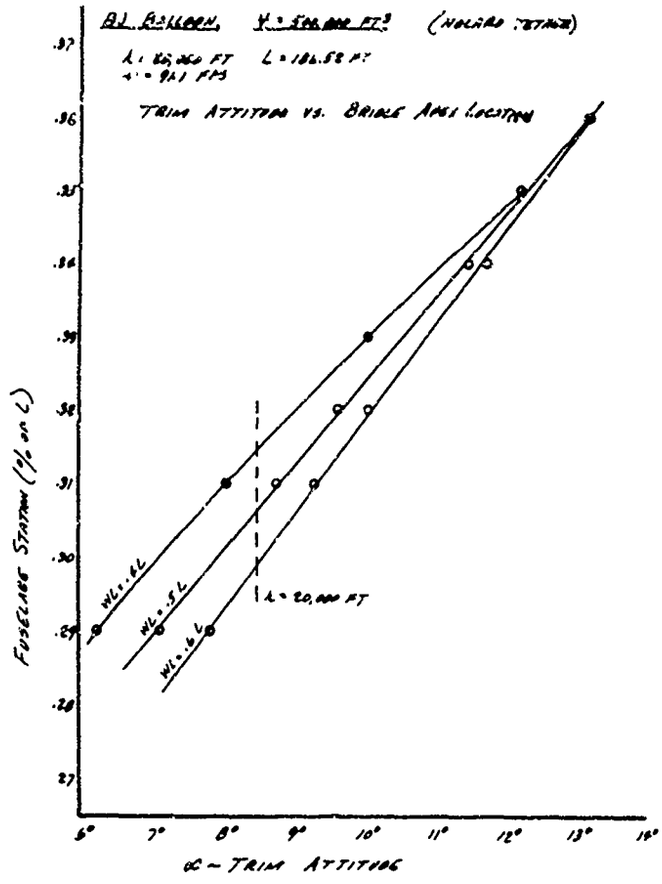

Figure 74

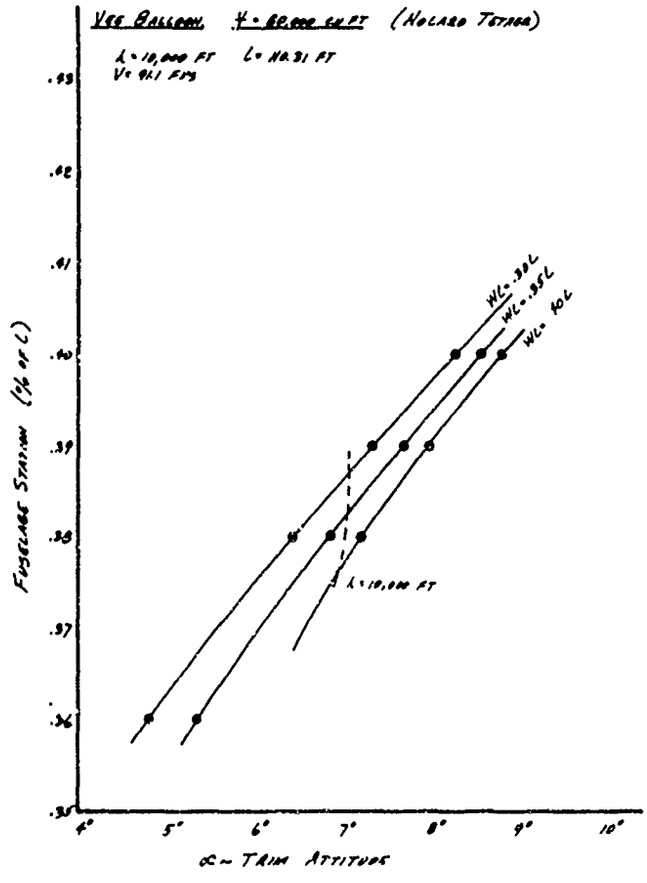

Figure 75

Figure 76

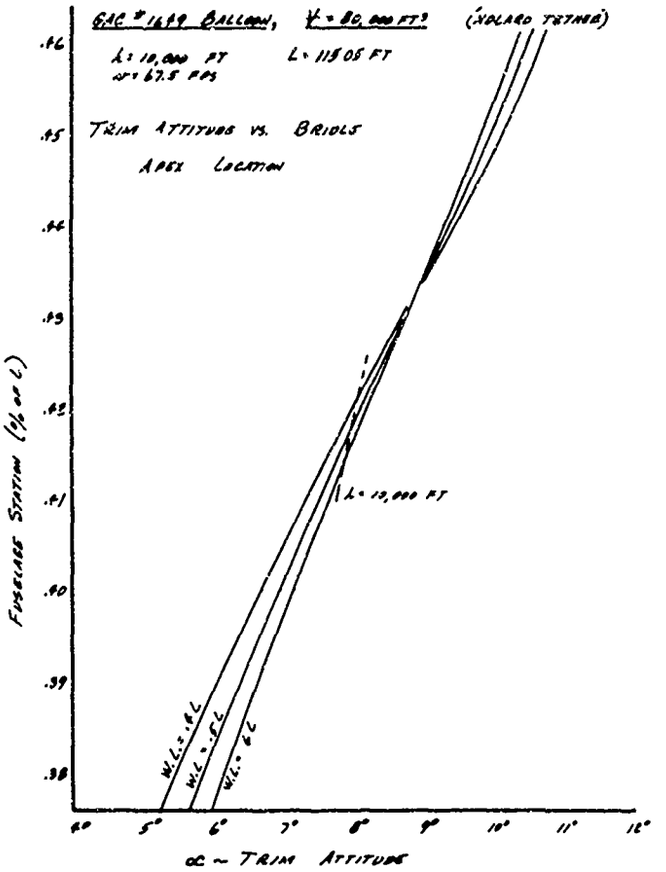

Figure 77

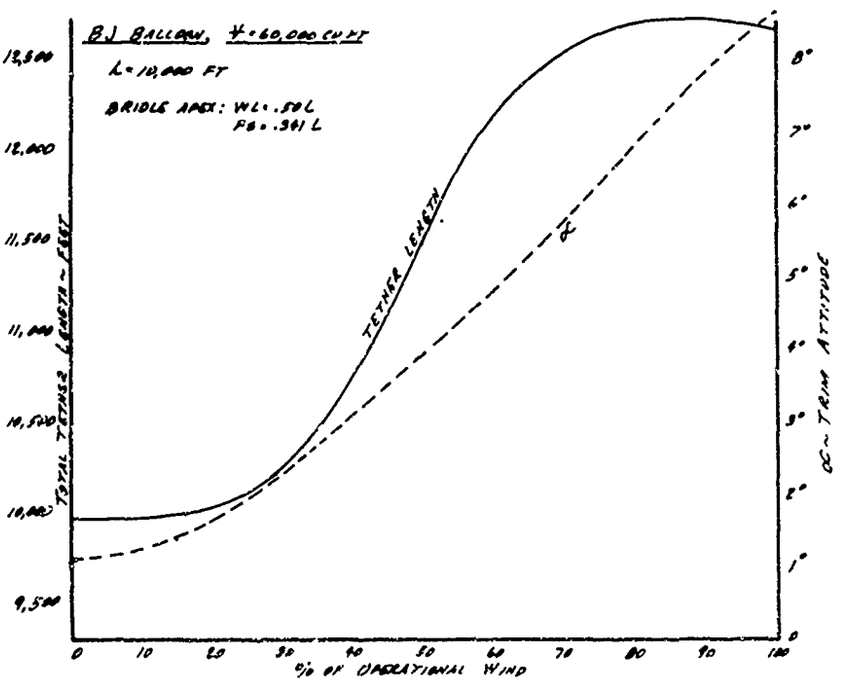

REFERENCES

1. Definition of Tethered Balloon Systems, Scientific Report No. 1, AFCRL-71-0213, 31 March 1971.

2. Doyle, George R, Jr.: Mathematical Model for the Ascent and Descent of a High-Altitude Tethered Balloon; Journal of Aircraft, Vol. 6, No. 5, September-October 1969.

3. Etkin, Bernard: Dynamics of Flight, Stability and Control, John Wiley & Sons, Inc., 1959

4. Perkins, Courtland D. and Hage, Robert E.: Airplane Performance Stability and Control, John Wiley and Sons, Inc., 1949

5. Jeffrey, N. E.: Influence of Design Features on Underwater Towed System Stability, AIAA Paper No. 68-124

6. Fröberg, Carl-Erik: Introduction to Numerical Analysis, Addison-Wesley Publishing Company, Inc., 1965.

7. Goldstein, Herbert PhD: Classical Mechanics, Addison-Wesley, Inc., 1965.